

UNIVERSITY OF SOUTHAMPTON

FACULTY OF ENVIRONMENTAL AND NATURAL SCIENCE

School of Ocean and Earth Science

**Benthic foraminiferal responses to mesoscale environmental
heterogeneity at the Porcupine Abyssal Plain, NE Atlantic**

by

Paris V. Stefanoudis

Thesis for the degree of Doctor of Philosophy

October_2016

UNIVERSITY OF SOUTHAMPTON

ABSTRACT

FACULTY OF ENVIRONMENTAL AND NATURAL SCIENCE

School of Ocean and Earth Science

Thesis for the degree of Doctor of Philosophy

**BENTHIC FORAMINIFERAL RESPONSES TO MESOSCALE
ENVIRONMENTAL HETEROGENEITY AT THE PORCUPINE ABYSSAL PLAIN,
NE ATLANTIC**

Paris V. Stefanoudis

Although our knowledge on the vast deep-sea biome has increased in recent decades, we still have a poor understanding of the processes regulating deep-sea diversity and assemblage composition, as well as their underlying natural variability in space and time. In the face of unprecedented anthropogenic impact on this environment, addressing this knowledge gap remains of paramount importance. In this thesis I focus on the effect of mesoscale (10s of kilometres) spatial heterogeneity, in the form of abyssal hills and surrounding abyssal plains, on benthic communities and specifically on foraminiferal faunas living at abyssal depths in the northeast Atlantic. 'Live' (Rose-Bengal-stained) and dead benthic foraminiferal assemblages, including rarely-studied soft-walled monothalamous species, were analysed based on a total of 16 Megacorer samples (0.25 cm² surface area, 0–1 sediment horizon, >150 µm sieve fraction) from five sites within the area of the Porcupine Abyssal Plain Sustained Observatory (PAP-SO, NE Atlantic, ~4850 m water depth). Three sites were located on the tops of small abyssal hills (~200–500 m elevation) and two on the adjacent abyssal plain. The main results of this analysis include the following. **(1) Description of new morphotypes of poorly known primitive benthic foraminifera associated with (i.e. sessile on) planktonic foraminiferal shells and mineral grains.** Some of these forms were more common on the hills, while others were more common on the plain. **(2) Agglutinated foraminifera selected particles of different sizes on the hills compared to the plain, which affected their test morphometry and visual appearance.** Distinct hydrodynamic conditions, and consequently distinct sediment granulometric characteristics between the two settings (hills, plain) resulted in foraminifera on the hills having more coarsely agglutinating tests. This information could be useful in palaeoecological interpretations of the fossil record. **(3) Live benthic foraminiferal assemblages were significantly influenced by seafloor topography.** Abyssal hills had a higher species density compared to the plain, supported a distinct fauna, and therefore tended to increase regional diversity. Enhanced bottom-water flow on hills, which affects organic matter supply and local sedimentology, were proposed to be responsible for these differences. **(4) During the transition from live to dead benthic foraminiferal faunas there was a significant loss of delicate agglutinated and organic-walled forms.** Unlike 'live' assemblages, the composition of the dead assemblages was very similar in hill and plain settings, suggesting that it would not be possible for paleoceanographers to differentiate between fossil foraminiferal faunas originating from these topographically contrasting settings. In conclusion, this study highlighted the significant effect of hills on agglutination patterns, assemblage composition and regional diversity of living benthic foraminifera. Since abyssal hills are one of the most common landforms on Earth, their presence may substantially enhance abyssal biodiversity, with important implications of deep-sea ecosystem functioning.

Table of Contents

Table of Contents	i
List of Tables	v
List of Figures	vii
List of Accompanying Materials	ix
DECLARATION OF AUTHORSHIP	xi
Acknowledgements	xiii
Chapter 1: Introduction	1
1.1 Benthic foraminifera	3
1.2 Previous studies in the northeast Atlantic.....	4
1.3 Research aim	8
1.4 Publication of portions of the thesis.....	10
References of Chapter 1.....	12
Chapter 2: Basal monothalamous and pseudochambered benthic foraminifera associated with planktonic foraminiferal shells and mineral grains from the Porcupine Abyssal Plain, NE Atlantic	27
Abstract	27
2.1 Introduction	28
2.2 Materials and Methods	30
2.2.1 Sample collection and laboratory processing.....	30
2.2.2 Light and scanning electron microscopy	31
2.3 Results	31
2.3.1 Entire benthic foraminiferal assemblages	31
2.3.2 Diversity of monothalamous and pseudochambered foraminifera ..	32
2.3.3 Occurrence at abyssal hills and abyssal plain sites	42
2.4 Discussion.....	43
2.4.1 Limitations of dataset	43
2.4.2 Comparisons with other studies	43
2.5 Concluding remarks	46
References of Chapter 2.....	47

Chapter 3: Agglutination of benthic foraminifera in relation to mesoscale bathymetric features in the abyssal NE Atlantic (Porcupine Abyssal Plain)	51
Abstract.....	51
3.1 Introduction.....	52
3.2 Materials and methods	53
3.2.1 Sample collection and study site.....	53
3.2.2 Test morphometry.....	55
3.2.3 Particle size analysis.....	57
3.2.4 Elemental composition.....	58
3.3 Results	60
3.3.1 Visual comparison of agglutinated foraminifera tests from hills and plain.....	60
3.3.2 Particle size analysis.....	62
3.3.3 Morphometric analysis	66
3.3.4 Elemental analysis	67
3.4 Discussion	69
3.4.1 Limitations of dataset	69
3.4.2 Do agglutinated foraminifera utilize different sized particles in hill and plain settings?.....	69
3.4.3 Does the composition of substratum affect test morphometry?	71
3.4.4 Evidence of mineral selectivity	73
3.4.5 Paleoceanographic significance.....	74
References of Chapter 3.....	76
Chapter 4: Abyssal hills: influence of topography on benthic foraminiferal assemblages	83
4.1 Introduction.....	83
4.2 Environmental characteristics of the study area	85
4.3 Materials and methods	87
4.3.1 Sample collection.....	87
4.3.2 Laboratory analysis.....	87
4.3.3 Light and scanning electron microscopy	88

4.3.4	Statistical analysis.....	89
4.4	Results	91
4.4.1	Density.....	91
4.4.2	Diversity	94
4.4.3	Assemblage composition	97
4.5	Discussion.....	99
4.5.1	Limitations of dataset	99
4.5.2	Influence of abyssal hills on foraminiferal faunas	99
4.5.3	Concluding remarks.....	105
	References of Chapter 4.....	107
Chapter 5:	Relationship between ‘live’ and dead benthic foraminiferal assemblages in the abyssal NE Atlantic	117
5.1	Introduction	118
5.2	Materials and methods	120
5.2.1	Characteristics of the study area	120
5.2.2	Sample collection.....	121
5.2.3	Sample processing	122
5.2.4	Light and scanning electron microscopy	122
5.2.5	Data processing.....	123
5.3	Results	124
5.3.1	Density.....	124
5.3.2	Diversity	124
5.3.3	Comparison of living and dead assemblages	126
5.4	Discussion.....	132
5.4.1	Limitations.....	132
5.4.2	To what extent are dead benthic foraminiferal assemblages representative of the original live fauna?	133
5.4.3	Taphonomic processes affecting the composition of dead assemblages	134
5.4.4	The influence of population dynamics on the composition of dead assemblages	137
5.4.5	<i>Bolivina spathulata</i>	139

5.4.6	Concluding remarks	140
	References of Chapter 5.....	142
Chapter 6:	Synthesis and future directions	151
6.1	Main conclusions.....	151
6.2	Limitations of data set	153
6.3	Suggestions for future work.....	154
6.4	Implications for understanding of the PAP-SO area and the wider abyss.....	165
	References of Chapter 6.....	167
Appendix A	Taxonomic Appendix	179
Appendix B	Formation of agglutinated cysts by the foraminiferan <i>Sphaeroidina bulloides</i> on the Porcupine Abyssal Plain (NE Atlantic).....	255

List of Tables

Table 1.1. Previous studies on modern deep-sea benthic foraminiferal assemblages from the northeast Atlantic.....	5
Table 2.1. Locality data.....	31
Table 2.2. Counts of monothalamid and pseudochambered morphotypes.....	32
Table 2.3. Occurrence of monothalamid and pseudochambered morphotypes...	33
Table 3.1. Locality data.....	55
Table 3.2. Summary statistics of test particle size composition for selected benthic foraminiferal species.....	62
Table 3.3. Mean percentage of the coarse sediment particle fraction per study site and topographic setting.....	65
Table 4.1. Site and station information.....	87
Table 4.2. Mean density of 'live' (Rose-Bengal-stained) specimens and mean number of species, per site and topographic setting.....	92
Table 4.3. Absolute and relative densities of the major groupings based on complete and fragmentary 'live' (Rose-Bengal-stained) specimens for each topographic setting.....	92
Table 4.4. Assessment of beta diversity via rarefaction with Hill numbers.....	96
Table 4.5. Variation in benthic foraminiferal assemblage composition between hill and plain samples and between sites as assessed by ANOSIM.....	98
Table 5.1. Site and station information.....	121
Table 5.2. Top 20 'live' (Rose-Bengal-stained) species with complete tests per sample and in all samples combined.....	128
Table 5.3. Top 20 dead species with complete tests per sample and in all samples combined.....	129
Table 5.4 Live/dead ratios for all major species, considering the 'entire' (fossilisable plus non-fossilisable) assemblage.....	131
Table 5.5 Live/dead ratios for all major species, considering potential fossil species only.....	132

Table 6.1. Site and station information.....	158
Table 6.2. Numbers of foraminiferal and metazoan morphospecies attached to dropstones.....	158

List of Figures

Fig. 2.1. Bathymetry map of the PAP-SO area.....	30
Fig. 2.2. Light and SEM photographs of some monothalamids.....	34
Fig. 2.3. Light and SEM photographs of some monothalamids.....	35
Fig. 2.4. Light and SEM photographs of some monothalamids.....	36
Fig. 2.5. Light and SEM photographs of some monothalamids.....	38
Fig. 2.6. Light and SEM photographs of some monothalamids.....	39
Fig. 2.7. Light and SEM photographs of some chain-like morphotypes.....	41
Fig. 3.1. Bathymetric map of the PAP-SO area.....	54
Fig. 3.2. Four main test morphometric descriptors.....	57
Plate 3.1. Light and SEM photographs of some species.....	59
Plate 3.2. Light and SEM photographs of some species.....	60
Plate 3.3. Light and SEM photographs of some species.....	61
Fig. 3.3. Particle size distribution for selected sediment samples (0–1 cm sediment horizon) and benthic foraminiferal tests.	63
Fig. 3.4. Elemental composition for selected sediment samples (0–1 cm sediment horizon) and benthic foraminiferal tests.....	68
Fig. 4.1. 3D topographic representation of the PAP-SO area.....	86
Fig. 4.2. ‘Live’ (Rose-Bengal-stained) species ranked by density for each topographic setting.....	94
Fig. 4.3. Sample-based rarefied benthic foraminiferal species richness scaled by (a) area sampled, and (b) number of individuals assessed.....	96
Fig. 4.4. MDS ordination plot of 16 Megacorer samples in the PAP-SO area, including all 134 species with complete tests.....	98
Fig. 5.1. 3D topographic representation of the PAP-SO area.....	121
Fig. 5.2. Biplot of rarefied estimated number of live and dead species.....	125
Fig. 5.3. MDS ordination plots of live and dead foraminiferal assemblage composition (log [x+1] transformed count data).....	127

Fig. 5.4. MDS ordination plot of live and dead foraminiferal assemblage composition (log [x+1] transformed relative abundance data).....	141
Fig. 6.1. Common metazoans attached to dropstones.....	159
Fig. 6.2. Common foraminifera attached to dropstones.....	160

List of Accompanying Materials

1 x CD-ROM containing supplementary material for:

Chapter 3

Supplementary Material 3.A. List of species used for morphometric, particle size and elemental analyses.

Supplementary Material 3.B. Results of morphometric analysis.

Supplementary Material 3.C. Results of elemental analysis.

Chapter 4

Supplementary Material 4.A. Seafloor topography of the PAP-SO area.

Supplementary Material 4.B. Assemblage characteristics of living assemblages against topographic setting.

Supplementary Material 4.C. Densities of living assemblages for 16 Megacorer samples.

Supplementary Material 4.D. SIMPER results.

Chapter 5

Supplementary Material 5.A. Assemblage characteristics of living and dead assemblages for 4 Megacorer samples.

Supplementary Material 5.B. Photographs of sediment cores.

DECLARATION OF AUTHORSHIP

I, Paris V. Stefanoudis

declare that this thesis entitled “Benthic foraminiferal responses to mesoscale environmental heterogeneity at the Porcupine Abyssal Plain, NE Atlantic” and the work presented in it are my own and has been generated by me as the result of my own original research.

I confirm that:

1. This work was done wholly or mainly while in candidature for a research degree at this University;
2. Where any part of this thesis has previously been submitted for a degree or any other qualification at this University or any other institution, this has been clearly stated;
3. Where I have consulted the published work of others, this is always clearly attributed;
4. Where I have quoted from the work of others, the source is always given. With the exception of such quotations, this thesis is entirely my own work;
5. I have acknowledged all main sources of help;
6. Where the thesis is based on work done by myself jointly with others, I have made clear exactly what was done by others and what I have contributed myself;
7. Parts of this work have been published as:

Stefanoudis, P.V., Gooday A.J., 2015. Basal monothalamous and pseudochambered foraminifera associated with planktonic foraminiferal shells and mineral grains from the Porcupine Abyssal Plain, NE Atlantic. *Marine Biodiversity*, 45, 357–369, doi:10.1007/s12526-014-0277-5.

Stefanoudis, P.V., Schiebel, R., Mallet, R., Durden, J.M., Bett, B.J., Gooday, A.J., 2016. Agglutination of benthic foraminifera in relation to mesoscale bathymetric features in the abyssal NE Atlantic (Porcupine Abyssal Plain). *Marine Micropaleontology*, 123, 15–28, doi:10.1016/j.marmicro.2015.12.005.

Stefanoudis, P.V., Bett, B.J., Gooday, A.J. (2016). Abyssal hills: Influence of topography on benthic foraminiferal assemblages. *Progress in Oceanography*, 148, 44–55, doi: 10.1016/j.pocean.2016.09.005.

Stefanoudis, P.V., Gooday, A.J. (2016). Formation of agglutinated cysts by the foraminiferan *Sphaeroidina bulloides* on the Porcupine Abyssal Plain (NE Atlantic). *Marine Biodiversity*, Online First, 1–3, doi:10.1007/s12526-015-0433-6.



Signed:

Date: 31 October 2016

Acknowledgements

This PhD was funded by the University of Southampton and the Natural Environmental Research Council (NERC) and contributed to the NERC-funded efforts of the Autonomous Ecological Survey of the Abyss project (AESAs; NE/H021787/1), the Porcupine Abyssal Plain Sustained Observatory (PAP-SO) programme, and the Marine Environmental Mapping Programme (MAREMAP).

I would like to thank my supervisors Andrew Gooday and Brian Bett for their constant help and support throughout my PhD. Their enthusiasm and working ethos has been a strong motivator for me and helped making the past 3.5 years a memorable and stress-free experience.

I am also grateful to Ralf Schiebel who supervised me during my three-month stay in the University of Angers; Frans Jorissen for kindly accepting to host me at the Laboratory of Recent and Fossil Bio-Indicators (BIAF), University of Angers; the Graduate School of Ocean and Earth Science, University of Southampton that provided funding for that time period (European Exchange Programme 2014). Many thanks to all the scientists who provided guidance during various stages of my PhD: Jen Durden, Aurelie Goineau, Laetitia Gunton, Matteo Ichino, Kirsty Morris, Henry Ruhl and Rui Vieira. Special thanks to my panel chair, Jon Copley.

I would also like to acknowledge the captain, crew and shipboard scientific party of RSS *James Cook* cruise 062 for the collection of the Megacore samples, without which this project would not be possible.

Last but not least, I am especially thankful to the people that were not involved in this research project, but instead were an integral part of my everyday life throughout this (PhD) era: my fiancée and partner in life Christina, my parents, my grandparents, my sisters and their families, and all of my friends from the National Oceanography Centre in Southampton. Their companion and support all these years made the PhD as a whole a most pleasant experience.

Chapter 1: Introduction

The oceans cover 71% of the earth's surface and in terms of volume encompass 99% of the available biosphere (Costanza, 1999; Costello et al., 2010), while the seafloor supports a living biomass of around 110 MtC globally (Wei et al., 2010). The deep sea, defined here as environments lying below 200 m depth, generally beyond the depth of the continental shelf break (UNESCO, 2009) and with insufficient light for net primary production by photosynthesis, represents about 91% of the available ocean floor (Harris et al., 2014). As such, it is the largest ecosystem on Earth, with a mean depth of 4.2 km, average temperatures <4 degrees Celcius, high pressures (average >400 atmospheres), and a seabed area of ~434,386,264 km² (Danovaro et al., 2014). However, at present only 5% of this vast environment has been explored using remote technology, while all physical samples collected from the deep seafloor combined represent <0.01% of its total surface area (Ramirez-Llodra et al., 2010).

For a long time the deep sea was thought of as a stable environment over ecological and geological time (Menzies, 1965). We know that this is not true, as the ocean floor is subject to a variety of disturbances operating across wide-ranging spatial and temporal scales (Danovaro et al., 2014; Gage and Tyler, 1991; Glover et al., 2010; Rex and Etter, 2010; Tyler, 1995). For example, on small spatial (<100 km²) and short temporal (<1 year) scales, strong disturbances arise from current activity (benthic storms) (Kerr, 1980) and down-slope or down-canyon sediment transport (Canals et al., 2006; Puig et al., 2003), which resuspend and organically enrich sediments, thereby affecting benthic communities (Aller, 1989; Thistle et al., 1991). Over larger areas and longer time frames, seasonality and interannual variability in food supply has a strong influence on growth, recruitment and migration of some species (Billett et al., 2001; Glover et al., 2002; Gooday, 2002; Tyler, 1988) and is a good predictor of deep-sea diversity patterns (Woolley et al., 2016). On decadal time scales, climatic oscillations such as the North Atlantic Oscillation (NAO) and El Nino Southern Oscillation (ENSO) in the Pacific may cause widespread changes in abyssal food supply (Ruhl et al., 2008; Smith et al., 2006). Over geological time scales, large climatic shifts, plate tectonics and associated continental movements, episodes of widespread deep-sea anoxia,

occasional mass sediment movements (submarine slumps and slides, turbidity currents) and volcanic eruptions among other phenomena, are suggested to have had global-scale impacts on the evolution (extinction, speciation, adaptive radiations) and geographic distribution (range shifts, local extinctions) of the deep-sea fauna (Jacobs and Lindberg, 1998; Masson, 1996; Priede and Froese, 2013; Thomas and Gooday, 1996; Yasuhara et al., 2009).

Although much has been learnt in recent decades, natural variation in the deep sea and processes underlying it remain poorly known, especially in non-chemosynthetic systems (Smith et al., 2009). Nevertheless, an improved understanding of natural phenomena on the ocean floor are essential in order to assess anthropogenic impacts on this environment. A wide variety of human activities (Rogers et al., 2015; Thiel, 2003), including benthic fisheries (Bailey et al., 2009; Clarke et al., 2015; Puig et al., 2012), mining of critical metals and elements (Wedding et al., 2013; 2015), mine-tailing placements (Ramirez-Llodra et al., 2015) and plastic pollution (Galil et al., 1995; Woodall et al., 2014) have, now or in the future, profound effects on the deep sea (Levin and Le Bris, 2015; Ramirez-Llodra et al., 2011) and the services it provides (Thurber et al., 2014). In addition, climate change is occurring at an unprecedented rate and is projected to warm the surface of the oceans by between 0.6 and 2.6 degrees Celsius by the end of the 21st century, depending on different emission scenarios (Collins et al., 2013; Mora et al., 2013). Surface ocean warming will result in increased stratification and reduced nutrient mixing, which in turn will negatively affect upper ocean biomass and surface primary production (Steinacher et al., 2010). At the same time increased uptake of carbon dioxide will depress pH (Byrne et al., 2010), with possible negative consequences for organisms with calcareous hard parts (Uthicke et al., 2013), including coccolithophores (Beaufort et al., 2011; Meyer and Riebesell, 2015) that are important primary producers in the euphotic zone. As deep-sea ecosystem functioning is primarily dependent on surface processes (food supply, deep-water formation and the oceanic 'conveyor belt'), climate change is expected to have profound implications for benthic communities (Jones et al., 2014). Reductions in food supply to benthic communities will have maximal impact at abyssal and hadal depths (3500–6500 and >6500 m water depth, respectively), which are already among the most food-stressed deep-sea environments (Jones et al., 2014; Smith et al., 2008).

Understanding the consequences of natural and human-induced impacts on deep-sea benthic ecosystems, requires improved knowledge of the natural variability of these ecosystems in space as well as time. This thesis focuses on the mesoscale (10s of kilometres) spatial variations of benthic communities, and specifically on foraminiferal faunas living at abyssal depths in the northeast Atlantic. The abyssal zone occupies by far the largest part of the ocean; it accounts for 27% of the total ocean depth range and covers almost 65% and 85% of earth's and ocean's surface, respectively (Harris et al., 2014; Watling et al., 2013). A network of plains (separated by mid-ocean ridges, island arcs and hadal trenches), hills and seamounts of various sizes, and the lower reaches of canyons, are among the diverse habitats found at these depths (Smith et al., 2008).

1.1 Benthic foraminifera

Benthic foraminifera are an enormously successful group of single-celled eukaryotic organisms ('protists') and a major component of the deep-sea benthos. These amoeboid protists are characterised by a netlike (granuloreticulate) system of pseudopodia and the presence of a shell ('test') that largely encloses the cytoplasmic body and is composed of one or more chambers (Goldstein, 1999). Molecular data place the foraminifera within the 'Supergroup' Rhizaria (Adl et al., 2012; Ruggiero et al., 2015) in close relationship with the Acantharea and Polycistinea (formerly 'radiolaria'), with which they form the rhizarian clade Rhetaria (Sierra et al., 2013). In some foraminiferal groups, the test is constructed from foreign particles (e.g. mineral grains, sponge spicules, shells of planktonic foraminifera) stuck together (agglutinated) by an organic or calcareous/organic cement (Bender, 1995; Bender and Hemleben, 1988). In others, the test is composed of calcium carbonate that is secreted by the organism itself (Hansen, 1999), while organic-walled forms (Loeblich and Tappan, 1987; Sen Gupta, 1999) and even 'naked' foraminifera that lack a test (Wilding, 2002) are also known.

As well as being a dominant life form in modern benthic communities, from intertidal to hadal depths, foraminifera have an excellent fossil record and are studied intensively by geologists (Jorissen et al., 2007). Much of this geological research uses knowledge of modern faunas to interpret fossil assemblages, but foraminifera

also have many more practical applications in geology and biology (Jones, 2013; Murray, 2006). In particular, the considerable value of foraminifera in environmental monitoring is being recognized increasingly (Alve et al., 2016; Schönfeld et al., 2012). The study of deep-sea benthic foraminifera, therefore, lies at the interface between biology and geology. However, because they have been studied mainly by geologists most attention has been paid to the 'hard-shelled' fossilisable taxa (Douglas and Woodruff, 1981; Jorissen et al., 2007; Murray, 1991), and much less is known about the soft-walled, predominantly monothalamous (i.e. single-chambered) taxa. Although known since the mid-1800s (e.g. Leidy, 1879; Rhumbler, 1913; reviewed in Gooday, 1990), these delicate organisms are difficult to study as many species, especially in deep-sea environments, have small, delicate tests that are destroyed or become unrecognisable when dried and provide taxonomists with relatively few morphological characters on which to base species definitions. Nevertheless, biodiversity studies taking into account soft-walled foraminifera reported that they represent a substantial component of meiofaunal communities (Enge et al., 2012; Gooday, 1986a, b, 1996; Gooday et al., 1998, 2000, 2004; Nozawa et al., 2006; Snider et al., 1984). Recently, sequencing of environmental DNA samples revealed that the vast majority of foraminifera in deep-sea sediments comprise monothalamous foraminifera ('monothalamids') (Lecroq et al., 2011; Lejzerowicz et al., 2014; Pawlowski et al., 2011). It is important for studies of benthic foraminifera to include monothalamids in order to avoid missing an important part of their biodiversity.

1.2 Previous studies in the northeast Atlantic

Numerous studies have focused on modern benthic foraminiferal faunas in the deep waters of the NE Atlantic (Table 1.1). The first published account was by Parker and Jones (1865) who described small agglutinated foraminifera in 39 sounding samples collected in 1857 between Newfoundland and Ireland by H.M.S. *Cyclops* during the first British survey for the north Atlantic submarine telegraph cable in 1857 (Rice, 1986). Important observations of large benthic foraminifera caught in dredge samples from the Scottish and Irish margins were made during the *Lightning* (1867) and *Porcupine* (1868–1869) expeditions

Table 1.1. Previous studies on modern deep-sea benthic foraminiferal assemblages from the northeast Atlantic; we did not include studies from the North Sea, Baltic Sea, and the Mediterranean. BIOTRANS = Biological Vertical Transport and Energetics in the Bethnic Boundary Layer of the Deep-Sea; MAP = Madeira Abyssal Plain; PAP = Porcupine Abyssal Plain; PCM = Portuguese continental margin; PSB = Porcupine Seabight.

Location	water depth (m)	Authors
A. Diversity studies		
A1. Continental margin		
Bay of Biscay	140–1993	Fontanier et al., 2002
	550	Fontanier et al., 2003
	550	Ernst and van der Zwaan, 2004
	80–2000	Duchemin et al., 2007
	550	Barras et al., 2010
Cape Juby + Cape Boyador	9–878	Colom, 1950
Celtic Sea	100–500	Dorst and Schönfeld, 2015
Celtic Sea + English Channel	13–1002	Murray, 1970
Celtic Sea + PSB	160–4262	Murray and Alve, 1994
coast off Galicia	110–655	Colom, 1952
continental shelf off Cameroon	10–100	Berthois et al., 1968
continental slope and rise off southwest Norway	144–3940	Mackensen et al., 1985
Darwin Mounds region	946–958	Hughes et al., 2004
Faeroe Channel	110–1189	Carpenter, 1868
Faeroe Channel + Rockall Trough	99–4453	Murray and Taplin, 1984
Gulf of Cadiz	103–1917	Schönfeld, 2002a
	103–1260	Schönfeld, 2002b
Gulf of Cascoigne	135–3200	Caralp et al., 1970
	135–4450	Pujos-Lamy, 1973
Gulf of Guinea	2475–4331	Levy et al., 1982
Norwegian Fjords	366–823	Sars, 1869
	55–914	Sars, 1872
N Atlantic + North Sea	9–1448	Heron-Allen and Earland, 1913
Norwegian-Greenland Sea	600–3500	Belanger and Streeter, 1980
off Cape Mondego + off Cape Sines + PCM	45–3905	Seiler, 1974
off SW coast of Ireland	1828	Green, 1889; Wright, 1886, 1889, 1890
off W Africa	32–1983	Haake, 1980
Porcupine basin	610–800	Coles et al., 1996
PCM	900	Koho et al., 2008b
	980–3125	Griveaud et al., 2010
	1000	Nardelli et al., 2010
PSB	1320–1340	Gooday, 1986a, b
	1320–1361	Gooday and Lamshead, 1989
	1320–1361	Lamshead and Gooday, 1990
	704–820	Rüggeberg et al., 2007
	696–982	Schönfeld et al., 2011
PSB + Rockall Bank	202–982	Margreth et al., 2009
PSB + western approaches	255–1600	Weston, 1985
Rockall Trough	1913–1980	Gooday and Hughes, 2002
	800–1000	Panieri, 2005
Rockall Trough + Hetton-Rockall Basin	1100–3569	Hughes et al., 2000
Rockall Trough + Rockall Bank + margin of British Isles	99–4453	Carpenter, 1870

Table 1.1. (continued)

Saharan coast of the Atlantic	22–1120	Le Calvez, 1972
SE Rockall Bank	469–1958	Morigi et al., 2012
southern PCM	250–3600	Schönfeld, 1997
A2. Open ocean		
BIOTRANS	4483–4538	Gooday, 1988c
BIOTRANS	3800–3550	Gooday, 1991
N Atlantic	2118–4673	Corliss et al., 2006
N Atlantic	2147–4820	Sun et al., 2006
PAP	4850	Smart and Gooday, 1997
PAP	4836–4847	Gooday et al., 2010b
PAP + BIOTRANS	3796–4680	Gooday et al., 2015
A3. Mixed		
N Atlantic + Arctic Oceans	0–4298	Parker and Jones, 1865
Biscay + off Morocco + off Sudan + Cape Verde	370–3655	de Folin, 1886
NW + NE Atlantic	1280–4820	Cushman and Henbest, 1940
Azores + Canary Islands + Cape Verde	2125–4235	Marie, 1946
south of Canary Islands + PSB	1484–4850	Gooday and Cook, 1984
N Atlantic + Norway-Greenland basin	115–5000	Lukashina, 1988a,b
PSB + BIOTRANS	1340–4561	Cartwright et al., 1989
Iceland Basin + BIOTRANS + PAP + MAP	2880–5519	Gooday et al. 1995
PAP + MAP + Cape Verde Abyssal Plain	4840–4950	Gooday, 1996
PSB + BIOTRANS + PAP	1340–4950	Gooday et al., 1998
Great Meteor Seamount	291–4096	Heinz et al. 2004
N Spain + Malin Sea	1–4450	Saidova, 2008
Bay of Biscay	320–4800	Mojtahid et al., 2010
A4. Canyons		
Cap Breton	632-647	Hess et al., 2005
	235–860	Hess and Jorissen, 2009
Cap de Creus	125–2100	Contreras-Rosales et al., 2012
Cap-Ferret	2800	Fontanier et al., 2005
	2800	Fontanier et al., 2008c
	300–3000	Duros et al., 2013, 2014
Cassidaigne	725-1529	Fontanier et al., 2012
Grand + Petit Rhône	350–2000	Fontanier et al., 2008b
Lisbon-Setubal	365–4450	Koho et al., 2008a
Nazaré	146–4976	Koho et al., 2007
	344–3518	Gooday et al., 2010a
	4300	Gooday et al., 2011
Saint-Tropez	373	Fontanier et al., 2008a
Whittard	300–3000	Duros et al., 2011, 2012
B. Taxonomic studies		
NE Atlantic	2000–4500	Gooday, 1983
PSB + off NW Africa	510–3018	Gooday, 1988b
PSB + off NW Africa + Iceland Basin	510–3018	Gooday, 1988a
PAP + PSB		Gooday, 1990
PAP + PSB + MAP	984–6059	Shires et al., 1994a
MAP	4950	Shires et al., 1994b

(Carpenter, 1868, 1870; Murray and Taplin, 1984). Later, Brady used some of Carpenter's material when he prepared his Challenger Report (1884), in which he described more than 900 species of benthic and planktonic foraminifera, from over 130 dredgings obtained around the world. This monumental work, was the first systematic description of foraminifera from bathyal and abyssal depths in all oceans except the Arctic and the Indian Ocean, and remains to this day an important source of information for taxonomy, morphology, biogeographic and bathymetric distribution of deep-sea benthic foraminifera. The *Challenger Expedition* was followed by an era of major national expeditions and surveys that lasted, except for brief intervals during the two major world wars, until the 1950s (reviewed in Menzies et al., 1973). These expeditions systematically visited and surveyed all of the world's major oceans, and resulted in major publications devoted to foraminifera, which include many descriptions of deep-sea species. The most important of these cruises were the *U.S.S. Albatross* (e.g. Flint, 1899; Cushman, 1918, 1920, 1922, 1923, 1931), *Terra Nova* (Heron-Allen and Earland, 1932) and *Discovery* (Heron-Allen and Earland, 1932; Earland, 1933, 1934, 1936) expeditions; the German Atlantic Expedition (Schott, 1935); Dutch *Siboga* Expedition (Höfker, 1927, 1951); Swedish Deep-Sea Expedition (Phleger and Parker, 1953; Schott, 1966); and Danish *Galathea* Expedition (Tendal and Hessler, 1977). Although most of these expeditions were conducted in parts of the world far beyond the NE Atlantic, they nevertheless contain descriptions of important foraminifera that are relevant to the present work.

More local oceanographic cruises and projects in the NE Atlantic have contributed to the literature on deep-sea foraminifera from this region. Early sampling campaigns were conducted in Norwegian Fjords (M. Sars, 1869; G. O. Sars 1872), various areas of the NE Atlantic and the western Mediterranean aboard the French vessels *Talisman* (1880–1882) and *Travailleur* (1883–1884) (Rice, 1980) leading to descriptions of the common deep-sea genus *Bathysiphon* (de Folin, 1886; Gooday, 1988c), off the southwest coast of Ireland (Green, 1889; Wright, 1886, 1889, 1990), and in the North Sea (Heron-Allen and Earland, 1913). After the second world war, the number of publications featuring benthic foraminifera has increased steadily, especially after the 1980s when foraminifera started to be routinely incorporated in large oceanographic programmes such as BIOTRANS (Biological Vertical Transport and Energetics in the Benthic

Boundary Layer of the Deep-Sea) (e.g. Gooday, 1988c, 1991; Gooday and Turley, 1990), BENBO (BENthic BOundary layer) (Gooday and Hughes, 2002; Hughes and Gooday, 2004), HERMES (Hotspot Ecosystem Research on the Margins of European Seas) (Gooday et al., 2010a; Koho et al., 2007), and HERMIONE (Hotspot Ecosystem Research and Man's Impact on European Seas) (Dorst and Schönfeld, 2013; Morigi et al., 2012).

The Porcupine Abyssal Plain has been the focus of detailed biological studies over the last 30 years (Billett and Rice, 2001; Rice et al., 1994) under a series of projects partly funded by the European Union, principally the BENGAL (High resolution temporal and spatial study of the benthic biology and geochemistry of a north-eastern Atlantic abyssal locality) programme. Research in this area has focused on metazoan meiofauna (Kalogeropoulou et al., 2010), polychaetes (Galeron et al., 2001; Laguionie-Marchais et al., 2013; Soto et al., 2010; Vanreusel et al., 2001), fishes (Bailey et al., 2009, Milligan et al., 2016), megafauna (Billett et al., 2001, 2010; Durden et al., 2015), sponges (Kahn et al., 2012), bacteria (Eardly et al., 2001), and benthic foraminifera (e.g. Gooday, 1996; Gooday et al., 2010b; see Table 1.1). In contrast to most research on deep-sea foraminifera the studies by Gooday and co-workers at the PAP have concerned 'entire assemblages', a term that denotes the inclusion monothalamids as well as hard-shelled multichambered taxa. A similar approach was adopted for the present study.

1.3 Research aim

The overarching aim of this thesis is to understand the effects of mesoscale topographic heterogeneity, in the form of abyssal hills and surrounding abyssal plains, on abyssal benthic communities, as represented by foraminifera. Abyssal hills are 100–1000 m high features that rise from topographically flat areas of seafloor and are estimated to be a globally dominant landscape element on the ocean floor (Harris et al., 2014). To achieve this objective, this work has focused on the area of the Porcupine Abyssal Plain Sustained Observatory (PAP-SO; 4850 water depth), located in the northeast Atlantic about 270 km southwest of Ireland. This is a relatively flat area populated by abyssal hills some 100–500 m

high, although one hill reaches a height of 1000 m above the seafloor (Klein and Mittelstaedt, 1992; Turnewitsch and Springer, 2001).

In Chapter 2, I describe some poorly-known benthic foraminifera from two localities within the PAP-SO area (one on top of a hill and one on the adjacent plain), which are associated with planktonic foraminiferal shells and mineral grains. I then compare these with similar foraminifera found in the abyssal Pacific.

In Chapter 3, I compare agglutination characteristics of benthic foraminiferal tests (morphometry, granulometric and chemical composition) from topographically contrasting locations (hills and plain). These data are compared with granulometric and elemental profiles of sediment samples from the same study sites in order to test for potential particle size and mineral selectivity by the foraminifera. Finally, I discuss how these findings are likely to have an impact on paleoceanographic studies.

In Chapter 4, I examine the effect of topography on benthic foraminiferal assemblage characteristics (density, diversity, species composition) by comparing benthic foraminiferal data from two plain and three hill locations within the PAP-SO area. Contrasting environmental conditions between the two habitats are invoked in order to explain the observed patterns. To conclude, I assess the contribution of hill-induced mesoscale habitat heterogeneity in abyssal foraminiferal diversity.

In Chapter 5, I ask to what extent are dead foraminiferal assemblages representative of the original 'live' (Rose-Bengal-stained) fauna. The contrasting population dynamics of different species, together with taphonomic processes operating over the last few hundreds years, are invoked to explain potential differences. I finish by examining if the effect of topography on modern faunas is maintained in the dead assemblages as well.

In Chapter 6, I synthesise knowledge on the effects of medium-scale habitat complexity on abyssal foraminiferal faunas from the PAP-SO area and create some new hypotheses that will hopefully stimulate future deep-sea research.

1.4 Publication of portions of the thesis

In accordance with the University of Southampton Three-Paper Thesis format requirements, the content of the chapters (text, tables, figures) of the thesis are presented verbatim, as they were submitted or accepted for publication. Therefore, some overlapping information exists between chapters. Tables and Figures have been renumbered, and cross-referencing between chapters has been added to comply with thesis formatting regulations.

Chapter 2. This chapter has been published in *Marine Biodiversity* as:

Stefanoudis, P.V., Gooday A.J., 2015. Basal monothalamous and pseudochambered foraminifera associated with planktonic foraminiferal shells and mineral grains from the Porcupine Abyssal Plain, NE Atlantic. *Marine Biodiversity*, 45, 357–369, doi:10.1007/s12526-014-0277-5.

P.V. Stefanoudis and A.J. Gooday analysed the sediment samples, indentified and photographed the foraminifera described in this paper. **P.V. Stefanoudis** wrote and edited the manuscript and A.J. Gooday provided comments and helped with the writing of the manuscript.

Chapter 3. This chapter has been published in *Marine Micropaleontology* as:

Stefanoudis, P.V., Schiebel, R., Mallet, R., Durden, J.M., Bett, B.J., Gooday, A.J., 2016. Agglutination of benthic foraminifera in relation to mesoscale bathymetric features in the abyssal NE Atlantic (Porcupine Abyssal Plain). *Marine Micropaleontology*, 123, 15–28, doi:10.1016/j.marmicro.2015.12.005.

P.V. Stefanoudis photographed the foraminifera illustrated in this paper, and carried out the morphometric and particle-size analyses for the foraminiferal tests as well as the elemental analysis for the sediment samples. **P.V. Stefanoudis** and R. Mallet performed the elemental analysis for the foraminiferal tests. J.M. Durden provided the particle size data for the sediment samples. Ralf Schiebel, B.J. Bett and A.J. Gooday provided advice on the data analysis and interpretation. **P.V. Stefanoudis** wrote and edited the manuscript. All authors provided comments and helped with the writing of the manuscript.

Chapter 4. This chapter has been published in *Progress in Oceanography* as: **Stefanoudis, P.V.**, Bett, B.J., Gooday, A.J. (2016). Abyssal hills: Influence of topography on benthic foraminiferal assemblages. *Progress in Oceanography*, 148, 44–55, doi: 10.1016/j.pocean.2016.09.005.

P.V. Stefanoudis analysed the sediment samples, identified and photographed the foraminifera described in this paper. A.J. Gooday assisted with the identification and taxonomy of the foraminifera. B.J. Bett and A.J. Gooday provided advice on the data analysis and interpretation. **P.V. Stefanoudis** wrote and edited the manuscript. All authors provided comments and helped with the writing of the manuscript.

Chapter 5. This chapter has been prepared as a draft manuscript for submission to *Deep-Sea Research Part I – Oceanographic Papers*, as:

Stefanoudis, P.V., Bett, B.J., Gooday, A.J., in prep. Dead assemblage formation in abyssal benthic foraminifera from the NE Atlantic.

P.V. Stefanoudis analysed the sediment samples, identified and photographed the foraminifera described in this paper. A.J. Gooday assisted with the identification and taxonomy of the foraminifera. B.J. Bett and A.J. Gooday provided advice on the data analysis and interpretation. **P.V. Stefanoudis** wrote and edited the manuscript. All authors provided comments and helped with the writing of the manuscript.

Appendix B. This appendix has been published in *Marine Biodiversity* as:

Stefanoudis, P.V., Gooday, A.J. (2016). Formation of agglutinated cysts by the foraminiferan *Sphaeroidina bulloides* on the Porcupine Abyssal Plain (NE Atlantic). *Marine Biodiversity*, Online First, 1–3, doi:10.1007/s12526-015-0433-6.

P.V. Stefanoudis photographed the *Sphaeroidina bulloides* specimens, wrote and edited the manuscript. A.J. Gooday provided comments and helped with the writing of the manuscript.

References of Chapter 1

- Adl, S.M., Simpson, A.G.B., Lane, C.E., Lukes, J., Bass, D., Bowser, S.S., Brown, M.W., Burki, F., Dunthorn, M., Hampl, V., Heiss, A., Hoppenrath, M., Lara, E., le Gall, L., Lynn, D.H., McManus, H., Mitchell, E.A.D., Mozley-Stanridge, S.E., Parfrey, L.W., Pawlowski, J., Rueckert, S., Shadwick, L., Schoch, C.L., Smirnov, A., Spiegel, F.W., 2012. The revised classification of eukaryotes. *Journal of Eukaryotic Microbiology*, 59, 429–493.
- Aller, J.Y., 1989. Quantifying sediment disturbance by bottom currents and its effect on benthic communities in a deep-sea western boundary zone. *Deep-Sea Research Part A—Oceanographic Research Papers*, 36, 901–934.
- Alve, E., Korsun, S., Schönfeld, J., Dijkstra, N., Golikova, E., Hess, S., Husum, K., Panieri, G., 2016. Foram-AMBI: A sensitivity index based on benthic foraminiferal faunas from North-East Atlantic and Arctic fjords, continental shelves and slopes. *Marine Micropaleontology*, 122, 1–12.
- Bailey, D.M., Collins, M.A., Gordon, J.D.M., Zuur, A.F., Priede, I.G., 2009. Long-term changes in deep-water fish populations in the northeast Atlantic: a deeper reaching effect of fisheries? *Proceedings of the Royal Society B-Biological Sciences*, 276, 1965–1969.
- Barras, C., Fontanier, C., Jorissen, F., Hohenegger, J., 2010. A comparison of spatial and temporal variability of living benthic foraminiferal faunas at 550m depth in the Bay of Biscay. *Micropaleontology*, 56, 275–295.
- Beaufort, L., Probert, I., de Garidel-Thoron, T., Bendif, E.M., Ruiz-Pino, D., Metzli, N., Goyet, C., Buchet, N., Coupel, P., Grelaud, M., Rost, B., Rickaby, R.E.M., de Vargas, C., 2011. Sensitivity of coccolithophores to carbonate chemistry and ocean acidification. *Nature*, 476, 80–83.
- Belanger, P.E., Streeter, S.S., 1980. Distribution and ecology of benthic foraminifera in the Norwegian-Greenland Sea. *Marine Micropaleontology*, 5, 401–428.
- Bender, H., Hemleben, C., 1988. Constructional aspects in test formation of some agglutinated foraminifera. *Abhandlungen der Geologischen Bundesanstalt*, 41, 13–12.
- Bender, H., 1995. Test structure and classification in agglutinated foraminifera. In: Kaminski, M.A., Geroch, S., Gasinski, M.A. (Eds.), *Proceedings of the Fourth International Workshop on Agglutinated Foraminifera*, Vol. 3 (pp. 27–70).
- Berthois, L., Crosnier, A., Le Calvez, Y., 1968. Contribution à l'étude sédimentologique du plateau continental dans la baie de Biafra. *Cahiers, O.R.S.T.O.M., série Océanographie*, 6, 55–86.
- Billett, D.S.M., Bett, B.J., Rice, A.L., Thurston, M.H., Galeron, J., Sibuet, M., Wolff, G.A., 2001. Long-term change in the megabenthos of the Porcupine Abyssal Plain (NE Atlantic). *Progress in Oceanography*, 50, 325–348.
- Billett, D.S.M., Rice, A.L., 2001. The BENGAL programme: introduction and overview. *Progress in Oceanography*, 50, 13–25.
- Billett, D.S.M., Bett, B.J., Reid, W.D.K., Boorman, B., Priede, I.G., 2010. Long-term change in the abyssal NE Atlantic: The 'Amperima Event' revisited. *Deep-Sea Research Part II—Topical Studies in Oceanography*, 57, 1406–1417.

- Brady, H.B., 1884. Report on the Foraminifera dredged by H.M.S. Challenger during the years 1873–1876: Report of the Scientific Results of the Voyage of H.M.S. Challenger, 1873–1876. *Zoology*, 9, 1–814.
- Byrne, R.H., Mecking, S., Feely, R.A., Liu, X.W., 2010. Direct observations of basin-wide acidification of the North Pacific Ocean. *Geophysical Research Letters*, 37.
- Canals, M., Puig, P., de Madron, X.D., Heussner, S., Palanques, A., Fabres, J., 2006. Flushing submarine canyons. *Nature*, 444, 354–357.
- Caralp, M., Lamy, A., Pujos, M., 1970. Contribution a la connaissance de la distribution bathymetrique des foraminiferes dans le Golfe de Gascogne. *Revista Espanola de Micropaleontologia*, 2, 55–84.
- Carpenter, W.B., 1868. Preliminary report of dredging operations in the seas to the north of the British Isles, caried by Her Majesty's steam-vessel "*Lightning*" by Dr Carpenter and Dr Wyville Thomson. *Proceedings of the Royal Society of London*, 17, 168–197.
- Carpenter, W.B., 1870. Preliminary report of the scientific exploration of the deep sea in H. M. surveying-vessel '*Porcupine*', during the summer of 1869. *Proceedings of the Royal Society of London*, 18, 397–453.
- Cartwright, N.G., Gooday, A.J., Jones, A.R., 1989. The morphology, internal organization, and taxonomic position of *Rhizammina algaeformis* Brady, a large, agglutinated, deep-sea foraminifer. *Journal of Foraminiferal Research*, 19, 115–125.
- Clarke, J., Milligan, R.J., Bailey, D.M., Neat, F.C., 2015. A scientific basis for regulating deep-sea fishing by depth. *Current Biology*, 25, 2597–2597.
- Coles G. P., Ainsworth, N.R., Whatley, R.C., Jones, R.W., 1996. Foraminifera and Ostracoda from Quaternary carbonate mounds associated with gas seepage in the Porcupine Basin, offshore western Ireland. *Revista Espanola de Micropaleontologia*, 28, 113–151.
- Collins, M., Knutti, R., Arblaster, J., Dufresne, J.-L., Fichfet, T., Friedlingstein, P., Gao, X., Gutowski, W.J., Johns, T., Krinner, G., Shongwe, M., Tebaldi, C., Weaver, A.J., Wehne, M., 2013. Long-term climate change: projections, commitments and irreversibility. In: Stocker, T.F., Qin, D., Plattner, G.-K., Tignor, M., Allen, S.K., Boschung, J., Nauels, A., Xia, Y., Bex, V., Midgley, P.M. (Eds.), *Climate Change 2013: The Physical Science Basis. Contribution of Working Group I to the Fifth Assessment Report of the International Panel on Climate Change* (pp. 1029–1136). Cambridge: Cambridge University Press.
- Colom, G., 1950. Estudio de los Foraminiferos de muestras de fondo recogidas entre los cabos Juby y Bojador. *Bolletín del Instituto Espanol de Oceanografía*, 28, 1–55.
- Colom, G., 1952. Foraminiferos de las costas de Galicia: (Campañas del "Xauen" en 1949 y 1950). *Bolletín del Instituto Espanol de Oceanografía*, 51, 1–59.
- Contreras-Rosales, L.A., Koho, K.A., Duijnste, I.A.P., de Stigter, H.C., Garcia, R., Koning, E., Epping, E., 2012. Living deep-sea benthic foraminifera from the Cap de Creus Canyon (western Mediterranean): Faunal-geochemical interactions. *Deep-Sea Research Part I—Oceanographic Research Papers*, 64, 22–42.
- Corliss, B.H., Sun, X., Brown, C.W., Showers, W.J., 2006. Influence of seasonal primary productivity on $\delta^{13}\text{C}$ of North Atlantic deep-sea benthic foraminifera. *Deep-Sea Research Part I—Oceanographic Research Papers*, 53, 740–746.

- Costanza, R., 1999. The ecological, economic, and social importance of the oceans. *Ecological Economics*, 31, 199–213.
- Costello, M.J., Cheung, A., De Hauwere, N., 2010. Surface area and the seabed area, volume, depth, slope, and topographic variation for the world's seas, oceans, and countries. *Environmental Science & Technology*, 44, 8821–8828.
- Cushman, J.A., 1918. The foraminifera of the Atlantic Ocean. Part 1. Astrorhizidae. *Bulletin of the United States National Museum*, 104, 1–111.
- Cushman, J.A., 1920. The foraminifera of the Atlantic Ocean. Part 2. Lituolidae. *Bulletin of the United States National Museum*, 104, 1–111.
- Cushman, J.A., 1922. The foraminifera of the Atlantic Ocean. Part 3. Textulariidae. *Bulletin of the United States National Museum*, 104, 1–149.
- Cushman, J.A., 1923. The foraminifera of the Atlantic Ocean. Part 4. Lagenidae. *Bulletin of the United States National Museum*, 104, 1–228.
- Cushman, J.A., 1931. The foraminifera of the Atlantic Ocean. Part 8. Rotaliidae, Amphisteginidae, Calcarinidae, Cymbaloporetidae, Globorotaliidae, Anomalinidae, Planorbulinidae, Rupertiidae, and Homotremidae. *Bulletin of the United States National Museum*, 104, 1–179.
- Cushman, J.A., Henbest, L.G., 1940. Part 2. Foraminifera. In: Bradley, W.H. (Ed.), *Geology and biology of North Atlantic deep-sea cores between Newfoundland and Ireland* (pp. 35–56).
- Danovaro, R., Snelgrove, P.V.R., Tyler, P., 2014. Challenging the paradigms of deep-sea ecology. *Trends in Ecology & Evolution*, 29, 465–475.
- de Folin, L., 1886. Les *Bathysiphons*; premieres pages d'une monographie du genre. *Actes de la Societe Linneenne de Bordeaux*, 40, 271–289.
- Dorst, S., Schönfeld, J., 2013. Diversity of benthic foraminifera on the shelf and slope of the NE Atlantic: analysis of datasets. *Journal of Foraminiferal Research*, 43, 238–254.
- Dorst, S., Schönfeld, J., 2015. Taxonomic notes on recent benthic foraminiferal species of the family Trochamminidae from the Celtic Sea. *Journal of Foraminiferal Research*, 45, 167–189.
- Douglas, R.G., Woodruff, F., 1981. Deep-sea foraminifera. In: Emiliani, C. (Ed.), *The sea* (pp. 1233–1328). Wiley, New York.
- Duchemin, G., Fontanier, C., Jorissen, F.J., Barras, C., Griveaud, C., 2007. Living small-sized (63–150 µm) foraminifera from mid-shelf to mid-slope environments in the Bay of Biscay. *Journal of Foraminiferal Research*, 37, 12–32.
- Durden, J.M., Bett, B.J., Jones, D.O.B., Huvenne, V.A.I., Ruhl, H.A., 2015. Abyssal hills – hidden source of increased habitat heterogeneity, benthic megafaunal biomass and diversity in the deep sea. *Progress in Oceanography*, 137, 209–218.
- Duros, P., Fontanier, C., Metzger, E., Pusceddu, A., Cesbron, F., de Stigter, H.C., Bianchelli, S., Danovaro, R., Jorissen, F.J., 2011. Live (stained) benthic foraminifera in the Whittard Canyon, Celtic margin (NE Atlantic). *Deep-Sea Research Part I—Oceanographic Research Papers*, 58, 128–146.
- Duros, P., Fontanier, C., de Stigter, H.C., Cesbron, F., Metzger, E., Jorissen, F.J., 2012. Live and dead benthic foraminiferal faunas from Whittard Canyon (NE Atlantic): Focus on taphonomic processes and paleo-environmental applications. *Marine Micropaleontology*, 94–95, 25–44.

- Duros, P., Fontanier, C., Metzger, E., Cesbron, F., Deflandre, B., Schmidt, S., Buscail, R., Zaragosi, S., Kerherve, P., Rigaud, S., Delgard, M.L., Jorissen, F.J., 2013. Live (stained) benthic foraminifera from the Cap-Ferret Canyon (Bay of Biscay, NE Atlantic): A comparison between the canyon axis and the surrounding areas. *Deep-Sea Research Part I—Oceanographic Research Papers*, 74, 98–114.
- Duros, P., Jorissen, F.J., Cesbron, F., Zaragosi, S., Schmidt, S., Metzger, E., Fontanier, C., 2014. Benthic foraminiferal thanatocoenoses from the Cap-Ferret Canyon area (NE Atlantic): A complex interplay between hydro-sedimentary and biological processes. *Deep-Sea Research Part I—Topical Studies in Oceanography*, 104, 145–163.
- Eardly, D.F., Carton, M.W., Gallagher, J.M., Patching, J.W., 2001. Bacterial abundance and activity in deep-sea sediments from the eastern North Atlantic. *Progress in Oceanography*, 50, 245–259.
- Earland, A., 1933. Foraminifera. Part II. South Georgia. *Discovery Reports*, Vol. 7 (pp. 27–138).
- Earland, A., 1934. Foraminifera. Part III. The Falklands sector of the Antarctic (excluding South Georgia). *Discovery Reports*, Vol. 10 (pp. 1–208).
- Earland, A., 1936. Foraminifera. Part IV. Additional records from the Weddel Sea sector from material obtained by the S.Y. 'Scotia'. *Discovery Reports*, Vol. 10 (pp. 1–76).
- Enge, A.J., Kucera, M., Heinz, P., 2012. Diversity and microhabitats of living benthic foraminifera in the abyssal Northeast Pacific. *Marine Micropaleontology*, 96–97, 84–104.
- Ernst, S., van der Zwaan, B., 2004. Effects of experimentally induced raised levels of organic flux and oxygen depletion on a continental slope benthic foraminiferal community. *Deep-Sea Research Part I—Oceanographic Research Papers*, 51, 1709–1739.
- Flint, J.M., 1899. Recent foraminifera. A descriptive catalogue of specimens dredged by the U.S. Fish Commission steamer Albatross. *Report of the United States National Museum for 1897* (pp. 249–349).
- Fontanier, C., Jorissen, F.J., Licari, L., Alexandre, A., Anschutz, P., Carbonel, P., 2002. Live benthic foraminiferal faunas from the Bay of Biscay: faunal density, composition, and microhabitats. *Deep-Sea Research Part I—Oceanographic Research Papers*, 49, 751–785.
- Fontanier, C., Jorissen, F., Chaillou, G., David, C., Anschutz, P., Lafon, V., 2003. Seasonal and interannual variability of benthic foraminiferal faunas at 550m depth in the Bay of Biscay. *Deep-Sea Research Part I—Oceanographic Research Papers*, 50, 457–494.
- Fontanier, C., Jorissen, F.J., Chaillou, G., Anschutz, P., Gremare, A., Griveaud, C., 2005. Live foraminiferal faunas from a 2800 m deep lower canyon station from the Bay of Biscay: Faunal response to focusing of refractory organic matter. *Deep-Sea Research Part I—Oceanographic Research Papers*, 52, 1189–1227.
- Fontanier, C., Jorissen, F., Geslin, E., Zaragosi, S., Duchemin, G., Laversin, M., Gaultier, M., 2008a. Live and dead foraminiferal faunas from Saint-Tropez Canyon (Bay of Fréjus): Observations based on in situ and incubated cores. *Journal of Foraminiferal Research*, 38, 137–156.
- Fontanier, C., Jorissen, F.J., Lansard, B., Mouret, A., Buscail, R., Schmidt, S., Kerherve, P., Buron, F., Zaragosi, S., Hunault, G., Ernoult, E., Artero, C., Anschutz, P., Rabouille, C., 2008b. Live foraminifera from the open slope between Grand Rhône and Petit Rhône Canyons (Gulf of

- Lions, NW Mediterranean). *Deep-Sea Research Part I—Oceanographic Research Papers*, 55, 1532–1553.
- Fontanier, C., Jorissen, F.J., Michel, E., Cortijo, E., Vidal, L., Anschutz, P., 2008c. Stable oxygen and carbon isotopes of live (stained) benthic foraminifera from Cap-Ferret Canyon (Bay of Biscay). *Journal of Foraminiferal Research*, 38, 39–51.
- Fontanier, C., Fabri, M.C., Buscail, R., Biscara, L., Koho, K., Reichart, G.J., Cossa, D., Galaup, S., Chabaud, G., Pigot, L., 2012. Deep-sea foraminifera from the Cassidaigne Canyon (NW Mediterranean): Assessing the environmental impact of bauxite red mud disposal. *Marine pollution bulletin*, 64, 1895–1910.
- Gage, J.D., Tyler, P.A., 1991. *Deep-sea biology: a natural history of organisms at the deep-sea floor*. Cambridge University Press.
- Galeron, J., Sibuet, M., Vanreusel, A., Mackenzie, K., Gooday, A.J., Dinet, A., Wolff, G.A., 2001. Temporal patterns among meiofauna and macrofauna taxa related to changes in sediment geochemistry at an abyssal NE Atlantic site. *Progress in Oceanography*, 50, 303–324.
- Galil, B.S., Golik, A., Turkay, M., 1995. Litter at the bottom of the sea: a seabed survey in the eastern Mediterranean. *Marine pollution bulletin*, 30, 22–24.
- Glover, A.G., Smith, C.R., Paterson, G.L.J., Wilson, G.D.F., Hawkins, L., Shearer, M., 2002. Polychaete species diversity in the central Pacific abyss: local and regional patterns, and relationships with productivity. *Marine Ecology Progress Series*, 240, 157–169.
- Glover, A.G., Gooday, A.J., Bailey, D.M., Billett, D.S.M., Chevaldonne, P., Colaco, A., Copley, J., Cuvelier, D., Desbruyeres, D., Kalogeropoulou, V., Klages, M., Lampadariou, N., Lejeune, C., Mestre, N.C., Paterson, G.L.J., Perez, T., Ruhl, H., Sarrazin, J., Soltwedel, T., Soto, E.H., Thatje, S., Tselepidis, A., Van Gaever, S., Vanreusel, A., 2010. Temporal change in deep-sea benthic ecosystems: a review of the evidence from recent time-series studies. *Advances in Marine Biology*, 58, 1–95.
- Goldstein, S.T., 1999. Foraminifera: a biological overview. In: Sen Gupta, B.K. (Ed.), *Benthic foraminiferal microhabitats below the sediment-water interface* (pp. 37–56). Dordrecht: Kluwer Academic Publishers.
- Gooday, A.J., 1983. *Bathysiphon rusticus* de Folin, 1886 and *Bathysiphon folini* n. sp.: two large agglutinated foraminifera abundant in abyssal NE Atlantic epibenthic sledge samples. *Journal of Foraminiferal Research*, 13, 262–276.
- Gooday, A.J., Cook, P.L., 1984. An association between komokiacean foraminifera (Protozoa) and paludicelline ctenostomes (Bryozoa) from the abyssal Northeast Atlantic. *Journal of Natural History*, 18, 765–784.
- Gooday, A.J., 1986a. Meiofaunal foraminiferans from the bathyal Porcupine Seabight (northeast Atlantic): size structure, standing stock, taxonomic composition, species-diversity and vertical-distribution in the sediment. *Deep Sea Research Part A—Oceanographic Research Papers*, 33, 1345–1373.
- Gooday, A.J., 1986b. Soft-shelled foraminifera in meiofaunal samples from the bathyal northeast Atlantic. *Sarsia*, 71, 275–287.
- Gooday, A.J., 1988a. A response by benthic foraminifera to the deposition of phytodetritus in the deep sea. *Nature*, 332, 70–73.

- Gooday, A.J., 1988b. The genus *Bathysiphon* (Protista, Foraminiferida) in the north-east Atlantic: a neotype for *B. filiformis* G.O. & M. Sars, 1872 and the description of a new species. *Journal of Natural History*, 22, 95–105.
- Gooday, A.J., 1988c. The genus *Bathysiphon* (Protista, Foraminiferida) in the NE Atlantic: revision of some species described by de Folin (1886). *Journal of Natural History*, 22, 71–93.
- Gooday, A.J., Lamshead, P.J.D., 1989. Influence of seasonally deposited phytodetritus on benthic foraminiferal populations in the bathyal northeast Atlantic: the species response. *Marine Ecology Progress Series*, 58, 53–67.
- Gooday, A.J., 1990. Recent deep-sea agglutinated foraminifera: a brief review. *Paleoecology, Biostratigraphy, Paleoceanography and Taxonomy of Agglutinated Foraminifera*, 327, 271–304.
- Gooday, A.J., Turley, C.M., Allen, J.A., 1990. Responses by benthic organisms to inputs of organic material to the ocean floor: a review. *Philosophical Transactions of the Royal Society A—Mathematical Physical and Engineering Sciences*, 331, 119–138.
- Gooday, A.J., 1991. Xenophyophores (Protista, Rhizopoda) in box-core samples from the Abyssal northeast Atlantic Ocean (BIOTRANS Area): their taxonomy, morphology, and ecology. *Journal of Foraminiferal Research*, 21, 197–212.
- Gooday, A.J., Carstens, M., Thiel, H., 1995. Microforaminifera and nanoforaminifera from abyssal northeast Atlantic sediments: a preliminary report. *Internationale Revue Der Gesamten Hydrobiologie*, 80, 361–383.
- Gooday, A.J., 1996. Epifaunal and shallow infaunal foraminiferal communities at three abyssal NE Atlantic sites subject to differing phytodetritus input regimes. *Deep-Sea Research Part I—Oceanographic Research Papers*, 43, 1395–1421.
- Gooday, A.J., Bett, B.J., Shires, R., Lamshead, P.J.D., 1998. Deep-sea benthic foraminiferal species diversity in the NE Atlantic and NW Arabian sea: a synthesis. *Deep-Sea Research Part II—Topical Studies in Oceanography*, 45, 165–201.
- Gooday, A.J., Bernhard, J.M., Levin, L.A., Suhr, S.B., 2000. Foraminifera in the Arabian Sea oxygen minimum zone and other oxygen-deficient settings: taxonomic composition, diversity, and relation to metazoan faunas. *Deep-Sea Research Part II—Topical Studies in Oceanography*, 47, 25–54.
- Gooday, A.J., 2002. Biological responses to seasonally varying fluxes of organic matter to the ocean floor: a review. *Journal of Oceanography*, 58, 305–332.
- Gooday, A.J., Hughes, J.A., 2002. Foraminifera associated with phytodetritus deposits at a bathyal site in the northern Rockall Trough (NE Atlantic): seasonal contrasts and a comparison of stained and dead assemblages. *Marine Micropaleontology*, 46, 83–110.
- Gooday, A.J., Hori, S., Todo, Y., Okamoto, T., Kitazato, H., Sabbatini, A., 2004. Soft-walled, monothalamous benthic foraminiferans in the Pacific, Indian and Atlantic Oceans: aspects of biodiversity and biogeography. *Deep-Sea Research Part I—Oceanographic Research Papers*, 51, 33–53.
- Gooday, A.J., da Silva, A.A., Koho, K.A., Lecroq, B., Pearce, R.B., 2010a. The 'mica sandwich'; a remarkable new genus of Foraminifera (Protista, Rhizaria) from the Nazaré Canyon (Portuguese margin, NE Atlantic). *Micropaleontology*, 56, 345–357.

- Gooday, A.J., Malzone, M.G., Bett, B.J., Lamont, P.A., 2010b. Decadal-scale changes in shallow-infaunal foraminiferal assemblages at the Porcupine Abyssal Plain, NE Atlantic. *Deep-Sea Research Part II—Topical Studies in Oceanography*, 57, 1362–1382.
- Gooday, A.J., da Silva, A.A., Pawlowski, J., 2011. Xenophyophores (Rhizaria, Foraminifera) from the Nazaré Canyon (Portuguese margin, NE Atlantic). *Deep-Sea Research Part II—Topical Studies in Oceanography*, 58, 2401–2419.
- Gooday, A.J., Goineau, A., Voltski, I., 2015. Abyssal foraminifera attached to polymetallic nodules from the eastern Clarion Clipperton Fracture Zone: a preliminary description and comparison with North Atlantic dropstone assemblages. *Marine Biodiversity*, 391–412.
- Green, W.S., 1889. Report of a deep-sea trawling cruise off the S.W. coast of Ireland, under the direction of Rev. W. Spotswood Green. *Annals and Magazine of Natural History, Series IV*, 4, 409–414.
- Griveaud, C., Jorissen, F., Anschutz, P., 2010. Spatial variability of live benthic foraminiferal faunas on the Portuguese margin. *Micropaleontology*, 56, 297–322.
- Haake, F.-W., 1980. Benthische Foraminiferen in Oberflächen-Sedimenten und Kernen des Ostatlantiks vor Senegal/Gambia (Westafrika). *Meteor Forschungs Ergebnisse*, 32, 1–29.
- Hansen, H.J., 1999. Shell construction in modern calcareous Foraminifera. In: Sen Gupta, B.K. (Ed.), *Modern Foraminifera* (pp. 57–70). Amsterdam: Elsevier.
- Harris, P.T., Macmillan-Lawler, M., Rupp, J., Baker, E.K., 2014. Geomorphology of the oceans. *Marine Geology*, 352, 4–24.
- Heinz, P., Ruepp, D., Hemleben, C., 2004. Benthic foraminifera assemblages at great meteor seamount. *Marine Biology*, 144, 985–998.
- Heron-Allen, E., Earland, A., 1913. On some foraminifera from the North Sea, etc, dredged by the Fisheries cruiser 'Goldseeker' (International North Sea Investigations—Scotland). II. On the distribution of *Saccamina sphaerica* (M. Sars) and *Psammosphaera fusca* (Schulze) in the North Sea: particularly with reference to the suggested identity of the two species. *Journal of the Royal Microscopical Society*, 1–26.
- Heron-Allen, E., Earland, A., 1932. Foraminifera. Part I. The ice-free area of the Falkland Islands and adjacent seas. *Discovery Reports*, IV, 291–460.
- Hess, S., Jorissen, F.J., Venet, V., Abu-Zied, R., 2005. Benthic foraminiferal recovery after recent turbidite deposition in Cap Breton Canyon, Bay of Biscay. *Journal of Foraminiferal Research*, 35, 114–129.
- Hess, S., Jorissen, F.J., 2009. Distribution patterns of living benthic foraminifera from Cap Breton canyon, Bay of Biscay: Faunal response to sediment instability. *Deep-Sea Research Part I—Oceanographic Research Papers*, 56, 1555–1578.
- Höfker, J., 1927. *The foraminifera of the Siboga Expedition. Part I. Families Tinoporidae, Rotaliidae, Nummulitidae, Amphisteginidae*. Leiden, Netherlands.
- Höfker, J., 1951. *The foraminifera of the Siboga Expedition. Part III*. Leiden, Netherlands.
- Hughes, J.A., Gooday, A.J., Murray, J.W., 2000. Distribution of live benthic Foraminifera at three oceanographically dissimilar sites in the northeast Atlantic: preliminary results. *Hydrobiologia*, 440, 227–238.

- Hughes, J.A., Gooday, A.J., 2004. Associations between living benthic foraminifera and dead tests of *Syringammina fragilissima* (Xenophyophorea) in the Darwin Mounds region (NE Atlantic). *Deep-Sea Research Part I–Oceanographic Research Papers*, 51, 1741–1758.
- Jacobs, D.K., Lindberg, D.R., 1998. Oxygen and evolutionary patterns in the sea: Onshore/offshore trends and recent recruitment of deep-sea faunas. *Proc Natl Acad Sci U S A*, 95, 9396–9401.
- Jones, D.O.B., Yool, A., Wei, C.L., Henson, S.A., Ruhl, H.A., Watson, R.A., Gehlen, M., 2014. Global reductions in seafloor biomass in response to climate change. *Global Change Biology*, 20, 1861–1872.
- Jones, R.W., 2013. *Foraminifera and their applications*. Cambridge, UK: Cambridge University Press.
- Jorissen, F.J., Fontanier, C., Thomas, E., 2007. Paleoceanographical proxies based on deep-sea benthic foraminiferal assemblage characteristics. In: Hillaire-Marcel, C., de Vernal, A. (Eds.), *Proxies in Late Cenozoic Paleoceanography: Pt. 2: Biological tracers and biomarkers* (pp. 263–326).
- Kahn, A.S., Ruhl, H.A., Smith, K.L., 2012. Temporal changes in deep-sea sponge populations are correlated to changes in surface climate and food supply. *Deep-Sea Research Part I–Oceanographic Research Papers*, 70, 36–41.
- Kalogeropoulou, V., Bett, B.J., Gooday, A.J., Lampadariou, N., Arbizu, P.M., Vanreusel, A., 2010. Temporal changes (1989–1999) in deep-sea metazoan meiofaunal assemblages on the Porcupine Abyssal Plain, NE Atlantic. *Deep-Sea Research Part II–Topical Studies in Oceanography*, 57, 1383–1395.
- Kerr, R.A., 1980. A new kind of storm beneath the sea. *Science*, 208, 484–486.
- Klein, H., Mittelstaedt, E., 1992. Currents and dispersion in the abyssal northeast Atlantic. Results from the NOAMP field program. *Deep-Sea Research Part I–Oceanographic Research Papers*, 39, 1727–1745.
- Koho, K.A., Kouwenhoven, J., de Stigter, H.C., van der Zwaan, G.J., 2007. Benthic foraminifera in the Nazaré Canyon, Portuguese continental margin: Sedimentary environments and disturbance. *Marine Micropaleontology*, 66, 27–51.
- Koho, K.A., Garcia, R., de Stigter, H.C., Epping, E., Koning, E., Kouwenhoven, T.J., van Der Zwaan, G.J., 2008a. Sedimentary labile organic carbon and pore water redox control on species distribution of benthic foraminifera: A case study from Lisbon-Setubal Canyon (southern Portugal). *Progress in Oceanography*, 79, 55–82.
- Koho, K.A., Langezaal, A.M., van Lith, Y.A., Duijnste, I.A.P., van der Zwaan, G.J., 2008b. The influence of a simulated diatom bloom on deep-sea benthic foraminifera and the activity of bacteria: A mesocosm study. *Deep-Sea Research Part I–Oceanographic Research Papers*, 55, 696–719.
- Laguionie-Marchais, C., Billett, D.S.M., Paterson, G.L.D., Ruhl, H.A., Soto, E.H., Smith, K.L., Thatje, S., 2013. Inter-annual dynamics of abyssal polychaete communities in the North East Pacific and North East Atlantic–A family-level study. *Deep-Sea Research Part I–Oceanographic Research Papers*, 75, 175–186.

- Lamshead, P.J.D., Gooday, A.J., 1990. The impact of seasonally deposited phytodetritus on epifaunal and shallow infaunal benthic foraminiferal populations in the bathyal northeast Atlantic: the assemblage response. *Deep-Sea Research Part A–Oceanographic Research Papers*, 37, 1263–1283.
- Le Calvez, Y., 1972. Etude ecologique de quelques foraminifères de la cote saharienne de l'Atlantique. *Revue des Travaux de l'Institut des Pêches Maritimes*, 36, 245–254.
- Lecroq, B., Lejzerowicz, F., Bachar, D., Christen, R., Esling, P., Baerlocher, L., Osteras, M., Farinelli, L., Pawlowski, J., 2011. Ultra-deep sequencing of foraminiferal microbarcodes unveils hidden richness of early monothalamous lineages in deep-sea sediments. *Proc Natl Acad Sci U S A*, 108, 13177–13182.
- Leidy, J., 1879. Freshwater rhizopods of North America. *United States Geological Survey of the Territories*, 12, 1–324.
- Lejzerowicz, F., Esling, P., Pawlowski, J., 2014. Patchiness of deep-sea benthic Foraminifera across the Southern Ocean: Insights from high-throughput DNA sequencing. *Deep-Sea Research Part II–Topical Studies in Oceanography*, 108, 17–26.
- Levin, L.A., Le Bris, N., 2015. The deep ocean under climate change. *Science*, 350, 766–768.
- Lévy, A., Mathieu, R., Poignant, A., Rosset-Moulinier, M., Rouvillois, A., 1982. Foraminifères benthiques actuels de sédiments profonds du golfe de Guinée. *Cahiers de Micropaleontologie*, 123–133.
- Loeblich, A.R., Tappan, H., 1987. *Foraminiferal genera and their classification*. New York: Van Nostrand Reinhold.
- Lukashina, N.P., 1988a. Benthic foraminifera communities and water masses of the North Atlantic and the Norway-Greenland Basin. *Oceanology*, 28, 612–617.
- Lukashina, N.P., 1988b. Distribution patterns of benthic foraminifera in the North Atlantic. *Oceanology*, 28, 492–497.
- Mackensen, A., Sejrup, H.P., Jansen, E., 1985. The distribution of living benthic foraminifera on the continental slope and rise off Southwest Norway. *Marine Micropaleontology*, 9, 275–306.
- Margreth, S., Ruggeberg, A., Spezzaferri, S., 2009. Benthic foraminifera as bioindicator for cold-water coral reef ecosystems along the Irish margin. *Deep-Sea Research Part I–Oceanographic Research Papers*, 56, 2216–2234.
- Marie, P., 1946. Sur la faune des foraminifères des îles atlantides et sur quelques récoltes du S/S "Talisman" (Campagne de 1883). In: Lechevalier, P. (Ed.), *Contribution à l'étude du peuplement des îles Atlantides*, Vol. 8 (pp. 295–324). Paris.
- Masson, D.G., 1996. Catastrophic collapse of the volcanic island of Hierro 15 ka ago and the history of landslides in the Canary Islands. *Geology*, 24, 231–234.
- Menzies, R.J., 1965. Conditions for the existence of life on the abyssal sea floor. *Oceanography and Marine Biology: An Annual Review*, 3, 195–210.
- Menzies, R.J., George, R.Y., Rowe, G.T., 1973. *Abyssal environment and ecology of the world oceans*. New York Wiley-Interscience.
- Meyer, J., Riebesell, U., 2015. Reviews and syntheses: responses of coccolithophores to ocean acidification: a meta-analysis. *Biogeosciences*, 12, 1671–1682.

- Milligan, R.J., Morris, K.J., Bett, B.J., Durden, J.M., Jones, D.O.B., Robert, K., Ruhl, H.A., Bailey, D.M., 2016. High resolution study of the spatial distributions of abyssal fishes by autonomous underwater vehicle. *Scientific Reports*, 6, 26095.
- Mojtahid, M., Griveaud, C., Fontanier, C., Anschutz, P., Jorissen, F.J., 2010. Live benthic foraminiferal faunas along a bathymetrical transect (140–4800m) in the Bay of Biscay (NE Atlantic). *Revue de micropaléontologie*, 53, 139–162.
- Mora, C., Wei, C.-L., Rollo, A., Amaro, T., Baco, A.R., Billett, D., Bopp, L., Chen, Q., Collier, M., Danovaro, R., 2013. Biotic and human vulnerability to projected changes in ocean biogeochemistry over the 21st century. *PLoS biology*, 11, e1001682.
- Morigi, C., Sabbatini, A., Vitale, G., Pancotti, I., Gooday, A.J., Duineveld, G.C.A., De Stigter, H.C., Danovaro, R., Negri, A., 2012. Foraminiferal biodiversity associated with cold-water coral carbonate mounds and open slope of SE Rockall Bank (Irish continental margin-NE Atlantic). *Deep-Sea Research Part I—Oceanographic Research Papers*, 59, 54–71.
- Murray, J.W., 1970. Foraminifers of the western approaches to the English Channel. *Micropaleontology*, 16, 471–485.
- Murray, J.W., Taplin, C.M., 1984. The WB Carpenter collection of foraminifera: a catalogue. *Journal of Micropalaeontology*, 3, 55–58.
- Murray, J.W., 1991. *Ecology and palaeoecology of benthic foraminifera*. New York: Longman Scientific & Technical.
- Murray, J.W., Alve, E., 1994. High diversity agglutinated foraminiferal assemblages from the NE Atlantic: dissolution experiments. In: Sejrup, H.P., Knudsen, K.L. (Eds.), *Late Cenozoic benthic foraminifera: taxonomy, ecology and stratigraphy* (pp. 33–51).
- Murray, J.W., 2006. *Ecology and applications of benthic foraminifera*. New York: Cambridge University Press.
- Nardelli, M.P., Jorissen, F.J., Pusceddu, A., Morigi, C., Dell'Anno, A., Danovaro, R., De Stigter, H.C., Negri, A., 2010. Living benthic foraminiferal assemblages along a latitudinal transect at 1000m depth off the Portuguese margin. *Micropaleontology*, 56, 323–344.
- Nozawa, F., Kitazato, H., Tsuchiya, M., Gooday, A.J., 2006. 'Live' benthic foraminifera at an abyssal site in the equatorial Pacific nodule province: Abundance, diversity and taxonomic composition. *Deep-Sea Research Part I—Oceanographic Research Papers*, 53, 1406–1422.
- Panieri, G., 2005. Benthic foraminifera associated with a hydrocarbon seep in the Rockall Trough (NE Atlantic). *Geobios*, 38, 247–255.
- Parker, W.K., Jones, T.R., 1865. On some foraminifera of the North Atlantic and Arctic Oceans during Davis Strait and Baffins Bay. *Philosophical Transactions of the Royal Society*, 155, 325–441.
- Pawlowski, J., Christen, R., Lecroq, B., Bachar, D., Shahbazkia, H.R., Amaral-Zettler, L., Guillou, L., 2011. Eukaryotic richness in the abyss: insights from pyrotag sequencing. *Plos One*, 6.
- Phleger, F.B., Parker, F.L., 1953. North Atlantic Foraminifera. *Reports of the Swedish Deep-Sea Expedition*, Vol. VI (pp. 1–122).
- Priede, I.G., Froese, R., 2013. Colonization of the deep sea by fishes. *Journal of fish Biology*, 83, 1528–1550.

- Puig, P., Ogston, A.S., Mullenbach, B.L., Nittrouer, C.A., Sternberg, R.W., 2003. Shelf-to-canyon sediment-transport processes on the Eel continental margin (northern California). *Marine Geology*, 193, 129–149.
- Puig, P., Canals, M., Company, J.B., Martin, J., Amblas, D., Lastras, G., Palanques, A., Calafat, A.M., 2012. Ploughing the deep sea floor. *Nature*, 489, 286–289.
- Pujos-Lamy, A., 1973. Repartition bathymetrique des foraminiferes benthiques profonds du Golfe de Gascogne. Comparaison avec d'autres aires oceaniques. *Revista Espanola de Micropaleontologia*, 5, 213–234.
- Ramirez-Llodra, E., Brandt, A., Danovaro, R., De Mol, B., Escobar, E., German, C.R., Levin, L.A., Martinez Arbizu, P., Menot, L., Buhl-Mortensen, P., Narayanaswamy, B.E., Smith, C.R., Tittensor, D.P., Tyler, P.A., Vanreusel, A., Vecchione, M., 2010. Deep, diverse and definitely different: unique attributes of the world's largest ecosystem. *Biogeosciences*, 7, 2851–2899.
- Ramirez-Llodra, E., Tyler, P.A., Baker, M.C., Bergstad, O.A., Clark, M.R., Escobar, E., Levin, L.A., Menot, L., Rowden, A.A., Smith, C.R., Van Dover, C.L., 2011. Man and the last great wilderness: human impact on the deep sea. *Plos One*, 6.
- Ramirez-Llodra, E., Trannum, H.C., Evenset, A., Levin, L.A., Andersson, M., Finne, T.E., Hilario, A., Flem, B., Christensen, G., Schaanning, M., Vanreusel, A., 2015. Submarine and deep-sea mine tailing placements: A review of current practices, environmental issues, natural analogs and knowledge gaps in Norway and internationally. *Marine pollution bulletin*, 97, 13–35.
- Rex, M.A., Etter, R.J., 2010. *Deep-sea biodiversity: pattern and scale*. Cambridge: Harvard University Press.
- Rhumbler, L., 1913. Die Foraminifere (Thalamophoren) der Plankton-Expedition. Teil II - Systematik: Arrhabdammidia, Arammodisclidia und Arnodosammidia. *Ergebnisse der Plankton-Expedition der Humboldt-Stiftung*, 3, 332–476.
- Rice, A.L., 1980. The beginnings of French oceanography: the cruise of the "Travailleur", July 1880. *Oceanologica Acta*, 3, 266–266.
- Rice, A.L., 1986. *British Oceanographic Vessel 1800–1950*. London: The Ray Society.
- Rice, A.L., Thurston, M.H., Bett, B.J., 1994. The IOSDL DEEPSEAS Program: introduction and photographic evidence for the presence and absence of a seasonal input of phytodetritus at contrasting abyssal sites in the northeastern Atlantic. *Deep-Sea Research Part I – Oceanographic Research Papers*, 41, 1305–1320.
- Rogers, A., Brierley, A., Croot, P., Cunha, M., Danovaro, R., Devey, C., Hoel, A., Ruhl, H., Sarradin, P.-M., Trevisanut, S., van den Hove, S., Vieira, H., Visbeck, M., Ostend., 2015. Delving Deeper: Critical challenges for 21st century deep-sea research. In: Larkin, K.E., Donaldson, K., McDonough, N. (Eds.), *Position Paper 22 of the European Marine Board* (p. 224). Ostend, Belgium.
- Rüggeberg, A., Dullo, C., Dorschel, B., Hebbeln, D., 2007. Environmental changes and growth history of a cold-water carbonate mound (Propeller Mound, Porcupine Seabight). *International Journal of Earth Sciences*, 96, 57–72.

- Ruggiero, M.A., Gordon, D.P., Orrell, T.M., Bailly, N., Bourgoïn, T., Brusca, R.C., Cavalier-Smith, T., Guiry, M.D., Kirk, P.M., 2015. A higher level classification of all living organisms. *Plos One*, 10, 1–60.
- Ruhl, H.A., Ellena, J.A., Smith, K.L., Jr., 2008. Connections between climate, food limitation, and carbon cycling in abyssal sediment communities. *Proceedings of the National Academy of Sciences*, 105, 17006–17011.
- Saidova, K.M., 2008. Benthic foraminifera communities of the Andaman Sea (Indian Ocean). *Oceanology*, 48, 517–523.
- Sars, G.O., 1872. Undersögelser over Hardangerfjordens Fauna. *Forhandlinger i Videnskabselskabet i Kristiania för 1871* (pp. 246–255).
- Sars, M., 1869. Fortsatte Bemaerkninger over det dyriske liys Udbredning i havets dybder. *Forhandlinger i Videnskabselskabet i Kristiania för 1868* (pp. 246–275).
- Schönfeld, J., 1997. The impact of the Mediterranean Outflow Water (MOW) on benthic foraminiferal assemblages and surface sediments at the southern Portuguese continental margin. *Marine Micropaleontology*, 29, 211–236.
- Schönfeld, J., 2002. A new benthic foraminiferal proxy for near-bottom current velocities in the Gulf of Cadiz, northeastern Atlantic Ocean. *Deep-Sea Research Part I—Oceanographic Research Papers*, 49, 1853–1875.
- Schönfeld, J., Dullo, W.C., Pfannkuche, O., Freiwald, A., Rüggeberg, A., Schmidt, S., Weston, J., 2011. Recent benthic foraminiferal assemblages from cold-water coral mounds in the Porcupine Seabight. *Facies*, 57, 187–213.
- Schönfeld, J., Alve, E., Geslin, E., Jorissen, F., Korsun, S., Spezzaferri, S., 2012. The FOBIMO (FORaminiferal Blo-MONitoring) initiative-towards a standardised protocol for soft-bottom benthic foraminiferal monitoring studies. *Marine Micropaleontology*, 94–95, 1–13.
- Schott, W., 1935. Die Foraminiferen in den Äquatorialen Teil des Atlantisches Ozeans. *Deutsche Atlantische Expedition*, 6, 411–616.
- Schott, W., 1966. Foraminiferen fauna und Stretigraphie der Tiefsee sediment im Nordatlantischen Ozean. *Report Swedish Deep-Sea Research Expedition*, Vol. VII (pp. 357–469).
- Seiler, W.C., 1974. Tiefenverteilung benthischer Foraminiferen am portugiesischen Kontinentalhang. *Meteor Forschungs Ergebnisse*, 23, 47–94.
- Sen Gupta, B.K., 1999. Systematics of modern foraminifera. In: Sen Gupta, B.K. (Ed.), *Modern foraminifera* (pp. 7–36). Amsterdam: Elsevier.
- Shires, R., Gooday, A.J., Jones, A.R., 1994a. The morphology and ecology of an abundant new komokiacean mudball (Komokiacea, Foraminiferida) from the bathyal and abyssal NE Atlantic. *Journal of Foraminiferal Research*, 24, 214–225.
- Shires, R., Gooday, A.J., Jones, A.R., 1994b. A new large agglutinated foraminifer (Arboramminidae n. fam.) from an oligotrophic site in the abyssal northeast Atlantic. *Journal of Foraminiferal Research*, 24, 149–157.
- Sierra, R., Matz, M.V., Aglyamova, G., Pillet, L., Decelle, J., Not, F., de Vargas, C., Pawlowski, J., 2013. Deep relationships of Rhizaria revealed by phylogenomics: A farewell to Haeckel's Radiolaria. *Molecular Phylogenetics and Evolution*, 67, 53–59.

- Smart, C.W., Gooday, A.J., 1997. Recent benthic foraminifera in the abyssal northeast Atlantic Ocean: relation to phytodetrital inputs. *Journal of Foraminiferal Research*, 27, 85–92.
- Smith, C.R., De Leo, F.C., Bernardino, A.F., Sweetman, A.K., Arbizu, P.M., 2008. Abyssal food limitation, ecosystem structure and climate change. *Trends in Ecology and Evolution*, 23, 518–528.
- Smith, K., Baldwin, R., Ruhl, H., Kahru, M., Mitchell, B., Kaufmann, R., 2006. Climate effect on food supply to depths greater than 4,000 meters in the northeast Pacific. *Limnology and Oceanography*, 51, 166–176.
- Smith, K.L., Ruhl, H.A., Bett, B.J., Billett, D.S., Lampitt, R.S., Kaufmann, R.S., 2009. Climate, carbon cycling, and deep-ocean ecosystems. *Proceedings of the National Academy of Sciences*, 106, 19211–19218.
- Snider, L.J., Burnett, B.R., Hessler, R.R., 1984. The composition and distribution of meiofauna and nanobiota in a central North Pacific deep-sea area. *Deep-Sea Research Part I—Oceanographic Research Papers*, 31, 1225–1249.
- Soto, E.H., Paterson, G.L.J., Billett, D.S.M., Hawkins, L.E., Galeron, J., Sibuet, M., 2010. Temporal variability in polychaete assemblages of the abyssal NE Atlantic Ocean. *Deep-Sea Research Part II—Topical Studies in Oceanography*, 57, 1396–1405.
- Steinacher, M., Joos, F., Frolicher, T.L., Bopp, L., Cadule, P., Cocco, V., Doney, S.C., Gehlen, M., Lindsay, K., Moore, J.K., Schneider, B., Segschneider, J., 2010. Projected 21st century decrease in marine productivity: a multi-model analysis. *Biogeosciences*, 7, 979–1005.
- Sun, X., Corliss, B.H., Brown, C.W., Showers, W.J., 2006. The effect of primary productivity and seasonality on the distribution of deep-sea benthic foraminifera in the North Atlantic. *Deep-Sea Research Part I—Oceanographic Research Papers*, 53, 28–47.
- Tendal, O.S., Hessler, R.R., 1977. An introduction to the biology and systematics of Komokiacea (Textulariina, Foraminiferida). *Galathea Report*, 14, 165–194.
- Thiel, H., 2003. Anthropogenic impacts on the deep sea. In: Tyler, P.A. (Ed.), *Ecosystems of the World* (pp. 427–472). Amsterdam: Elsevier.
- Thistle, D., Ertman, S.C., Fauchald, K., 1991. The fauna of the HEBBLE site: patterns in standing stock and sediment-dynamic effects. *Marine Geology*, 99, 413–422.
- Thomas, E., Gooday, A.J., 1996. Cenozoic deep-sea benthic foraminifers: Tracers for changes in oceanic productivity? *Geology*, 24, 355–358.
- Thurber, A.R., Sweetman, A.K., Narayanaswamy, B.E., Jones, D.O.B., Ingels, J., Hansman, R.L., 2014. Ecosystem function and services provided by the deep sea. *Biogeosciences*, 11, 3941–3963.
- Turnewitsch, R., Springer, B.M., 2001. Do bottom mixed layers influence ²³⁴Th dynamics in the abyssal near-bottom water column? *Deep-Sea Research Part I—Oceanographic Research Papers*, 48, 1279–1307.
- Tyler, P.A., 1988. Seasonality in the deep sea. *Oceanography and Marine Biology: An Annual Review*, 26, 227–258.
- Tyler, P.A., 1995. Conditions for the existence of life at the deep-sea floor: An update. *Oceanography and Marine Biology: An Annual Review*, 33, 221–244.

- UNESCO, 2009. Global Open Oceans and Deep Seabed (GOODS) – Biogeographic Classification. *IOC Technical Series* (pp. 1–87). Paris, UNESCO-IOC.
- Uthicke, S., Momigliano, P., Fabricius, K.E., 2013. High risk of extinction of benthic foraminifera in this century due to ocean acidification. *Scientific Reports*, 3.
- Vanreusel, A., Cosson-Sarradin, N., Gooday, A.J., Paterson, G.L.J., Galeron, J., Sibuet, M., Vincx, M., 2001. Evidence for episodic recruitment in a small opheliid polychaete species from the abyssal NE Atlantic. *Progress in Oceanography*, 50, 285–301.
- Watling, L., Guinotte, J., Clark, M.R., Smith, C.R., 2013. A proposed biogeography of the deep ocean floor. *Progress in Oceanography*, 111, 91–112.
- Wedding, L.M., Friedlander, A.M., Kittinger, J.N., Watling, L., Gaines, S.D., Bennett, M., Hardy, S.M., Smith, C.R., 2013. From principles to practice: a spatial approach to systematic conservation planning in the deep sea. *Proceedings of the Royal Society B-Biological Sciences*, 280, 1–10.
- Wedding, L.M., Reiter, S.M., Smith, C.R., Gjerde, K.M., Kittinger, J.N., Friedlander, A.M., Gaines, S.D., Clark, M.R., Thurnherr, A.M., Hardy, S.M., Crowder, L.B., 2015. Managing mining of the deep seabed. *Science*, 349, 144–145.
- Wei, C.L., Rowe, G.T., Hubbard, G.F., Scheltema, A.H., Wilson, G.D.F., Petrescu, I., Foster, J.M., Wicksten, M.K., Chen, M., Davenport, R., Soliman, Y., Wang, Y.N., 2010. Bathymetric zonation of deep-sea macrofauna in relation to export of surface phytoplankton production. *Marine Ecology Progress Series*, 399, 1–14.
- Weston, J.F., 1985. Comparison between recent benthic foraminiferal faunas of the Porcupine Seabight and Western Approaches continental slope *Journal of Micropalaeontology*, 4, 165–183.
- Wilding, T.A., 2002. Taxonomy and ecology of *Toxisarcon alba*, sp. nov. from Loch Linnhe, west coast of Scotland, UK. *Journal of Foraminiferal Research*, 32, 358–363.
- Woodall, L.C., Sanchez-Vidal, A., Canals, M., Paterson, G.L.J., Coppock, R., Sleight, V., Calafat, A., Rogers, A.D., Narayanaswamy, B.E., Thompson, R.C., 2014. The deep sea is a major sink for microplastic debris. *Royal Society Open Science*, 1, 1–8.
- Woolley, S.N.C., Tittensor, D.P., Dunstan, P.K., Guillera-Aroita, G., Lahoz-Monfort, J.J., Wintle, B.A., Worm, B., O'Hara, T.D., 2016. Deep-sea diversity patterns are shaped by energy availability. *Nature*, 533, 393–396.
- Wright, J., 1886. First report on the marine fauna of the south-west of Ireland. *Proceedings of the Royal Irish Academy, Series 2*, 4, 607–614.
- Wright, J., 1889. Report of a deep-sea trawling cruise off the south-west coast of Ireland, under the direction of Rev. W. Spotswood Green. *Annals and Magazine of Natural history*, 4, 447–449.
- Wright, J., 1890. Deep-sea trawling off the S.W. coast of Ireland. *Annals and Magazine of Natural History*, 5, 124.
- Yasuhara, M., Hunt, G., Cronin, T.M., Okahashi, H., 2009. Temporal latitudinal-gradient dynamics and tropical instability of deep-sea species diversity. *Proc Natl Acad Sci U S A*, 106, 21717–21720.

Chapter 2: Basal monothalamous and pseudochambered benthic foraminifera associated with planktonic foraminiferal shells and mineral grains from the Porcupine Abyssal Plain, NE Atlantic

Abstract

We present a survey of 'live' (stained) and dead monothalamous (single-chambered, mainly spherical) and pseudochambered (chain-like) foraminifera associated with planktonic foraminiferal shells and mineral grains, based on two samples from one abyssal plain site (P4, 4851 m water depth) and one abyssal hill site (H4, 4365 m water depth) on the Porcupine Abyssal Plain Sustained Observatory (PAP-SO) area, northeast Atlantic. Our study is the first to focus on this poorly known component of abyssal foraminiferal faunas and highlight their abundances and diversity at the PAP-SO. In both samples these monothalamids and pseudochambered forms represented 31–33% and 23–36%, respectively, of the entire live and dead foraminiferal assemblage (>150 μm , 0–1 cm sediment layer). Among 1,112 stained and dead specimens we recognise a total of 18 distinct morphotypes on the basis of test characteristics. Another 144 specimens could not be assigned to any morphotype and are regarded as indeterminate. Most of the monothalamids are small (<150 μm), although some incorporate planktonic foraminiferal shells to create larger structures. In absolute terms, stained and dead individuals of these morphotypes were more abundant at the abyssal hill site, although data from additional samples are needed to confirm if this is representative of differences between abyssal hills and the surrounding abyssal plain at the PAP-SO. Agglutinated spheres and domes similar to some of our abyssal forms have been reported from shelf and slope settings, but they are generally much larger. Small agglutinated spheres are very common in the abyssal Pacific, at depths close to or below the carbonate compensation depth (CCD). However, they are composed largely of siliceous particles, including mineral grains, radiolarians and diatom fragments. In contrast, carbonate oozes at

the PAP-SO, situated above the CCD, are rich in coccoliths and planktonic foraminiferal shells, which are used in the construction of agglutinated spheres and domes. These results underline the important contribution made by largely underestimated foraminiferal taxa to abyssal communities.

2.1 Introduction

Benthic foraminifera are one of the most abundant and species-rich groups in the deep sea, often accounting for >50% of the meiofauna (Gooday, 2014; Snider et al., 1984) and in some areas a large proportion of the macrofauna (Tendal and Hessler, 1977). Diversity and distributional patterns of hard-shelled calcareous and robustly agglutinated forms (mainly multichambered) have been widely documented (Gooday and Jorissen, 2012; Murray, 1991, 2013), but relatively little is known about organic-walled and delicately agglutinated, predominantly monothalamous (single-chambered) species, hereafter termed monothalamids (Pawlowski et al., 2013). Due to their fragile nature these taxa have a poor fossil record (Mackensen et al., 1990; Tappan and Loeblich, 1988) resulting in an incomplete picture of past foraminiferal communities. In modern oceans these delicate species can constitute a dominant element of deep-sea foraminiferal assemblages (Bernstein et al., 1978; Nozawa et al., 2006; Snider et al., 1984; Tendal and Hessler, 1977), particularly at abyssal plains below the carbonate compensation depth (CCD) (Schröder et al., 1988).

Monothalamids encompass a wide variety of organic-walled and agglutinated taxa with spherical, flask-shaped, tubular or more complex test morphologies and in some cases a soft, flexible test wall. Their internal structure is relatively simple and deep-sea species often contain masses of waste pellets, termed stercomata. They represent the basal radiation of foraminifera that gave rise to morphologically diverse groups of multichambered calcareous and agglutinated forms (Pawlowski et al., 2003, 2013). Monothalamids are generally poorly known and usually overlooked in faunal studies of the deep-sea benthos. Many species are undescribed and their often simple morphologies, which lack prominent features, make their identification problematic. Nevertheless, monothalamids are a highly diverse group, often constituting >30% of the total foraminiferal species pool, and are thought to represent a significant undocumented source of biodiversity on the

ocean floor (Enge et al., 2012; Gooday et al., 2004). Recently developed molecular techniques, including ultra-deep sequencing of foraminiferal microbarcodes in environmental DNA samples, have emphasised their dominance (>80%) in deep-sea foraminiferal assemblages (Lecroq et al., 2011).

During the analysis of foraminiferal samples from the Porcupine Abyssal Plain Sustained Observatory (PAP-SO) area in the northeast Atlantic (4850 m water depth), we encountered monothalamids and chain-like agglutinated forms (considered pseudochambered *sensu* Mikhalevich 2005) that were associated with planktonic foraminiferal shells and mineral grains. The vast majority comprised tiny agglutinated spheres and domes (50–150 μm) that formed larger structures (often >300 μm) by incorporating planktonic shells and mineral grains as part of their test or by using these as a substrate. Small trochamminaceans (<100 μm) from the same area are also commonly found on the shells of planktonic foraminifera (Gooday et al., 2010).

Benthic foraminifera attached to hard substrates have been known to science for well over a century (Loeblich and Tappan, 1987). Scientific expeditions in the Southern Ocean and the North Atlantic Ocean reported organic-walled and agglutinated foraminiferal species, some of them monothalamous, that are sessile on a variety of substrates such as stones, molluscan shells, sponge spicules and benthic foraminiferal shells (Earland 1933, 1934, 1936; Heron-Allen and Earland, 1913, 1932). However, most of these studies described attached forms from shelf and the slope settings (sublittoral to upper bathyal) and none of them concern tiny agglutinated foraminifera from the abyssal deep sea.

The purpose of this paper is to: (1) briefly characterise these primitive monothalamids and chain-like taxa from the PAP-SO that live attached to, or are lodged between, planktonic shells or mineral grains; (2) compare them with similar forms found in other ocean basins such as the Pacific; (3) assess their contribution to the abundance and diversity of the entire foraminiferal assemblages at the PAP-SO.

2.2 Materials and Methods

2.2.1 Sample collection and laboratory processing

Two core tube samples (25.5 cm² surface area) were collected during R.S.S. *James Cook* Cruise 062 (JC062) (July-August 2011) at an abyssal plain site (P4; station JC062-77, 4851 m water depth) and a somewhat shallower, abyssal hill site (H4; station JC062-126, 4365 m water depth) within the area of the PAP-SO (Fig. 2.1; Table 2.1). Onboard the ship, the cores were sliced into layers down to 10 cm depth and each slice fixed in 10% buffered formalin. The present work, which is part of a larger study of foraminifera from the PAP-SO, is based on the 0–1 cm sediment layer.

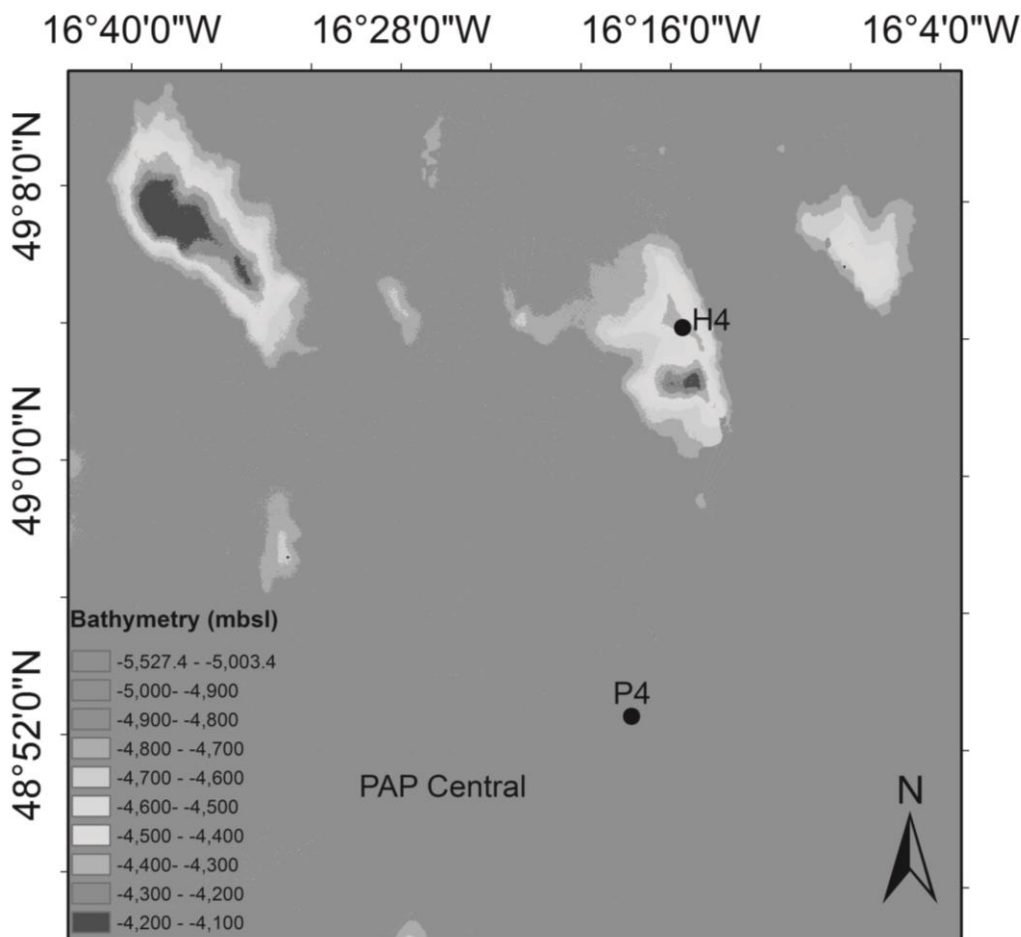


Fig. 2.1. Bathymetry map of the PAP-SO area showing the positions of our two study sites, P4 (abyssal plain site) and H4 (abyssal hill site), in relation to the PAP central site, which is the focus of long-term time-series sampling at the Porcupine Abyssal Plain Sustained Observatory (e.g. Gooday et al. 2010). Bathymetry map of the PAP-SO area showing the positions of our two study sites, P4 (abyssal plain site) and H4 (abyssal hill site), in relation to the PAP central site, which is the focus of long-term time-series sampling at the Porcupine Abyssal Plain Sustained Observatory (e.g. Gooday et al. 2010).

Table 2.1. Locality data.

Station	Date	Latitude (°N)	Longitude (°W)	Depth (m)	Topography
JC062-77	August 2011	48.875	16.293	4851	Abyssal Plain (P4)
JC062-126	August 2011	49.074	16.264	4365	Abyssal Hill (H4)

In the laboratory, the 0–0.5 cm and 0.5–1.0 cm slices of cores from the P4 and H4 sites were gently washed through two sieves (mesh sizes: 300 μm and 150 μm) using filtered tap water. Residues $>300 \mu\text{m}$ and 150–300 μm were stained with Rose Bengal (1 g dissolved in 1 L tap water) overnight and sorted for all ‘live’ (stained) and dead foraminifera in water in a Petri dish under a binocular microscope. In order to ensure that the stained material was foraminiferal protoplasm, specimens were transferred to glass slides with glycerine and examined under a high power compound microscope. Delicate taxa were either stored on glass cavity slides in glycerol or in 2-ml Nalgene cryovials in 10% buffered formalin. The specimens considered in the present chapter were informally assigned to morphotypes (morphologically similar specimens) on the basis of test morphology and wall structure.

2.2.2 Light and scanning electron microscopy

Specimens placed in water in a glass cavity slide were photographed using a NIKON Coolpix 4500 camera mounted on an Olympus SZX10 compound microscope. Selected specimens were dried onto aluminium scanning electron microscopy (SEM) stubs, gold sputter coated and subsequently examined by SEM using a LEO 1450VP (variable pressure) scanning electron microscope.

2.3 Results

2.3.1 Entire benthic foraminiferal assemblages

Densities for the entire live assemblage (i.e. all foraminiferal taxa, multichambered as well as monothalamids, in the 150–300 and $>300\text{-}\mu\text{m}$ fractions combined) were 50 individuals $\times 10 \text{ cm}^{-2}$ at the abyssal plain site (P4) and 79 individuals $\times 10 \text{ cm}^{-2}$ at the abyssal hill site (H4). The corresponding values for the entire dead assemblages were 391 individuals $\times 10 \text{ cm}^{-2}$ (P4) and 1,040 individuals $\times 10 \text{ cm}^{-2}$ (H4). For the monothalamids and pseudo-chambered forms considered here, 42

Table 2.2. Counts (N) of monothalamid and pseudochambered morphotypes, including fragments and indeterminate specimens, from the 0–0.5 cm and 0.5–1 cm sediment layers. Densities (individuals per 10 cm²) are shown in parentheses after the counts per sample. Also shown are their relative abundance (%) amongst the entire ‘Live’ (stained) and Dead assemblage (multichambered and monothalamid taxa) from the two samples (>150- μ m fraction) for the two layers combined (i.e. 0–1 cm). The percentages for the ?Live category represents their proportion among the total number of monothalamids and pseudochambered morphotypes present in the 0–1 cm sediment layer.

	‘Live’ (stained)			Dead			?Live		
	N		%	N		%	N		%
	0–0.5	0.5–1	0–1	0–0.5	0.5–1	0–1	0–0.5	0.5–1	0–1
SL (cm)									
P4	29 (11.4)	13 (5.1)	33.1	340 (133)	16 (6.3)	35.7	22 (8.6)	20 (7.8)	9.6
H4	50 (19.6)	13 (5.1)	31.3	437 (171)	160 (62.7)	22.5	17 (6.7)	139 (54.5)	19.1

?Live unclear whether live or dead, SL sediment layer, P4 abyssal plain, H4 abyssal hill.

live individuals (16.5 individuals \times 10 cm⁻²) were counted at the abyssal plain site (P4) and 63 live individuals (24.7 individuals \times 10 cm⁻²) at the abyssal hill site (H4). The corresponding values for the dead assemblages were 356 individuals (139.3 individuals \times 10 cm⁻²) (P4) and 597 individuals (234.1 individuals \times 10 cm⁻²) (H4).

The majority of the specimens (live and dead) in both sites were concentrated in the 0–0.5 cm sediment layer (Table 2.2). In both samples these two groups represented 31–33% and 23–36% of the live and dead fauna respectively (Table 2.2). In the case of an additional 42 (P4) and 156 (H4) individuals it was impossible to determine using Rose Bengal staining if they were live or dead. These ambiguous specimens represented 10% and 20% of the total number of monothalamids and pseudochambered forms found at the abyssal plain and abyssal hill site, respectively (Table 2.2).

2.3.2 Diversity of monothalamous and pseudochambered foraminifera

Overall, we recognised a total of 18 distinct forms among 1112 monothalamous and pseudochambered foraminifera picked from the samples at the two sites (Table 2.3). None can be placed in a described species. We regard them as morphotypes, although those with consistent, well-defined morphologies are probably distinct species. A further 144 monothalamous specimens could not be

assigned to any morphotype and were regarded indeterminate. They will not be considered further.

Table 2.3. Occurrence of monothalamid and pseudo-chambered morphotypes associated with planktonic foraminiferal shells and mineral grains in PAP-SO samples (>150- μ m fraction).

Morphotypes ^a	Figure	P4 (abyssal plain)			H4 (abyssal hill)		
		L	D	?live	L	D	?live
<i>Monothalamids attached to or lodged between planktonic foraminiferal shells</i>							
1) Thin-walled sphere	2.2a,b	0	0	3	2	0	0
2) Sphere with long flimsy tubes	2.2c,d,e	3	78	8	7	113	1
3) Dome with cap attached to large planktonic foraminiferal shell	2.2f,g,h	1	34	0	7	55	0
4) Delicate thick-walled sphere with red-stained interior	2.3a,b,c,d,e	9	0	0	0	0	0
5) Round, slightly opaque sphere with red-stained interior	2.3f,g,h	1	0	0	1	0	0
6) <i>Crithionina</i> -like sphere	2.3i,j,k	0	5	0	1	7	1
7) 'Classic dome'	2.4a,b,c,d	19	155	12	30	271	25
8) Sphere with short tube	2.4e,f	1	2	0	3	29	0
9) Red sphere with stercomata, between planktonic shells	2.5a,b,c,d,e	5	9	0	5	2	3
10) Thin-walled red sphere attached to large planktonic shell	2.5f,g	1	0	0	3	0	1
11) Soft sphere lodged between two planktonic shells	2.5h	2	0	0	0	4	0
<i>Monothalamids associated with mineral grains</i>							
12) Monothalamids associated with mineral grains	2.6a,b,c	0	4	0	4	90	0
<i>Monothalamids associated with tubes</i>							
13) Spherical chamber with tubes	2.6d,e,f	0	0	0	0	8	0
14) Short, soft-walled tube	2.6g,h,i	0	0	0	0	1	0
<i>Pseudo-chambered (chain-like) forms</i>							
15) Double dome	2.7a,b,c	0	0	0	0	4	0
16) Pseudo-chambers linked with stolons	2.7d,e,f	0	15	0	0	9	0
17) Chain with thick tube	2.7g,h,i	0	1	0	0	0	0
18) Indeterminate chain of chambers	2.7j,k,l	0	53	0	0	4	0
Total		42	356	23	63	597	31

L = 'live' (stained), D = dead, ?Live = unclear whether live or dead

^aThe numbers in this column correspond to those in the text

2.3.2.1 Monothalamids attached to or lodged between planktonic foraminiferal shells

The majority (11) of the 18 forms are soft spheres that are sessile on a planktonic foraminiferal shell or are lodged between two or more planktonic shells. These monothalamous foraminifera exhibit a wide morphological diversity and contain some of the most abundant forms (Table 2.3). They include the following types.

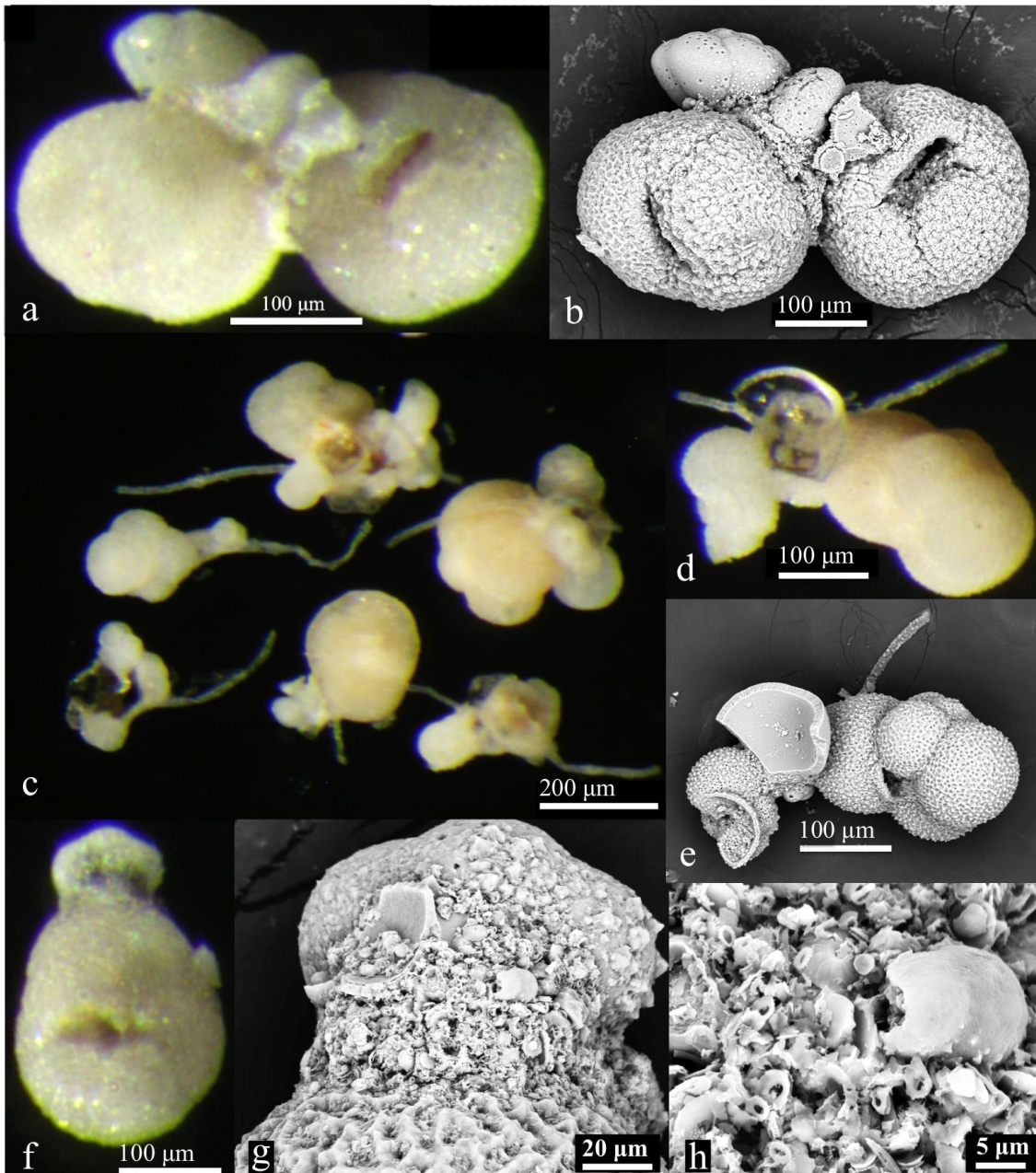


Fig. 2.2. Monothalamids attached to, or lodged between, planktonic foraminiferal shells. Reflected light images (a, c, d, f); SEM images (b, e, g, h). Thin-walled sphere (a, b). Sphere with long flimsy tubes (c–e). Dome with cap attached to large planktonic foraminiferal shell (f–h).

1. *Thin-walled sphere* (Fig. 2.2a, b; Type 1 in Table 2.3). A thin-walled agglutinated sphere (<150 µm in maximum dimension) containing stercomata usually confined between several (>2) planktonic shells.
2. *Sphere with long flimsy tubes* (Fig. 2.2c–e; Type 2 in Table 2.3). Easily recognisable and abundant form with one or more long flimsy tubes extending out of the main, approximately spherical, test. In some cases, the tubes are 2 to 3 times the length of the main test, which is between 100–150 µm in maximum dimension. The specimens are attached to one or more planktonic shells and occasionally incorporate small quartz grains, in which case the

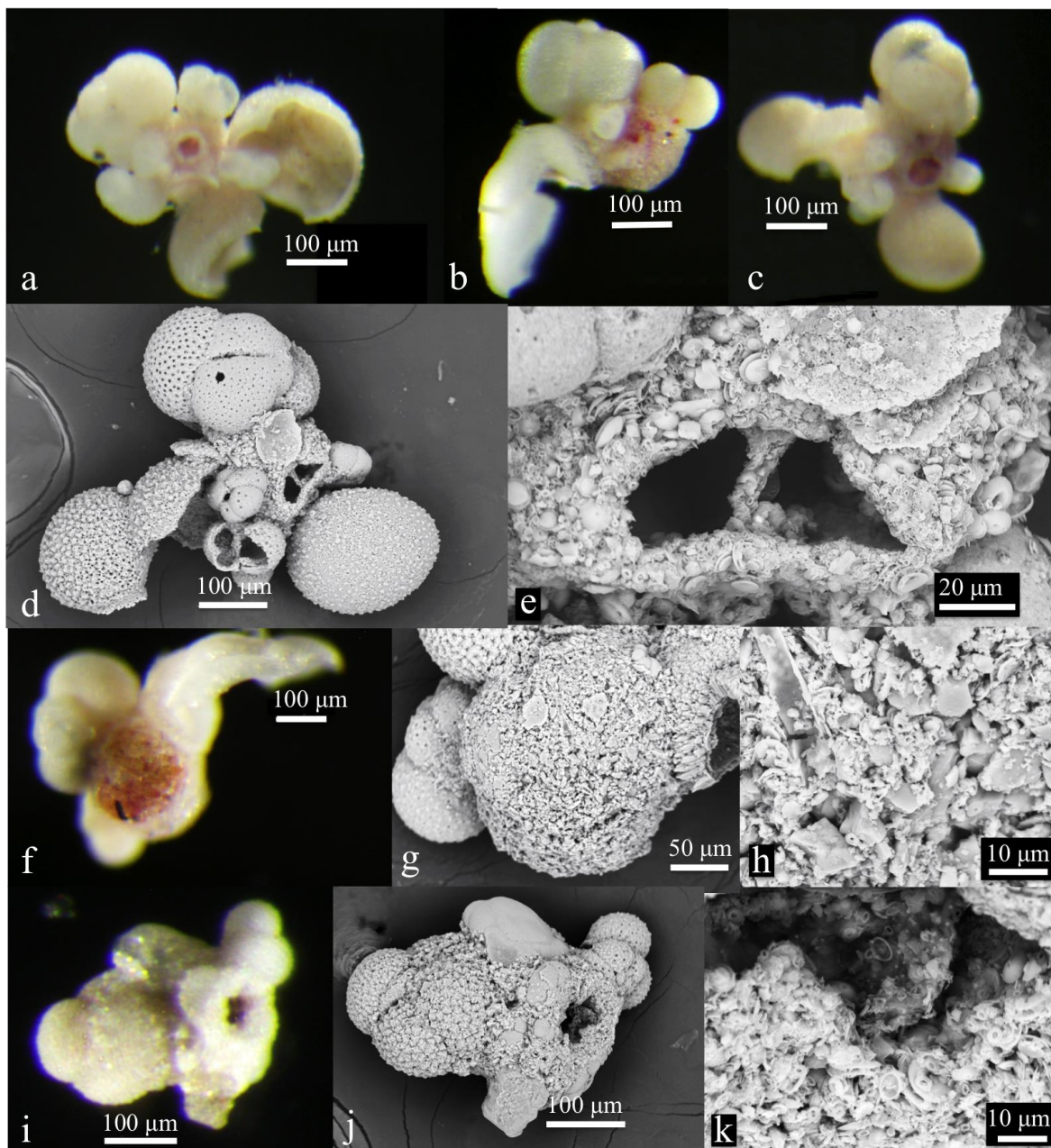


Fig. 2.3. Monothalamids attached to, or lodged between, planktonic foraminiferal shells. Reflected light images (a–c, f, i); SEM images (d, e, g, h, j, k). Delicate thick-walled spheres with red stained interior (a–c); SEM images of the third (c) specimen (d, e). Round, slightly opaque sphere with red stained interior (f–h). *Crithionina*-like sphere (i–k).

specimens are somewhat larger (approx. 200 μm) (Fig. 2.2c).

3. *Dome with cap attached to large planktonic foraminiferal shell* (Fig. 2.2f–h; Type 3 in Table 2.3). A small dome (approx. 100 μm) attached to a large planktonic shell on one side and capped by a much smaller shell on the other side. This simple type is very common in both sites (Table 2.3). The wall is mainly composed of coccoliths (Fig. 2.2h).
4. *Delicate thick-walled sphere with red-stained interior* (Fig. 2.3a–e; Type 4 in Table 2.3). Agglutinated spherical test with red-stained protoplasm,

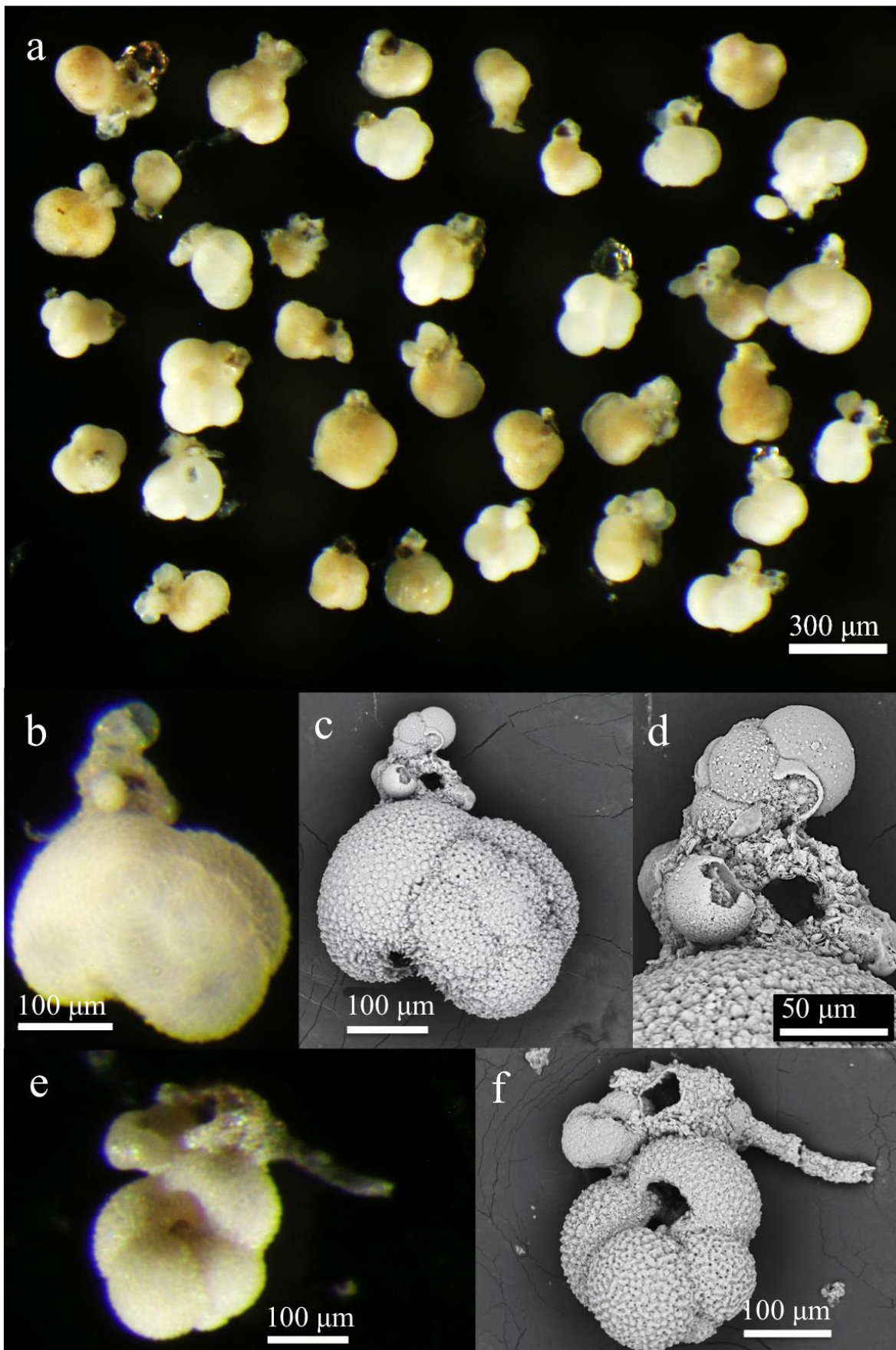


Fig. 2.4. Monothalamids attached to, or lodged between, planktonic foraminiferal shells. Reflected light images (a, b, e); SEM images (c, d, f). 'Classic dome' (a–d). Sphere with short tube (e, f).

containing sparse stercomata. It usually forms a large structure $>300\ \mu\text{m}$ due to the incorporation of several large planktonic shells, although the sphere itself is never more than $100\ \mu\text{m}$ in diameter. The test has a thick wall and is commonly exposed on one end (i.e. not covered by planktonic shells). A typical feature is the presence of one or more round openings on the exposed surface through which the red-stained test interior is visible. These openings are encircled by a slightly raised rim (Fig. 2.3a–c) and appear to be a natural feature rather than the result of damage to the test wall. When dried on a SEM stub, the sphere shrinks and the openings deform, indicating that the wall is flexible to some degree (Fig. 2.3d, e).

5. *Round, slightly opaque sphere with red-stained interior* (Fig. 2.3f–h; Type 5 in Table 2.3). Round agglutinated sphere (approx. $200\ \mu\text{m}$ diameter) with a few attached planktonic shells. The agglutinated material of the test comprises a mixture of coccoliths and small mineral grains, in many cases plate-like, giving the sphere a slightly reflective and opaque appearance. The interior contains stercomata but these cannot be seen clearly through the wall.
6. *Crithionina-like sphere* (Fig. 2.3i–k; Type 6 in Table 2.3). A distinctive form with a thick white test made of finely agglutinated particles (mainly coccoliths). These specimens resemble the well-known agglutinated genus *Crithionina*, although they are much smaller ($<150\ \mu\text{m}$) than any described species of the genus.
7. *'Classic dome'* (Fig. 2.4a–d; Type 7 in Table 2.3). Small (approx. $100\ \mu\text{m}$ diameter), more or less spherical agglutinated sphere on top of a large planktonic shell, with many smaller shells incorporated into the test, occasionally also mineral grains. It contains numerous stercomata, which makes it difficult to distinguish live from dead individuals. This monothalamid is termed 'classic dome', and is by far the most abundant morphotype at both sites.
8. *Sphere with short tube* (Fig. 2.4e, f; Type 8 in Table 2.3). Monothalamous morphotype incorporating planktonic shells and similar in appearance to the 'classic dome'. It differs in that the test gives rise to a short tube, rarely longer than the main test ($100\text{--}150\ \mu\text{m}$ diameter). SEM images reveal coccoliths as the main agglutinated constituent for both the test and the tube.
9. *Red sphere with stercomata, between planktonic shells* (Fig. 2.5a–e; Type 9 in Table 2.3). An agglutinated, more or less spherical test (approx. $100\ \mu\text{m}$

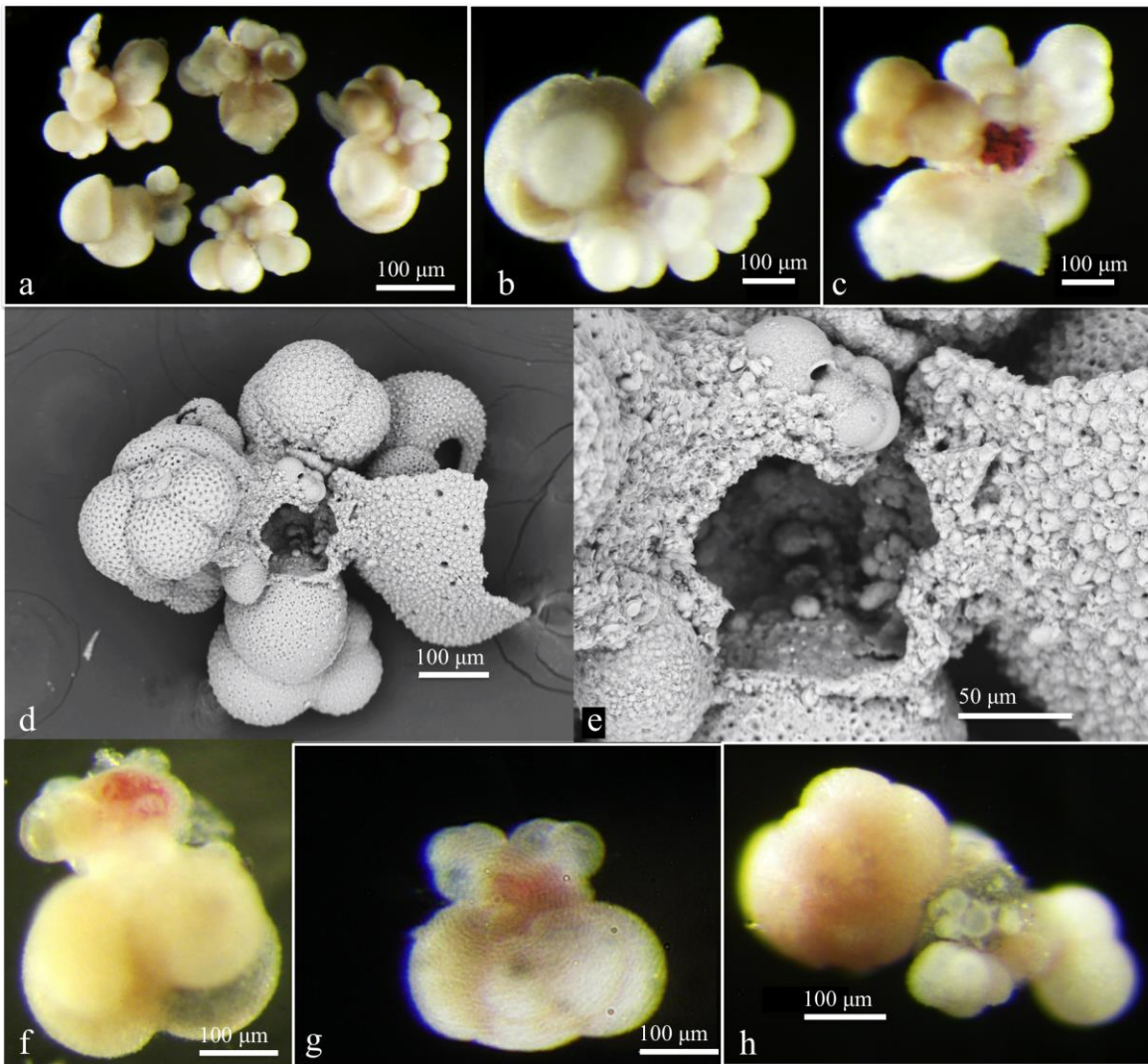


Fig. 2.5. Monothalamids attached to, or lodged between, planktonic foraminiferal shells. Reflected light images (a–c, f–h); SEM images (d, e). Red sphere with stercomata, between planktonic shells (a–e). Thin-walled red sphere attached to large planktonic shell (f, g). Soft sphere lodged between two planktonic shells (h).

diameter) attached to planktonic shells to form a much larger, irregular-shaped structure. In most specimens some shells have to be removed in order to reveal the sphere (Fig. 2.5b, c). As the sphere contains numerous large stercomata, stained individuals have a dark-red colour. When dried on the SEM stub the sphere shrinks, but stercomata are still clearly visible (Fig. 2.5e).

10. *Thin-walled red sphere attached to large planktonic shell* (Fig 2.5f, g; Type 10 in Table 2.3). Agglutinated sphere (100–150 μm diameter) attached to a large planktonic shell and incorporating smaller shells in its test. This form resembles ‘classic dome’, but has a thinner wall and specimens are always brightly stained, suggesting that stercomata are absent or sparse.
11. *Soft sphere lodged between two planktonic shells* (Fig. 2.5h; Type 11 in Table

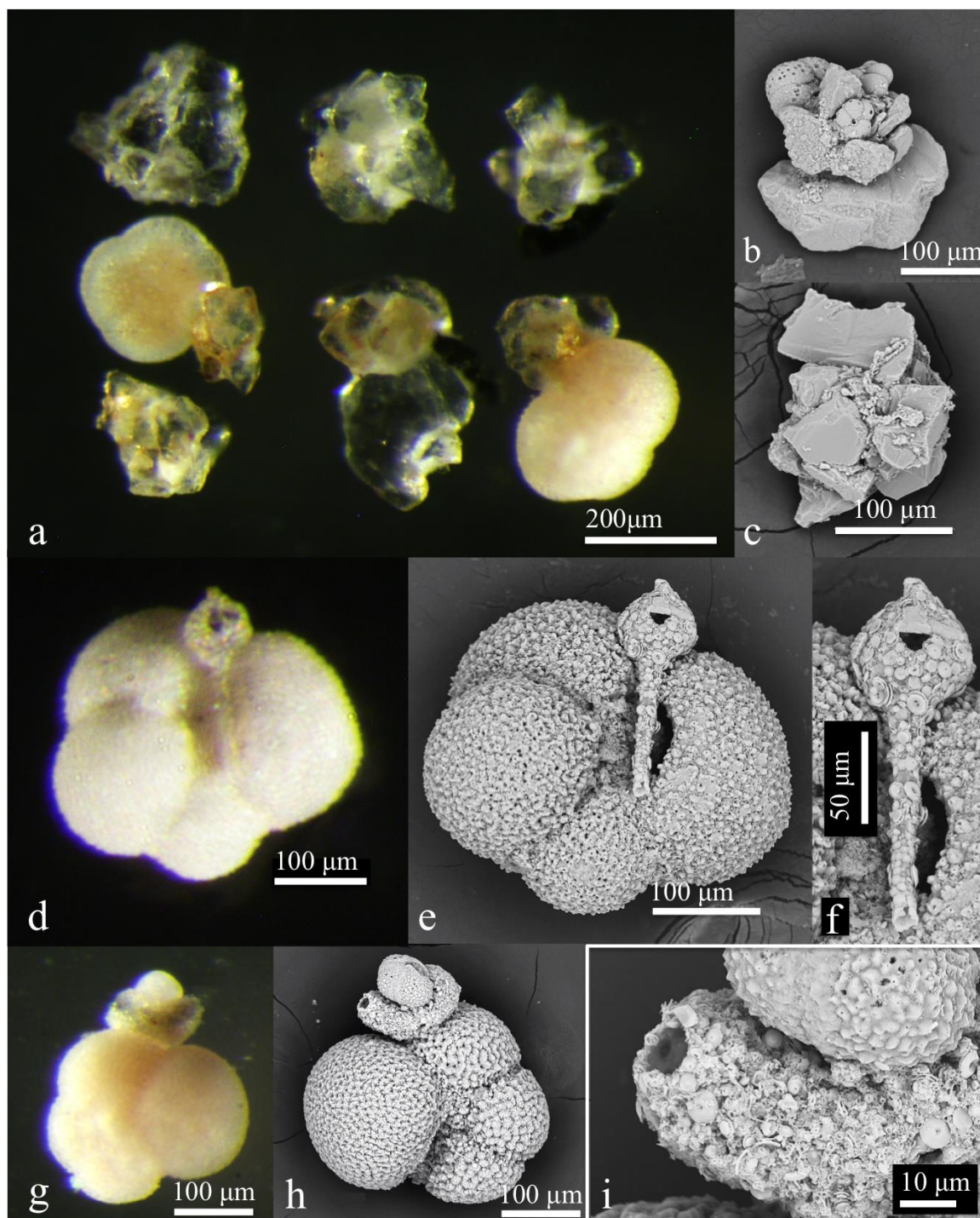


Fig. 2.6. Monothalamid associated with mineral grains and tubes. Reflected light images (a, d, g); SEM images (b, c, e, f, h, i). Monothalamids utilising yellow, orange and transparent mineral grains for constructing their test (a); SEM images of a specimen attached to a planktonic shell (b) and a free-living form (c). Spherical chamber with tubes (d–f). Short, soft-walled tube (g–i).

2.3). Finely agglutinated sphere with flexible wall and smooth surface, lodged between two large planktonic shells. The test (approx. 100 μm in maximum dimension) of the single specimen incorporates tiny planktonic shells, imparting a whitish/grey colour when viewed under the stereomicroscope. The faded grey colour suggests that the protoplasm contains stercomata.

2.3.2.2 Monothalamids associated with mineral grains

12. *Monothalamids associated with mineral grains* (Fig. 2.6a–c; Type 12 in Table 2.3). The foraminiferans in this category are small, spherical or domed monothalamids that use mineral grains to construct their test. The grains comprise a variety of whitish, yellow and orange particles, some of them plate-like, thus often resembling the agglutinated genus *Psammospaera*. They are found either free-living, with maximum dimension up to 150 μm , or attached to planktonic foraminiferal shells and/or quartz grains, to form much larger structures. The spheres and domes included in this category are difficult to separate into distinct morphotypes.

2.3.2.3 Tubular monothalamids

The following tubular morphotypes are associated with planktonic shells.

13. *Spherical chamber with tubes* (Fig. 2.6d–f; Type 13 in Table 2.3). This form comprises a small (approx. 50 μm diameter), spherical, agglutinated chamber that gives rise to two narrow rigid tubes (each approximately 100 μm long and 15 μm diameter) from opposite ends of its test, although only the base of one tube is present in the figured specimen. Large coccoliths are the main agglutinated particle.
14. *Short, soft-walled tube* (Fig. 2.6g–i; Type 14 in Table 2.3). A short (<150 μm), curved, soft-walled tube, open at both ends and apparently complete, sitting on top of a planktonic foraminiferal shell.

2.3.2.4 Pseudochambered (chain-like) forms

A number of forms have tests comprising a series of swellings or chamber-like segments (regarded as pseudochambers), which are sessile on, or surrounded by, planktonic foraminiferal shells. We recognise four forms based on the number of pseudochambers and planktonic shells involved, and the presence/absence of stercomata.

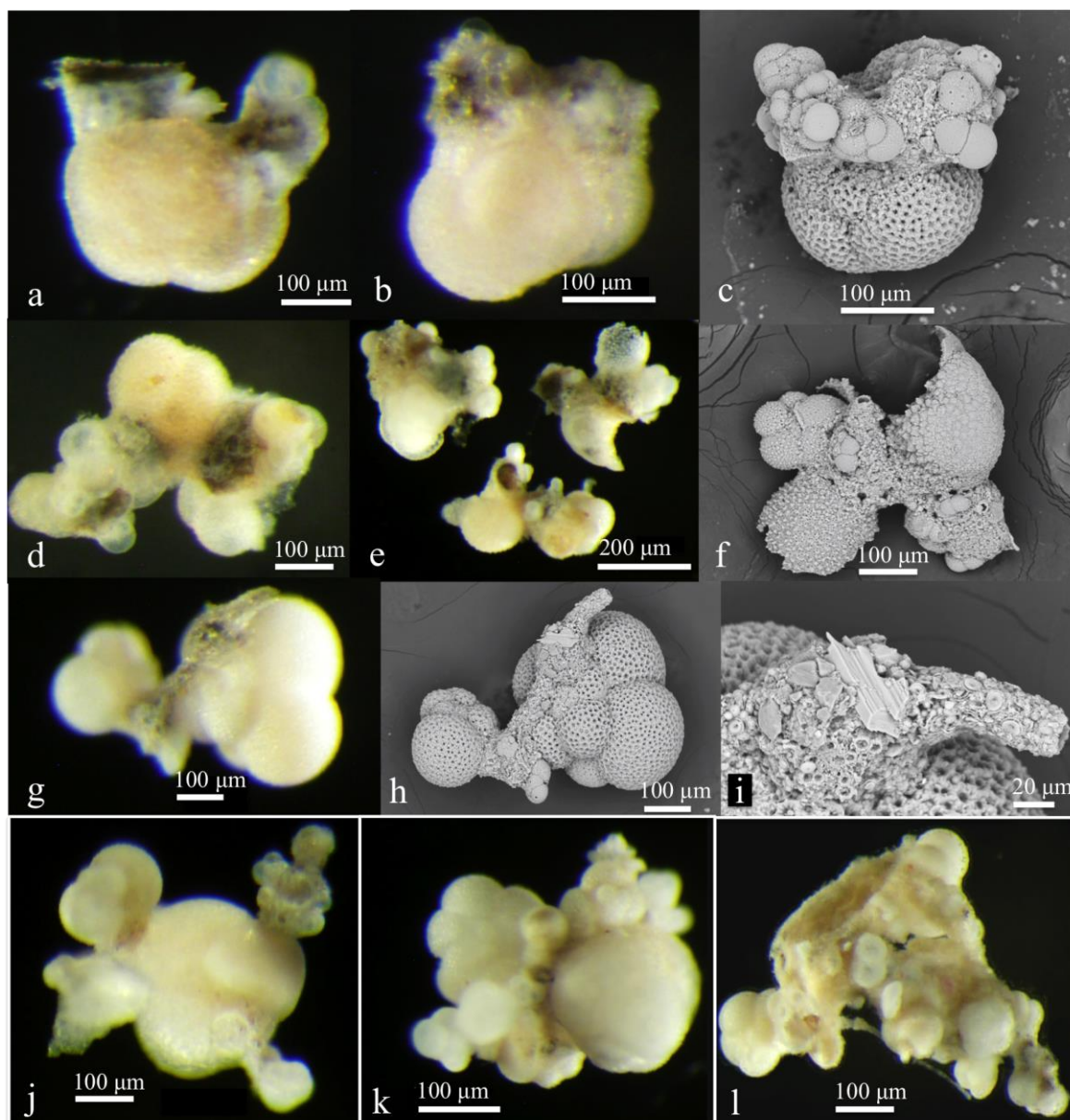


Fig. 2.7. Pseudochambered (chain-like) morphotypes. Reflected light images (a, b, d, e, g, j–l); SEM images (c, f, h, i). Double dome (a–c). Pseudochambers linked with stolons (d–f). Chain with thick tube (g–i). Indeterminate chain of chambers (j–l).

15. *Double dome* (Fig. 2.7a–c; Type 15 in Table 2.3). Two more or less spherical domes attached to a planktonic shell, each approximately 100 μm long, linked by a short ‘bridge’ and containing dark stercomata. Both domes are composed of small planktonic shells set in a matrix of coccoliths.
16. *Pseudochambers linked with stolons* (Fig. 2.7d–f; Type 16 in Table 2.3). Domed pseudochambers (approx. 100 μm diameter) associated with planktonic shells containing dark stercomata and linked by narrow stolons made of coccoliths. In some cases the stolons are open at one end (Fig. 2.7f). This morphotype resembles “double dome” but the pseudochambers are flatter and shrink when dried on a SEM stub.

17. *Chain with thick tube* (Fig. 2.7g–i; Type 17 in Table 2.3) Two pseudochambers (approx. 50 and 100 μm long) connected by a relatively thick tube and attached to two large planktonic shells. The entire structure (pseudochambers and tube) is about 300 μm long. The wall is composed of coccoliths and mineral grains imparting a shiny appearance under the stereomicroscope.
18. *Indeterminate chain of chambers* (Fig. 2.7j–l; Type 18 in Table 2.3). Complex chains comprising several pseudochambers of variable size that incorporate small planktonic foraminiferal shells, extending across one or more large planktonic shells and connected with narrow stolons. The incorporation of planktonic shells makes the arrangement of the pseudochambers and the relationship between them very difficult to decipher.

2.3.3 Occurrence at abyssal hills and abyssal plain sites

Our examination of the two samples suggests some differences in the contribution of morphotypes between the abyssal hill and abyssal plain sites. However, analyses of additional replicates will be necessary to confirm or refute these patterns. In absolute terms, monothalamid and pseudochambered foraminifera were more abundant at the abyssal hill site (H4) compared to the abyssal plain site (P4), for both the live (25 vs. 17 individuals $\times 10 \text{ cm}^{-2}$) and the dead fauna (234 vs. 139 individuals $\times 10 \text{ cm}^{-2}$) (see Table 2.2). Most morphotypes, including the three most abundant ones (Types 2–3, 7 in Table 2.3), had comparable relative abundances (i.e. percentage of the total number of monothalamids) at both sites, but there were some exceptions. Monothalamids with test composed of mineral grains (Type 12 in Table 2.3) were found almost exclusively at the abyssal hill site, while delicate thick-walled spheres with red stained interior (Type 4 in Table 2.3) were only encountered on the abyssal plain site. Moreover, spheres with short tube (Type 8 in Table 2.3) were more abundant at the abyssal hill site, while pseudochambered forms (Types 15–18, Table 2.3) were more abundant at the abyssal plain site. Some monothalamids (Types 13–14 in Table 2.3) and pseudochambered forms (Types 15, 17 in Table 2.3) were confined either to the abyssal hill or abyssal plain site, but as they were all uncommon, and in some cases were singletons, little can be concluded regarding their distribution.

2.4 Discussion

2.4.1 Limitations of dataset

Because of their delicate nature, the foraminifera described here might be vulnerable to mechanical damage, particularly during the sieving of sediment samples. Those particularly prone to breakage would include chain-like forms in which the segments are joined by fragile stolons that often span more than one planktonic shell (Fig. 2.7). The sieving process was carried out as gently as possible and most of the specimens that we examined appeared to be intact. It is possible that the 'spheres with long flimsy tubes' (Fig. 2.2c–e) represent fragments of chain-like formations in which the tubes link together several chambers, although we have no direct evidence for this interpretation.

The recognition of live individuals was sometimes problematic, particularly in the case of forms in which the test contents were dominated by stercomata, for example the 'classic dome' (Fig. 2.4a; Type 7 in Table 2.3). Another problem in some forms was that the central chamber was obscured by planktonic shells, which had to be removed in order to reveal whether or not the contents were stained (e.g. Fig. 2.5a–c; Type 9 in Table 2.3). This procedure both damages the specimen and is time-consuming. Because of these problems, the numbers of live specimens may have been underestimated. Because the present analysis was confined to the 0–1 cm sediment layer, further staining of deeper layers is necessary to examine if these foraminifera live at greater depths within the sediment. Moreover, as this study was based on only two samples, replicates are needed in order to confirm the differences between the abyssal hill and abyssal plain sites.

2.4.2 Comparisons with other studies

2.4.2.1 Continental margins monothalamids

There are certain similarities between the abyssal morphotypes considered here and monothalamous foraminifera illustrated in earlier publications. In particular, monothalamids associated with mineral grains resemble some illustrations of

Psammosphaera fusca from the North Sea (Heron-Allen and Earland 1913; e.g. Plate II Fig. 3.10– 3.12). Here, specimens of *P. fusca* used a variety of particles to construct their tests, mainly mineral grains but also dead foraminiferal shells. Heron-Allen and Earland (1913) reported both free-living and sessile forms of this species, the latter attached to sponge spicules, larger foraminiferal tests and molluscan shells. These authors also recorded *Crithionina mamilla*, which was found on similar substrates. This species resembles our *Crithionina*-like sphere in having a white thick-walled test. However, *P. fusca* and *C. mamilla* were reported from shelf and slope settings (16–1,600 m) rather than abyssal depths and were much larger (approx. 550–1,150 μm) than our morphotypes, which in most cases did not exceed 150 μm . Differences in food supply linked to differences in depth probably explain their larger size.

2.4.2.2 Abyssal environments: differences between Atlantic and Pacific monothalamids

Snider et al. (1984) analysed boxcore samples taken at 5800 m depth in the North Pacific in order to assess the composition and distribution of the meiofauna and nanofauna. They found that an important part of the abundance and biomass of benthic foraminifera comprised small (<100 μm diameter) ‘sac-shaped’ individuals, which they called *Crithionina*. These were presumably some sorts of agglutinated spheres. In the Kaplan East area of the abyssal eastern Equatorial Pacific, Nozawa et al. (2006) reported tiny free-living agglutinated spheres termed ‘indeterminate psammosphaerids’ that were consistently more abundant (usually 60–80% of the total live assemblage) than other foraminifera. A small (<100 μm diameter) agglutinated spherical form was described from the Kaplan Central site by Ohkawara et al. (2009) as *Saccamina minimus*. This species incorporated radiolarian tests and shard-like diatom fragments in its test and contained stercomata.

The abundance of small agglutinated spheres at abyssal sites in both the Pacific and Atlantic Ocean (Goody et al. 1995; our samples) is striking. However, they differ in the nature of particles used to construct the test - mainly siliceous in the Pacific and mainly calcareous in the Atlantic. Much of the abyssal Pacific lies close to or below the CCD (Berger, 1978) and thus few planktonic foraminiferal shells

are available in seafloor sediments. As a result, most agglutinated spheres are made of fine mineral particles and siliceous biogenic material, mainly radiolarians and diatom fragments (Nozawa et al., 2006; Ohkawara et al., 2009). They are also predominantly free-living and not attached to substrates. At the PAP-SO, on the other hand, the CCD is much deeper (Biscaye et al., 1976) and the sediment is mainly a carbonate ooze with abundant planktonic foraminiferal shells and coccoliths, which monothalamous spheres and domes use to construct their tests. In particular, they typically incorporate planktonic shells into their test or attach themselves to the surfaces of large planktonic shells. As a result, they often form large and complex structures (>300 μm), which appear superficially quite different from the tiny monothalamids found in the Pacific Ocean.

2.4.2.3 Distribution across the abyssal plain and abyssal plain sites

Topographic high points can generate distinctive environmental conditions. Thistle et al. (1999) reported faunal and ecological differences between high points (seamounts) and flat areas. High points tend to have stronger currents (Roden, 1987) and coarser sediment (Levin and Thomas, 1989). Our abyssal hill site resembles a small seamount (see Fig. 2.1; Table 2.1). Thus, we would expect stronger currents and coarser sediment compared with the abyssal plain site, which might affect the abundance and species composition of sediment-dwelling fauna (Kaufmann et al., 1989; Levin et al., 1994), including the foraminifera (Kaminski, 1985). Our observations suggest that this is true for monothalamous and pseudo-chambered foraminifera, as their densities are greater at the abyssal hill site. Furthermore, monothalamids that incorporate mineral grains as part of their test are almost exclusively restricted to this elevated setting where larger quartz grains are available. Taking into account the patchy distribution of benthic foraminifera in abyssal environments (Bernstein et al., 1978; Bernstein and Meador, 1979), replicate samples will clearly be necessary to confirm this pattern. However, if confirmed, this would have implications for the role of abyssal hills in generating faunal heterogeneity.

2.5 Concluding remarks

Our preliminary study provides evidence for the prevalence of certain types of basal ('primitive') foraminifera at the PAP-SO area of the northeast Atlantic. They represent a subset of the diverse and largely undescribed monothalamids that flourish in the deep sea and represent an important component of abyssal benthic communities. The forms that we describe are all associated with planktonic foraminiferal shells, an important component of the sand fraction of sediments at the PAP-SO, which is situated above the CCD. In the abyssal Pacific, where the CCD is shallower, radiolarian tests take the place of planktonic foraminifera as sand-sized components of the sediment. Currently, there are many problems associated with the study of these abyssal monothalamids, among them, distinguishing live from dead individuals and obtaining molecular genetic data in order to address their phylogenetic relationships. These remain important challenges for the future.

The fossil record of monothalamous foraminifera is generally poor (Tappan and Loeblich, 1988). Some apparently delicate agglutinated species have been found in ancient marine sediments (e.g. Nestell et al. 2009; Nestell and Tolmacheva 2004) and agglutinated tests that resemble testate amoebae are known from Neoproterozoic sediments (Porter and Knoll, 2000). We are not aware of any forms in the fossil record similar to those described here, although it is possible that they may be discovered eventually in Late Cretaceous sediments deposited in the North Atlantic and Western Tethys (now Western Mediterranean) Oceans, in some cases above the CCD. These sediments have yielded diverse deep-water agglutinated foraminiferal assemblages (e.g. Kuhnt and Kaminski 1989; Kuhnt et al. 1989), some resembling komokiaceans. The planktonic shells from which many of the PAP-SO forms are constructed could easily become detached, causing the test structure to disintegrate, but the organic components might survive fossilisation.

References of Chapter 2

- Berger, W.H., 1978. Sedimentation of deep-sea carbonate; maps and models of variations and fluctuations. *Journal of Foraminiferal Research*, 8, 286–302.
- Bernstein, B.B., Hessler, R.R., Smith, R., Jumars, P.A., 1978. Spatial dispersion of benthic foraminifera in abyssal central North Pacific. *Limnology and Oceanography*, 23, 401–416.
- Bernstein, B.B., Meador, J.P., 1979. Temporal persistence of biological patch structure in an abyssal benthic community. *Marine Biology*, 51, 179–183.
- Biscaye, P.E., Kolla, V., Turekian, K.K., 1976. Distribution of calcium carbonate in surface sediments of the Atlantic Ocean. *Journal of geophysical research*, 81, 2595–2603.
- Earland, A., 1933. Foraminifera. Part II. South Georgia. *Discovery Reports*, Vol. 7 (pp. 27–138).
- Earland, A., 1934. Foraminifera. Part III. The Falklands sector of the Antarctic (excluding South Georgia). *Discovery Reports*, Vol. 10 (pp. 1–208).
- Earland, A., 1936. Foraminifera. Part IV. Additional records from the Weddel Sea sector from material obtained by the S.Y. 'Scotia'. *Discovery Reports*, Vol. 10 (pp. 1–76).
- Enge, A.J., Kucera, M., Heinz, P., 2012. Diversity and microhabitats of living benthic foraminifera in the abyssal Northeast Pacific. *Marine Micropaleontology*, 96–97, 84–104.
- Gooday, A.J., Carstens, M., Thiel, H., 1995. Microforaminifera and nanoforaminifera from abyssal northeast Atlantic sediments: a preliminary report. *Internationale Revue Der Gesamten Hydrobiologie*, 80, 361–383.
- Gooday, A.J., Hori, S., Todo, Y., Okamoto, T., Kitazato, H., Sabbatini, A., 2004. Soft-walled, monothalamous benthic foraminiferans in the Pacific, Indian and Atlantic Oceans: aspects of biodiversity and biogeography. *Deep-Sea Research Part I–Oceanographic Research Papers*, 51, 33–53.
- Gooday, A.J., Malzone, M.G., Bett, B.J., Lamont, P.A., 2010. Decadal-scale changes in shallow-infaunal foraminiferal assemblages at the Porcupine Abyssal Plain, NE Atlantic. *Deep-Sea Research Part II–Topical Studies in Oceanography*, 57, 1362–1382.
- Gooday, A.J., Jorissen, F.J., 2012. Benthic foraminiferal biogeography: controls on global distribution patterns in deep-water settings. *Annual Review of Marine Science*, 4, 237–262.
- Gooday, A.J., 2014. Deep-sea benthic foraminifera. *Reference Module in Earth Systems and Environmental Sciences* (pp. 1–20).
- Heron-Allen, E., Earland, A., 1913. On some foraminifera from the North Sea, etc, dredged by the Fisheries cruiser 'Goldseeker' (International North Sea Investigations—Scotland). II. On the distribution of *Saccamina sphaerica* (M. Sars) and *Psammosphaera fusca* (Schulze) in the North Sea: particularly with reference to the suggested identity of the two species. *Journal of the Royal Microscopical Society*, 1–26.
- Heron-Allen, E., Earland, A., 1932. Foraminifera. Part I. The ice-free area of the Falkland Islands and adjacent seas. *Discovery Reports*, IV, 291–460.
- Kaminski, M.A., 1985. Evidence for control of abyssal agglutinated foraminiferal community structure by substrate disturbance: results from the HEBBLE area. *Marine Geology*, 66, 113–131.

- Kaufmann, R.S., Wakefield, W.W., Genin, A., 1989. Distribution of epibenthic megafauna and lebensspuren on two central North Pacific seamounts. *Deep-Sea Research Part I—Oceanographic Research Papers*, 36, 1863–1896.
- Kuhnt, W., Kaminski, M.A., 1989. Upper Cretaceous deep-water agglutinated benthic foraminiferal assemblages from the Western Mediterranean and adjacent areas. In: Wiedmann, J. (Ed.), *Cretaceous of the Western Tethys, Proceedings of the Third International Cretaceous Symposium, Tübingen* (pp. 91–120). Stuttgart: Scheizerbart'sche Verlagsbuchhandlung.
- Lecroq, B., Lejzerowicz, F., Bachar, D., Christen, R., Esling, P., Baerlocher, L., Osteras, M., Farinelli, L., Pawlowski, J., 2011. Ultra-deep sequencing of foraminiferal microbarcodes unveils hidden richness of early monothalamous lineages in deep-sea sediments. *Proc Natl Acad Sci U S A*, 108, 13177–13182.
- Levin, L.A., Thomas, C.L., 1989. The influence of hydrodynamic regime on infaunal assemblages inhabiting carbonate sediments on central Pacific seamounts. *Deep-Sea Research Part A—Oceanographic Research Papers*, 36, 1897–1915.
- Levin, L.A., Leithold, E.L., Gross, T.F., Huggett, C.L., Dibacco, C., 1994. Contrasting effects of substrate mobility on infaunal assemblages inhabiting two high-energy settings on Fieberling Guyot. *Journal of Marine Research*, 52, 489–522.
- Loeblich, A.R., Tappan, H., 1987. *Foraminiferal genera and their classification*. New York: Van Nostrand Reinhold.
- Mackensen, A., Grobe, H., Kuhn, G., Fütterer, D.K., 1990. Benthic foraminiferal assemblages from the eastern Weddell Sea between 68° and 73° S: Distribution, ecology and fossilization potential. *Marine Micropaleontology*, 16, 241–283.
- Mikhalevich, V.I., 2005. Polymerization and oligomerization in foraminiferal evolution. *Methods and Applications in Micropalaeontology*, 124, 117–141.
- Murray, J.W., 1991. *Ecology and palaeoecology of benthic foraminifera*. New York: Longman Scientific & Technical.
- Murray, J.W., 2013. Living benthic foraminifera: biogeographical distributions and the significance of rare morphospecies. *Journal of Micropalaeontology*, 32, 1–58.
- Nestell, G.P., Tolmacheva, T.Y., 2004. Early ordovician foraminifers from the Lava River Section, northwestern Russia. *Micropaleontology*, 50, 253–280.
- Nestell, G.P., Sudar, M.N., Jovanovic, D., Kolar-Jurkovsek, T., 2009. Latest Permian foraminifers from the Vlasic mountain area, northwestern Serbia. *Micropaleontology*, 55, 495–513.
- Nozawa, F., Kitazato, H., Tsuchiya, M., Gooday, A.J., 2006. 'Live' benthic foraminifera at an abyssal site in the equatorial Pacific nodule province: Abundance, diversity and taxonomic composition. *Deep-Sea Research Part I—Oceanographic Research Papers*, 53, 1406–1422.
- Ohkawara, N., Kitazato, H., Uematsu, K., Gooday, A.J., 2009. A minute new species of *Saccamina* (monothalamous Foraminifera; Protista) from the abyssal Pacific. *Journal of Micropalaeontology*, 28, 143–151.
- Pawlowski, J., Holzmann, M., Berney, C., Fahrni, J., Gooday, A.J., Cedhagen, T., Habura, A., Bowser, S.S., 2003. The evolution of early Foraminifera. *Proceedings of the National Academy of Sciences*, 30, 11494–11498.

- Pawlowski, J., Holzmann, M., Tyszka, J., 2013. New supraordinal classification of Foraminifera: molecules meet morphology. *Marine Micropaleontology*, 100, 1–10.
- Porter, S.M., Knoll, A.H., 2000. Testate amoebae in the Neoproterozoic Era: evidence from vase-shaped microfossils in the Chuar Group, Grand Canyon. *Paleobiology*, 26, 360–385.
- Roden, G.I., 1987. Effects of seamounts and seamount chains on ocean circulation and thermohaline structure. In: Keating, B.H., Fryer, P., Batiza, R., Boehlert, G.W. (Eds.), *Seamounts, Islands and Atolls* (pp. 335–354). Washington, D. C: American Geophysical Union.
- Schröder, C.J., Scott, D.B., Medioli, F.S., Bernstein, B.B., Hessler, R.R., 1988. Larger agglutinated Foraminifera: comparison of assemblages from central North Pacific and Western North Atlantic (Nares Abyssal Plain). *Journal of Foraminiferal Research*, 18, 25–41.
- Snider, L.J., Burnett, B.R., Hessler, R.R., 1984. The composition and distribution of meiofauna and nanobiota in a central North Pacific deep-sea area. *Deep-Sea Research Part I—Oceanographic Research Papers*, 31, 1225–1249.
- Tappan, H., Loeblich, A.R., 1988. Foraminiferal evolution, diversification, and extinction. *Journal of Paleontology*, 62, 695–714.
- Tendal, O.S., Hessler, R.R., 1977. An introduction to the biology and systematics of Komokiacea (Textulariina, Foraminiferida). *Galathea Report*, 14, 165–194.
- Thistle, D., Levin, L.A., Gooday, A.J., Pfannkuche, O., Lambshead, P.J.D., 1999. Physical reworking by near-bottom flow alters the metazoan meiofauna of Fieberling Guyot (northeast Pacific). *Deep-Sea Research Part I—Oceanographic Research Papers*, 46, 2041–2052.

Chapter 3: Agglutination of benthic foraminifera in relation to mesoscale bathymetric features in the abyssal NE Atlantic (Porcupine Abyssal Plain)

Abstract

Abyssal hills, small topographic features rising above the abyssal seafloor (<1000 m altitude), have distinct environmental characteristics compared to abyssal plains, notably the presence of coarser-grained sediments. As a result, they are a major source of habitat heterogeneity in the deep sea. The aim of this study was to investigate whether there is a link between abyssal hills and the test characteristics of selected agglutinated benthic foraminiferal species. We analysed 1) the overall morphometry, and 2) the granulometric and chemical (elemental) characteristics of the agglutinated tests of ten common foraminiferal species (*Adercotryma glomerata*, *Ammobaculites agglutinans*, *Cribrostomoides subglobosus*, *Lagenammina* aff. *arenulata*, *Nodulina dentaliniformis*, *Portatrochammina murrayi*, *Recurvoides* sp. 1 and three *Reophax* sp.) at four sites (two on top of abyssal hills and two on the adjacent plain) in the area of the Porcupine Abyssal Plain Sustained Observatory, northeast Atlantic. The foraminiferal test data were compared with the particle size distribution and elemental composition of sediments from the study sites in order to explore possible grain size and mineral selectivity. We found differences in the visual appearance of the tests (i.e. the degree of irregularity in their shape), which was confirmed by morphometric analyses, related to seafloor topography. The agglutinated foraminifera selected different sized particles on hills and plains, reflecting the distinct granulometric characteristics of these settings. These characteristics (incorporation of coarse particles, test morphometry) could provide evidence for the recognition of ancient abyssal hill environments, as well as other palaeoceanographic settings that were characterised by enhanced current flow. Furthermore, analyses of sediment samples from the hill and plain sites using wavelength dispersive X-ray fluorescence (WD-XRF) yielded different elemental profiles from the plains, probably a result of winnowing on the hills, although all

samples were carbonate-rich. In contrast, the majority of the agglutinated tests were rich in silica, suggesting a preferential selection for quartz.

3.1 Introduction

Abyssal plains are vast areas of the ocean floor situated at water depths between 3500 and 6500 m. They make up almost two-thirds of the Earth's surface (Watling et al., 2013), yet despite their immense size they have received disproportionately little scientific attention compared to other ocean habitats (Stuart et al., 2008). Often regarded as topographically homogeneous, abyssal plains are populated by abyssal hills, typically up to a few hundred meters in height and a few kilometres in width. These represent one of the most important geomorphic features in the oceans (Goff and Arbic, 2010; Heezen and Holcombe, 1965; Heezen et al., 1959). Abyssal hills share many environmental characteristics with larger underwater features such as submarine knolls and seamounts (Yesson et al., 2011), which led to the term seamount being applied to any topographic rise >100 m high (Clark et al., 2010; Pitcher et al., 2007). However, here we retain the term 'abyssal hills' for relatively low (<1000 m) topographic rises located on the abyssal seafloor, and treat them as distinct topographic entities. Abyssal hills increase habitat complexity on the seafloor and may potentially alter benthic faunal patterns and diversity (Rex and Etter, 2010; Snelgrove and Smith, 2002). There is an extensive literature on the effects of habitat heterogeneity on benthic diversity patterns. Studies have focussed mainly on the finer spatial scales (centimetres to metres) represented by biogenic structures and the patchy distribution of organic matter (Gooday, 1986; Hasemann and Soltwedel, 2011; Levin et al., 1986; Thistle and Eckman, 1990; Warren et al., 2013) but have also addressed broader scales (mesoscale, i.e. decimetres to kilometres) by comparing assemblages from environmentally contrasting sites (Baldrighi et al., 2014; Gage et al., 1995; Kaminski, 1985; Thistle, 1983). However, very few studies (e.g., Durden et al., 2015) have explored the impacts of abyssal hills on deep-sea communities and none has dealt with meiofaunal groups such as the foraminifera.

Benthic foraminifera are a successful group of largely marine testate protists within the Rhizaria (Adl et al., 2012; Ruggiero et al., 2015). The 'tests' (shells) of some species are preserved in marine sediments and represent important

proxies in palaeoceanography. They are a major component of modern soft-bottom meio- and macro-faunal communities on abyssal plains and play an important role in ecological processes on the ocean floor (Gooday et al., 1992). During the analysis of foraminiferal samples collected in the area of the Porcupine Abyssal Plain Sustained Observatory (PAP-SO; Hartman et al., 2012) in the northeast Atlantic (4850 m water depth), we found variation in the community composition of benthic foraminiferal assemblages obtained at sites on the tops of abyssal hills and on the adjacent abyssal plain (Stefanoudis et al., 2015). In addition, we observed apparent differences in the agglutination patterns (size and nature of the cemented particles) and morphology of benthic foraminiferal tests in relation to these two topographic settings (i.e. hills vs. plain). The overall aim of this study was to investigate whether and how environmental differences between the hills and the plain affect the construction of agglutinated benthic foraminiferal tests in this region. Specifically, we were interested in 1) whether the same species select particles of different (a) sizes and (b) composition in these two settings, and 2) the extent to which any differences in particle selection influences the test morphology. To address these questions, we analysed the overall morphometry as well as the granulometric and chemical (elemental) characteristics of the agglutinated tests of selected common foraminiferal species in the PAP-SO area.

3.2 Materials and methods

3.2.1 Sample collection and study site

Samples were collected during RRS *James Cook* Cruise 062 (JC062, 24 July to 29 August 2011; Ruhl, 2012) in the vicinity of the PAP-SO area. They were obtained using a Bowers and Connelly Megacorer (Gage and Bett, 2005) equipped with core tubes (59 mm internal diameter) from two abyssal plain sites (P1, P2) and two abyssal hill sites (H1, H4) (Fig. 3.1; Table 3.1). Distances between sites were in the range of tens of kilometres. On board the ship the cores were sliced into 0.5-cm-thick layers down to 2 cm sediment depth, followed by 1-cm-thick layers from 2 to 10 cm depth, and each slice fixed in 10% Borax buffered formalin. The present contribution is based on material retained on a 150- μ m sieve from the 0–1 cm sediment horizon of eight core tube samples.

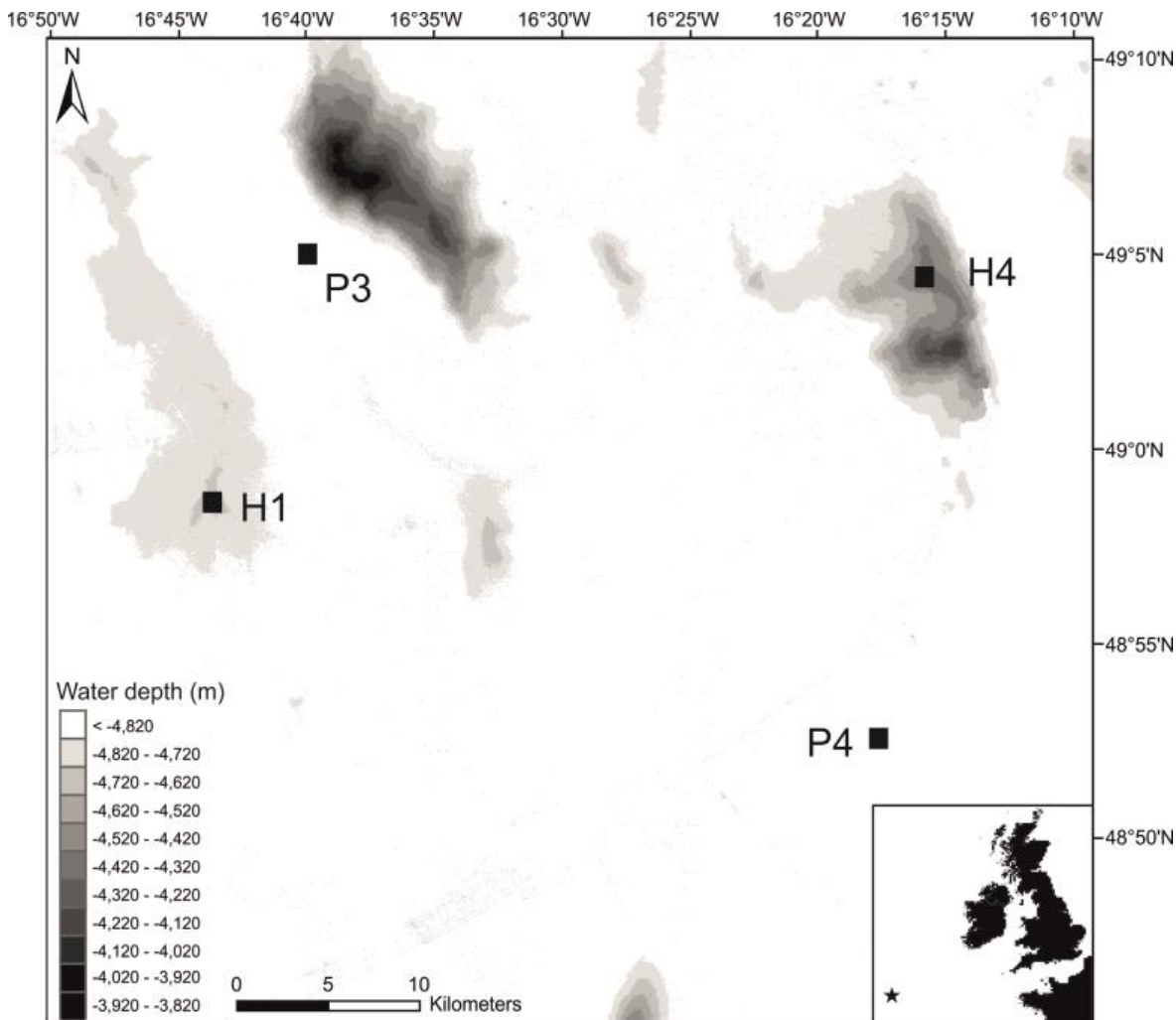


Fig. 3.1. Bathymetric map of the PAP-SO area indicating the location of the four study sites, P3 and P4 (abyssal plain sites), H1 and H4 (abyssal hill sites). The inset indicates the general location of the Porcupine Abyssal Plain in the northeast Atlantic Ocean.

Sixty-five foraminiferal specimens (23 from abyssal plain sites, and 42 from abyssal hill sites) belonging to 10 agglutinated taxa were included in the analysis (Table 3.1). The selection of species was based on their numerical abundance and an initial assessment of the variability in the size and nature of the agglutinated particles that constituted their tests. The species, the number of specimens of each examined, and the types of analyses employed, are detailed in Supplementary Material 3.A. A brief description of the species is given in Appendix A.

Durden et al. (2015) present data on the physical characteristics for our sampling sites. Particle size distribution (0–5 cm sediment horizon) at all sites was bimodal, with peaks at 4 and 200 μm and a trough at 22.9 μm . The fine sediment fraction (<23 μm) comprised mainly coccoliths, while the coarser fraction (23–1000 μm)

Table 3.1. Locality data. N₁= number of replicate samples from which foraminiferal specimens have been collected and used in this study. N₂= number of specimens analysed from each site. N₃= Number of sediment samples for particle size analysis. N₄= Number of sediment samples for elemental analysis. For geographical position of sites consult Fig. 3.1.

Site	Topography	Centre Latitude (°N)	Centre Longitude (°W)	Water depth (m)	N ₁	N ₂	N ₃	N ₄
P3	Abyssal plain	49.083	16.667	4851–4853	1	4	5	1
P4	Abyssal plain	48.877	16.293	4849–4851	2	19	5	2
H1	Abyssal hill	48.978	16.728	4669–4679	3	16	5	1
H4	Abyssal hill	49.074	16.243	4339–4388	2	26	2	1

was dominated by foraminiferal tests, indicating sediments with high carbonate content (i.e. carbonate ooze).

The size contrast between the two sediment components generated the bimodal particle-size distribution observed in all samples. The coarser fraction constituted a higher proportion of the sediment on the abyssal hills, where larger mineral grains, including pebbles to cobble-sized ice-rafted stones were also observed, enhancing the larger of the two size peaks. Median seabed slope was greater and more variable at the abyssal hill sites compared to the plain sites, and the slope of H4 (8.6°) was more than double that of H1 (4.0°). Organic matter input estimated from seabed images and expressed either as the percentage of the seafloor covered by phytodetritus or as median detritus aggregate size, did not vary spatially in the PAP-SO area.

3.2.2 Test morphometry

Initially, all 65 specimens were photographed under an incident light microscope (Leica Z16-APO). The majority (56) were then examined by scanning electron microscopy (SEM) using an environmental Zeiss EVO LS10 at variable pressure. The number of SEM images was lower than the number of light microscope images because some delicately agglutinated species collapsed upon transfer to SEM stubs (mostly specimens of *Nodulina dentaliniformis*). Subsequently, both sets of images were processed and a total of 31 morphometric parameters were obtained using image analysis software (analySIS version 5.0, Olympus Soft Imaging Solutions). The resulting morphometric data from both sets of microscopic

images were compared for consistency. As there were no significant statistical differences, the light transmission microscopy dataset, which was based on a larger number of specimens (65 compared to 56 SEM images), was selected for further analyses of the overall test morphometry (see Supplementary Material 3.A). Tests incorporating long spicules (mostly belonging to *Reophax* sp. 28) were not included in the analysis as the image analysis software overestimated their surface area, lowering the total number of specimens suitable for morphometric comparisons to 60 (see Supplementary Material 3.A).

Multivariate assessment of the data was computed using PRIMER 6 (Clarke and Gorley, 2006). Euclidean distance similarity matrices were created for the morphometric data and their relation to topography was explored using Multi-dimensional Scaling (MDS) and Analysis of Similarities (ANOSIM). We first worked on the complete set of morphometric parameters before focusing on the following reduced set of four parameters (see Fig. 3.2) that seemed to drive most variation in the data: (i) Convexity, defined as the ratio between the actual measured test area (an irregular surface) and an imaginary smooth envelope that encloses the test (Fig. 3.2a); (ii) Maximum to Minimum Diameter ratio (Fig. 3.2b); (iii) Perimeter to Area ratio (Fig. 3.2c); and (iv) Sphericity, which gives information about the roundness of the test (Fig. 3.2d). In general, specimens with more irregular, “bumpier” morphologies will tend to have lower convexity and sphericity values, and higher perimeter to area and maximum to minimum diameter ratios, while the opposite will hold true for specimens with smooth surfaces and a more circular appearance. We assessed the effect of individual parameters using the Student's t and Mann–Whitney U tests, for normally (Shapiro–Wilk test; $p > 0.05$) and non-normally (Shapiro–Wilk test; $p < 0.05$) distributed data, respectively. The relationship of these parameters to topography was assessed using morphometric data from all species as well as focusing on four species (*Adercotryma glomerata*, *Lagenammia* aff. *arenulata*, *N. dentaliniformis* and *Reophax* sp. 21) that were represented by enough specimens (≥ 3) in both settings to permit statistical comparisons (see Supplementary Material 3.A).

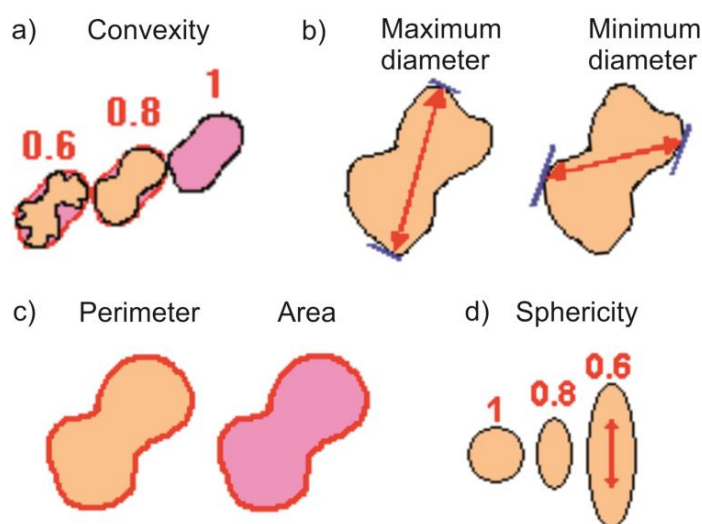


Fig. 3.2. The four morphometric descriptors driving most variation in the data (iconography from analySIS version 5.0, Olympus Soft Imaging Solutions). (a) Convexity. (b) Maximum to Minimum Diameter ratio. (c) Perimeter to Area ratio. (d) Sphericity.

3.2.3 Particle size analysis

Test particle size was measured from a set of 56 SEM images. Initially, an automated counting procedure was used, similar to the one described in (Armynot du Châtelet et al., 2013c). However, it could not cope well with the heterogeneous nature of the particles found in the foraminiferal tests and therefore its use was discontinued. Instead, measurements were made manually using ImageJ (Rasband, W.S., ImageJ, U.S. National Institutes of Health, Bethesda, Maryland, USA, <http://imagej.nih.gov/ij/>, 1997–2014), and restricted to particles $\geq 10 \mu\text{m}$. Size was determined as the longest axis dimension of the grains. In order to relate particle size to topography, the data were divided into 25 size classes based on the geometric mean particle diameter, spanning grain sizes 10–295 μm , and the resulting particle size distributions were compared. The effect of topography could be tested further for four species (*A. glomerata*, *Lagenammia* aff. *arenulata*, *Reophax* sp. 21, *Reophax* sp. 28) that were represented by sufficient specimens (≥ 3) in both settings.

Grain size characteristics for the four study sites were assessed from seventeen samples (Fig. 3.1; Table 3.1) that were obtained using a Bowers and Connelly Megacorer equipped with multiple core tubes (59 and 100 mm internal diameter) (Gage and Bett, 2005). On board the ship the cores were sliced in three layers (0–1, 1–3, 3–5 cm) and each slice was stored in plastic bags with no preservative for

later analysis. Sediment particle size distributions were measured by laser diffraction using a Malvern Mastersizer, after homogenisation (particles >2 mm removed), dispersal in a 0.05% (NaPO₃)₆ solution (Abbireddy and Clayton, 2009), and mechanical agitation. Detected particle sizes ranged from 0.01 to 2000 µm. The percentage of particles >63 µm in the sediments of each site and topographic setting was also estimated, as in deep-sea environments it can serve as a proxy of current activity (McCave and Hall, 2006; McCave et al., 1995). The present contribution is based on material from the 0–1 cm sediment horizon. In order to test for particle size selectivity by the foraminifera, we compared particle-size distribution data from the tests and the sediment samples, focusing on particles within the 10–295 µm range, which covers the same 25 size classes used to analyse foraminiferal grains.

3.2.4 Elemental composition

Quantitative estimates of the elemental composition of 56 benthic foraminiferal tests (see Supplementary Material 3.A) were carried out using an Environmental Scanning Electron Microscope (ESEM) (Zeiss EVO LS10) equipped with an Energy-Dispersive Spectroscopy (EDS) device (X-Max, Oxford Instruments).

The elemental composition of sediments from the hills and plains was determined by applying wavelength-dispersive X-ray fluorescence (WD-XRF) techniques to five samples, three from the plains and two from the hills (Table 3.1). Major elements were determined in fused beads obtained following fusion with a pure lithium borate flux in a Pt–Au vessel at c. 1100 °C. Lithium tetraborate (Fluxana, Germany) was used to dissolve the samples prior to major element determinations. Trace elements were analysed using pressed powder pellets. A Philips MAGIX-PRO automatic sequential WD X-ray fluorescence spectrometer was used to determine element concentrations. The elements were excited by means of a 4 kW Rh end-window X-ray tube. The instrument was calibrated using a wide range of international geochemical reference samples; accuracy was typically within 5% of the consensus value when an international reference sample was run as an unknown. The 2σ precision is typically 1–5%. Following conventional practice in geochemistry, the major element compositions were expressed as oxides. We then calculated the proportion of each element separately based on their atomic number in order to compare sediment elemental data with the elemental composition of the tests.

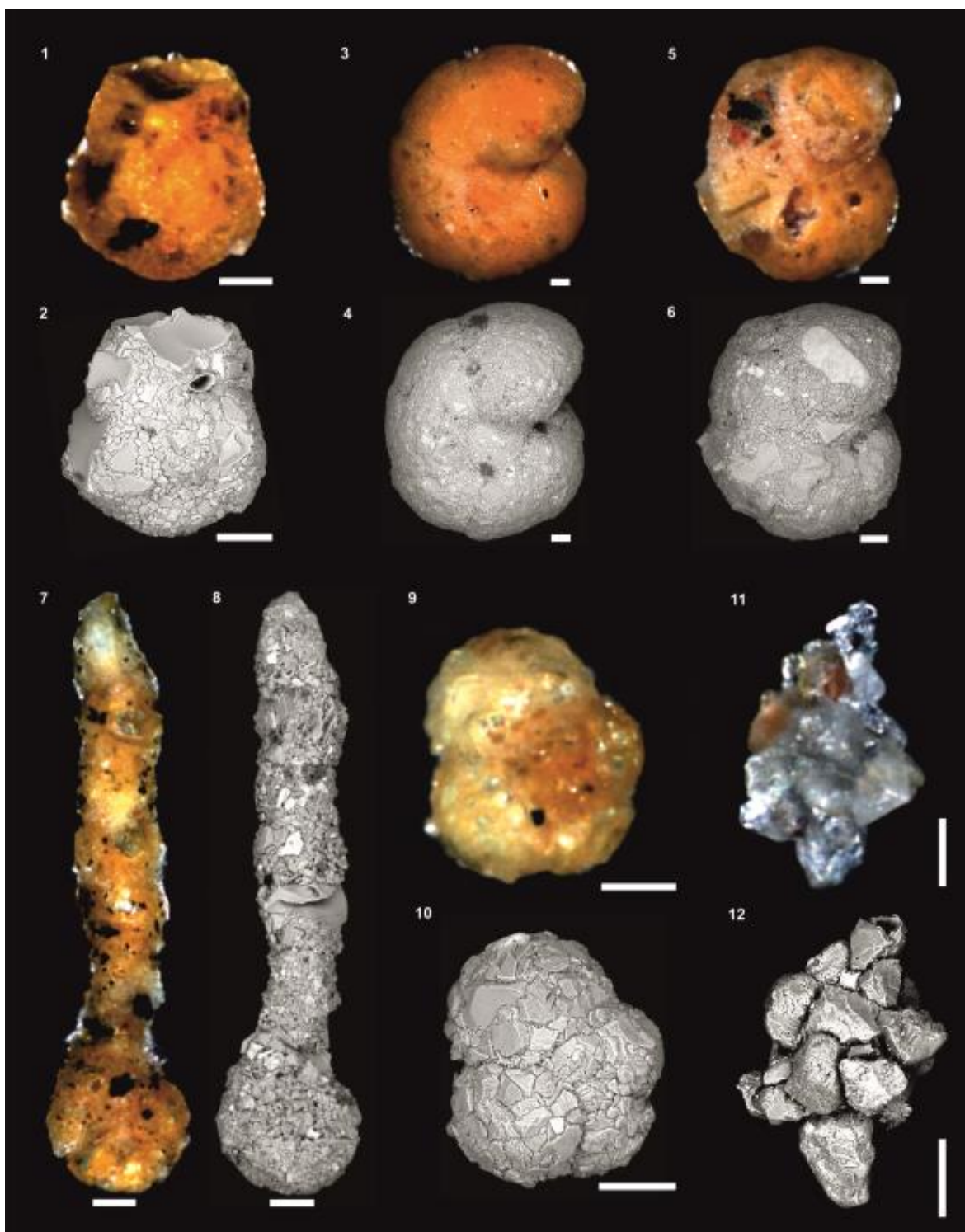


Plate 3.1. Light and SEM photographs of some species used in this study along with the site of collection. Figs. 1–2. *Recurvoides* sp. 1 (H1). Figs. 3–6. *Cribrostomoides subglobosus*: 3–4 (P3); 5–6 (H4). Figs. 7–8. *Ammobaculites agglutinans* (H1). Figs. 9–10. *Portatrochammina murrayi* (H4). Figs. 11–12. *Reophax* sp. 9 (H4). Scale bars = 100 μ m.

3.3 Results

3.3.1 Visual comparison of agglutinated foraminifera tests from hills and plain

The ten species used in this study are illustrated in Plates 3.1–3.3 and brief descriptions given in Appendix A. There were clear differences in the visual appearance of tests from topographically high and low sites. Specimens from the hills incorporated a higher number of larger particles (i.e. $>100\ \mu\text{m}$) (Table 3.2) in their test walls, which gave them a more or less irregular ('lumpier') appearance with rougher surfaces than those from the plain sites (Plates 3.1, Figs. 3–6; 3.2; 3.3).

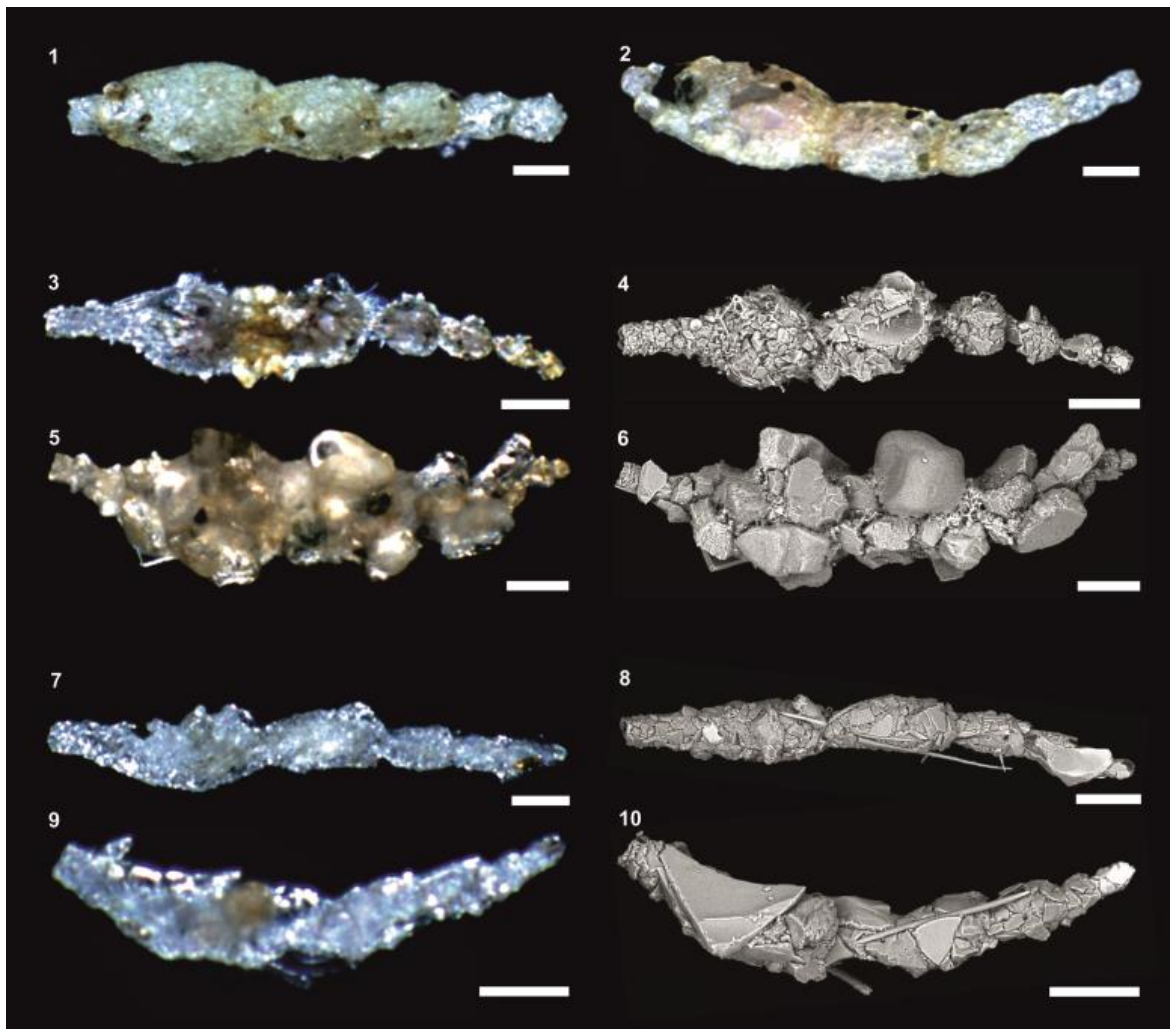


Plate 3.2. Light and SEM photographs of some species used in this study along with the site of collection. Figs. 1–2. *Nodulina dentaliniformis*: 1, (P4); 2, (H4). Figs. 3–6. *Reophax* sp. 21: 3–4, (P4); 5–6, (H4). Figs. 7–10. *Reophax* sp. 28: 7–8, (P4); 9–10, (H1). Scale bars = 100 μm .

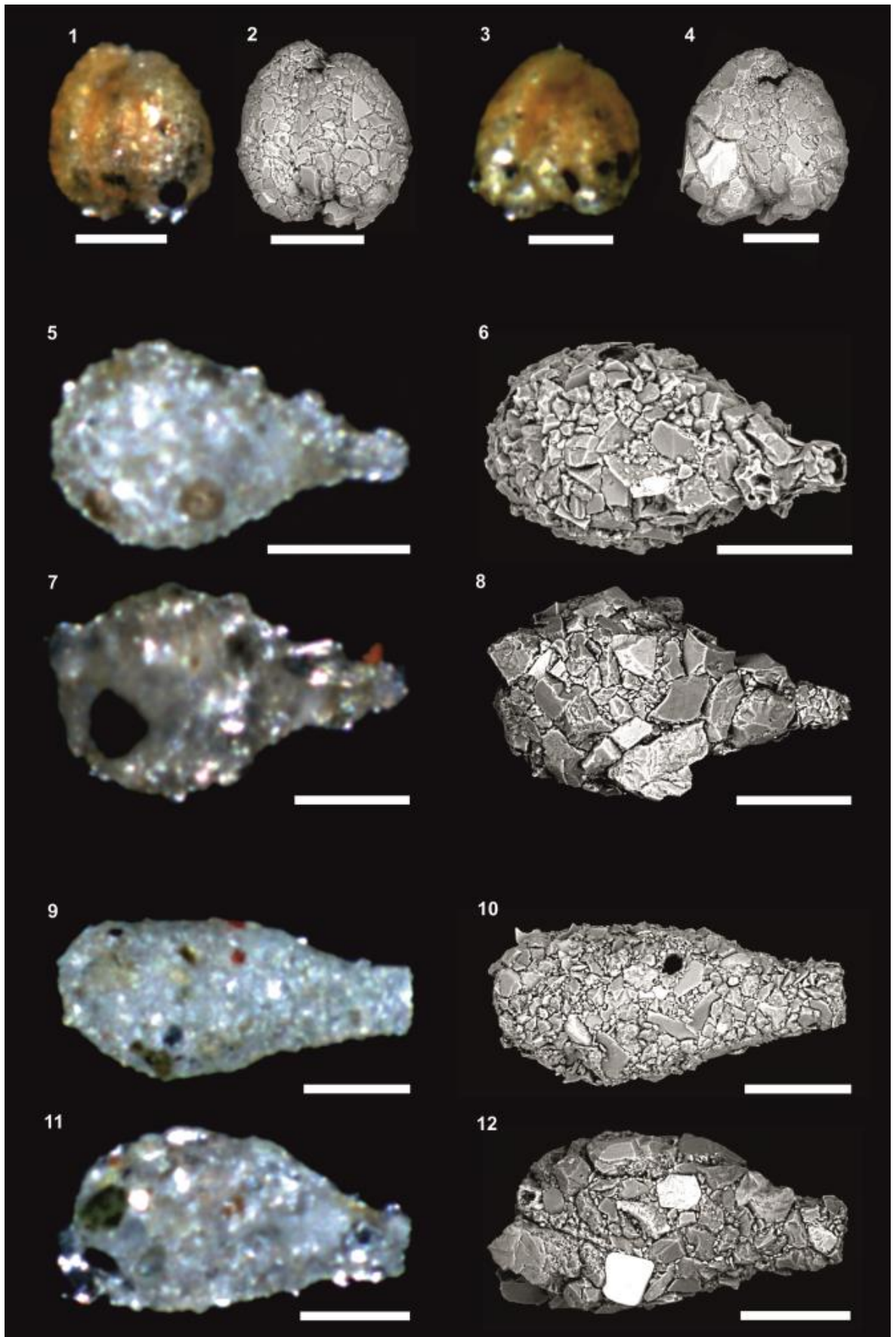


Plate 3.3. Light and SEM photographs of some species used in this study along with the site of collection. Figs. 1–4. *Adercotryma glomerata*: 1–2, (P4); 3–4, (H4). Figs. 5–10. *Lagenamma* aff. *arenulata*: 1st morphotype, 5–6, (P4), 7–8 (H4); 2nd morphotype, 9–10 (P4), 11–12 (H4). Scale bars = 100 μ m.

In certain species, notably *Reophax* sp. 21, which utilised some conspicuously large grains up to almost 300 μm in size), the effect of these larger particles on the shape and appearance of the test was particularly evident (Plate 3.2, Figs. 5–6). However, these striking differences did not hamper the recognition of species that were common to the two settings (e.g., Plate 3.2, Figs. 3–10).

3.3.2 Particle size analysis

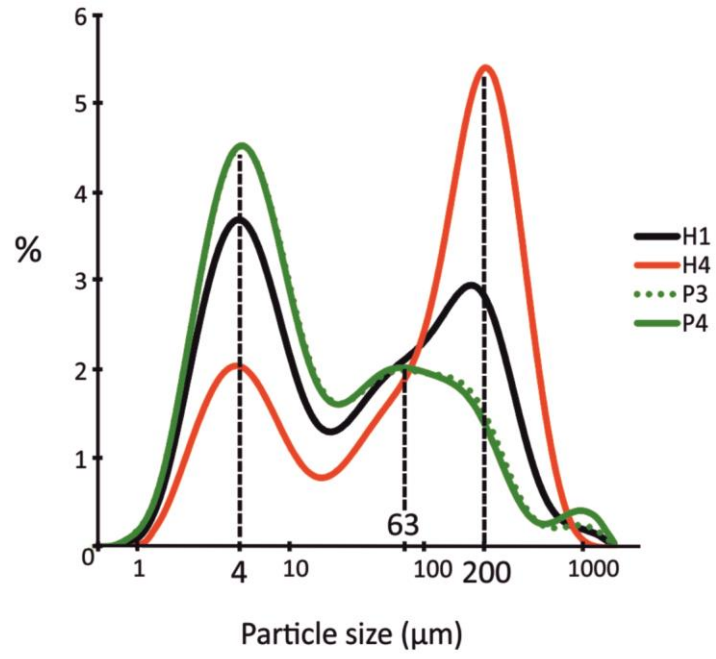
A summary of test particle size data for the agglutinated foraminifera is given in Table 3.2. In general, the average size and standard deviation of test particles was higher for hill specimens, although median values were comparable between hills and plains. ANOSIM results showed that the overall particle size composition of tests (i.e. taking into account all 25 particle size classes) was not related ($p > 0.05$) to the topographic setting. At the species level, only *A. glomerata* showed significant differences in particle size (ANOSIM, $p = 0.048$), with abyssal hill specimens utilising coarser particles on average (Table 3.2).

Sediment particle size distributions for the four studied sites were bimodal with peaks at approximately 4 μm and 200 μm (Fig. 3.3a), although on average the abyssal hills had a greater proportion of coarser material ($>63 \mu\text{m}$) compared to the plain sites (Student's t , $p < 0.05$) (Fig. 3.3a; Table 3.3). Within the 10–295 μm size range, which spanned the data we used to test for particle size selectivity by the foraminifera, ANOSIM found statistically significant differences ($p < 0.01$) in particle size composition between hill and plain sediments.

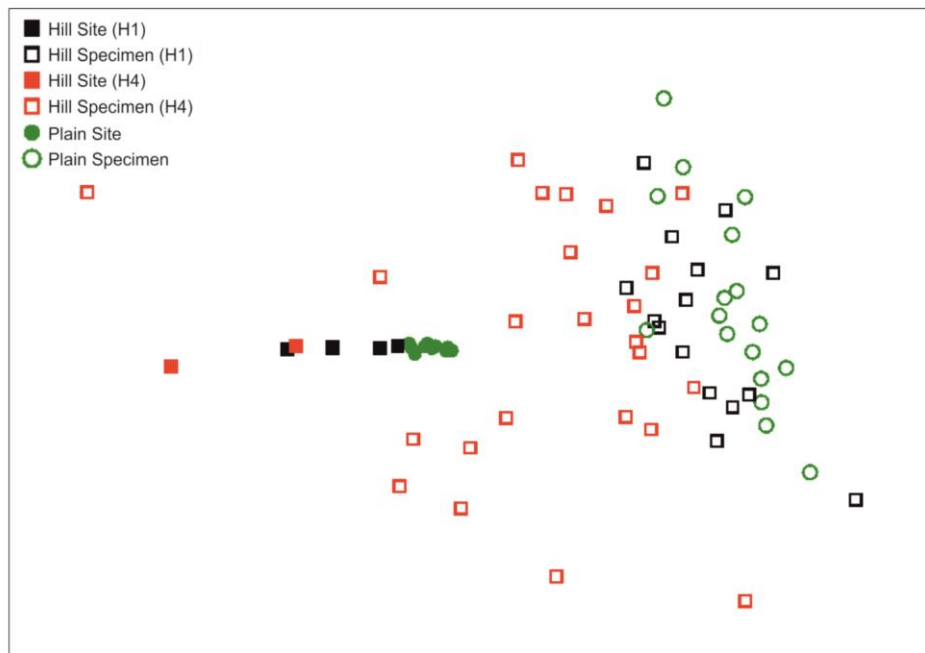
Table 3.2. Summary statistics of test particle size composition for species found in both hills and plains and all species for each setting combined.

Species	Plains				Hills			
	Mean (μm)	Median (μm)	SD	>100 μm	Mean (μm)	Median (μm)	SD	>100 μm
<i>Adercotryma glomerata</i>	19.0	17.2	7.9	0%	25.6	18.5	18.1	0.8%
<i>Cribrostomoides subglobosus</i>	25.1	22.1	12.3	0.1%	24	19.3	22.7	1.7%
<i>Lagenammina</i> aff. <i>arenulata</i>	22.6	19.7	11.4	0.2%	28.8	21.1	21.8	1.6%
<i>Recurvoides</i> sp. 1	15.7	14.3	5.5	0.0%	24.8	19.6	16.1	0.3%
<i>Reophax</i> sp. 21	21.1	17.1	15.7	0.3%	33.6	19.3	35.9	6.3%
<i>Reophax</i> sp. 28	21.7	18.6	13.2	0.3%	25.3	18.5	23.2	1.4%
All species	22.1	19.3	12.0	0.1%	27	19.3	23.8	2%

a)



b)



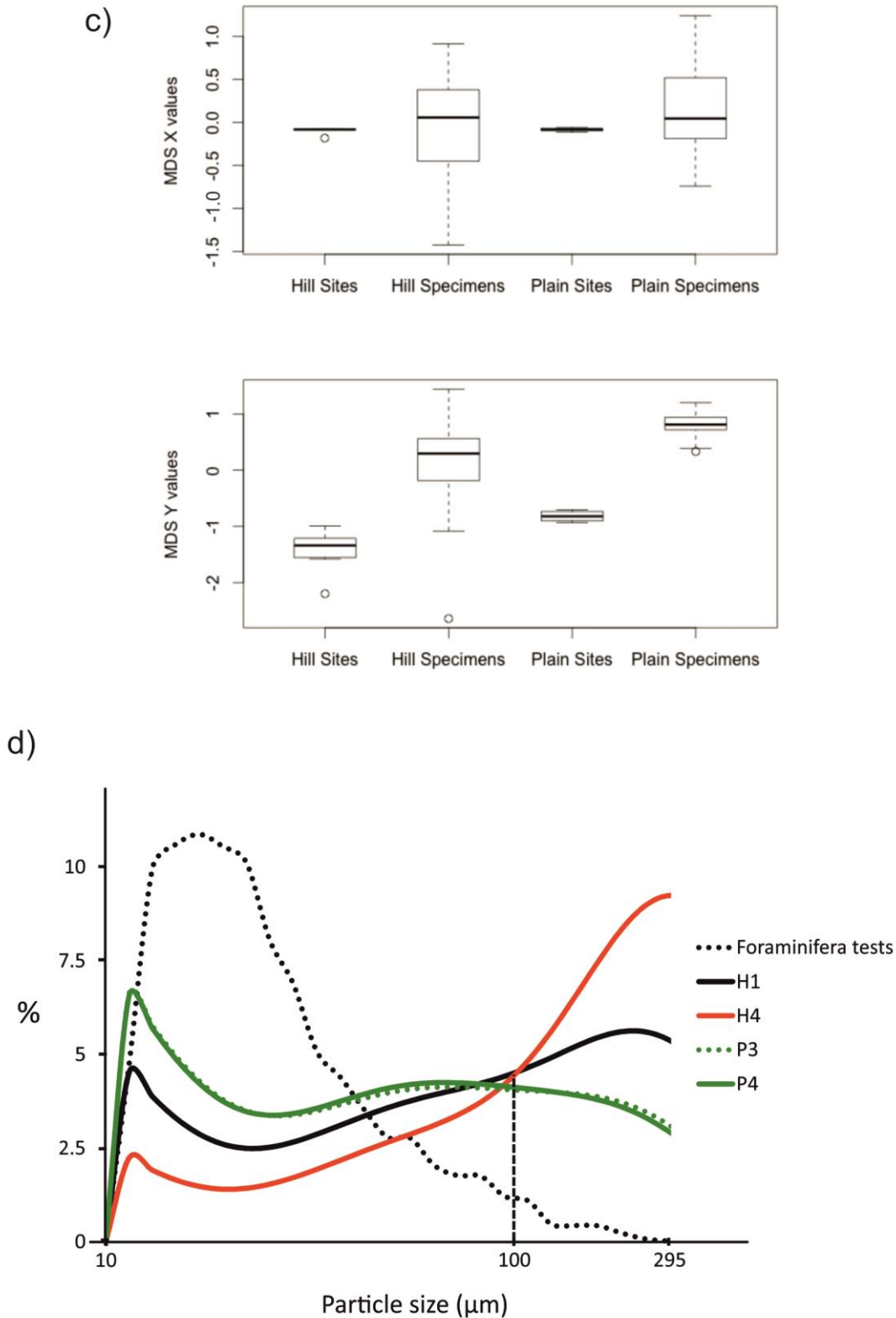


Fig. 3.3. (a) Mean particle size distribution (0–1 cm sediment horizon) of sediment samples from the four study sites. (b) MDS on the particle size distribution of 56 benthic foraminiferal tests and seventeen sediment samples from four sites. (c) Box–Whisker plots of the MDS x- and y-ordinate for the sediment samples and foraminiferal tests against topography. d) Mean particle size distribution (0–1 cm sediment horizon) of the foraminiferal tests and sediment samples from the four study sites.

Table 3.3. Mean percentages of the coarse sediment particle fraction (>63 μm) against the whole range of measured particles (0.01–2000 μm) for each of the four study sites and topographic settings.

Site	>63 μm (%)
P3	24.8
P4	24.9
H1	38.2
H4	63

An MDS ordination based on the particle size data derived from all ten species (56 specimens) and four sites (17 sediment samples) revealed differences between test and sediment samples (Fig. 3.3b). On an MDS plot the distance between two points corresponds to their degree of similarity in composition (i.e. closely spaced points are compositionally similar). Box–Whisker plots of the MDS x and y-ordinates against topography indicated that foraminiferal tests from the two hills contained particles that spanned a wider size range than those from the plain (Fig. 3.3c), reflecting the greater abundance of coarse particles available in these settings. Consistent with the above-mentioned ANOSIM results, hill and plain specimens did not form well-defined groupings and had significant overlap (Fig. 3.3b).

Sediment samples from the four sites exhibited lower levels of particle size variability compared to the tests. In the case of the plain sediments this was particularly evident from plots of the MDS x and y-ordinates against topography (Fig. 3.3c). Sediment samples were also clearly separated from most of the tests (Fig. 3.3b). This was to be expected, as the sediment particle data used extends several size classes below and above the studied size range (10–295 μm). Consequently, sediment samples had higher proportions of coarser particles compared to the foraminifera, which always included only a few coarse grains in their tests (Fig. 3.3d).

Unlike the foraminiferal tests, hill and plain sediment samples showed no overlap on the MDS plot, further highlighting their different particle size compositions (Fig. 3.3b). Interestingly, H1 sediment samples were positioned between the plain (P3, P4) and the H4 samples, indicating an intermediate composition. In order to explore this further, an additional ANOSIM of sediment particle data against study

site was performed. Initial results were significant ($p < 0.01$), and further pairwise comparisons revealed that the particle size composition was similar between the two plain samples (P3, P4), but significantly different from the hill site H1 (P3 vs. H1, $p = 0.016$; P4 vs. H1, $p < 0.01$). Unfortunately, the low number of sediment samples (2) from H4 did not permit pairwise comparisons with the rest of the sites, but based on their positioning on the ordination plot (Fig. 3.3b) we assume that the particle size composition is different from both plain samples, and perhaps from H1 as well.

In the light of these findings, we wanted to explore the inconsistency between the coarser sediments on the hills (especially at H4) and the apparent lack of correlation between test particle size and topographic setting. To do this we performed an additional ANOSIM on particle size data from all 56 tests against the study sites P4, H1 and H4 (P3 had particle data only from two specimens and thus could not be compared). This analysis yielded significant results ($p = 0.021$). Additional pairwise comparisons demonstrated that specimens from H4 had significantly different particle size composition compared to specimens from P4 ($p < 0.01$) as well as H1 ($p = 0.036$), whereas H1 specimens were not different from P4.

3.3.3 Morphometric analysis

Multivariate analysis of morphometric data (31 parameters) did not reveal significant differences in test morphology between foraminiferal tests from abyssal hills and plains. Further analyses using a reduced set of four parameters (convexity, maximum to minimum diameter ratio, perimeter to area ratio and sphericity) produced significant results (ANOSIM, $p < 0.01$), although further tests did not attribute this variation to any single morphometric character.

At the species level, ANOSIM with 31 morphometric parameters yielded significant differences related to topography only in the case of *A. glomerata* ($p = 0.035$). *Reophax* sp. 21 showed variation in test morphometry between hills and plains only when taking into account the reduced set of four parameters (ANOSIM, $p = 0.018$). Furthermore, Student's *t* and Mann–Whitney U tests identified differences in the convexity and sphericity of *N. dentaliniformis* ($p = 0.027$ and $p = 0.048$,

respectively) as well as in the maximum to minimum diameter ratio and sphericity of *Reophax* sp.21 ($p < 0.01$ in both cases).

All the morphometric characters estimated for the studied specimens can be found in Supplementary Material 3.B.

3.3.4 Elemental analysis

ESEM–EDS identified a total of 16 elements (10 major and 6 trace) from 56 benthic foraminiferal tests. Silica (Si) was by far the most abundant element, reflecting high quartz content, consistent with peaks in Si and oxygen (O) in most EDS spectra. WD-XRF identified a total of 11 major elements and 21 trace elements in the five sediment samples taken from the four study sites. Ca was the dominant element, with CaO constituting approximately 39% in all samples (41% and 37% in hill and plains samples, respectively) reflecting the presence of carbonate oozes at the PAP-SO. The next most abundant element was Si, with SiO constituting approximately 15% in all samples (14% and 17% in hill and plain samples, respectively).

The elemental composition of the foraminiferal tests was markedly different from that of the sediment samples (ANOSIM, $p < 0.01$; Fig. 3.4a). There was no significant correlation with topographic setting for all studied material (56 tests belonging to 10 species) or for individual species (*A. glomerata*, *Lagenammia* aff. *arenulata*, *N. dentaliniformis* and *Reophax* sp. 21). This was further demonstrated by the considerable overlap of species from both settings in the MDS plot (Fig. 3.4b). On the other hand, MDS of the sediment elemental data yielded distinct clusters for abyssal hill and abyssal plain sites, respectively (Fig. 3.4c). An additional t-test on the MDS X-ordinate of the five sediment samples was significant ($p < 0.01$), indicating distinct elemental profiles for abyssal hills and plain.

All the data used for the elemental analysis can be found in Supplementary Material 3.C.

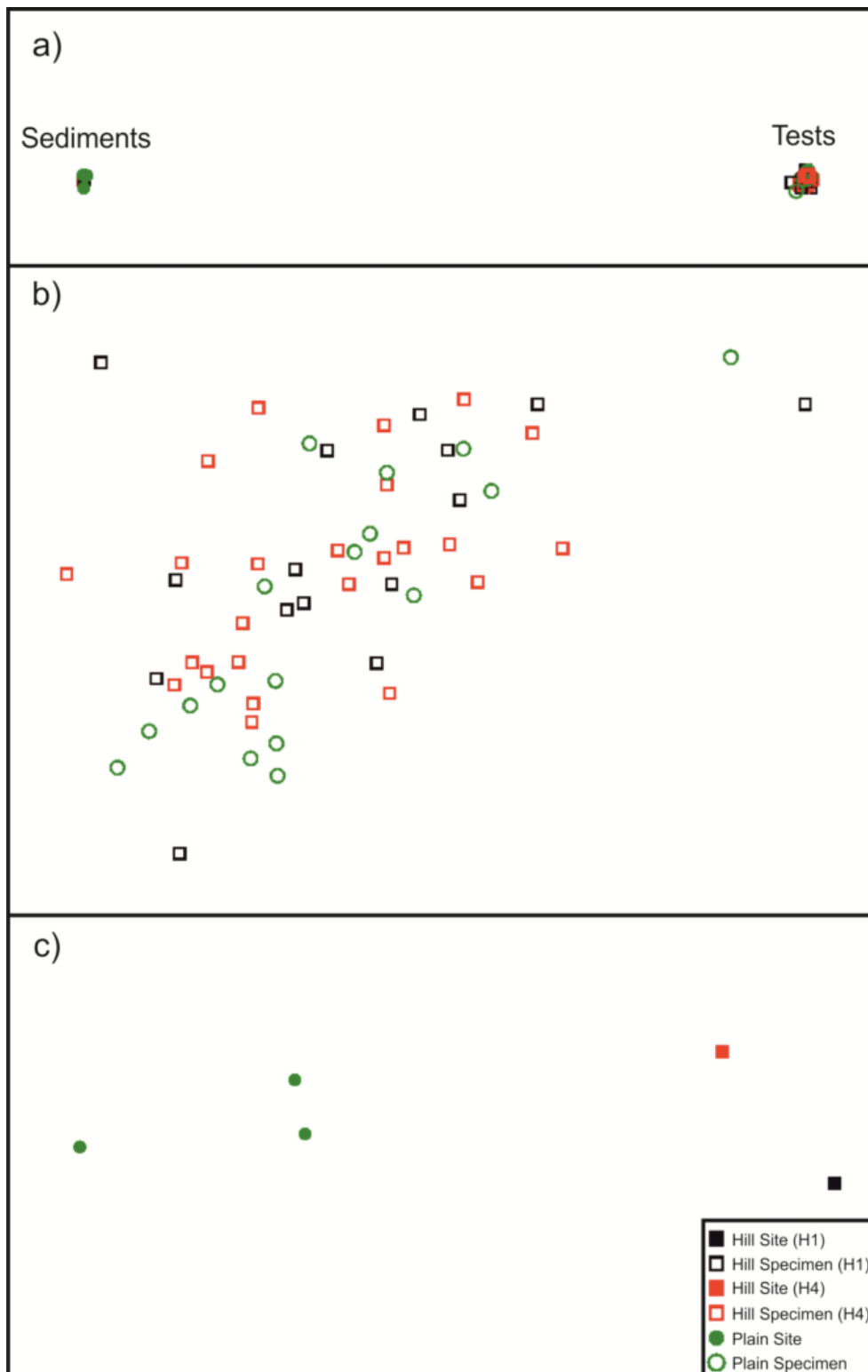


Fig. 3.4. (a) MDS on the elemental composition (13 common elements: 10 major, 3 trace) of 56 benthic foraminiferal tests and five sediment samples from four sites. (b) MDS on the elemental composition (16 elements: 10 major, 6 trace) of the 56 benthic foraminiferal tests. (c) MDS on the elemental (32 elements: 11 major, 21 trace) composition of the five sediment samples.

3.4 Discussion

3.4.1 Limitations of dataset

As our samples were fixed in formalin, we could not obtain molecular data to support our contention that the same foraminiferal species occur at the hill and plain sites. However, we took considerable care to compare specimens using light and scanning electron microscopy and are confident that similar specimens can be considered conspecific on the basis of morphological characters (see Appendix A).

The particle size analysis of the agglutinated tests was based on two-dimensional SEM images in which only one side of each specimen was visible. In addition, particles $<10\ \mu\text{m}$ were too small to be reliably measured from SEM images and therefore this finest sediment fraction could not be included in the analysis. Creating an automated, accurate and high-resolution (sub-micron scale) method for counting the entire range of agglutinated particles in benthic foraminiferal tests remains a challenge for the future.

3.4.2 Do agglutinated foraminifera utilize different sized particles in hill and plain settings?

In the deep sea, areas with elevated current activity have been shown to consist of coarse-grained sediments as a result of winnowing processes (Aller, 1989; Kaminski, 1985; Schröder, 1988); these areas include topographic high points such as seamounts (Genin et al., 1986; Levin and Nittrouer, 1987; Levin and Thomas, 1989). Although we lack current-meter data for our specific study sites, sediment grain-size distributions provide some indication of the hydrodynamic regime at our study sites. In the deep sea, sediments of the 10–63 μm range (sortable silt) are thought to be most easily eroded by current activity (McCave and Hall, 2006; McCave et al., 1995). Thus, higher proportions of particles $>63\ \mu\text{m}$ should be an indicator of enhanced current flow. This has been empirically established for a large abyssal hill (height $>900\ \text{m}$) in the PAP-SO area, where numerical modelling predictions of higher flow intensity above parts of the topographic feature correlated well with actual grain-size patterns (i.e. higher proportions of particles $>63\ \mu\text{m}$) found the sedimentary record (Turnewitsch et al.,

2013; Turnewitsch et al., 2004). The sediments on the abyssal hills that we sampled consisted, on average, of greater proportions of particles $>63\ \mu\text{m}$ compared to the adjacent abyssal plain (Fig. 3.3a; Table 3.3). In addition, hill sites from this area (including H1 and H4), were found to have greater median seabed slope compared to plain sites (including P3 and P4) (Durden et al., 2015). Considering the above, substantial hydrographic differences between our hill and plain sites (i.e. elevated current activity above the hills) are likely. These differences were found to have a significant effect on the faunal composition of benthic foraminifera from the same sites (Stefanoudis et al., 2015) and are going to be discussed in more detail in chapter 4.

Our present results suggest that differences in sediment granulometry between our plain and hill sites are reflected in differences in foraminiferal test agglutination. Specimens collected from abyssal hills agglutinated larger particles, mirroring the coarser nature of the surrounding sediments. This was evident simply from a visual comparison of specimens from the hill and plain settings, with the latter having a more irregular morphology than the former (Plates 3.1, Figs. 3–6; 3.2; 3.3), although those differences were not confirmed by numerical analyses. Similarly, at the species level statistical analyses revealed no significant differences in test particle size composition with topography for the rest of the species, except in the case of *A. glomerata*. This is probably because the number of large agglutinated grains ($>100\ \mu\text{m}$) was low in relation to the finer-grained component. A few coarse grains incorporated in an otherwise finely agglutinated foraminiferal test can have a disproportionate effect on its overall shape and appearance (e.g. Plate 3.2, Figs. 3–6). Another factor may be that we grouped together the two abyssal hill sites (H1 and H4), despite their significant bathymetric differences (see Table 3.1). H4 was located at the top of the highest and steepest hill and was characterised by a much larger fraction of particles $>63\ \mu\text{m}$ compared to H1 (Table 3.3). Similarly, pairwise comparisons using ANOSIM revealed that specimens from H4 had significantly coarser agglutination than those from H1. By amalgamating data from these two topographic high sites and comparing them to the plain, statistical differences in test particle size composition of foraminifera became insignificant.

Previous studies have suggested that particle selection by size occurs in some species of agglutinated foraminifera (Allen et al., 1999; Bartholdy et al., 2005; Bowser and Bernhard, 1993; Bowser et al., 2002; Gooday et al., 1995; Salami, 1976; Sliter, 1968). However, based on visual inspection of the specimens combined with statistical tests, we conclude that the agglutinated foraminiferal species included in this study were not selecting for particular particle sizes. Instead, the composition of their tests reflected the sedimentary environment in which they resided. In some early culture experiments, Slama (1954) observed that *Ammobaculites*, a genus included in the present study (Plate 3.3, Figs. 7–8), indiscriminately agglutinated particles of different composition and size. Since then, further studies have demonstrated non-selectivity for particle size in some agglutinated foraminifera (Armynot du Châtelet et al., 2013a,b; Buchanan and Hedley, 1960; Thomsen and Rasmussen, 2008; Wells, 1985). In a comparative study of benthic foraminiferal assemblages between two deep-sea habitats in the central north Pacific and western north Atlantic, Schröder (1986) and Schröder et al. (1988) found that certain species, including their *Reophax scorpiurus*, which resembles *Reophax* sp. 21 of the present study (see Appendix A), were non-selective for particle size and thus exhibited wide morphological variability in different sedimentary environments. Moreover, *Cyclammina pusilla* that usually uses small quartz grains for test construction was found to also incorporate volcanic ash grains in its test, as soon as these particles became prevalent in the sediments following the 1991 Mt Pinatubo eruption (Hess et al., 2000).

3.4.3 Does the composition of substratum affect test morphometry?

To our knowledge, only a few studies have examined the relationship between substratum and the test morphometry of agglutinated foraminifera. Hada (1957) observed that foraminifera living in coarser sediments have coarser test surfaces. Haake (1977) noted that tests of *Textularia pseudogamen* become broader (i.e. higher width/length ratio) on coarser sediments. Schröder (1986) and Schröder et al. (1988) commented on the intraspecific morphological variability of *Reophax* species as a response to different substratum characteristics (see previous section). Recently, Mancin et al. (2015) noted changes in the wall thickness of some agglutinated foraminifera that were linked to tephra deposits. With the exception of Haake (1977), the results from the rest of the studies were qualitative

as they were mainly based on visual observation of the tests. Such approaches can be informative and have been successfully applied in paleoenvironmental studies (e.g. Kaminski and Schröder, 1987). However, in order to detect trends in the shape of agglutinated tests under different environmental conditions, quantitative morphometric data are necessary. The present work is the first to investigate changes in test morphology related to different sedimentary environments both qualitatively (i.e. visual observation of tests) and quantitatively (i.e. by using a range of morphometric parameters).

We failed to find clear evidence for differences in particle size selection between the agglutinated foraminiferal tests from the hill and plain sites, despite the different granulometric profiles of the two topographic settings. Nevertheless, all species that could be compared directly had more irregularly shaped tests at the highest site (H4) as a result of the incorporation of a relatively few large grains (Plates 3.1, Figs. 3–6; 3.2; 3.3). This was particularly evident in the case of *Reophax* sp. 21. These obvious visual differences were confirmed by morphometric analyses. A comparison of all agglutinated tests between abyssal hill and plain sites demonstrated that there is a systematic morphometric difference that could not be expressed in terms of a single character. Instead, a combination of four parameters (convexity, maximum to minimum diameter ratio, perimeter to area ratio and sphericity) was more effective in differentiating tests from the two settings.

At the species level, differences in test morphology related to topography were significant for *A. glomerata*, *N. dentaliniformis* and *Reophax* sp. 21. In the case of *A. glomerata* it was the combined effect of all 31 morphometric parameters that drove the difference. Specimens from the plain sites were finely agglutinated with smooth and circular tests (Plate 3.3, Figs. 1–2), similar to previous descriptions of this species (see Appendix A), while hill specimens had a rougher surface (Plate 3.3, Figs. 3–4), a reflection of the coarser sediment fractions present in these settings. However, their general shape and outline remained recognisable in both cases and there was little doubt that they represented the same morphospecies. Specimens of *N. dentaliniformis* from the plain sites had low convexity and sphericity values consistent with their elongate tests (Plate 3.2, Fig. 3.1), while hill specimens commonly agglutinated large, rounded to sub-rounded grains, resulting

in a more spherical test (Plate 3.2, Fig. 3.2). Similarly, specimens of *Reophax* sp. 21 from the hills had lower maximum to minimum diameter ratios and higher sphericity than those from the plain. In this case, the incorporation of large particles obscured the basic test morphology, which often made identification more difficult (Plate 3.2, Figs. 5–6.). We conclude that the incorporation of large grains tends to make elongate tests more spherical in shape (*N. dentaliniformis*, *Reophax* sp. 21), and make spherical tests less spherical (*A. glomerata*).

3.4.4 Evidence of mineral selectivity

ESEM–EDS analyses revealed significant overlaps in the elemental composition of agglutinated tests in relation to topographic setting. In contrast, the elemental composition of hill and plain sediments was different when using the MDS x-ordinate as a variable in a Student's t-test ($p < 0.01$), most likely as result of the different environmental conditions prevalent in the two settings. For example, Turnewitsch et al. (2004) demonstrated hydrodynamic near-bottom sorting and selective deposition/erosion of particles of differing sizes and chemical composition on a large abyssal hill in the PAP-SO area. They concluded that area of increasing near-bottom flow (erosiveness) tended to have higher concentrations of large and heavy particles (e.g. Zircon) than more quiescent sites. In our case, sediments from the hill sites are subject to winnowing processes that preferentially remove the finer particles (e.g. coccoliths, small quartz grains) from the hilltops and deposit them on the adjacent plain, leaving the hill sediments enriched with coarser material (e.g. dead planktonic foraminifera tests, pebble to cobble-sized ice-rafted stones). It is likely that such processes are responsible for the distinct elemental profiles in the two settings.

The clear differences in the elemental composition of the tests and the sediments (Fig. 3.4a) indicated that foraminiferans favour certain minerals. The sediment at the PAP-SO is a carbonate ooze and as a result, many species found in the same area have tests made of planktonic foraminifera shells, including species of *Reophax* and *Lagenammia* (Goody et al., 2010, Figs. 13A–B; 14F). Thus the presence of agglutinated taxa with tests made exclusively of mineral grains indicates a certain degree of mineral selection. Based on EDS spectra, all the foraminifera in our samples had tests composed largely of quartz grains that were

held together by organic cement (Bender, 1989, 1995; Bender and Hemleben, 1988) regardless of species or site of origin. Quartz has been identified as the main test component of agglutinated foraminifera in marginal marine settings (Allen et al., 1999), the deep sea (Gooday, 1986; Gooday and Claugher, 1989) and in ancient marine environments (Mancin, 2001; Mancin et al., 2012), including carbonate-dominated habitats where this mineral occurred only in negligible amounts (Jørgensen, 1977). The selection of a quartz as a test component must confer certain benefits for the agglutinated foraminifera. Quartz is a stable mineral, with a consistent density and high resistance to weathering (Drever, 1985). Its use could help to make agglutinated foraminiferal tests more robust (Mancin et al., 2012), at least in the case of species with firmly cemented tests like *A. glomerata*, *Cribrostomoides* spp. or *Ammobaculites agglutinans* (Schröder, 1988), of which are present in our study sites (Plates 3.1, Figs. 3–10; 3.3, Figs. 1–4). Benthic foraminifera (mainly calcareous) living in physically stressed coastal habitats have stronger tests than those from nearby more tranquil localities (Wetmore, 1987). It is possible that a similar relationship applies in hydrographically different deep-sea settings.

3.4.5 Paleooceanographic significance

The rich fossil record of benthic foraminifera makes them ideal tools for paleoenvironmental reconstructions. Traditionally, there has been an emphasis on calcareous taxa due to their high fossilization potential (Gooday, 2003; Jorissen et al., 2007; Rohling and Cooke, 2003). However, agglutinated foraminifera are sometimes a major component of fossil assemblages, especially in “flysch-type” or “high latitude slope deep-water agglutinated foraminifera” faunas (Brouwer, 1965; Gradstein and Berggren, 1981; Kaminski et al., 1989a, b, 1995; Nagy et al., 1997, 2000; Peryt et al., 1997, 2004; Reolid et al., 2008, 2010; Setoyama et al., 2011; Waskowska, 2011) and can convey important palaeoecological information (Alve and Murray, 1999; Jones and Charnock, 1985; Murray and Alve, 1999a, b; Murray and Alve, 2001; Murray et al., 2011). Careful analysis has shown that modern agglutinated assemblages provide effective proxies for inferring past ecological conditions (Jones, 1999; Jones et al., 2005; Kaminski and Schröder, 1987; Kender et al., 2008; Nagy, 1992; Preece et al., 1999). Additional studies on modern agglutinated foraminiferal faunas will help to refine their use in paleoceanography.

The present results indicate that some abyssal NE Atlantic species are fairly consistent in terms of their test elemental composition, and hence presumably their selection of particular minerals (predominately quartz). Although we found no statistical support for selection of particles in terms of size, there were differences in terms of the visual appearance and overall morphometry of the tests, which were more irregularly shaped ('lumpier') at the hill sites, H4 in particular. These characteristics (incorporation of coarse particles, test morphometry) could provide evidence for the recognition of ancient abyssal hills environments, as well as other palaeoceanographic settings that were characterised by enhanced current flow (Kaminski, 1985; Kaminski and Schröder, 1987; Nagy et al., 1997). Certain taxa are clearly better suited to this task than others. In accordance with our findings, *A. glomerata*, *Cribrostomoides subglobosus* and species of the genus *Reophax* have been elsewhere reported to reflect the nature of the surrounding sediments (Schröder et al., 1988). These taxa, which are an important component of modern foraminiferal assemblages in the PAP-SO area, could be potential indicators of ancient environments exposed to enhanced near-bottom flow, complementing proxies based on the analysis of sediment characteristics.

References of Chapter 3

- Abbireddy, C.O.R., Clayton, C.R.I., 2009. A review of modern particle sizing methods. *Proceedings of the Institution of Civil Engineers-Geotechnical Engineering*, 162, 193–201.
- Adl, S.M., Simpson, A.G.B., Lane, C.E., Lukes, J., Bass, D., Bowser, S.S., Brown, M.W., Burki, F., Dunthorn, M., Hampl, V., Heiss, A., Hoppenrath, M., Lara, E., le Gall, L., Lynn, D.H., McManus, H., Mitchell, E.A.D., Mozley-Stanridge, S.E., Parfrey, L.W., Pawlowski, J., Rueckert, S., Shadwick, L., Schoch, C.L., Smirnov, A., Spiegel, F.W., 2012. The revised classification of eukaryotes. *Journal of Eukaryotic Microbiology*, 59, 429–493.
- Allen, K., Roberts, S., Murray, J.W., 1999. Marginal marine agglutinated foraminifera: affinities for mineral phases. *Journal of Micropalaeontology*, 18, 183–191.
- Aller, J.Y., 1989. Quantifying sediment disturbance by bottom currents and its effect on benthic communities in a deep-sea western boundary zone. *Deep-Sea Research Part A—Oceanographic Research Papers*, 36, 901–934.
- Alve, E., Murray, J.W., 1999. Marginal marine environments of the Skagerrak and Kattegat: a baseline study of living (stained) benthic foraminiferal ecology. *Palaeogeography Palaeoclimatology Palaeoecology*, 146, 171–193.
- Armynot du Châtelet, E., Bout-Roumazeilles, V., Coccioni, R., Frontalini, F., Guillot, F., Kaminski, M.A., Recourt, P., Riboulleau, A., Trentesaux, A., Tribovillard, N., Ventalon, S., 2013a. Environmental control on shell structure and composition of agglutinated foraminifera along a proximal-distal transect in the Marmara Sea. *Marine Geology*, 335, 114–128.
- Armynot du Châtelet, E., Frontalini, F., Guillot, F., Recourt, P., Ventalon, S., 2013b. Surface analysis of agglutinated benthic foraminifera through ESEM-EDS and Raman analyses: An expeditious approach for tracing mineral diversity. *Marine Micropaleontology*, 105, 18–29.
- Armynot du Châtelet, E., Noiriel, C., Delaine, M., 2013c. Three-dimensional morphological and mineralogical characterization of testate amebae. *Microscopy and Microanalysis*, 19, 1511–1522.
- Baldrighi, E., Lavaleye, M., Aliani, S., Conversi, A., Manini, E., 2014. Large spatial scale variability in bathyal macrobenthos abundance, biomass, α - and β -diversity along the Mediterranean continental margin. *Plos One*, 9, e107261.
- Bartholdy, J., Leipe, T., Frenzel, P., Tauber, F., Bahlo, R., 2005. High resolution single particle analysis by scanning electron microscopy: a new tool to investigate the mineral composition of agglutinated foraminifers. *Methods and Applications in Micropalaeontology*, 124, 53–65.
- Bender, H., Hemleben, C., 1988. Constructional aspects in test formation of some agglutinated foraminifera. *Abhandlungen der Geologischen Bundesanstalt*, 41, 13–12.
- Bender, H., 1989. Gehäuseaufbau, Gehäusegenese und Biologie agglutiniertes Foraminiferen (Sarcodina, Textulariina). *Jahrbuch der Geologischen Bundesanstalt*, 133, 259–347.
- Bender, H., 1995. Test structure and classification in agglutinated foraminifera. In: Kaminski, M.A., Geroch, S., Gasinski, M.A. (Eds.), *Proceedings of the Fourth International Workshop on Agglutinated Foraminifera*, Vol. 3 (pp. 27–70).

- Bowser, S.S., Bernhard, J.M., 1993. Structure, bioadhesive distribution and elastic properties of the agglutinated test of *Astrammmina rara* (Protozoa, Foraminiferida). *Journal of Eukaryotic Microbiology*, 40, 121–131.
- Bowser, S.S., Bernhard, J.M., Habura, A., Gooday, A.J., 2002. Structure, taxonomy and ecology of *Astrammmina triangularis* (Earland), an allogromiid-like agglutinated foraminifer from Explorers Cove, Antarctica. *Journal of Foraminiferal Research*, 32, 364–374.
- Brouwer, J., 1965. Agglutinated foraminiferal faunas from some turbiditic sequences I, II. *Proceedings Koninklijke Nederlandse Akademie van Wetenschappen series B*, 68, 309–334.
- Buchanan, J.B., Hedley, R.H., 1960. A contribution to the biology of *Astrorhiza limicola* (Foraminifera). *Journal of the Marine Biological Association of the United Kingdom*, 39, 549–560.
- Clark, M.R., Rowden, A.A., Schlacher, T., Williams, A., Consalvey, M., Stocks, K.I., Rogers, A.D., O'Hara, T.D., White, M., Shank, T.M., Hall-Spencer, J.M., 2010. The ecology of seamounts: structure, function, and human impacts. *Annual Review of Marine Science*, 2, 253–278.
- Clarke, K.R., Gorley, R.N., 2006. *PRIMER v6: User Manual/Tutorial*. PRIMER-E, Plymouth, UK.
- Drever, J.I., 1985. *The Chemistry of Weathering*. New York, Reidel.
- Durden, J.M., Bett, B.J., Jones, D.O.B., Huvenne, V.A.I., Ruhl, H.A., 2015. Abyssal hills – hidden source of increased habitat heterogeneity, benthic megafaunal biomass and diversity in the deep sea. *Progress in Oceanography*, 137, 209–218.
- Gage, J.D., Lamont, P.A., Tyler, P.A., 1995. Deep-sea macrobenthic communities at contrasting sites off Portugal, preliminary results. I Introduction and diversity comparisons. *Internationale Revue Der Gesamten Hydrobiologie*, 80, 235–250.
- Gage, J.D., Bett, B.J., 2005. Deep-sea benthic sampling. In: Eleftheriou, A., MacIntyre, A.D. (Eds.), *Methods for the study of marine benthos*, 3rd ed. (pp. 273–325). Oxford, UK: Blackwell Scientific.
- Genin, A., Dayton, P.K., Lonsdale, P.F., Spiess, F.N., 1986. Corals on seamount peaks provide evidence of current acceleration over deep-sea topography. *Nature*, 322, 59–61.
- Goff, J.A., Arbic, B.K., 2010. Global prediction of abyssal hill roughness statistics for use in ocean models from digital maps of paleo-spreading rate, paleo-ridge orientation, and sediment thickness. *Ocean Modelling*, 32, 36–43.
- Gooday, A.J., 1986. Meiofaunal foraminiferans from the bathyal Porcupine Seabight (northeast Atlantic): size structure, standing stock, taxonomic composition, species-diversity and vertical-distribution in the sediment. *Deep Sea Research Part A–Oceanographic Research Papers*, 33, 1345–1373.
- Gooday, A.J., Claugher, D., 1989. The genus *Bathysiphon* (Protista, Foraminiferida) in the northeast Atlantic: SEM observations on the wall structure of seven species. *Journal of Natural History*, 23, 591–611.
- Gooday, A.J., Levin, L.A., Linke, P., Heeger, T., 1992. The role of benthic foraminifera in deep-sea food webs and carbon cycling. *Deep-Sea Food Chains and the Global Carbon Cycle*, 360, 63–91.

- Gooday, A.J., Nott, J.A., Davis, S., Mann, S., 1995. Apatite particles in the test wall of the large agglutinated foraminifer *Bathysiphon major* (Protista). *Journal of the Marine Biological Association of the United Kingdom*, 75, 469–481.
- Gooday, A.J., 2003. Benthic foraminifera (protista) as tools in deep-water palaeoceanography: Environmental influences on faunal characteristics. *Advances in Marine Biology*, 46, 1–90.
- Gooday, A.J., Malzone, M.G., Bett, B.J., Lamont, P.A., 2010. Decadal-scale changes in shallow-infaunal foraminiferal assemblages at the Porcupine Abyssal Plain, NE Atlantic. *Deep-Sea Research Part II–Topical Studies in Oceanography*, 57, 1362–1382.
- Gradstein, F.M., Berggren, W.A., 1981. Flysch-type agglutinated foraminifera and the Maestrichtian to Paleogene history of the Labrador and North Seas. *Marine Micropaleontology*, 6, 211–268.
- Haake, F.-W., 1977. Living benthic foraminifera in the Adriatic Sea: influence of water depth and sediment. *The Journal of Foraminiferal Research*, 7, 62–75.
- Hada, Y., 1957. Biology of the arenaceous foraminifera. *Journal of Science of the Suzugamine Women's College, Hiroshima, Japan*, 3, 31–50.
- Hartman, S.E., Lampitt, R.S., Larkin, K.E., Pagnani, M., Campbell, J., Gkritzalis, T., Jiang, Z.P., Pebody, C.A., Ruhl, H.A., Gooday, A.J., Bett, B.J., Billett, D.S.M., Provost, P., McLachlan, R., Turton, J.D., Lankester, S., 2012. The Porcupine Abyssal Plain fixed-point sustained observatory (PAP-SO): variations and trends from the Northeast Atlantic fixed-point time-series. *ICES Journal of Marine Science: Journal du Conseil*, 69, 776–783.
- Hasemann, C., Soltwedel, T., 2011. Small-scale heterogeneity in deep-sea nematode communities around biogenic structures. *Plos One*, 6, 1–13.
- Heezen, B.C., Tharp, M., Ewing, M., 1959. The floors of the oceans: I. The North Atlantic. *Geological Society of America Special Paper*, 65, 1–126.
- Heezen, B.C., Holcombe, T.L., 1965. Geographic distribution of bottom roughness in the North Atlantic. (p. 41). Palisades, New York, N.Y.: Lamont Geological Observatory, Columbia University.
- Hess, S., Kuhnt, W., Spivey, B., Kaminski, M.A., Whittaker, J.E., 2000. Ash grains of the 1991 Mt Pinatubo eruption as a tracer in Rose Bengal stained deep sea agglutinated foraminifera: How old is Freddy? In: Hart, M.B., Kaminski, M.A., Smart, C.W. (Eds.), *Proceedings of the Fifth International Workshop on Agglutinated Foraminifera* (p. 126).
- Jones, R.W., Charnock, M.A., 1985. Morphogroups of agglutinated foraminifera. Their life positions and feeding habits and potential applicability in (paleo)ecological studies. *Revue de Paléobiologie*, 4, 311–320.
- Jones, R.W., 1999. Forties Field (North Sea) revisited: a demonstration of the value of historical micropalaeontological data. *Biostratigraphy in Production and Development Geology*, 152, 185–200.
- Jones, R.W., Pickering, K.T., Boudagher-Fadel, M., Matthews, S., 2005. Preliminary observations on the micropalaeontological characterization of submarine fan/channel sub-environments, Ainsa System, south-central Pyrenees, Spain. *Recent Developments in Applied Biostratigraphy*, 55–68.

- Jørgensen, N.O., 1977. Wall structure of some arenaceous foraminifera from the Maastrichtian White Chalk (Denmark) *Journal of Foraminiferal Research*, 7, 313–321.
- Jorissen, F.J., Fontanier, C., Thomas, E., 2007. Paleoceanographical proxies based on deep-sea benthic foraminiferal assemblage characteristics. In: Hillaire-Marcel, C., de Vernal, A. (Eds.), *Proxies in Late Cenozoic Paleoceanography: Pt. 2: Biological tracers and biomarkers* (pp. 263–326).
- Kaminski, M.A., 1985. Evidence for control of abyssal agglutinated foraminiferal community structure by substrate disturbance: results from the HEBBLE area. *Marine Geology*, 66, 113–131.
- Kaminski, M.A., Schröder, C.J., 1987. Environmental analysis of deep-sea agglutinated foraminifera: can we distinguish tranquil from disturbed environments? In: Barnette, S.C., Butler, D.M. (Eds.), *Gulf Coast Section SEPM Foundation Eighth Annual Research Conference. Selected papers and illustrated abstracts* (pp. 90–93).
- Kaminski, M.A., Gradstein, F.M., Berggren, W.A., 1989a. Paleogene benthic foraminifer biostratigraphy and paleoecology at Site 647, southern Labrador Sea. *Proceedings of the Ocean Drilling Program: Scientific Results*, 105, 705–730.
- Kaminski, M.A., Gradstein, F.M., Scott, D.B., Mackinnon, K.D., 1989b. Neogene benthic foraminiferal stratigraphy and deep water history of Sites 645, 646, and 647, Baffin Bay and Labrador Sea. *Proceedings of the Ocean Drilling Program: Scientific Results*, 105, 731–756.
- Kaminski, M.A., Boersma, M., Tyszka, J., Holbourn, A.E.L., 1995. Response of deep-water agglutinated foraminifera to dysoxic conditions in the California Borderland basins. In: Kaminski, M.A., Geroch, S., Gasifski, M.A. (Eds.), *Proceedings of the Fourth International Workshop on Agglutinated Foraminifera, Kraków, Poland, September 12-19, 1993* (pp. 131–140).
- Kender, S., Kaminski, M.A., Jones, R.W., 2008. Early to middle Miocene foraminifera from the deep-sea Congo Fan, offshore Angola. *Micropaleontology*, 54, 477–568.
- Levin, L.A., Demaster, D.J., Mccann, L.D., Thomas, C.L., 1986. Effects of giant protozoans (class Xenophyophorea) on deep-seamount benthos. *Marine Ecology Progress Series*, 29, 99–104.
- Levin, L.A., Nittrouer, C.A., 1987. Textural characteristics of sediments on deep seamounts in the eastern Pacific Ocean between 10°N and 30°N. *Seamounts, Islands, and Atolls*, 43, 187–203.
- Levin, L.A., Thomas, C.L., 1989. The influence of hydrodynamic regime on infaunal assemblages inhabiting carbonate sediments on central Pacific seamounts. *Deep-Sea Research Part A—Oceanographic Research Papers*, 36, 1897–1915.
- Mancin, N., 2001. Agglutinated foraminifera from the Epiligurian succession (Middle Eocene/Lower Miocene, Northern Apennines, Italy): Scanning electron microscopic characterization and paleoenvironmental implications. *Journal of Foraminiferal Research*, 31, 294–308.
- Mancin, N., Basso, E., Pirini, C., Kaminski, M.A., 2012. Selective mineral composition, functional test morphology and paleoecology of the agglutinated foraminiferal genus *Colominella* Popescu, 1998 in the Mediterranean Pliocene (Liguria, Italy). *Geologica Carpathica*, 63, 491–502.

- Mancin, N., Basso, E., Lupi, C., Cobianchi, M., Hayward, B.W., 2015. The agglutinated foraminifera from the SW Pacific bathyal sediments of the last 550 kyr: Relationship with the deposition of tephra layers. *Marine Micropaleontology*, 115, 39–58.
- McCave, I.N., Manighetti, B., Robinson, S.G., 1995. Sortable silt and fine sediment size composition slicing: parameters for paleocurrent speed and paleoceanography. *Paleoceanography*, 10, 593–610.
- McCave, I.N., Hall, I.R., 2006. Size sorting in marine muds: Processes, pitfalls, and prospects for paleoflow-speed proxies. *Geochemistry Geophysics Geosystems*, 7, 1–37.
- Murray, J.W., Alve, E., 1999a. Taphonomic experiments on marginal marine foraminiferal assemblages: how much ecological information is preserved? *Palaeogeography Palaeoclimatology Palaeoecology*, 149, 183–197.
- Murray, J.W., Alve, E., 1999b. Natural dissolution of modern shallow water benthic foraminifera: taphonomic effects on the palaeoecological record. *Palaeogeography Palaeoclimatology Palaeoecology*, 146, 195–209.
- Murray, J.W., Alve, E., 2001. Do calcareous dominated shelf foraminiferal assemblages leave worthwhile ecological information after their dissolution? In: M. B. Hart, M. A. Kaminski, Smart, C.W. (Eds.), *Proceedings of the Fifth International Workshop on Agglutinated Foraminifera, Plymouth, U.K., September 6–16, 1997* (pp. 311–331).
- Murray, J.W., Alve, E., Jones, B.W., 2011. A new look at modern agglutinated benthic foraminiferal morphogroups: their value in palaeoecological interpretation. *Palaeogeography Palaeoclimatology Palaeoecology*, 309, 229–241.
- Nagy, J., 1992. Environmental significance of foraminiferal morphogroups in Jurassic North Sea deltas. *Palaeogeography Palaeoclimatology Palaeoecology*, 95, 111–134.
- Nagy, J., Kaminski, M.A., Johnsen, K., Mittlehner, A.G., 1997. Foraminiferal, palynomorph, and diatom biostratigraphy and paleoenvironments of the Tork Formation: a reference section for the Paleocene–Eocene transition in the western Barents Sea. In: Hass, H.C., Kaminski, M.A. (Eds.), *Contributions to the Micropaleontology and Paleoceanography of the Northern North Atlantic*, Vol. 5 (pp. 15–38).
- Nagy, J., Kaminski, M.A., Kuhnt, W., Bremer, M.A., 2000. Agglutinated foraminifera from neritic to bathyal facies in the Palaeogene of Spitsbergen and the Barents Sea In: Hart, M.B., Kaminski, M.A., Smart, C.W. (Eds.), *Proceedings of the Fifth International Workshop on Agglutinated Foraminifera*. (pp. 333–361).
- Peryt, D., Lahodynsky, R., Durakiewicz, T., 1997. Deep-water agglutinated foraminiferal changes and stable isotope profiles across the Cretaceous–Paleogene boundary in the Rotwandgraben section, Eastern Alps (Austria). *Palaeogeography Palaeoclimatology Palaeoecology*, 132, 287–307.
- Peryt, D., Alegret, L., Molina, E., 2004. Agglutinated foraminifera and their response to the Cretaceous/Paleogene (K/P) boundary event at Ain Settara, Tunisia. In: Bubik, M., Kaminski, M.A. (Eds.), *Proceedings of the Sixth International Workshop on Agglutinated Foraminifera* (pp. 393–412).
- Pitcher, T.J., Morato, T., Hart, P.J.B., Clark, M.R., Haggan, N., Santos, R.S., 2007. *Seamounts: ecology, fisheries, and conservation*. Oxford, UK: Blackwell.

- Preece, R.C., Kaminski, M.A., Dignes, T.W., 1999. Miocene benthonic foraminiferal morphogroups in an oxygen minimum zone, offshore Cabinda. In: Cameron, N.R., Bate, R.H., Clure, V.S. (Eds.), *The oil and gas habitats of the South Atlantic* (pp. 267–282).
- Reolid, M., Rodriguez-Tovar, F.J., Nagy, J., Oloriz, F., 2008. Benthic foraminiferal morphogroups of mid to outer shelf environments of the Late Jurassic (Prebetic Zone, southern Spain): Characterization of biofacies and environmental significance. *Palaeogeography Palaeoclimatology Palaeoecology*, 261, 280–299.
- Reolid, M., Nagy, J., Rodriguez-Tovar, F.J., 2010. Ecostratigraphic trends of Jurassic agglutinated foraminiferal assemblages as a response to sea-level changes in shelf deposits of Svalbard (Norway). *Palaeogeography Palaeoclimatology Palaeoecology*, 293, 184–196.
- Rex, M.A., Etter, R.J., 2010. *Deep-sea biodiversity: pattern and scale*. Cambridge: Harvard University Press.
- Rohling, E.J., Cooke, S., 2003. Stable oxygen and carbon isotopes in foraminiferal carbonate shells. In: Gupta, B.K.S. (Ed.), *Modern foraminifera* (pp. 239–258). Netherlands: Springer
- Ruggiero, M.A., Gordon, D.P., Orrell, T.M., Bailly, N., Bourgoin, T., Brusca, R.C., Cavalier-Smith, T., Guiry, M.D., Kirk, P.M., 2015. A higher level classification of all living organisms. *Plos One*, 10, 1–60.
- Ruhl, H.A., 2012. RRS James Cook Cruise 62, 24 Jul-29 Aug 2011. Porcupine Abyssal Plain - sustained observatory research. *National Oceanography Centre Cruise Report* (p. 119). Southampton, UK: National Oceanography Centre.
- Salami, M.B., 1976. Biology of *Trochammina* cf. *T. quadriloba* Høglund (1947), an agglutinating foraminifer. *Journal of Foraminiferal Research*, 6, 142–153.
- Schröder, C.J., 1986. Deep-water arenaceous foraminifera in the northwest Atlantic Ocean *Canadian Technical Report of Hydrography and Ocean Sciences*, 71, 1–191.
- Schröder, C.J., 1988. Subsurface preservation of agglutinated foraminifera in the Northwest Atlantic Ocean. *Abhandlungen der Geologischen Bundesanstalt*, 41, 325–336.
- Schröder, C.J., Scott, D.B., Medioli, F.S., Bernstein, B.B., Hessler, R.R., 1988. Larger agglutinated Foraminifera: comparison of assemblages from central North Pacific and Western North Atlantic (Nares Abyssal Plain). *Journal of Foraminiferal Research*, 18, 25–41.
- Setoyama, E., Kaminski, M.A., Tyszka, J., 2011. The Late Cretaceous-Early Paleocene palaeobathymetric trends in the southwestern Barents Sea – Palaeoenvironmental implications of benthic foraminiferal assemblage analysis. *Palaeogeography Palaeoclimatology Palaeoecology*, 307, 44–58.
- Slama, D.C., 1954. Arenaceous tests in foraminifera: an experiment. *The Micropaleontologist*, 8, 33–34.
- Sliter, W.V., 1968. Shell material variation in the agglutinated foraminifer *Trochammina pacifica* Cushman. *Tulane Studies Geology and Paleontology*, 6, 80–84.
- Snelgrove, P.V.R., Smith, C.R., 2002. A riot of species in an environmental calm: The paradox of the species-rich deep-sea floor. *Oceanography and Marine Biology: An Annual Review*, 40, 311–342.

- Stefanoudis, P.V., Bett, B.J., Gooday, A.J., 2015. Hills and plains: the influence of topography on deep-sea benthic foraminiferal assemblages. *14th Deep-Sea Biology Symposium* (pp. 174–175): UA Editora, Universidade De Aveiro.
- Stuart, C.T., Arbizu, P.M., Smith, C.R., Molodtsova, T., Brandt, A., Etter, R.J., Escobar-Briones, E., Fabri, M.C., Rex, M.A., 2008. CeDAMar global database of abyssal biological sampling. *Aquatic Biology*, 4, 143–145.
- Thistle, D., 1983. The stability time hypothesis as a predictor of diversity in deep-sea soft-bottom communities: a test. *Deep-Sea Research Part A–Oceanographic Research Papers*, 30, 267–277.
- Thistle, D., Eckman, J.E., 1990. The effect of a biologically produced structure on the benthic copepods of a deep-sea site. *Deep-Sea Research Part A–Oceanographic Research Papers*, 37, 541–554.
- Thomsen, E., Rasmussen, T.L., 2008. Coccolith-agglutinating foraminifera from the early Cretaceous and how they constructed their tests. *Journal of Foraminiferal Research*, 38, 193–214.
- Turnewitsch, R., Reyss, J.L., Chapman, D.C., Thomson, J., Lampitt, R.S., 2004. Evidence for a sedimentary fingerprint of an asymmetric flow field surrounding a short seamount. *Earth and Planetary Science Letters*, 222, 1023–1036.
- Turnewitsch, R., Falahat, S., Nycander, J., Dale, A., Scott, R.B., Furnival, D., 2013. Deep-sea fluid and sediment dynamics—Influence of hill- to seamount-scale seafloor topography. *Earth-Science Reviews*, 127, 203–241.
- Warren, R., VanDerWal, J., Price, J., Welbergen, J.A., Atkinson, I., Ramirez-Villegas, J., Osborn, T.J., Jarvis, A., Shoo, L.P., Williams, S.E., 2013. Quantifying the benefit of early climate change mitigation in avoiding biodiversity loss. *Nature Climate Change*, 3, 678–682.
- Waskowska, A., 2011. Response of Early Eocene deep-water benthic foraminifera to volcanic ash falls in the Polish Outer Carpathians: Palaeocological implications. *Palaeogeography Palaeoclimatology Palaeoecology*, 305, 50–64.
- Watling, L., Guinotte, J., Clark, M.R., Smith, C.R., 2013. A proposed biogeography of the deep ocean floor. *Progress in Oceanography*, 111, 91–112.
- Wells, P.E., 1985. Recent agglutinated benthonic Foraminifera (Suborder Textulariina) of Wellington Harbor, New Zealand. *New Zealand Journal of Marine and Freshwater Research*, 19, 575–599.
- Yesson, C., Clark, M.R., Taylor, M.L., Rogers, A.D., 2011. The global distribution of seamounts based on 30 arc seconds bathymetry data. *Deep-Sea Research Part I–Oceanographic Research Papers*, 58, 442–453.

Chapter 4: Abyssal hills: influence of topography on benthic foraminiferal assemblages

Abstract

Abyssal plains, often thought of as vast flat areas, encompass a variety of terrains including abyssal hills, features that constitute the single largest landscape type on Earth. The potential influence on deep-sea benthic faunas of mesoscale habitat complexity arising from the presence of abyssal hills is still poorly understood. To address this issue we focus on benthic foraminifera (testate protists) in the >150- μm fraction of Megacorer samples (0–1 cm layer) collected at five different sites in the area of the Porcupine Abyssal Plain Sustained Observatory (NE Atlantic, 4850 m water depth). Three sites are located on the tops of small abyssal hills (~200–500 m elevation) and two on the adjacent abyssal plain. We examined benthic foraminiferal assemblage characteristics (standing stock, diversity, composition) in relation to seafloor topography (hills vs. plain). Density and rarefied diversity were not significantly different between the hills and the plain. Nevertheless, hills do support a higher species density (i.e. species per unit area), a distinct fauna, and act to increase the regional species pool. Topographically enhanced bottom-water flows that influence food availability and sediment type are suggested as the most likely mechanisms responsible for these differences. Our findings highlight the potential importance of mesoscale heterogeneity introduced by relatively modest topography in regulating abyssal foraminiferal diversity. Given the predominance of abyssal hill terrain in the global ocean, we suggest the need to include faunal data from abyssal hills in assessments of abyssal ecology.

4.1 Introduction

The abyssal zone (~3500–6500 m water depth) occupies 27% of the entire ocean depth range as well as almost 65% and 85% of Earth's surface and ocean floor, respectively (Harris et al., 2014; Watling et al., 2013). However, only an estimated 1.4×10^{-9} % of this large biome has been sampled to date (Stuart et al., 2008). Most of that sampling effort has been focused on abyssal plains, topographically flat (i.e.

homogeneous) soft-bottom areas of the ocean (Heezen and Laughton, 1963). The plains are commonly regarded as the dominant topographic feature of the abyss, with the result that the terms abyssal plain and abyssal zone are often been used interchangeably in the scientific literature (e.g. Ebbe et al., 2010; Ramirez-Llodra et al., 2010; Stuart et al., 2008). On the other hand, marine geologists and geophysicists have reported the presence of numerous abyssal hills, small topographic rises <1000 m in height, for almost 60 years (Goff, 1998; Heezen et al., 1959; Macdonald et al., 1996). Recently, Harris et al. (2014) estimated that hills (300–1000 m in height) cover almost 50% and >40% of the abyssal and global seafloor, respectively, making them the most pervasive landform on Earth as well as in the abyss. It is clear that the widespread occurrence of abyssal hills in the oceans increases mesoscale (metre to kilometre) habitat heterogeneity and complexity in the abyss (Bell, 1979), with potentially significant effects on the density, diversity and distribution of deep-sea benthic organisms (Rex and Etter, 2010; Snelgrove and Smith, 2002).

Deep-sea studies investigating the effects of habitat heterogeneity on benthic faunas have focused mainly on small spatial scales (centimetres to metres) represented by biogenic structures and the patchy distribution of organic matter (Buhl-Mortensen et al., 2010; Grassle and Morse-Porteous, 1987; Hasemann and Soltwedel, 2011; Levin et al., 1986; Rice and Lambshead, 1994). Others have addressed broader scales by comparing assemblages from environmentally contrasting habitats (Gage et al., 1995; Kaminski, 1985; Menot et al., 2010; Schönfeld, 1997, 2002a; Thistle, 1983). However, only a few recent studies (e.g., Durden et al., 2015, on megafauna; Laguionie-Marchais, 2015, on macrofauna; Morris et al., 2016, on megafauna and organic matter supply) have considered the impacts of abyssal hills on deep-sea communities and none has focused on smaller organisms such as foraminifera.

Benthic foraminifera are single-celled eukaryotes (protists) that produce a 'test' (shell) and are very common in marine environments from intertidal mudflats to the greatest ocean depths. In the deep sea they often account for >50% of the meiofauna (32 or 63 to 300 μm) (Gooday, 2014; Snider et al., 1984), while larger species constitute a significant proportion of the macrofauna (300–1000 μm) (Bernstein et al., 1978; Tendal and Hessler, 1977) and even the megafauna (e.g.,

Gooday et al., 2011; Amon et al., 2016). Foraminifera play an important role in ecological processes on the seafloor (e.g. Gooday et al., 1992, 2008) and their abundance is closely related to levels of organic matter input and dissolved oxygen concentrations in the near-bottom water (e.g. Jorissen et al., 1995). In addition, calcareous benthic foraminifera have an excellent fossil record and are commonly utilized as proxies for reconstructing past ocean conditions (Gooday, 2003; Jorissen et al., 2007).

The aim of this study was to examine the potential effects of seafloor topography on benthic foraminiferal assemblages from the Porcupine Abyssal Plain Sustained Observatory area (PAP-SO, Hartman et al., 2012) in the Northeast Atlantic (4850 m water depth), a largely flat area populated by a number of abyssal hills (see Supplementary Material 4.A). There has been a long history of research at the PAP-SO dating back to the 1980s (Lampitt et al., 2010a), including foraminiferal studies (Gooday et al., 2010; Stefanoudis and Gooday, 2015; Chapter 2). However, the ecological significance of the abyssal hills in this area has only recently been appreciated (Durden et al., 2015; Morris et al., 2016). An earlier investigation established that differences in sediment characteristics between the hills and the adjacent plain had a significant effect in the agglutination patterns and test morphometry of certain benthic foraminifera (Stefanoudis et al., 2016; Chapter 3). Here, we investigate whether abyssal hills: i) modify standing stocks of benthic foraminifera, ii) influence foraminiferan diversity, locally and/or regionally, and iii) support distinct benthic foraminiferal communities compared to the adjacent plain.

4.2 Environmental characteristics of the study area

The water column overlying the PAP-SO area is subject to seasonal fluctuations in primary production and fluxes of organic matter to the seafloor (Rice et al., 1994). Deep ocean particle flux has been monitored since 1989 using sediment traps (Frigstad et al., 2015; Lampitt et al., 2010b). Sedimentation rates on the plain in the PAP-SO area are around 3.5 cm ky⁻¹ (Billett and Rice, 2001). Oxygen penetrates at least 25 cm into the sediment (Rutgers van der Loeff and Lavaleye, 1986). Both hill and plain sediments have a bimodal particle size distribution, with a

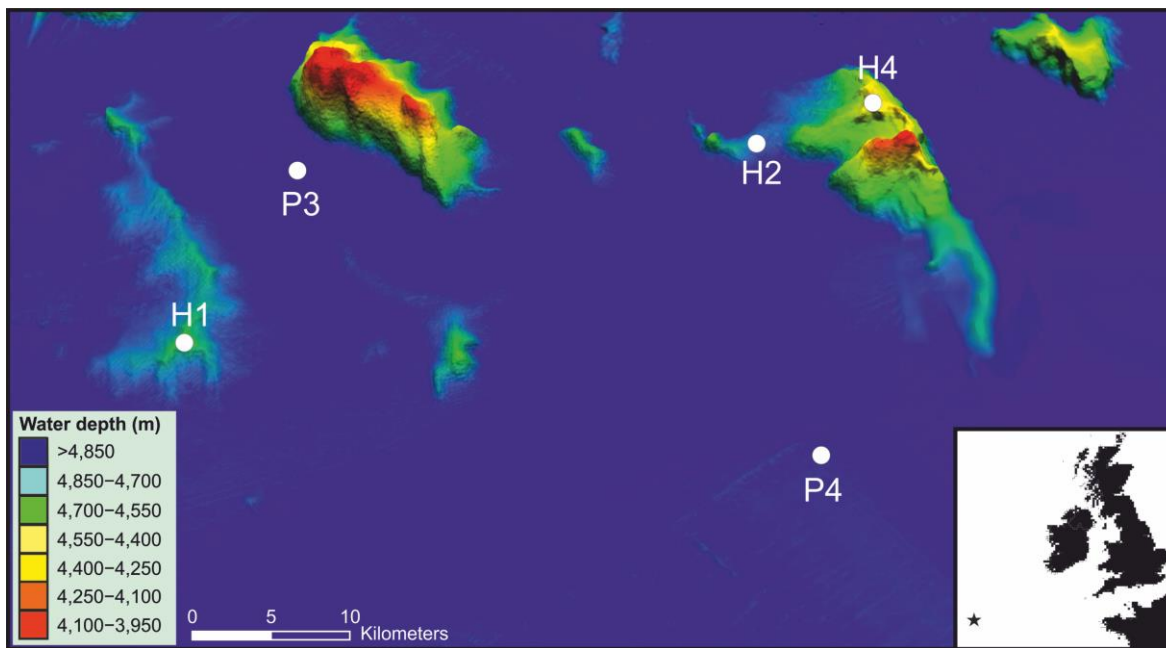


Fig. 4.1. 3D topographic representation of the PAP-SO area (48.79 to 49.21 °N, 16.03 to 16.93 °W) indicating the approximate location and bathymetry of the five study sites H1, H2 and H4 (abyssal hill sites) and P3 and P4 (abyssal plain sites). The inset shows the general location (star) of the Porcupine Abyssal Plain in the Northeast Atlantic Ocean.

trough at 22.9 μm (Durden et al., 2015). The sediments are carbonate oozes with particles $<23 \mu\text{m}$ comprising mainly coccoliths, while the sediment fraction 23–1000 μm is dominated by planktonic foraminiferal tests. However, sediments at the hill sites (H1, H2 and H4; Fig. 4.1) have a significantly higher fraction of coarser-grained material ($>63 \mu\text{m}$) than plain sites (P3, P4; Fig. 4.1) (38–64% on the hills vs. 25% on the plain; see Stefanoudis et al., 2016; Chapter 3, Table 3.3 therein), for both the 0–1 and 0–5 cm sediment horizons (Durden et al., 2015; Stefanoudis et al., 2016; Chapter 3). Some ice-rafted dropstones that serve as a hard substratum for sessile organisms are also known from the hills. Median seabed slope is greater and more variable at the abyssal hill sites compared to the plain. Potential organic matter input, expressed either as the percentage of the seafloor covered by phytodetritus or as median detrital aggregate size, did not vary between hills and plain (Durden et al., 2015) at the time samples for the present study were collected, although some variation has been detected subsequently (Morris et al., 2016). However, significant temporal variations, both seasonal and inter-annual, in organic matter supply do occur (Bett et al., 2001), and may be influenced by seafloor topography (Turnewitsch et al., 2015).

4.3 Materials and methods

4.3.1 Sample collection

Samples were collected during RRS *James Cook* Cruise 062 (JC062, 24 July to 29 August 2011; Ruhl, 2012) in the vicinity of the PAP-SO. They were obtained using a Bowers and Connelly Megacorer (Gage and Bett, 2005), equipped with 59 mm internal diameter core tubes, from two abyssal plain sites (P1, P2) and three abyssal hill sites (H1, H2, H4) (Fig. 4.1). Distances between sites were in the range of tens of kilometres (i.e. mesoscale). On board the ship the cores were sliced into 0.5-cm-thick layers down to 2 cm sediment depth, followed by 1-cm-thick layers from 2 to 10 cm depth, and each slice was fixed in 10% buffered formalin. The present contribution is based on material retained on a 150- μ m mesh sieve from the 0–1 cm sediment horizon from 16 Megacore samples, with up to four replicates per site (Table 4.1).

Table 4.1. Site and station information for each core used in the present study.

Site	Station	Topography	Water depth (m)	Latitude (°N)	Longitude (°W)
H1	JC062-53	Hill	4679	48.977	16.727
	JC062-60	Hill	4673	48.977	16.728
	JC062-61	Hill	4673	48.979	16.728
	JC062-115	Hill	4669	48.978	16.729
H2	JC062-129	Hill	4775	49.091	16.314
H4	JC062-123	Hill	4382	49.074	16.260
	JC062-126	Hill	4365	49.074	16.264
	JC062-128	Hill	4339	49.076	16.314
P3	JC062-66	Plain	4852	49.085	16.666
	JC062-67	Plain	4851	49.083	16.667
	JC062-101	Plain	4851	49.083	16.667
	JC062-131	Plain	4851	49.082	16.666
P4	JC062-73	Plain	4851	48.879	16.294
	JC062-75	Plain	4849	48.877	16.297
	JC062-76	Plain	4849	48.876	16.292
	JC062-77	Plain	4851	48.875	16.293

4.3.2 Laboratory analysis

In the laboratory, the 0–0.5 cm and 0.5–1.0 cm slices of cores were gently washed through two sieves (mesh sizes 300 and 150 μ m) using filtered tap water.

Residues >300 and 150–300 μ m were stained with Rose Bengal (1 g dissolved in 1 L tap water) overnight and sorted for ‘live’ (stained) benthic foraminifera in water in a Petri dish under a binocular microscope. We did not include komokiaceans or

small dome-like foraminifera associated with planktonic foraminiferal shells and mineral grains (Stefanoudis and Gooday, 2015; Chapter 2), with the exception of two easily recognizable morphotypes (*Psammosphaera* sp. 1 and 'White domes'; see taxonomic notes in Appendix A). These forms are omitted because they are difficult to separate into species and do not stain well with Rose Bengal, making the recognition of 'live' specimens problematic. For the rest, in order to ensure that the stained material was foraminiferal protoplasm, specimens were transferred to glass slides with glycerin and examined under a high-power compound microscope. This enabled us to distinguish 'fresh' cellular material from decayed cytoplasm, accumulations of bacteria, or inhabiting organisms. If necessary, thick-walled agglutinated tests were broken open to expose the material inside. Only specimens with most chambers stained were considered to be 'live'. In the case of many monothalamids, the test contained numerous stercomata (waste pellets) that decay after death into a grey powder. We regarded the 'fresh' (undegraded) appearance of stercomata as an additional indication that specimens were alive when collected. Delicate taxa were either stored on glass cavity slides in glycerol or in 2 ml Nalgene cryovials in 10% buffered formalin (4% borax buffered formaldehyde solution).

4.3.3 Light and scanning electron microscopy

Specimens placed in glycerol on a glass cavity slide were photographed using either a NIKON Coolpix 4500 camera mounted on an Olympus SZX10 compound microscope or a Leica Z16-APO incident light microscope. Selected specimens were dried onto aluminium stubs and examined by scanning electron microscopy (SEM) using a LEO 1450VP (variable pressure) or an environmental Zeiss EVO LS10 (variable pressure) instrument. The taxonomic scheme we followed was a combination of those proposed by Loeblich and Tappan (1987) and Pawlowski et al. (2013).

4.3.4 Statistical analysis

In order to test for differences in density with respect to topography (hills vs. plain) or site at either the assemblage level (for complete and fragmentary specimens separately) or the species level we performed analysis of variance (ANOVA), where necessary followed by Tukey's or Games-Howell (for homogeneous and non-homogeneous data, respectively) pairwise comparisons (SPSS v22) on log (x+1) transformed count data (see e.g. Sokal and Rohlf, 2012). For the species-level comparisons we used only species with complete tests that were 'common' (relative abundance >2% in at least one sample). In an attempt to reduce the reporting of 'false positive' results, we followed the method of Benjamini and Hochberg (1995) in controlling the false discovery rate (SPSS v22). We calculated the reciprocal Berger-Parker dominance index (N/N_{\max}) (Magurran, 2004), where N_{\max} and N are the number of individuals of the most abundant species and all species combined in a sample, respectively. An increased value of the index accompanies an increase in diversity and a reduction in dominance. Rank-density plots were constructed for all species in order to detect changes in dominance and ranking order between habitats.

Rarefied alpha diversity indexes (species richness, exponential Shannon index, inverse Simpson index, Chao 1; see e.g. Magurran, 2004) were calculated using the EstimateS 9 software package (Colwell, 2013), based on count data for complete specimens, and compared against seafloor topography (hills vs. plain) or site using ANOVA and Tukey's post-hoc pairwise comparisons (SPSS v22). Subsequently, we created two sets of sample-based rarefaction curves scaled by sampled seabed area and by number of individuals to examine species density (i.e. number of species per unit area), an important concept that may be particularly valuable in comparisons of contrasting organic matter supply regimes, and species richness (i.e. number of species per individuals), respectively (Chazdon et al., 1998; Gotelli and Colwell, 2001). In addition, we estimated beta diversity (β_w) for the eight hill and the eight plain samples separately as well as for all 16 samples of our dataset combined, using the formula proposed by Whittaker (1960, 1972), and commonly referred to as Whittaker's diversity index (Magurran, 2004):

$$\beta_w = \gamma / \bar{\alpha}.$$

In our case $\bar{\alpha}$ is the average sample diversity rarefied to 50 individuals (the lowest number of individuals found in a single sample that could be placed into a morphospecies), and γ is the total diversity (i.e. combining all samples of a category) rarefied to 400 individuals (i.e. eight replicate samples of 50 individuals). This form of beta diversity quantifies how many times as rich the entire dataset is compared to its constituent sampling units (Tuomisto, 2010), and hence, is a measure of variability in community structure among samples (Anderson et al., 2011). We calculated beta diversity based on three of Hill's numbers (Chao et al., 2014a): species richness ${}^0D = S$, exponential Shannon index ${}^1D = \exp(-\sum p_i \log p_i)$ and inverse Simpson index ${}^2D = 1 / \sum p_i^2$ (see also Chao et al., 2012, 2014b; Jost 2007), where p_i is the proportional abundance of the i -th morphospecies. As indicated by Gotelli and Chao (2013), 0D takes into account the number of species in the assemblage but not their relative abundances; 1D weights species in proportion to their frequency of occurrence, and can be interpreted as the number of 'typical species' in the assemblage; and 2D is weighted towards the most common (i.e. abundant) species and represents the number of very abundant species in the assemblage.

Trends in the structure of foraminiferal communities were explored using multivariate statistics such as global and pairwise analysis of similarities (ANOSIM) and non-metric multidimensional scaling (MDS) ordinations in PRIMER 6 (Clarke and Gorley, 2006). The analyses were based on Bray Curtis dissimilarity of raw (i.e. untransformed) and transformed ($\log[x+1]$ transformed, square-root transformed, fourth-root transformed, presence-absence) density data for complete specimens. To examine the impact of rarity we considered three versions of these data: i) all species, ii) only species with a relative abundance >2% in at least one sample, and iii) only species with a relative abundance >5% in at least one sample. The PRIMER routine, SIMPER (similarity percentages) was used to assess dissimilarity in foraminiferal composition by topography and site and identify those species contributing to within-group similarity. Spearman's rank correlation was used to assess the strength of the association between MDS ordines and proportion of the coarse sediment particle fraction (>63 μm) at each site, using particle size data as presented by Durden et al. (2015), Stefanoudis et al. (2016) and in chapter 3.

4.4 Results

4.4.1 Density

4.4.1.1 Total fauna

A total of 2102 obviously complete and 'live' (Rose-Bengal-stained) foraminiferal specimens was picked from the 16 Megacorer samples (Table 4.2). The density of complete specimens from abyssal hill samples ranged from 62 to 322 (mean 155 ± 76 standard deviation) individuals per sample (i.e. 25.5 cm^2) compared with 70 to 175 (mean 108 ± 35) indiv. per sample on the plain (Table 4.2 and Supplementary Material 4.B.1). Hill sites had higher mean densities than plain sites, especially in the case of site H4, situated on top of a large hill (Fig. 4.1). However, statistical comparisons of density against topography or site did not reveal any significant differences (ANOVA, $p > 0.05$).

In addition to the complete specimens, we recorded 2447 fragmented stained tests from all samples. Almost all (~99%) represented tubular morphospecies. Numbers varied considerably, ranging from 0 to 197 (mean 92 ± 79) indiv. per sample on the hills, against 2 to 1183 (mean 214 ± 409) indiv. per sample on the plain (Table 4.2; Supplementary Material 4.B.1). Again, statistical comparisons of density by seafloor topography or site did not detect significant differences in densities (ANOVA, $p < 0.05$).

4.4.1.2 Major taxa and groupings

The complete individuals that could be assigned to morphospecies (either described or undescribed) comprised the majority (85%) of all picked specimens, the remainder being indeterminate. As some species could not be placed easily in any higher taxon, the major groupings in Table 4.3 (for data per site see Supplementary Material 4.B.2; 4.B.3) represent a pragmatic mix of formal taxa (mainly multichambered groups) and informal morphology-based groupings (most monothalamids). More than half belonged to two multichambered agglutinated

Table 4.2. Mean density of 'live' (Rose-Bengal-stained) specimens (complete and fragmentary) and mean number of species, per site and topographic setting (hills, plain). (N: density of complete specimens, NF: density of fragments, S_N: number of species with complete tests, S_{N+NF}: number of species including fragmentary tests). Densities per 10 cm² are included in order to facilitate comparisons with other studies.

	H1	H2	H4	Hills	P3	P4	Plain
Density							
N 25.5 cm ²	115	134	215	155	112	104	108
N 10 cm ²	45	53	84	61	44	41	42
NF 25.5 cm ²	77	11	138	92	387	41	214
NF 10 cm ²	30	4	54	36	152	16	84
Species richness							
S _N	35	39	47	40	34	35	34
S _{N+NF}	41	41	56	47	38	38	39

Table 4.3. Absolute and relative (%) densities (number of specimens per eight Megacorer samples, i.e. 204 cm²) of the major taxa and informal groupings based on complete (N) and fragmentary (NF) 'live' (Rose-Bengal-stained) specimens for each topographic setting. (S_{N+NF}: number of species including complete and fragmentary specimens, *significant difference between hill and plain samples, ANOVA, p<0.05). The informal term 'saccamminids' is used for flask-shaped monothalamids with one or two apertures.

Major grouping	Hills					Plain				
	N	N%	NF	NF%	S _{N+NF}	N	N%	NF	NF%	S _{N+NF}
Monothalamids										
<i>Lagenammia</i>	88	7.1	0	0.0	8	114	13.2	0	0.0	8
<i>Nodellum</i> -like	45*	3.6	0	0.0	3	8*	0.9	0	0.0	2
Organic-walled	36	2.9	0	0.0	3	7	0.8	3	0.2	3
'Saccamminids'	44	3.6	0	0.0	6	36	4.2	0	0.0	8
Spheres (no aperture)	65	5.2	0	0.0	5	19	2.2	0	0.0	3
Tubular	7	0.6	725	98.8	24	2	0.2	1704	99.4	16
Others	143	11.6	1	0.1	3	77	8.9	0	0.0	3
Multichambered										
Ammodiscacea	1	0.1	0	0.0	1	2	0.2	0	0.0	2
Hormosinacea	273	22	5	0.7	24	234	27.1	3	0.2	20
Lageniida	10	0.8	0	0.0	6	14	1.6	0	0.0	8
Milioliida	34	2.7	0	0.0	5	15	1.7	0	0.0	4
Rotaliida	137	11.1	0	0.0	20	145	16.8	0	0.0	18
Textulariida	68	5.5	0	0.0	11	43	5	3	0.2	9
Trochamminacea	288	23.2	3	0.4	11	147	17	0	0	6
Total numbers	1239		734		130	863		1713		110

groups, the Hormosinacea and the Trochamminacea, and the calcareous Rotaliida. Among the monothalamids (single-chambered taxa; *sensu* Pawlowski et al., 2013), species of the genus *Lagenammia* were the most abundant. Delicate

and soft-walled agglutinated spheres without apertures (including representatives of the Psammosphaeridae), 'saccamminids' (agglutinated flasks and similar morphotypes with apertures) and organic-walled taxa ('allogromiids'), were never very abundant either in absolute or relative terms (Table 4.3). Many other monothalamids (grouped as 'Others' in Table 4.3) could not be assigned easily to recognised taxa. The only group that was significantly more abundant in one topographic setting comprised the *Nodellum*-like forms (tubular or 'segmented' organic-walled taxa of uncertain affinity), which overall were more common on the hills than the plain (ANOVA, $p < 0.05$; Table 4.3).

Hormosinaceans (i.e. *Reophax*, *Hormosina* and similar uniserial agglutinated genera) and rotaliids were the most speciose groups at both hills and plain sites. In general, all groups had similar numbers of species at different sites and in different topographic settings, except for trochamminaceans, which were more speciose at H4 than at the other sites (pairwise comparisons, $p < 0.05$ in all cases; see also Supplementary Material 4.B.3).

The overwhelming majority (~99%) of fragmentary specimens were agglutinated tubes (i.e., tubular monothalamids). These also represented a significant proportion (15–19%) of the total number of species found in each setting (Table 4.3 and Supplementary Material 4.B.3), highlighting the importance of considering fragments in assessments of abyssal benthic foraminiferal diversity.

4.4.1.3 Key species

Supplementary Material 4.B.4–4.B.6 summarise the ten most abundant morphospecies with complete and fragmentary tests, respectively, in all samples and in each topographic setting. These taxa are briefly described and illustrated in Appendix A. The densities of 'common' species (relative abundance $> 2\%$ in at least one sample) were not significantly different between hill and plain sites (ANOVA, $p < 0.05$). However, there were significant differences in relation to site (ANOVA and pairwise comparisons, $p < 0.05$) for four species: *Nodellum*-like sp. (H4 $>$ P3, P4), *Psammosphaera* sp. 1 (H4 $>$ H1, P3, P4), *Reophax* sp. 23 (H1, P4 $>$ P3), and *Portatrochammina murrayi* (H4 $>$ P4). Six species (*Adercotryma*

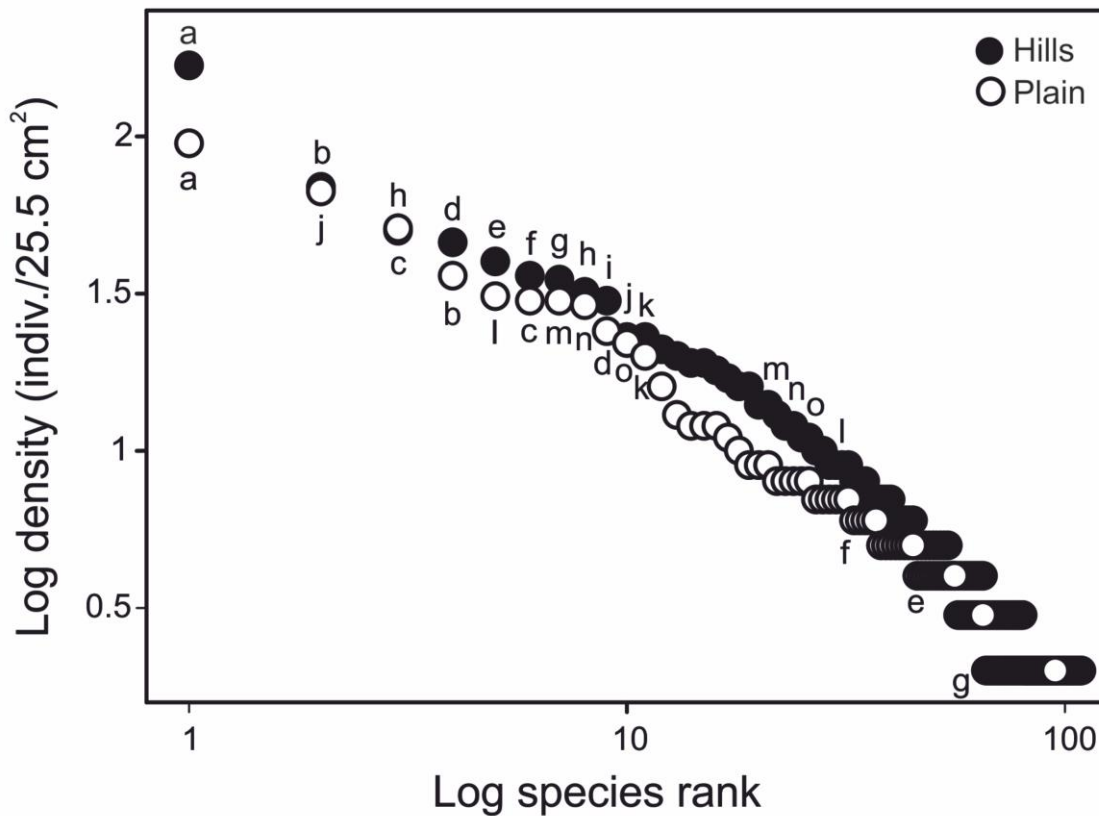


Fig. 4.2. Species ranked by density (individuals per 25.5 cm²). Hill (filled circles) and plain (open circles) are indicated separately, with abundant species keyed as follows: a) *Adercotryma glomerata*, b) *Reophax* sp. 21, c) *Nodulina dentaliniformis*, d) *Lagenammina* aff. *arenulata*, e) *Psammosphaera* sp. 1, f) *Nodellum*-like sp., g) Organic-walled domes, h) *Epistominella exigua*, i) *Recurvoides* sp. 1, j) *Thurammina albicans*, k) *Lagenammina* sp. 19, l) *Reophax bilocularis*, m) *Reophax* sp. 19, n) *Reophax* sp. 28.

glomerata, *Lagenammina* aff. *arenulata*, *Reophax* sp. 21, *Nodulina dentaliniformis*, *Epistominella exigua*, *Thurammina albicans*) were among the top 10 on the hills and on the plain, although their ranking was not consistent between settings (Fig. 4.2; Supplementary Material 4.B.5). Overall, hill assemblages seemed to exhibit slightly higher levels of dominance compared to the plain, mainly driven by the high density of *A. glomerata* (Fig. 4.2), although this difference was not statistically significant (inverse Berger-Parker index, ANOVA, $p > 0.05$). Similarly, six of the top 10 species with fragmentary tests (*Rhizammina algaeformis* and five other tubular spp.) were recorded in both hill and plain samples (Supplementary Material 4.B.6).

4.4.2 Diversity

A total of 158 morphospecies (complete and fragmentary tests) was recognised in all samples (see Supplementary Material 4.C for the complete dataset), 130 from

the hill samples and 110 from the plain samples (Table 4.3). Eighty-two species were found in both habitats, while 48 and 28 species were found exclusively on the hills and the plain, respectively. A detailed taxonomic appendix and illustrations for each species can be found in Appendix A.

Rarefied sample (alpha; $\bar{\alpha}$) diversity indexes (species richness, exponential Shannon index, inverse Simpson index, Chao 1) showed no significant variation with respect to topographic setting (hills vs. plain) or site (ANOVA and Tukey's test, $p > 0.05$). Sample-based rarefaction curves suggested that hills had a somewhat higher species density (number of species per unit area) (Fig. 4.3a) but when scaled to number of individuals (species richness) both settings were almost identical (Fig. 4.3b). Based on the eight samples we analysed from each topographic setting, Chao 1 (an asymptotic estimator of species richness) indicated that there were still species to be discovered on the hills (expected species number: 119–172, mean = 134) and the plain (expected species number: 112–205, mean = 138).

According to the three metrics (0D , 1D , 2D), rarefied $\bar{\alpha}$ diversity was marginally higher on the hills compared to the plain and the combined hill and plain samples. However, β_w and rarefied γ diversity appeared to be consistently higher in the combined hill and plain samples than in the hills or the plain samples analysed separately (Table 4.4). In qualitative terms, this may indicate that hills harbour some species not often encountered on the plain. Taken together with the rank abundance distribution (Fig. 4.2), these results suggest that the benthic foraminiferal assemblages on hills are somewhat richer in species than the plain assemblages, but have comparable numbers of 'typical' (in terms of frequency of occurrence) as well as 'common' (in terms of density) species.

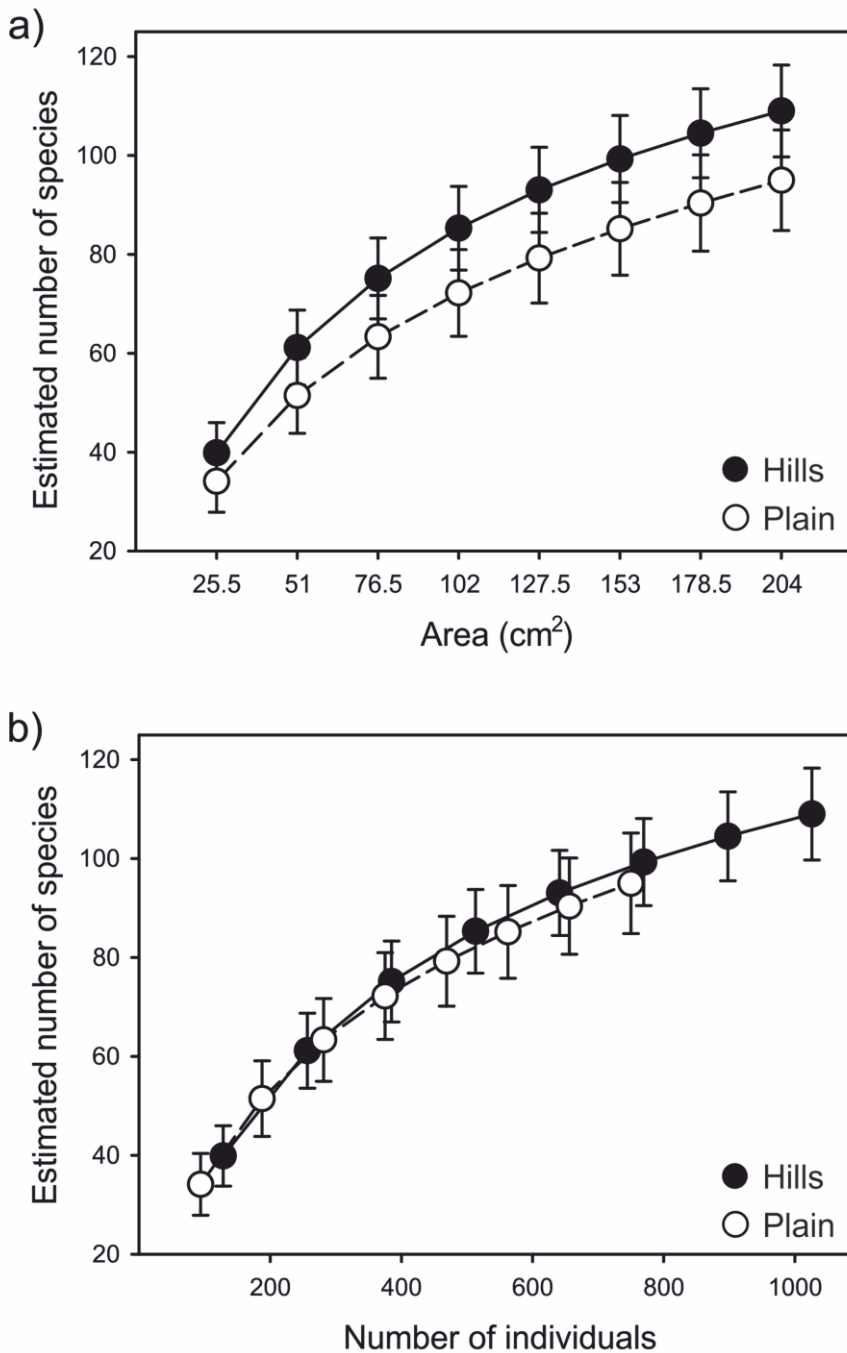


Fig. 4.3. Sample-based rarefied benthic foraminiferal morphospecies richness scaled by (a) area sampled (species density), and (b) number of individuals assessed (species richness) for combined hill (filled circles) and plain (open circles) samples.

Table 4.4. Assessment of beta diversity via rarefaction with Hill numbers (0D , species richness; 1D , exponential Shannon; 2D , inverse Simpson), $\bar{\alpha}$ rarefied to 50 individuals, and γ rarefied to 400 individuals. $\beta_w = \gamma/\bar{\alpha}$.

	0D			1D			2D		
	$\bar{\alpha}$	β_w	γ	$\bar{\alpha}$	β_w	γ	$\bar{\alpha}$	β_w	Γ
Hills	25.1	3.2	81.1	19	2.1	40.3	14.4	1.5	21.1
Plain	24.8	3.1	77.4	18.8	2.1	38.8	14	1.6	22.7
Hills and plain	25	3.4	83.9	18.9	2.3	43.1	14.2	1.7	23.6

4.4.3 Assemblage composition

Differences in benthic foraminiferal assemblage composition with topography and site was assessed by ANOSIM based on three different sets of density data (all species with complete specimens; only species with a relative abundance >2% in at least one sample; only species with a relative abundance >5% in at least one sample) for the 134 species with complete tests (see Supplementary Material 4.C). In all pairwise cases, topography appeared to exert a significant (ANOSIM, $p < 0.05$) effect on composition, with significant (ANOSIM, $p < 0.05$) variation between sites detected in 14 of the 15 cases tested (Table 4.5). Where a significant difference was detected between sites, site H4 (large hill) was always distinct (ANOSIM, $p < 0.05$) from one or both of the plain sites P3 and P4, and on five occasions from site H1 (Table 4.5).

An MDS ordination plot based on $\log(x+1)$ -transformed data of all 134 species was constructed to visualise differences in assemblage composition (Fig. 4.4; Table 4.5). On an MDS plot the distance between two points corresponds to their degree of similarity in composition (i.e. closely spaced points are compositionally similar). The stress value of the resultant plot was somewhat high (0.22), i.e. the full variation in the dataset was not well captured in two dimensions. There is considerable overlap of some hill and plain samples (H1, P3) and significant topographic variation in assemblage composition is not apparent. Nevertheless, the large hill (H4) was well separated from both the plain sites (P3, P4) and the other hill sites (H1, H2), reflecting the distinctive nature of the H4 assemblage. Spearman's rank correlation of the MDS x-ordinates, which best separate hill and plain sites, and the coarse sediment (>63 μm) particle fraction in each site, resulted in a significant ($p = 0.01$) relationship between foram species composition and local sedimentology. SIMPER analysis (see Supplementary Material 4.D for detailed results by topography and site) on the same dataset showed that the mean similarity (43%) among hill samples was driven most by *A. glomerata* (13%), *Reophax* sp. 21, *N. dentaliniformis* and *Lagenammia* aff. *arenulata* (all 7%), while mean similarity (44%) among plain samples was driven most by *A. glomerata* (11%), *Lagenammia* sp. 19 (9%), *Reophax* sp. 21 and *E. exigua* (both 8%). In contrast, mean dissimilarity (59%) between hill and plain samples was driven by several species, each contributing modestly to that dissimilarity (0.4–2.5%;

Supplementary Material 4.D).

Table 4.5. Variation in benthic foraminiferal assemblage composition between hill and plain samples (Topo) and between sites as assessed by ANOSIM. Results are tabulated for three versions of the dataset and five data transformations (see text), and indicate the global result (Topo/Site) and significant ($p < 0.05$) pairwise tests between individual sites.

Dataset	Factor	Transformation				
		None	Log	Sqrt	Frt	P/A
All	Topo	<0.05	<0.05	<0.05	<0.05	<0.05
	Site	<0.01 H4 vs. H1, P3, P4	<0.01 H4 vs. P3, P4	<0.01 H4 vs. P3, P4	<0.05 H4 vs. P3, P4	<0.05 H4 vs. P4
>2%	Topo	<0.05	<0.05	<0.05	<0.05	<0.01
	Site	<0.01 H4 vs. H1, P3, P4	<0.01 H4 vs. P3, P4	<0.01 H4 vs. P3, P4	<0.05 H4 vs. P3, P4	<0.05 H4 vs. P3, P4
>5%	Topo	<0.05	<0.05	<0.01	<0.05	<0.05
	Site	<0.01 H4 vs. H1, P3, P4	<0.01 H4 vs. H1, P3	<0.01 H4 vs. H1, P3, P4	<0.05 H4 vs. P3	Ns

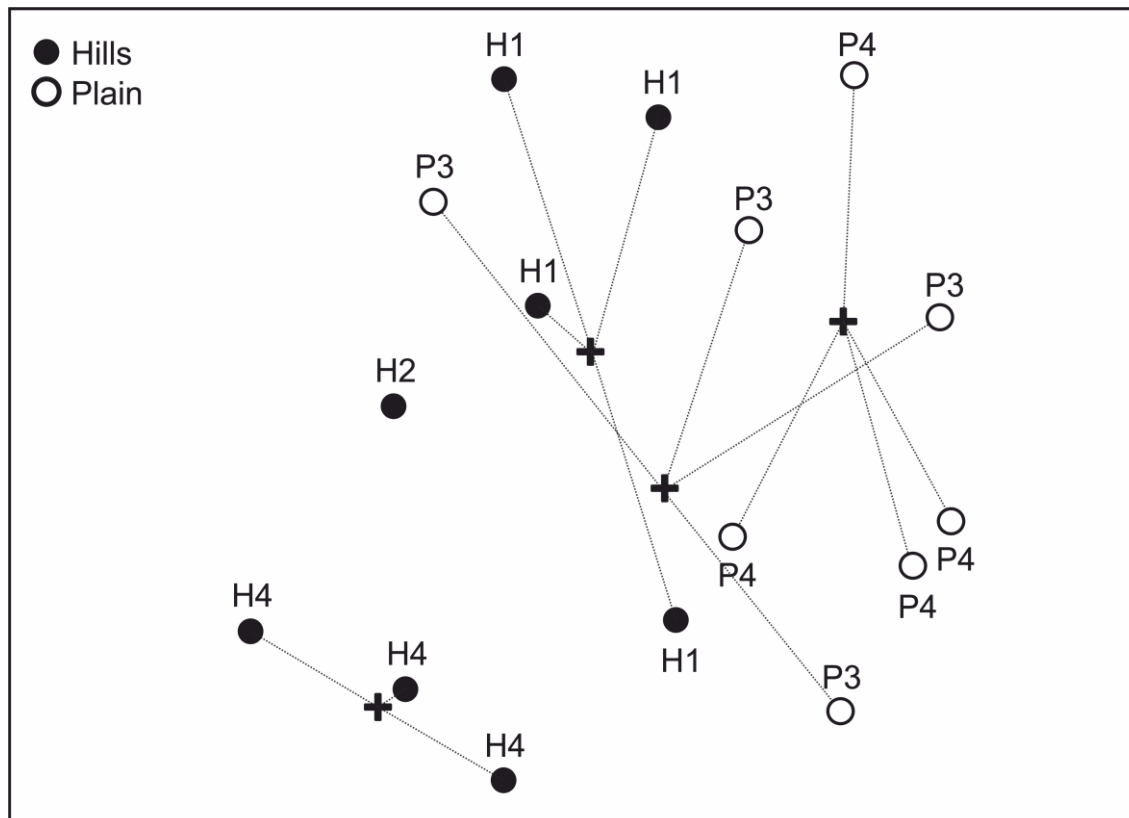


Fig. 4.4. MDS ordination plot of 16 Megacorer samples in the PAP-SO area, including all 134 species with complete tests. Filled circles represent hill samples, open circles the plain samples, site replicates are shown linked to their corresponding centroids (solid crosses). (Based on Bray-Curtis dissimilarity of $\log[x+1]$ transformed density).

4.5 Discussion

4.5.1 Limitations of dataset

This study was limited to foraminiferal tests retained on a 150- μm mesh sieve. Analysis of finer sieve fractions would have yielded additional information on smaller, shallow-infaunal species that can be more responsive to freshly deposited organic matter (Gooday, 1988; 1993; Sun et al., 2006). However, previous studies based on $>150\text{-}\mu\text{m}$ residues have succeeded in establishing ecologically meaningful links between patterns in benthic foraminiferal assemblages (density, diversity, community composition) and environmental parameters (Barras et al., 2010; Caille et al., 2015; Fontanier et al., 2002; Goineau et al., 2012; Mojtahid et al., 2010), while size-fractionated data from the NE Atlantic (>150 and $>63\ \mu\text{m}$) resulted in similar correlations between diversity measures and benthic foraminiferal densities (Gooday et al., 2012). The main advantage of analysing the $>150\text{-}\mu\text{m}$ sieve fractions is that it is less time-consuming than finer fractions, making it possible to process a larger number of replicates.

4.5.2 Influence of abyssal hills on foraminiferal faunas

Topographic features on the scale of hills are associated with turbulent mixing above the seabed (Garrett and Kunze, 2007; Kunze and Llewellyn-Smith, 2004; Nash et al., 2007). This process modifies the distribution, settling and availability of organic matter (Clark et al., 2010; Genin et al., 1986), the quantity and quality of which influence benthic foraminiferal standing stocks (Altenbach et al., 1999; Caralp, 1989; Fontanier et al., 2002; Koho et al., 2008).

Although we lack specific near-bottom current-speed data for our study sites, we can use the proportion of coarser sediments particles ($>63\mu\text{m}$) on the PAP-SO abyssal hills (Durden *et al.*, 2015; Stefanoudis et al., 2016; Chapter 3) as a proxy of enhanced flows. This is based on the assumption that particles $<63\ \mu\text{m}$ are more readily transported by currents (McCave and Hall, 2006; McCave et al., 1995), as has been empirically established for another abyssal hill within the PAP-SO area (Turnewitsch et al., 2004, 2013). A recent study in the PAP-SO area by Turnewitsch et al. (2015) found less, but fresher, organic material in hill sediments

when compared to adjacent plain sediments. The authors suggested that organic material deposited on the hill was readily advected and redeposited downstream, and/or that the reduced surface area of the coarser particles comprising hill sediments could have decreased the potential for sorptive organic-matter preservation (Arnarson and Keil, 2001; Curry et al., 2007). Another recent study of the PAP-SO area reported that there was no difference in apparent organic matter supply (seafloor phytodetritus cover; median detrital aggregate size) to the hills or the plain, but that seabed cover was minimal (between 0 and ~3%) (Durden et al., 2015). That survey occurred after the seasonal peak in deposition. A more detailed study of a single PAP-SO hill by Morris et al. (2016) revealed a much higher phytodetritus cover (c. 45%) and showed that modest topography (80 m elevation) had fractionally higher cover than the adjacent plain. Morris et al. (2016) also supported the previous observations of Durden et al. (2015) of a substantially higher biomass of megabenthos on the hill than the plain. Both studies strongly suggest that lateral transport of organic matter plays a major role in the benthic ecology of abyssal hill communities. Taken together, these observations suggest that total organic matter availability is generally greater on the hills than on the plain, but that its residence time may be reduced.

4.5.2.1 Density

Higher organic matter availability on the hills could partially explain the higher foraminiferal densities compared to the surrounding plain in the PAP-SO area (Table 4.2), although statistical comparisons suggested that these differences were not significant (ANOVA, $p > 0.05$). Enhanced current velocities and therefore increased organic matter supply on the hills could also lead to more suspension-feeding organisms (e.g. Kaufmann et al., 1989). Both Durden et al. (2015) and Morris et al. (2016) recorded 3- to 5-fold increases in megabenthic biomass between PAP-SO plain and hill sites, with much of the increase attributable to suspension feeding taxa. This suggests that densities of epifaunal foraminiferal species inferred to be suspension feeders, notably tubular monothalamids (Jones and Charnock, 1985; Kaminski et al., 2015; Mullineaux, 1987; Murray et al., 2011; Veillette et al., 2007) and certain calcareous species (e.g. *Cibicides* spp., *Cibicoides* spp., *Discanomalina* spp.) (Linke and Lutze, 1993; Lutze and Altenbach, 1988; Lutze and Thiel, 1989; Schönfeld, 1997, 2002b), might be higher

on the hills. However, with the exception of the *Nodellum*-like group, which is unlikely to include suspension feeders, we did not find any significant increase in the density of any taxonomic or morphology-based groups linked to seafloor topography (Table 4.3).

Positive relationships between bottom currents and faunal density have been invoked to explain faunal density patterns in the deep sea. For example, Kaminski (1985) compared two abyssal locations with contrasting current regimes in the NW Atlantic and found that agglutinated benthic foraminiferal abundance was greater where bottom-water flow was enhanced at the HEBBLE site, which is subject to episodic high-velocity current flows ('benthic storms'), than at the nearby tranquil HEBBLE Shallow site. Kaminski (1985) attributed this difference to sediment heterogeneity and did not consider potential differences in food supply between the two areas. Thistle et al. (1985) reported that macrofaunal and meiofaunal abundance was higher at the high-energy HEBBLE site than on the Horizon Guyot perimeter. The authors concluded that the strong near-bottom currents at the HEBBLE site promoted bacterial growth and an enhanced flux of suspended food particles. Seamounts have been shown to support enhanced densities of epibenthic megafaunal biomass when compared to slope habitats (Rowden et al., 2010) due to an elevated food supply in the former. On the other hand, current-swept regions can also be characterised by depressed faunal densities. For example, Koho et al. (2007) found low standing stocks of benthic foraminifera in the highly disturbed axis of the upper Nazaré Canyon, which experiences frequent sediment resuspension and gravity flows. Similarly, strong near-bottom flows have been shown to depress the abundance of metazoan macrofauna (Levin and Thomas, 1989) and meiofauna (Thistle and Levin, 1998) on seamounts,.

The literature reviewed above suggests that the effect of near-bottom currents on benthic faunas can be either negative or positive depending on the faunal group and the intensity of the disturbance (Levin et al., 2001). Strong, erosive currents will negatively impact benthic faunal density, including that of foraminifera, by eroding surficial sediments and the individuals living in them (Aller, 1997). Moderate currents, such as those present on the hills in the PAP-SO area, will increase food supply by delivering organic matter and promoting bacteria growth

(Aller, 1989; Thistle et al., 1985), potentially leading to enhanced benthic faunal density.

4.5.2.2 Diversity

In general, the hills supported more species than the plain (130 vs. 110) (Table 4.3). Alpha, beta, and gamma measures of diversity were in most cases marginally higher on hills than on the plain (Table 4.4). However, statistical comparisons of rarefied alpha diversity indexes (species richness, exponential Shannon index, inverse Simpson index, Chao 1) by topography and site did not reveal any significant differences (ANOVA, $p > 0.05$). Taking our samples as a whole, hills had similar dominance values (inverse Berger-Parker index results; Fig. 4.2) but higher species density (i.e. more species per unit area) (Fig. 4.3a), and when added to samples from the plain acted to increase regional beta and gamma diversity (Table 4.4). The increased species density suggests enhanced organic matter supply (Section 4.5.2; also Levin et al., 2001; Rowden et al., 2010), while the increase in regional diversity may be indicative of additional habitat heterogeneity (e.g. variation in sediment particle size distributions; Durden et al., 2015; Stefanoudis et al., 2016; Chapter 3).

Comparisons of benthic foraminiferal diversity between contrasting habitats are relatively scarce. In coastal waters, variation of organic-matter supply is reported to be a major driver of foraminiferal diversity (Mojtahid et al., 2009). In deeper waters, foraminiferal communities are less diverse in areas disturbed by high intensity bottom-water currents and with coarser sediments, than at undisturbed locations (Kaminski, 1985). As in the case of density, data on the effects of currents on deep-sea metazoan species diversity are rather contradictory. Macrofaunal diversity appears markedly depressed by high current flow (Gage et al., 1995; Harriague et al., 2014). On the other hand, meiofaunal diversity is reported to be similar at hydrodynamically contrasting sites (Harriague et al., 2014; Thistle, 1983), although enhanced diversity due to strong near-bottom flow has also been recorded (Thistle, 1998). Comparisons between seamounts and adjacent slope sites have revealed similar levels of mollusk, coral and ophiuroid species richness and/or rates of endemism (Castelin et al., 2011; Hall-Spencer et al., 2007; O'Hara, 2007).

These results suggest that the response to hydrodynamically-induced disturbance of diversity, like that of density, can be both negative and positive and may vary between faunal groups (see also Thistle et al., 1991). Levin et al. (2001) predicted a unimodal relationship between flow strength and diversity, whereby diversity is maximal at intermediate flows rates, although they added that there are few direct observations to support this model. The different aspects of diversity are variously impacted and controlled by different factors, including habitat heterogeneity, disturbance, and productivity (McClain and Barry, 2010) several of which may operate in our study area. We suspect that different sediment characteristics, together with moderately increased near-bottom water flows, and hence enhanced organic matter supply, are all likely to influence diversity in the PAP-SO area, although it is difficult to disentangle their separate influences (e.g., Svensson et al., 2012).

4.5.2.3 Assemblage characteristics

There were significant differences in benthic foraminiferal community composition related to seafloor topography (hills vs. plain). Assessments by ANOSIM and MDS suggested that relatively distinct assemblages occupy the hills, particularly the largest hill (H4) (Table 4.5; Fig. 4.4). Around 48 species, most of them uncommon (Table 4.5, Supplementary Material 4.D), were only recorded in hill samples (hills: 130 vs. plain: 110; Table 4.3, Supplementary Material 4.C). More importantly, there were relatively subtle changes between the two settings in the density of individual species that collectively make the assemblages distinctive (Table 4.5; Fig. 4.4), although these were significant only in the case of *Nodellum*-like sp. [H4>P3, P4], *Psammosphaera* sp. 1 [H4>H1, P3, P4], *Reophax* sp. 23 [H1, P4>P3], and *Portatrochammina murrayi* [H4>P4] (Table 4.3; Fig. 4.2; Supplementary Material 4.D).

Substratum heterogeneity has often been used to explain deep-sea diversity patterns and changes in benthic community composition (Etter and Grassle, 1992; Hecker, 1990; Kaufmann et al., 1989; Leduc et al., 2012; Levin et al., 1994; Sautya et al., 2011), including benthic foraminifera (Kaminski, 1985; Murray, 2006). For example, Mackensen et al. (1985) reported a distinct foraminiferal

assemblage dominated by *Trifarina angulosa* on the upper part of the Norwegian continental slope, apparently linked to the coarse-grained sediments and strong prevailing bottom currents. Similarly, Schönfeld (1997, 2002a, b) recorded distinct foraminiferal assemblages from the Gulf of Cadiz and the southern Portuguese continental margin related to local hydrography and sedimentary facies. In the South Atlantic Ocean, Mackensen et al. (1995) found that the hydrodynamic properties of the benthic environment, and the related sediment grain size parameters, to be among the main environmental factors controlling foraminiferal faunas. Schmiedl et al. (1997) also concluded that the grain size characteristics influenced the distribution pattern of agglutinated foraminifera such as *Lagenammina*, *Psammosphaera*, *Reophax*, *Rhizammina*, all of which are present in our study area.

Although there is some evidence for a difference in organic matter supply to hill and plain sites in the PAP-SO area (Durden et al., 2015; Turnewitsch et al., 2015; Morris et al., 2016), we suggest that substratum variation (i.e. coarser sediments on hills; see Durden et al., 2015; Stefanoudis et al., 2016; Chapter 3) is most likely the main driver of differences in foraminiferal assemblage composition (as distinct from density and diversity changes). This is supported by the statistically significant correlation between MDS x-ordinates and the coarser (>63 µm) particle fraction at each site. Durden et al. (2015) reached a similar conclusion for the PAP-SO megafauna. However, sediment granulometry and sedimentary organic carbon typically covary, with coarser sediments having a lower organic carbon content than finer ones (Arnarson and Keil, 2001; Curry et al., 2007). Hence grain size may only be influencing foraminiferal community attributes indirectly.

If substratum is the main driver of foraminiferal community composition, then the fact that the assemblages on the large hill (H4) and the plain are significantly different, whereas those on the two small hills (H1, H2) and the plain are much closer (Table 4.5), suggests that there should be little difference in sediment granulometry between the small hills and the plain. Nevertheless, Stefanoudis et al., (2016) found significant granulometric differences (ANOSIM, $p < 0.05$) between H1 and the two plain sites (P3 and P4) (see also chapter 3). Although we had too few sediment samples from H4 ($n=2$) to perform similar statistical comparisons, the fact that there is a higher percentage of coarse particles (>63 µm) in H4 than in

H1 sediments (63% and 38%, respectively; Stefanoudis et al., 2016; Chapter 3), is a good indication that sediments at H4 differ granulometrically from those of the plain. This is also clear from an MDS plot of granulometric profiles from H1, H4, P1 and P2 (Stefanoudis et al., 2016; Chapter 3, Fig. 4.3b therein), which shows that the particle size composition of H4 is distinct from the plain and quite possibly from H1 as well. These considerations suggest that topographically enhanced bottom currents, and hence coarser sediments, on the hills modify the composition of the foraminiferal communities when compared to the finer-grained sediments and more quiescent conditions on the abyssal plain. These differences are most evident (i.e. statistically significant) when comparing the large hill (H4) and the flat P3 and P4 sites. The two smaller hills (H1, H2), where the sediments contain less coarse-grained material than at H4 and foraminiferal assemblages have an intermediate composition (Fig. 4.4; SIMPER results between sites in Supplementary Material 4.D), fall between these extremes.

Assemblage characteristics might be further influenced by the occurrence at the sediment surface of dropstones (ice-rafted glacial erratics; Lisitzin, 2002), found exclusively on the hills. Although not present in samples analysed for this study, dropstones are an important source of small-scale habitat heterogeneity, providing 'islands' of solid substratum against a background of soft sediment. They typically host sessile species not found in the sediments (Gooday et al., 2015), and hence largely absent from abyssal plain samples.

4.5.3 Concluding remarks

The questions we sought to answer in this study were: do abyssal hills modify the i) density, ii) diversity, iii) and species composition of foraminiferal assemblages, and if so, iv) is mesoscale diversity enhanced? Although we recorded enhanced density and diversity on hills, these differences were not statistically significant. However, we did demonstrate that hills had a higher species density (potentially related to increased organic matter supply), and harboured species not found on the plain (most likely related to sediment characteristics), thereby increasing the pool of benthic foraminiferal species within the PAP-SO area. Most importantly, by combining data from abyssal hills and the neighboring plain the regional diversity was enhanced. These findings highlight the influence of mesoscale heterogeneity,

linked to relatively modest topography, on the benthic foraminiferal communities of the PAP-SO area.

Abyssal hill terrain is the dominant feature of the abyssal realm (Harris et al., 2014), and represents an important source of habitat heterogeneity. Deep-sea macrohabitat diversity has been argued to be a significant contributor to global nematode diversity (Vanreusel et al., 2010), continental margin and slope diversity (Levin and Dayton, 2009; Levin and Sibuet, 2012) and regional deep-sea diversity (Levin et al., 2001). Our results support those general conclusions, and suggest that we need to also consider the influence of abyssal hills on abyssal biodiversity. Although these features pose some practical challenges in terms of sample collection, the increased availability of remotely operated and autonomous underwater vehicles, and dynamically positioned research vessels with good swathe bathymetry capability, as well as modern, hydraulically damped sediment coring systems, should make such studies more common. The juxtaposition of habitat heterogeneity, physical disturbance, and productivity variations over relatively small spatial scales, and generally remote from human impacts, at least in the Atlantic Ocean, suggests that abyssal hill terrain can be an effective focus for ecological hypothesis testing.

References of Chapter 4

- Aller, J.Y., 1989. Quantifying sediment disturbance by bottom currents and its effect on benthic communities in a deep-sea western boundary zone. *Deep-Sea Research Part A–Oceanographic Research Papers*, 36, 901–934.
- Aller, J.Y., 1997. Benthic community response to temporal and spatial gradients in physical disturbance within a deep-sea western boundary region. *Deep-Sea Research Part I–Oceanographic Research Papers*, 44, 39–69.
- Altenbach, A.V., Pflaumann, U., Schiebel, R., Thies, A., Timm, S., Trauth, M., 1999. Scaling percentages and distributional patterns of benthic foraminifera with flux rates of organic carbon. *Journal of Foraminiferal Research*, 29, 173–185.
- Amon, D.J., Amanda F. Ziegler, Thomas G. Dahlgren, Adrian G. Glover, Aurélie Goineau, Andrew J. Gooday, Helena Wiklund, Smith, C.R., 2016. Insights into the abundance and diversity of abyssal megafauna in a polymetallic-nodule region in the eastern Clarion-Clipperton Zone. *Scientific Reports*, 6, 30492.
- Anderson, M.J., Crist, T.O., Chase, J.M., Vellend, M., Inouye, B.D., Freestone, A.L., Sanders, N.J., Cornell, H.V., Comita, L.S., Davies, K.F., Harrison, S.P., Kraft, N.J.B., Stegen, J.C., Swenson, N.G., 2011. Navigating the multiple meanings of beta diversity: a roadmap for the practicing ecologist. *Ecology Letters*, 14, 19–28.
- Arnarson, T.S., Keil, R.G., 2001. Organic-mineral interactions in marine sediments studied using density fractionation and X-ray photoelectron spectroscopy. *Organic Geochemistry*, 32, 1401–1415.
- Barras, C., Fontanier, C., Jorissen, F., Hohenegger, J., 2010. A comparison of spatial and temporal variability of living benthic foraminiferal faunas at 550m depth in the Bay of Biscay. *Micropaleontology*, 56, 275–295.
- Bell, T.H., 1979. Mesoscale sea floor roughness. *Deep-Sea Research Part A–Oceanographic Research Papers*, 26, 65–76.
- Benjamini, Y., Hochberg, Y., 1995. Controlling the false discovery rate: A practical and powerful approach to multiple testing. *Journal of the Royal Statistical Society Series B–Methodological*, 57, 289–300.
- Bernstein, B.B., Hessler, R.R., Smith, R., Jumars, P.A., 1978. Spatial dispersion of benthic foraminifera in abyssal central North Pacific. *Limnology and Oceanography*, 23, 401–416.
- Bett, B.J., Malzone, M.G., Narayanaswamy, B.E., Wigham, B.D., 2001. Temporal variability in phytodetritus and megabenthic activity at the seabed in the deep Northeast Atlantic. *Progress in Oceanography*, 50, 349–368.
- Billett, D.S.M., Rice, A.L., 2001. The BENGAL programme: introduction and overview. *Progress in Oceanography*, 50, 13–25.
- Buhl-Mortensen, L., Vanreusel, A., Gooday, A.J., Levin, L.A., Priede, I.G., Buhl-Mortensen, P., Gheerardyn, H., King, N.J., Raes, M., 2010. Biological structures as a source of habitat heterogeneity and biodiversity on the deep ocean margins. *Marine Ecology*, 31, 21–50.

- Caralp, M.H., 1989. Abundance of *Bulimina exilis* and *Melonis barleeanum*: Relationship to the quality of marine organic-matter. *Geo-Marine Letters*, 9, 37–43.
- Castelin, M., Puillandre, N., Lozouet, P., Sysoev, A., de Forges, B.R., Samadi, S., 2011. Molluscan species richness and endemism on New Caledonian seamounts: Are they enhanced compared to adjacent slopes? *Deep-Sea Research Part I–Oceanographic Research Papers*, 58, 637–646.
- Caulle, C., Mojtahid, M., Gooday, A.J., Jorissen, F.J., Kitazato, H., 2015. Living (Rose-Bengal-stained) benthic foraminiferal faunas along a strong bottom-water oxygen gradient on the Indian margin (Arabian Sea). *Biogeosciences*, 12, 5005–5019.
- Chao, A., Chiu, C.H., Hsieh, T.C., 2012. Proposing a resolution to debates on diversity partitioning. *Ecology*, 93, 2037–2051.
- Chao, A., Gotelli, N.J., Hsieh, T.C., Sander, E.L., Ma, K.H., Colwell, R.K., Ellison, A.M., 2014a. Rarefaction and extrapolation with Hill numbers: a framework for sampling and estimation in species diversity studies. *Ecological monographs*, 84, 45–67.
- Chao, A.N., Chiu, C.H., Jost, L., 2014b. Unifying species diversity, phylogenetic diversity, functional diversity, and related similarity and differentiation measures through Hill numbers. *Annual Review of Ecology, Evolution, and Systematics*, Vol 45, 45, 297–324.
- Chazdon, R.L., Colwell, R.K., Denslow, J.S., Guariguata, M.R., 1998. Statistical methods for estimating species richness of woody regeneration in primary and secondary rain forests of NE Costa Rica. In: Dallmeier, F., Comiskey, J.A. (Eds.), *Forest biodiversity research, monitoring and modeling: Conceptual background and Old World case studies* (pp. 285–309). Paris: Parthenon Publishing.
- Clark, M.R., Rowden, A.A., Schlacher, T., Williams, A., Consalvey, M., Stocks, K.I., Rogers, A.D., O'Hara, T.D., White, M., Shank, T.M., Hall-Spencer, J.M., 2010. The ecology of seamounts: structure, function, and human impacts. *Annual Review of Marine Science*, 2, 253–278.
- Clarke, K.R., Gorley, R.N., 2006. *PRIMER v6: User Manual/Tutorial*. PRIMER-E, Plymouth, UK.
- Colwell, R.K., 2013. EstimateS: Statistical estimation of species richness and shared species from samples. Version 9 and earlier. User's Guide and application.
- Curry, K.J., Bennett, R.H., Mayer, L.M., Curry, A., Abril, M., Biesiot, P.M., Hulbert, M.H., 2007. Direct visualization of clay microfabric signatures driving organic matter preservation in fine-grained sediment. *Geochimica Et Cosmochimica Acta*, 71, 1709–1720.
- Durden, J.M., Bett, B.J., Jones, D.O.B., Huvenne, V.A.I., Ruhl, H.A., 2015. Abyssal hills – hidden source of increased habitat heterogeneity, benthic megafaunal biomass and diversity in the deep sea. *Progress in Oceanography*, 137, 209–218.
- Ebbe, B., Billett, D., Brandt, A., Ellingsen, K., Glover, A.G., Keller, S., Malyutina, M., Arbizu, P.M., Molodtsova, T., Rex, M., Smith, C.R., Tselepidis, A., 2010. Chapter 8 - Diversity of abyssal marine life. In: McIntyre, A.D. (Ed.), *Life in the World's Oceans* (pp. 139–160): Blackwell Publishing Ltd.
- Etter, R.J., Grassle, J.F., 1992. Patterns of species diversity in the deep sea as a function of sediment particle size diversity. *Nature*, 360, 576–578.

- Fontanier, C., Jorissen, F.J., Licari, L., Alexandre, A., Anschutz, P., Carbonel, P., 2002. Live benthic foraminiferal faunas from the Bay of Biscay: faunal density, composition, and microhabitats. *Deep-Sea Research Part I—Oceanographic Research Papers*, 49, 751–785.
- Frigstad, H., Henson, S.A., Hartman, S.E., Omar, A.M., Jeansson, E., Cole, H., Pebody, C., Lampitt, R.S., 2015. Links between surface productivity and deep ocean particle flux at the Porcupine Abyssal Plain sustained observatory. *Biogeosciences*, 12, 5885–5897.
- Gage, J.D., Lamont, P.A., Tyler, P.A., 1995. Deep-sea macrobenthic communities at contrasting sites off Portugal, preliminary results. I Introduction and diversity comparisons. *Internationale Revue Der Gesamten Hydrobiologie*, 80, 235–250.
- Gage, J.D., Bett, B.J., 2005. Deep-sea benthic sampling. In: Eleftheriou, A., MacIntyre, A.D. (Eds.), *Methods for the study of marine benthos*, 3rd ed. (pp. 273–325). Oxford, UK: Blackwell Scientific.
- Garrett, C., Kunze, E., 2007. Internal tide generation in the deep ocean. *Annual Review of Fluid Mechanics*, 39, 57–87.
- Genin, A., Dayton, P.K., Lonsdale, P.F., Spiess, F.N., 1986. Corals on seamount peaks provide evidence of current acceleration over deep-sea topography. *Nature*, 322, 59–61.
- Goff, J.A., 1998. Finding chaos in abyssal hills. *Nature*, 392, 224–227.
- Goineau, A., Fontanier, C., Jorissen, F., Buscail, R., Kerhervé, P., Cathalot, C., Pruski, A., Bourgeois, S., Metzger, E., Legrand, E., 2012. Temporal variability of live (stained) benthic foraminiferal faunas in a river-dominated shelf—faunal response to rapid changes of the river influence (Rhône prodelta, NW Mediterranean). *Biogeosciences*, 9, 1367–1388.
- Gooday, A.J., Levin, L.A., Linke, P., Heeger, T., 1992. The role of benthic foraminifera in deep-sea food webs and carbon cycling. *Deep-Sea Food Chains and the Global Carbon Cycle*, 360, 63–91.
- Gooday, A.J., 2003. Benthic foraminifera (protista) as tools in deep-water palaeoceanography: Environmental influences on faunal characteristics. *Advances in Marine Biology*, 46, 1–90.
- Gooday, A.J., Nomaki, H., Kitazato, H., 2008. Modern deep-sea benthic foraminifera: a brief review of their morphology-based biodiversity and trophic diversity. *Geological Society, London, Special Publications*, 303, 97–119.
- Gooday, A.J., Malzone, M.G., Bett, B.J., Lamont, P.A., 2010. Decadal-scale changes in shallow-infaunal foraminiferal assemblages at the Porcupine Abyssal Plain, NE Atlantic. *Deep-Sea Research Part II—Topical Studies in Oceanography*, 57, 1362–1382.
- Gooday, A.J., da Silva, A.A., Pawlowski, J., 2011. Xenophyophores (Rhizaria, Foraminifera) from the Nazaré Canyon (Portuguese margin, NE Atlantic). *Deep-Sea Research Part II—Topical Studies in Oceanography*, 58, 2401–2419.
- Gooday, A.J., Bett, B.J., Jones, D.O.B., Kitazato, H., 2012. The influence of productivity on abyssal foraminiferal biodiversity. *Marine Biodiversity*, 42, 415–431.
- Gooday, A.J., 2014. Deep-sea benthic foraminifera. *Reference Module in Earth Systems and Environmental Sciences* (pp. 1–20).
- Gooday, A.J., Goineau, A., Voltski, I., 2015. Abyssal foraminifera attached to polymetallic nodules from the eastern Clarion Clipperton Fracture Zone: a preliminary description and comparison with North Atlantic dropstone assemblages. *Marine Biodiversity*, 391–412.

- Gotelli, N.J., Colwell, R.K., 2001. Quantifying biodiversity: procedures and pitfalls in the measurement and comparison of species richness. *Ecology Letters*, 4, 379–391.
- Gotelli, N.J., Chao, A., 2013. Measuring and estimating species richness, species diversity, and biotic similarity from sampling data. In: Levin, S.A. (Ed.), *Encyclopedia of Biodiversity*, 2nd Edition, Vol. 5 (pp. 195–211). Waltham, MA: Academic Press.
- Grassle, J.F., Morse-Porteous, L.S., 1987. Macrofaunal colonization of disturbed deep-sea environments and the structure of deep-sea benthic communities. *Deep-Sea Research Part A—Oceanographic Research Papers*, 34, 1911–1950.
- Hall-Spencer, J., Rogers, A., Davies, J., Foggo, A., 2007. Deep-sea coral distribution on seamounts, oceanic islands, and continental slopes in the Northeast Atlantic. In: George, R.Y., Cairns, S.D. (Eds.), *Conservation and Adaptive Management of Seamount and Deep-Sea Coral Ecosystems* (pp. 135–146). Rosenstiel, School of Marine and Atmospheric Science, University of Miami.
- Harriague, A.C., Bavestrello, G., Bo, M., Borghini, M., Castellano, M., Majorana, M., Massa, F., Montella, A., Povero, P., Misic, C., 2014. Linking environmental forcing and trophic supply to benthic communities in the Vercelli Seamount area (Tyrrhenian Sea). *Plos One*, 9, 1–10.
- Harris, P.T., Macmillan-Lawler, M., Rupp, J., Baker, E.K., 2014. Geomorphology of the oceans. *Marine Geology*, 352, 4–24.
- Hartman, S.E., Lampitt, R.S., Larkin, K.E., Pagnani, M., Campbell, J., Gkritzalis, T., Jiang, Z.P., Pebody, C.A., Ruhl, H.A., Gooday, A.J., Bett, B.J., Billett, D.S.M., Provost, P., McLachlan, R., Turton, J.D., Lankester, S., 2012. The Porcupine Abyssal Plain fixed-point sustained observatory (PAP-SO): variations and trends from the Northeast Atlantic fixed-point time-series. *ICES Journal of Marine Science: Journal du Conseil*, 69, 776–783.
- Hasemann, C., Soltwedel, T., 2011. Small-scale heterogeneity in deep-sea nematode communities around biogenic structures. *Plos One*, 6, 1–13.
- Hecker, B., 1990. Variation in megafaunal assemblages on the continental margin south of New England. *Deep-Sea Research Part A—Oceanographic Research Papers*, 37, 37–57.
- Heezen, B.C., Tharp, M., Ewing, M., 1959. The floors of the oceans: I. The North Atlantic. *Geological Society of America Special Paper*, 65, 1–126.
- Heezen, B.C., Laughton, A.S., 1963. Abyssal plains. In: Hill, M.N. (Ed.), *The Earth Beneath the Sea* Vol. 3 (pp. 312–364): Wiley Interscience.
- Jones, R.W., Charnock, M.A., 1985. Morphogroups of agglutinated foraminifera. Their life positions and feeding habits and potential applicability in (paleo)ecological studies. *Revue de Paléobiologie*, 4, 311–320.
- Jorissen, F.J., de Stigter, H.C., Widmark, J.G.V., 1995. A conceptual model explaining benthic foraminiferal microhabitats. *Marine Micropaleontology*, 26, 3–15.
- Jorissen, F.J., Fontanier, C., Thomas, E., 2007. Paleooceanographical proxies based on deep-sea benthic foraminiferal assemblage characteristics. In: Hillaire-Marcel, C., de Vernal, A. (Eds.), *Proxies in Late Cenozoic Paleooceanography: Pt. 2: Biological tracers and biomarkers* (pp. 263–326).
- Jost, L., 2006. Entropy and diversity. *Oikos*, 113, 363–375.

- Kaminski, M.A., 1985. Evidence for control of abyssal agglutinated foraminiferal community structure by substrate disturbance: results from the HEBBLE area. *Marine Geology*, 66, 113–131.
- Kaminski, M.A., Niessen, F., Party, P.S.G., 2015. Modern agglutinated foraminifera from the Hovgard Ridge, Fram Strait, west of Spitsbergen: evidence for a deep bottom current. *Annales Societatis Geologorum Poloniae*, 85, 309–320.
- Kaufmann, R.S., Wakefield, W.W., Genin, A., 1989. Distribution of epibenthic megafauna and lebensspuren on two central North Pacific seamounts. *Deep-Sea Research Part I–Oceanographic Research Papers*, 36, 1863–1896.
- Koho, K.A., Kouwenhoven, J., de Stigter, H.C., van der Zwaan, G.J., 2007. Benthic foraminifera in the Nazaré Canyon, Portuguese continental margin: Sedimentary environments and disturbance. *Marine Micropaleontology*, 66, 27–51.
- Koho, K.A., Garcia, R., de Stigter, H.C., Epping, E., Koning, E., Kouwenhoven, T.J., van Der Zwaan, G.J., 2008. Sedimentary labile organic carbon and pore water redox control on species distribution of benthic foraminifera: A case study from Lisbon-Setubal Canyon (southern Portugal). *Progress in Oceanography*, 79, 55–82.
- Kunze, E., Llewellyn-Smith, S.G., 2004. The role of small-scale topography in turbulent mixing of the global ocean. *Oceanography*, 17, 55–64.
- Laguionie-Marchais, C., 2015. Polychaete community structure and biodiversity change in space and time at the abyssal seafloor. Doctoral thesis. *University of Southampton, Ocean & Earth Science* (p. 301).
- Lampitt, R.S., Billett, D.S.M., Martin, A.P., 2010a. The sustained observatory over the Porcupine Abyssal Plain (PAP): Insights from time series observations and process studies *Deep-Sea Research Part II–Topical Studies in Oceanography*, 57, 1267–1271.
- Lampitt, R.S., Salter, I., de Cuevas, B.A., Hartman, S., Larkin, K.E., Pebody, C.A., 2010b. Long-term variability of downward particle flux in the deep northeast Atlantic: Causes and trends. *Deep-Sea Research Part II–Topical Studies in Oceanography*, 57, 1346–1361.
- Leduc, D., Rowden, A.A., Probert, P.K., Pilditch, C.A., Nodder, S.D., Vanreusel, A., Duineveld, G.C.A., Witbaard, R., 2012. Further evidence for the effect of particle-size diversity on deep-sea benthic biodiversity. *Deep-Sea Research Part I–Oceanographic Research Papers*, 63, 164–169.
- Levin, L.A., Demaster, D.J., Mccann, L.D., Thomas, C.L., 1986. Effects of giant protozoans (class Xenophyophorea) on deep-seamount benthos. *Marine Ecology Progress Series*, 29, 99–104.
- Levin, L.A., Thomas, C.L., 1989. The influence of hydrodynamic regime on infaunal assemblages inhabiting carbonate sediments on central Pacific seamounts. *Deep-Sea Research Part A–Oceanographic Research Papers*, 36, 1897–1915.
- Levin, L.A., Leithold, E.L., Gross, T.F., Huggett, C.L., Dibacco, C., 1994. Contrasting effects of substrate mobility on infaunal assemblages inhabiting two high-energy settings on Fieberling Guyot. *Journal of Marine Research*, 52, 489–522.
- Levin, L.A., Etter, R.J., Rex, M.A., Gooday, A.J., Smith, C.R., Pineda, J., Stuart, C.T., R., H.R., Pawson, D., 2001. Environmental influences on regional deep-sea species diversity. *Annual Review of Ecology and Systematics*, 32, 51–93.

- Levin, L.A., Dayton, P.K., 2009. Ecological theory and continental margins: where shallow meets deep. *Trends in Ecology & Evolution*, 24, 606–617.
- Levin, L.A., Sibuet, M., 2012. Understanding continental margin biodiversity: a new imperative. *Annual Review of Marine Science*, Vol 4, 4, 79–112.
- Linke, P., Lutze, G.F., 1993. Microhabitat preferences of benthic foraminifera - a static concept or a dynamic adaptation to optimize food acquisition. *Marine Micropaleontology*, 20, 215–234.
- Lisitzin, A.P., 2002. *Sea-ice and iceberg sedimentation in the ocean: recent and past*. Berlin: Springer-Verlag.
- Loeblich, A.R., Tappan, H., 1987. *Foraminiferal genera and their classification*. New York: Van Nostrand Reinhold.
- Lutze, G.F., Altenbach, A.V., 1988. *Rupertina stabilis* (Wallich), a highly adapted, Suspension feeding foraminifer. *Meyniana*, 40, 55–69.
- Lutze, G.F., Thiel, H., 1989. Epibenthic foraminifera from elevated microhabitats : *Cibicidoides wuellerstorfi* and *Planulina ariminensis*. *Journal of Foraminiferal Research*, 19, 153–158.
- Macdonald, K.C., Fox, P.J., Alexander, R.T., Pockalny, R., Gente, P., 1996. Volcanic growth faults and the origin of Pacific abyssal hills. *Nature*, 380, 125–129.
- Mackensen, A., Sejrup, H.P., Jansen, E., 1985. The distribution of living benthic foraminifera on the continental slope and rise off Southwest Norway. *Marine Micropaleontology*, 9, 275–306.
- Mackensen, A., Schmiedl, G., Harloff, J., Giese, M., 1995. Deep-sea foraminifera in the South Atlantic ocean: Ecology and assemblage generation. *Micropaleontology*, 41, 342–358.
- Magurran, A.E., 2004. *Measuring Biological Diversity*. Oxford: Blackwell Science.
- McCave, I.N., Manighetti, B., Robinson, S.G., 1995. Sortable silt and fine sediment size composition slicing: parameters for paleocurrent speed and paleoceanography. *Paleoceanography*, 10, 593–610.
- McCave, I.N., Hall, I.R., 2006. Size sorting in marine muds: Processes, pitfalls, and prospects for paleoflow-speed proxies. *Geochemistry Geophysics Geosystems*, 7, 1–37.
- McClain, C.R., Barry, J.P., 2010. Habitat heterogeneity, disturbance, and productivity work in concert to regulate biodiversity in deep submarine canyons. *Ecology*, 91, 964–976.
- Menot, L., Galeron, J., Olu, K., Caprais, J.C., Crassous, P., Khripounoff, A., Sibuet, M., 2010. Spatial heterogeneity of macrofaunal communities in and near a giant pockmark area in the deep Gulf of Guinea. *Marine Ecology*, 31, 78–93.
- Mojtahid, M., Jorissen, F., Lansard, B., Fontanier, C., Bombled, B., Rabouille, C., 2009. Spatial distribution of live benthic foraminifera in the Rhône prodelta: Faunal response to a continental-marine organic matter gradient. *Marine Micropaleontology*, 70, 177–200.
- Mojtahid, M., Griveaud, C., Fontanier, C., Anschutz, P., Jorissen, F.J., 2010. Live benthic foraminiferal faunas along a bathymetrical transect (140–4800m) in the Bay of Biscay (NE Atlantic). *Revue de micropaléontologie*, 53, 139–162.
- Morris, K., Bett, B., Durden, J., Benoist, N., Huvenne, V., Jones, D., Robert, K., Ichino, M., Wolff, G., Ruhl, H., 2016. Landscape-scale spatial heterogeneity in phytodetrital cover and megafauna biomass in the abyss links to modest topographic variation. *Scientific Reports*, 6, 34080.

- Mullineaux, L.S., 1987. Organisms encrusting manganese nodules and crusts: distribution and abundance at three North Pacific sites. *Deep-Sea Research Part I—Oceanographic Research Papers*, 34.
- Murray, J.W., 2006. *Ecology and applications of benthic foraminifera*. New York: Cambridge University Press.
- Murray, J.W., Alve, E., Jones, B.W., 2011. A new look at modern agglutinated benthic foraminiferal morphogroups: their value in palaeoecological interpretation. *Palaeogeography Palaeoclimatology Palaeoecology*, 309, 229–241.
- Nash, J.D., Alford, M.H., Kunze, E., Martini, K., Kelly, S., 2007. Hotspots of deep ocean mixing on the Oregon continental slope. *Geophysical Research Letters*, 34, 1–6.
- O'Hara, T.D., 2007. Seamounts: centres of endemism or species richness for ophiuroids? *Global Ecology and Biogeography*, 16, 720–732.
- Pawlowski, J., Holzmann, M., Tyszka, J., 2013. New supraordinal classification of Foraminifera: molecules meet morphology. *Marine Micropaleontology*, 100, 1–10.
- Ramirez-Llodra, E., Brandt, A., Danovaro, R., De Mol, B., Escobar, E., German, C.R., Levin, L.A., Martinez Arbizu, P., Menot, L., Buhl-Mortensen, P., Narayanaswamy, B.E., Smith, C.R., Tittensor, D.P., Tyler, P.A., Vanreusel, A., Vecchione, M., 2010. Deep, diverse and definitely different: unique attributes of the world's largest ecosystem. *Biogeosciences*, 7, 2851–2899.
- Rex, M.A., Etter, R.J., 2010. *Deep-sea biodiversity: pattern and scale*. Cambridge: Harvard University Press.
- Rice, A.L., Lamshead, P.J.D., 1994. Patch dynamics in the deep-sea benthos: the role of a heterogeneous supply of organic matter. In: Giller, P.S., Hildrew, A.G., Raffaelli, D.G. (Eds.), *Aquatic ecology. Scale, pattern and process - The 34th Symposium of the British Ecological Society* (pp. 469–497). Oxford, UK: Blackwell Scientific.
- Rice, A.L., Thurston, M.H., Bett, B.J., 1994. The IOSDL DEEPSEAS Program: introduction and photographic evidence for the presence and absence of a seasonal input of phytodetritus at contrasting abyssal sites in the northeastern Atlantic. *Deep-Sea Research Part I—Oceanographic Research Papers*, 41, 1305–1320.
- Rowden, A.A., Schlacher, T.A., Williams, A., Clark, M.R., Stewart, R., Althaus, F., Bowden, D.A., Consalvey, M., Robinson, W., Dowdney, J., 2010. A test of the seamount oasis hypothesis: seamounts support higher epibenthic megafaunal biomass than adjacent slopes. *Marine Ecology*, 31, 95–106.
- Ruhl, H.A., 2012. RRS James Cook Cruise 62, 24 Jul-29 Aug 2011. Porcupine Abyssal Plain - sustained observatory research. *National Oceanography Centre Cruise Report* (p. 119). Southampton, UK: National Oceanography Centre.
- Rutgers van der Loeff, M., Lavaleye, M., 1986. Sediments, fauna, and the dispersal of radionuclides at the NE Atlantic dumpsite for low-level radioactive waste. *Report of the Dutch DORA program* (p. 134). Texel: Netherlands Institute for Sea Research.
- Sautya, S., Ingole, B., Ray, D., Stohr, S., Samudrala, K., Raju, K.A.K., Mudholkar, A., 2011. Megafaunal community structure of Andaman seamounts including the Back-arc Basin - a quantitative exploration from the Indian Ocean. *Plos One*, 6.

- Schmiedl, G., Mackensen, A., Müller, P., 1997. Recent benthic foraminifera from the eastern South Atlantic Ocean: dependence on food supply and water masses. *Marine Micropaleontology*, 32, 249–287.
- Schönfeld, J., 1997. The impact of the Mediterranean Outflow Water (MOW) on benthic foraminiferal assemblages and surface sediments at the southern Portuguese continental margin. *Marine Micropaleontology*, 29, 211–236.
- Schönfeld, J., 2002a. Recent benthic foraminiferal assemblages in deep high-energy environments from the Gulf of Cadiz (Spain). *Marine Micropaleontology*, 44, 141–162.
- Schönfeld, J., 2002b. A new benthic foraminiferal proxy for near-bottom current velocities in the Gulf of Cadiz, northeastern Atlantic Ocean. *Deep-Sea Research Part I–Oceanographic Research Papers*, 49, 1853–1875.
- Snelgrove, P.V.R., Smith, C.R., 2002. A riot of species in an environmental calm: The paradox of the species-rich deep-sea floor. *Oceanography and Marine Biology: An Annual Review*, 40, 311–342.
- Snider, L.J., Burnett, B.R., Hessler, R.R., 1984. The composition and distribution of meiofauna and nanobiota in a central North Pacific deep-sea area. *Deep-Sea Research Part I–Oceanographic Research Papers*, 31, 1225–1249.
- Sokal, R.R., Rohlf, J.F., 2012. *Biometry: the principles and practice of statistics in biological research*. New York: W. H. Freeman and Company.
- Stefanoudis, P.V., Gooday, A.J., 2015. Basal monothalamous and pseudochambered benthic foraminifera associated with planktonic foraminiferal shells and mineral grains from the Porcupine Abyssal Plain, NE Atlantic. *Marine Biodiversity*, 45, 357–369.
- Stefanoudis, P.V., Schiebel, R., Mallet, R., Durden, J.M., Bett, B.J., Gooday, A.J., 2016. Agglutination of benthic foraminifera in relation to mesoscale bathymetric features in the abyssal NE Atlantic (Porcupine Abyssal Plain). *Marine Micropaleontology*, 123, 15–28.
- Stuart, C.T., Arbizu, P.M., Smith, C.R., Molodtsova, T., Brandt, A., Etter, R.J., Escobar-Briones, E., Fabri, M.C., Rex, M.A., 2008. CeDAMar global database of abyssal biological sampling. *Aquatic Biology*, 4, 143–145.
- Svensson, J.R., Lindegarth, M., Jonsson, P.R., Pavia, H., 2012. Disturbance-diversity models: what do they really predict and how are they tested? *Proceedings of the Royal Society B–Biological Sciences*, 279, 2163–2170.
- Tendal, O.S., Hessler, R.R., 1977. An introduction to the biology and systematics of Komokiacea (Textulariina, Foraminiferida). *Galathea Report*, 14, 165–194.
- Thistle, D., 1983. The stability time hypothesis as a predictor of diversity in deep-sea soft-bottom communities: a test. *Deep-Sea Research Part A–Oceanographic Research Papers*, 30, 267–277.
- Thistle, D., Yingst, J.Y., Fauchald, K., 1985. A deep-sea benthic community exposed to strong near-bottom currents on the Scotian Rise (Western Atlantic). *Marine Geology*, 66, 91–112.
- Thistle, D., Ertman, S.C., Fauchald, K., 1991. The fauna of the HEBBLE site: patterns in standing stock and sediment-dynamic effects. *Marine Geology*, 99, 413–422.
- Thistle, D., 1998. Harpacticoid copepod diversity at two physically reworked sites in the deep sea. *Deep-Sea Research Part II–Topical Studies in Oceanography*, 45, 13–24.

- Thistle, D., Levin, L.A., 1998. The effect of experimentally increased near-bottom flow on metazoan meiofauna at a deep-sea site, with comparison data on macrofauna. *Deep-Sea Research Part I—Oceanographic Research Papers*, 45, 625–638.
- Tuomisto, H., 2010. A diversity of beta diversities: straightening up a concept gone awry. Part 1. Defining beta diversity as a function of alpha and gamma diversity. *Ecography*, 33, 2–22.
- Turnewitsch, R., Reyss, J.L., Chapman, D.C., Thomson, J., Lampitt, R.S., 2004. Evidence for a sedimentary fingerprint of an asymmetric flow field surrounding a short seamount. *Earth and Planetary Science Letters*, 222, 1023–1036.
- Turnewitsch, R., Falahat, S., Nycander, J., Dale, A., Scott, R.B., Furnival, D., 2013. Deep-sea fluid and sediment dynamics—Influence of hill- to seamount-scale seafloor topography. *Earth-Science Reviews*, 127, 203–241.
- Turnewitsch, R., Lahajnar, N., Haeckel, M., Christiansen, B., 2015. An abyssal hill fractionates organic and inorganic matter in deep-sea surface sediments. *Geophysical Research Letters*, 42, 7663–7672.
- Vanreusel, A., Fonseca, G., Danovaro, R., da Silva, M.C., Esteves, A.M., Ferrero, T., Gad, G., Galtsova, V., Gambi, C., Genevois, V.D., Ingels, J., Ingole, B., Lampadariou, N., Merckx, B., Miljutin, D., Miljutina, M., Muthumbi, A., Netto, S., Portnova, D., Radziejewska, T., Raes, M., Tchesunov, A., Vanaverbeke, J., Van Gaeve, S., Venekey, V., Bezerra, T.N., Flint, H., Copley, J., Pape, E., Zeppilli, D., Martinez, P.A., Galeron, J., 2010. The contribution of deep-sea macrohabitat heterogeneity to global nematode diversity. *Marine Ecology*, 31, 6–20.
- Veillette, J., Sarrazin, J., Gooday, A.J., Galeron, J., Caprais, J.C., Vangriesheim, A., Etoubleau, J., Christian, J.R., Juniper, S.K., 2007. Ferromanganese nodule fauna in the Tropical North Pacific Ocean: Species richness, faunal cover and spatial distribution. *Deep-Sea Research Part I—Oceanographic Research Papers*, 54, 1912–1935.
- Watling, L., Guinotte, J., Clark, M.R., Smith, C.R., 2013. A proposed biogeography of the deep ocean floor. *Progress in Oceanography*, 111, 91–112.
- Whittaker, R.H., 1960. Vegetation of the Siskiyou mountains, Oregon and California. *Ecological monographs*, 30, 279–338.
- Whittaker, R.H., 1972. Evolution and measurement of species diversity. *International Association for Plant Taxonomy*, 21, 213–251.

Chapter 5: Relationship between ‘live’ and dead benthic foraminiferal assemblages in the abyssal NE Atlantic

Abstract

Dead foraminiferal assemblages within the sediment mixed layer provide an integrated, time-averaged view of the foraminiferal fauna, while the relationship between dead and live assemblages reflects the population dynamics of different species together with taphonomic processes operating over the last few hundred years. Here, we analysed four samples for ‘live’ (Rose-Bengal-stained) and dead benthic foraminifera (0–1 cm sediment layer, >150 µm) from four sites in the area of the Porcupine Abyssal Plain Sustained Observatory (PAP-SO; NE Atlantic, 4850 m water depth). Two sites were located on abyssal hills and two on the adjacent abyssal plain. Our results indicate that the transition from live to dead benthic foraminiferal assemblages involved a significant loss of delicate agglutinated and organic-walled tests (e.g. *Lagenammia*, *Nodellum*, *Reophax*) with poor preservation potential, and to a lesser extent that of some relatively fragile calcareous tests (mostly miliolids), possibly a result of dissolution. Other processes, such as the transport of tests by bottom currents and predation, are unlikely to have substantially altered the composition of dead faunas. Positive live to dead ratios suggest that some species (notably *Epistominella exigua* and *Bolivina spathulata*) may have responded to recent phytodetritus input. Although the composition of live assemblages seemed to be influenced by seafloor topography (abyssal hills vs. plain), no important relation was found for dead assemblages. We suggest that PAP-SO fossil assemblages are likely to be comparable across topographically contrasting sites, and dominated by calcareous and some robust agglutinated forms with calcitic cement (e.g. *Eggerella*).

5.1 Introduction

Benthic foraminifera are a hugely successful group of unicellular eukaryotes within the Supergroup Rhizaria (Ruggiero et al., 2015), most of which form a 'test' (shell) made of organic matter, agglutinated sediment particles or secreted calcium carbonate. They are extremely common in most marine sediments but particularly in the deep sea (>200 m water depth) where they often account for >50% of the meiofauna (32–300 μm) (Gooday, 2014; Snider et al., 1984) and a significant proportion of the macrofauna (>300 μm) (Gooday et al., 2007; Tendal and Hessler, 1977). Robust secreted (calcitic) or agglutinated foraminiferal tests are preserved in marine sediments in excellent condition and provide a continuous fossil record starting in the early Cambrian (McIlroy et al., 2001). This, in combination with their high sensitivity to environmental conditions, makes foraminiferal tests widely used as proxies for reconstructing ancient oceans, particularly during the Cenozoic (Fischer and Wefer, 1999; Gooday, 2003; Jorissen et al., 2007).

The use of benthic foraminifera as tools in paleoceanographic studies necessitates a good knowledge of the ecology of modern species as well as the bias that is introduced during the transition from a living community into a dead and subsequently fossil assemblage. For a theoretical approach to assemblage formation see the works of Loubere and Gary (1990), Loubere et al. (1993) and Loubere (1997). Dead assemblages are found within the surface mixed layer where sediment is being bioturbated by macrofaunal and megafaunal organisms. A mixture of life and taphonomic processes controls dead assemblage composition. Life processes include species-specific rates of test production (i.e. reproduction and death), which dictate the contribution of tests from the living fauna to the sediment (de Stigter et al., 1999; Murray, 1976). Taphonomy occurs over the course of months to years and includes the following processes: 1) Microbial decomposition of fragile agglutinated tests that contain easily degradable organic cement (e.g. komokiaceans, organic-walled and most agglutinated taxa) (Schröder, 1988), and dissolution of thin-walled calcareous tests within the lysocline (Berger et al., 1982) and below the carbonate compensation depth (CCD) (Saidova, 1965, 1966). 2) Post-mortem transport of small-sized tests by

bottom currents (Murray, 2003; Snyder et al., 1990). (3) Destruction of tests by metazoan predation, passive ingestion by deposit-feeding organisms, and other forms of biological activity (Culver and Lipps, 2003). (4) Mixing by bioturbation (Bouchet et al., 2009; Moodley, 1990).

The surface mixed layer overlies the 'fossil sediment' where the dead assemblage, now buried below the reach of biological activity, is transformed into the fossil assemblage. Additional changes in faunal composition are predominantly governed by pore-water geochemistry and sediment compaction (Mackensen and Douglas, 1989; Schröder, 1988).

Several previous studies have focused on comparisons between live and dead assemblages in coastal (Goineau et al., 2015; Murray and Alve, 1999; Murray and Pudsey, 2004), shelf (Douglas et al., 1980; Mendes et al., 2013) or bathyal settings (Duros et al., 2012; Duros et al., 2014; Fontanier et al., 2014; Mackensen and Douglas, 1989; Schumacher et al., 2007). However, only those of Bernstein and Meador (1979) in the Central Pacific, Schröder (1988) in the NW Atlantic, Loubere and Rayray (2016) in the European Arctic Margin, Mackensen et al. (1993) in the South Atlantic, and Mackensen et al. (1990) and Harloff and Mackensen (1997) in the Weddell Sea have been conducted partly or entirely at abyssal depths (i.e. >3500 m).

The area of the Porcupine Abyssal Plain Sustained Observatory (PAP-SO, Hartman et al., 2012), located in the northeast Atlantic (4850 m water depth), has been studied for almost three decades (Lampitt et al., 2010a). Although the live foraminiferal faunas are well known (Gooday, 1996; Gooday et al., 2010; Chapter 4), and post-glacial (the last 15,000 years) fossil faunas in a long core were analysed by Smart (2008), the dead faunas at the PAP-SO site have never been examined. Studies of dead core-top assemblages, and their relationship to corresponding live assemblages provide insights into initial post-mortem changes unaffected by diagenetic effects. With this in mind, we analysed the top sediment layer (0–1 cm) of four samples for 'live' (Rose-Bengal-stained) and dead benthic foraminifera from four sites in the PAP-SO area, two on top of abyssal hills and two on the adjacent abyssal plain. We then asked the following questions. (1) To

what extent are dead foraminiferal assemblages representative of the original live fauna? (2) Based on these comparisons, which factors seem to influence the composition of dead assemblages? (3) Are faunal differences between the hill and plain settings reflected in the dead assemblages?

5.2 Materials and methods

5.2.1 Characteristics of the study area

The PAP-SO area is subject to seasonal fluctuations in surface ocean primary production and consequent fluxes of organic matter to the seafloor (Rice et al., 1994). Particle flux has been monitored since 1989 using sediment traps, with a peak typically occurring in summer (Frigstad et al., 2015; Lampitt et al., 2001; Lampitt et al., 2010b). Long-term sediment accumulation rates on the plain are around 3.5 cm ky⁻¹ (Rice et al., 1991; Thomson et al., 1993), with oxygen penetrating to at least 25 cm sediment depth (van der Loeff and Lavaleye, 1986), and the sediment mixed layer being around 11 cm thick (Smith and Rabouille, 2002). The lysocline has been estimated to lie between 4700–4900 m (Biscaye et al., 1976; van der Loeff and Lavaleye, 1986) and the CCD at about 5200 m (Biscaye et al., 1976). Due to winnowing processes ice-rafted dropstones (~few mm in size) are frequently exposed on hills but not on the plain (Durden et al., 2015). The silt and clay content of hill sediments is appreciably lower than plain sediments (Chapter 3; Durden et al., 2015; Stefanoudis et al., 2016). These observations strongly suggest significant winnowing of fine particles from hill sediments, and consequently reduced sediment accumulation rates on hills. The strong seasonal signal in organic matter supply to the seafloor (e.g. Bett et al., 2001), coupled with the substantial variation in the silt and clay content of hill and plain sediments complicates the interpretation of sedimentary organic matter content (Turnewitsch et al., 2015). However, a c. three-fold increase in megafaunal biomass on hill compared to plain locations provides a strong indication of the relative input of organic matter (Durden et al., 2015; Morris et al., 2016).

5.2.2 Sample collection

Samples were collected during RSS *James Cook* cruise 062 (JC062, 24 July to 29 August 2011; Ruhl, 2012) and were obtained using a Bowers and Connelly Megacorer (Gage and Bett, 2005) fitted with 59 mm internal diameter cores tubes,

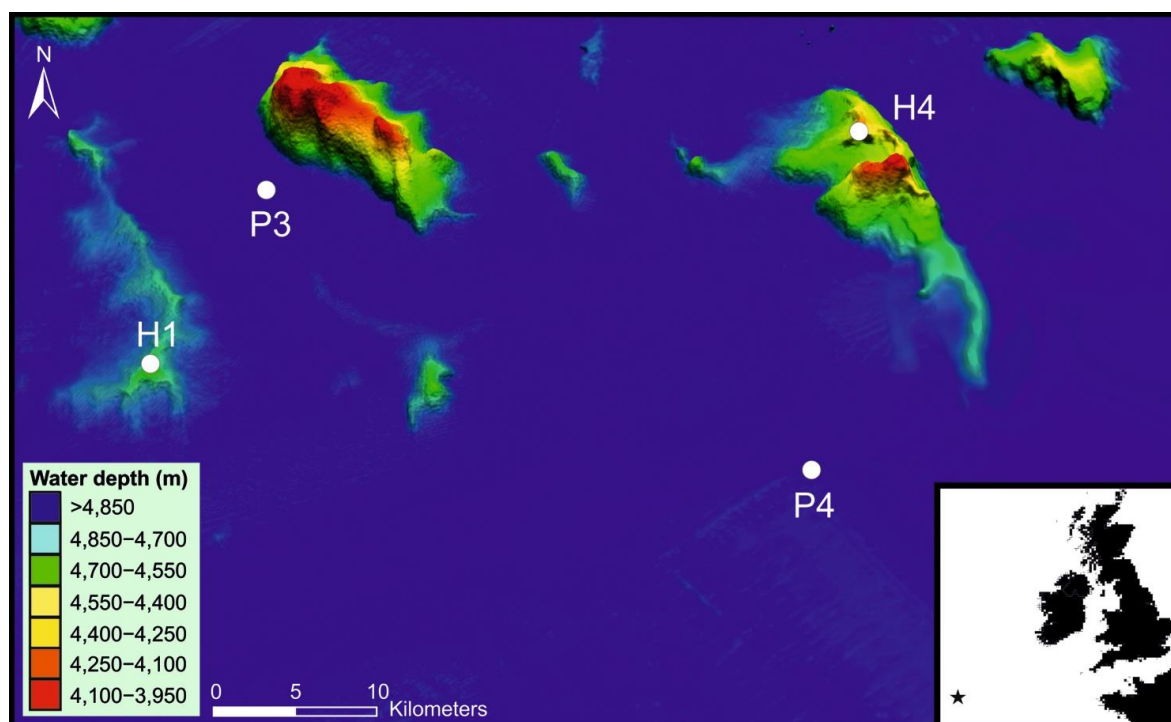


Figure 5.1. 3D topographic representation of the PAP-SO area (48.79 to 49.21 °N, 16.03 to 16.93 °W) indicating the approximate location and bathymetry of the four study sites, H1 and H4 (abyssal hill sites) and P3 and P4 (abyssal plain sites). The inset shows the general location (star) of the Porcupine Abyssal Plain in the Northeast Atlantic Ocean.

Table 5.1. Site and station information.

Site	Station	Topography	Water depth (m)	Latitude (°N)	Longitude (°W)	Date sampled
H1	JC062-053	Abyssal Hill	4679	48.977	16.727	05.08.2011
H4	JC062-126	Abyssal Hill	4365	49.074	16.264	22.08.2011
P3	JC062-101	Abyssal Plain	4851	49.083	16.667	17.08.2011
P4	JC062-077	Abyssal Plain	4851	48.875	16.293	11.08.2011

from two abyssal plain sites (P1, P2) and two abyssal hill sites (H1, H4) (Fig. 5.1). On recovery the cores were sliced into 0.5 cm layers to 2 cm sediment depth, followed by 1 cm layers from 2 to 10 cm depth, and each slice fixed in 10% Borax buffered formalin. The present contribution is based on material retained on a 150-

μm sieve from the 0–1 cm sediment horizon from four samples, one from each site (Table 5.1).

5.2.3 Sample processing

In the laboratory, the 0–0.5 cm and 0.5–1.0 cm slices of cores were gently washed through two sieves (300 μm and 150 μm) using filtered tap water. Residues >300 μm and 150–300 μm were stained with Rose Bengal (1 $\text{g}\cdot\text{L}^{-1}$) overnight and sorted for all ‘live’ (stained) and dead benthic foraminifera under a binocular microscope. We did not include komokiaceans or small dome-like foraminifera associated with planktonic foraminiferal shells and mineral grains (Chapter 2; Stefanoudis and Gooday, 2015), with the exception of two easily recognizable morphotypes (*Psammosphaera* sp. 1 and ‘white domes’; see taxonomic notes in Appendix A). These forms are not taken into account, as they are difficult to separate into species and are poorly stained with Rose Bengal, making the distinction between live and dead specimens difficult. For the rest of the picked material, in order to ensure that the stained material was foraminiferal protoplasm, specimens were transferred to glass slides with glycerin and examined under a transmission light microscope. This enabled the distinction of ‘fresh’ cellular material from decayed cytoplasm, accumulations of bacteria, or other inhabiting organisms. Where necessary, thick-walled agglutinated tests were broken open to expose the material inside. Only specimens with most chambers stained were considered to be live. In the case of many monothalamids, the test contained numerous stercomata (waste pellets) that decay after death into a grey powder. Thus, the ‘fresh’ (undegraded) appearance of stercomata was an additional indication that specimens were alive when collected. Delicate taxa were either stored on glass cavity slides in glycerol or in 2 ml Nalgene cryovials in 10% buffered formalin (4% borax buffered formaldehyde solution).

5.2.4 Light and scanning electron microscopy

Specimens were photographed using either a NIKON Coolpix 4500 camera mounted on an Olympus SZX10 compound microscope, or a Canon EOS 60D mounted on an Olympus SZX7 compound microscope, or a Canon EOS 350D

mounted on a Leica Z16-APO incident light microscope. Selected specimens were dried onto aluminium stubs and examined by scanning electron microscopy (SEM) using a LEO 1450VP (variable pressure) or an environmental Zeiss EVO LS10 (variable pressure) instrument. The taxonomic scheme we followed was a combination of those proposed by Loeblich and Tappan (1987) and Pawlowski et al. (2013).

5.2.5 Data processing

For the purposes of analysis we partitioned our data in three ways: (a) 'live' (Rose-Bengal-stained) versus 'dead' specimens; (b) 'entire' (fossilisable plus non-fossilisable taxa) versus 'potential fossil fauna', the latter consisting of calcareous taxa and agglutinates with a calcitic cement, such as *Eggerella* and *Karrerella* (Harloff and Mackensen, 1997; Mackensen et al., 1990; Mackensen et al., 1995; Schmiedl et al., 1997); and (c) 'common' versus 'rare' species, the former consisting of species having a relative abundance >5% in the live or dead fraction of at least one sample. Rarefied alpha diversity indexes (species richness, exponential Shannon index, inverse Simpson index, Chao 1; see e.g. Magurran, 2004) were assessed via individual-based rarefaction (e.g. Colwell et al., 2012) implemented using EstimateS (9.1.0, viceroy.eeb.uconn.edu/estimates), based on count data for complete specimens. Community composition was examined on the basis of faunal dissimilarity (Bray-Curtis), calculated following a range of transformations (none; log [x+1]; square-root; fourth-root; presence-absence) on the count data for complete specimens, visualised with non-metric multi-dimensional scaling ordination (MDS), and assessed using analysis of similarities (PRIMER 6, Clarke and Gorley, 2006). Multivariate dispersion (MVDISP), a measure of community heterogeneity, was also estimated in PRIMER.

We calculated live to dead ratios (L/D; Jorissen and Wittling, 1999) for all 'common' species in two ways: 1) using count (N) data (L_N/D_N), and 2) using relative abundance (%) data ($L\%/D\%$), that are less affected by the substantially higher numbers of tests in the dead fauna. Only the latter ratio has been used for live-dead comparisons in previous studies (e.g. Jorissen & Wittling, 1999; Duros et al., 2014; Goineau et al., 2015). For the L/D ratios of potential fossil species, we

first calculated corrected relative abundances for all species in the living and dead assemblages after discounting all non-fossilising agglutinated species (i.e. agglutinated species with an organic cement).

5.3 Results

5.3.1 Density

A total of 512 obviously complete live foraminiferal specimens, 85–163 (mean 128 \pm 33 standard deviation) individuals per sample, was picked from the four samples. About half belonged to the Hormosinacea (agglutinated) and the Rotaliida (calcareous), both multichambered groups. In addition to the complete specimens, we recorded 43 fragmented stained tests (12–28 per sample), the majority (77%) of them tubular monothalamids. The same samples yielded a total of 4686 obviously complete, dead foraminiferal specimens, 571–2122 per sample. Almost two-thirds (63%) of these were rotaliids, with the next most abundant group being the multichambered textulariids (agglutinated) (~8% of the total dead assemblage). Fragments of dead tests ranged from 261 to 528 per sample (total 1527), of which more than two-thirds (72%) were tubular and almost all of the rest (~25%) were members of the Miliolida (calcareous; mostly *Pyrgo* spp. and *Quinqueloculina* spp.). Densities per major grouping for the live and dead assemblages are given in Supplementary Material 5.A.1.

5.3.2 Diversity

The majority (~88%) of all complete live tests could be assigned to morphospecies (either described or undescribed), the remainder being indeterminate. In total, 76 species were identified, with 29–46 species being present in each sample. Most (~86%) of the live fragments could be assigned to 10 morphospecies, mainly tubular monothalamids, with 0–5 species per sample. The total number of species with a live test (complete and fragments) was 83. In the case of the dead assemblage, almost all (99%) of the specimens with complete tests could be assigned to a morphospecies. In total, 152 species were identified, with 75–114

per sample. Three quarters of the dead fragments could be assigned to 24 morphospecies (7–17 per sample), most of them tubular monothalamids. The total number of species with dead tests (complete and fragments) was 163. The numbers of live and dead species in each major grouping are summarised in Supplementary Material 5.A.2. A brief description and representative illustration for each species is given in Appendix B.

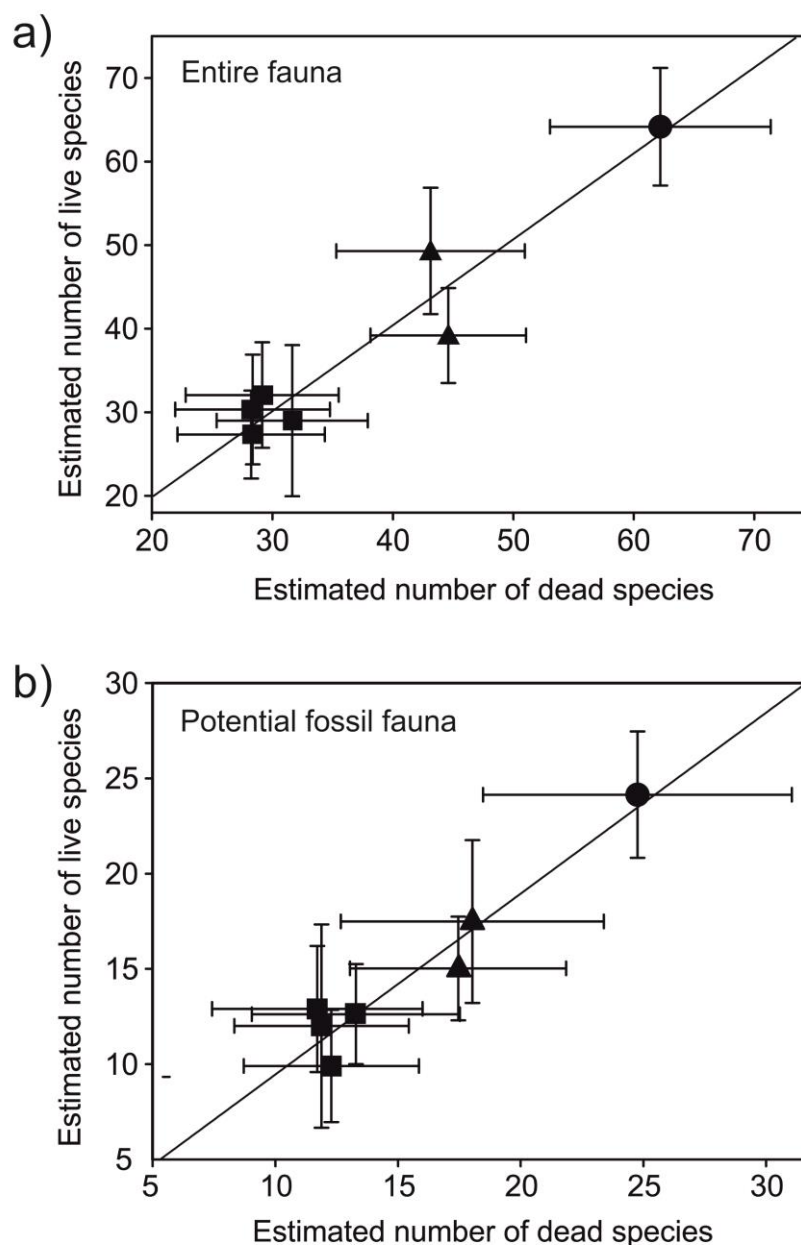


Figure 5.2. Biplot of rarefied estimated number of live and dead species for each individual sample (square), samples grouped by topography (hills, plain; triangle) and all samples combined (circle), for the entire (a) and potential fossil fauna (b), respectively. (Data shown as mean and 95% confidence interval; line: linear least squares fit).

Rarefied alpha diversity indexes (species richness, exponential Shannon index, inverse Simpson index, Chao 1) were comparable (ANOVA, $p < 0.05$) between the live and dead assemblages, for both the entire and the potential fossil fauna. In addition, we found that the rarefied estimated number of live species was always linearly correlated with that of the dead fraction for individual samples, samples grouped by setting (hills, plain), as well as for all samples combined (Fig. 5.2). This was especially true for the potential fossil fauna, where most of the samples were fairly close to the best-fit line. For the entire fauna, most samples were slightly above the best-fit line, indicating that for the same number of individuals the number of live species was slightly higher than in the case of the potential fossil assemblage.

5.3.3 Comparison of living and dead assemblages

5.3.3.1 Species composition

Live and dead assemblages were highly distinct in terms of their species composition (Fig. 5.3). When the entire assemblage was considered, ANOSIM assessment indicated a significant ($p < 0.05$) difference in the assemblages regardless of prior data transformation. When only the common species were considered, ANOSIM again indicated a significant ($p < 0.05$) difference in the assemblages except in the case of simple presence absence assessment. Multivariate dispersion was always less in the dead than in the live assemblage ($MVDISP_{\text{dead}} < MVDISP_{\text{live}}$), indicating that the dead assemblages were more homogeneous in their composition. Identical results were obtained when only the potential fossil faunas were considered. The 2-d MDS plots suggested common ecological trends (e.g. plain to hill comparisons) in both the live and dead assemblages whether assessed in terms of the entire fauna (Fig. 5.3a) or only the fossilisable component (Fig. 5.3b), although that trend was always more pronounced in the live fauna. Similarly, the live to dead trend (e.g. live plain to dead plain) in species composition appeared to be consistent between both plains and hills, whether assessed in terms of the total fauna or only the fossilisable component.

5.3.3.2 Abundant species

The 20 top-ranked species from the entire assemblage, per sample and in all samples combined, are summarised in Table 5.2. The four most common species with consistently high rankings across all four samples were *Adercotryma glomerata* (ranked in the top three in three out of four samples), *Epistominella exigua* (ranked in the top five in all four samples), *Reophax* sp. 21 (ranked in the top four in all four samples) and *Lagenammia* aff. *arenulata* (ranked in the top

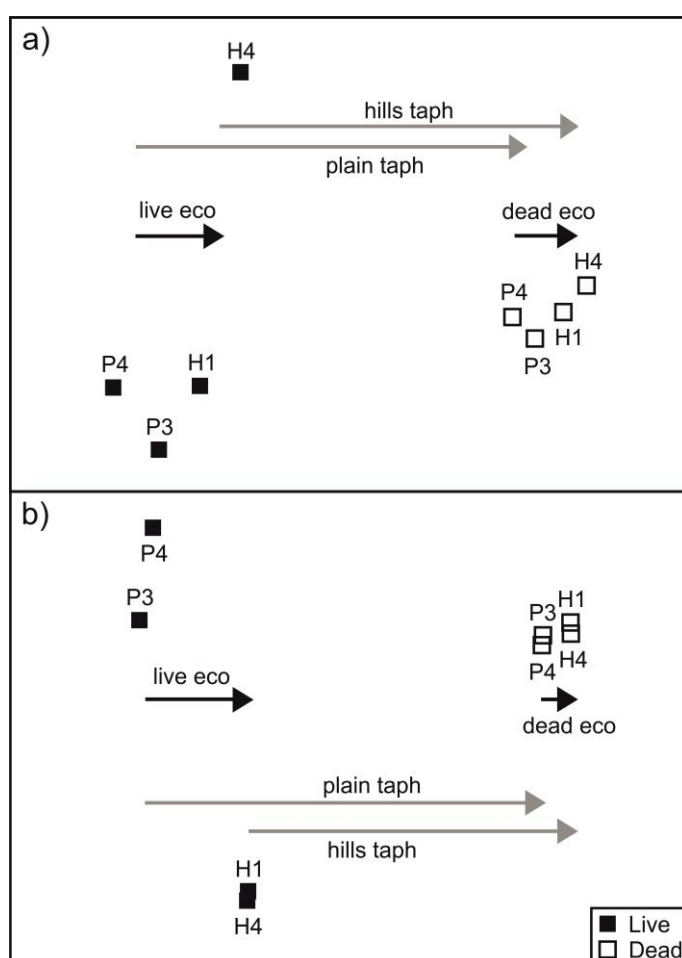


Fig. 5.3. 2-d non-metric multi-dimensional scaling ordination plots of live (solid symbols) and dead (open symbols) foraminiferal assemblage composition from plain (circles) and hill (triangles) sites on the PAP-SO area, based on Bray-Curtis dissimilarity of $\log(x+1)$ transformed data. (a) Entire assemblage. (b) Potential fossil assemblage. Black arrows illustrate the degree of ecological variation in assemblage composition within the living and dead fraction, while grey arrows indicate the amount of taphonomic change in assemblage composition per topographic setting.

Table 5.2. Top 20 'live' (Rose-Bengal-stained) species with complete tests per sample and in all samples combined (final column). N = total number of specimens. *A. glomerata* = *Adercotryma glomerata*, *A. shannoni* = *Ammoglobigerina shannoni*, *B. aff. earleandi* = *Bolivina earleandi*, *B. spathulata* = *Bolivina spathulata*, *C. wuellerstorfi* = *Cibicides wuellerstorfi*, *E. bradyi* = *Eggerella bradyi*, *E. exigua* = *Epistominella exigua*, *G. subglobosa* = *Globocassidulina subglobosa*, *L. aff. arenulata* = *Lagenammia aff. arenulata*, *N. dentaliniformis* = *Nodulina dentaliniformis*, *N. umboniferus* = *Nuttaliides umboniferus*, *O. globosa* = *Oolina globosa*, *O. tenerus* = *Oridorsalis tenerus*, *O. umbonatus* = *Oridorsalis umbonatus*, *P. aurantiaca* = *Placopsilinella aurantiaca*, *P. murrayi* = *Portatrochammina murrayi*, *P. murrhina* = *Pyro murrhina*, *R. agglutinatus* = *Reophax agglutinatus*, *R. bilocularis* = *Reophax bilocularis*, *Q. venusta* = *Quinqueloculina venusta*, *S. bulloides* = *Sphaeroidina bulloides*, *S. tenuis* = *Spirosigmoilina tenuis*, *T. albicans* = *Thurammina albicans*.

Rank	H1	N	Rank	H4	N	Rank	P3	N	Rank	P4	N	Rank	Total	N
	Species			Species			Species			Species			Species	
1	White domes	15	1	<i>A. glomerata</i>	24	1	<i>E. exigua</i>	16	1	<i>E. exigua</i>	13	1	<i>A. glomerata</i>	46
2	<i>L. aff. arenulata</i>	14	2	<i>Nodellum</i> -like sp.	9	2	<i>Reophax</i> sp. 28	14	2	<i>A. glomerata</i>	9	2	<i>E. exigua</i>	43
3	<i>A. glomerata</i>	11	3	<i>Reophax</i> sp. 21	8	3	<i>B. spathulata</i>	10	3	<i>R. bilocularis</i>	6	3	<i>Reophax</i> sp. 21	30
4	<i>Reophax</i> sp. 21	10	4	<i>E. exigua</i>	7	4	<i>N. dentaliniformis</i>	8	4	<i>L. aff. arenulata</i>	4	4	<i>L. aff. arenulata</i>	20
5	<i>E. exigua</i>	7	4	<i>S. bulloides</i>	7	4	<i>Reophax</i> sp. 21	8	4	<i>Reophax</i> sp. 9	4	5	<i>Reophax</i> sp. 28	20
6	<i>Reophax</i> sp. 19	6	6	<i>A. shannoni</i>	5	6	<i>G. subglobosa</i>	5	4	<i>Reophax</i> sp. 21	4	6	White domes	19
6	<i>T. albicans</i>	6	7	<i>Psammospaera</i> sp. 1	4	6	<i>Reophax</i> sp. 19	5	7	<i>Lagenammia</i> sp. 3	3	7	<i>Reophax</i> sp. 19	14
8	<i>G. subglobosa</i>	5	7	<i>Reophax</i> sp. 9	4	8	White domes	4	7	<i>Reophax</i> sp. 19	3	8	<i>G. subglobosa</i>	13
8	<i>Lagenammia</i> sp. 19	5	7	<i>P. murrhina</i>	4	9	<i>C. wuellerstorfi</i>	3	7	<i>T. albicans</i>	3	8	<i>Nodellum</i> -like sp.	13
8	<i>O. umbonatus</i>	5	10	<i>P. murrayi</i>	3	9	<i>S. bulloides</i>	3	10	<i>M. barleeanus</i>	2	8	<i>N. dentaliniformis</i>	13
8	<i>P. murrhina</i>	5	10	<i>R. agglutinatus</i>	3	9	<i>T. albicans</i>	3	10	<i>P. murrhina</i>	2	8	<i>P. murrhina</i>	13
8	<i>Reophax</i> sp. 23	5	10	<i>R. bilocularis</i>	3	12	<i>A. glomerata</i>	2	20	Multiple (18) spp.	1	8	<i>Reophax</i> sp. 9	13
8	<i>Reophax</i> sp. 28	5	13	<i>C. wuellerstorfi</i>	2	12	<i>B. aff. earleandi</i>	2				13	<i>S. bulloides</i>	12
8	<i>Reophax</i> sp. 110/111	5	13	<i>E. bradyi</i>	2	12	<i>E. bradyi</i>	2				13	<i>T. albicans</i>	12
15	<i>Bathysiphon</i> sp. 1	4	13	<i>G. subglobosa</i>	2	12	<i>L. aff. arenulata</i>	2				15	<i>B. spathulata</i>	10
15	<i>Reophax</i> sp. 9	4	13	<i>N. umboniferus</i>	2	12	<i>Lagenammia</i> sp. 19	2				16	<i>C. wuellerstorfi</i>	8
17	<i>Nodellum</i> -like sp.	3	13	<i>O. tenerus</i>	2	12	<i>O. globosa</i>	2				16	<i>Lagenammia</i> sp. 19	8
17	<i>N. dentaliniformis</i>	3	13	<i>P. aurantiaca</i>	2	12	<i>P. murrhina</i>	2				16	<i>O. umbonatus</i>	8
17	<i>Q. venusta</i>	3	13	<i>S. tenuis</i>	2	12	<i>Reophax</i> sp. 27	2				16	<i>R. bilocularis</i>	8
17	<i>Reophax</i> sp.8	3	20	Multiple (21) spp.	1	20	Multiple (15) spp.	1				20	<i>Reophax</i> sp. 23	7

Table 5.3. Top 20 dead species with complete tests per sample and in all samples combined (final column). N = total number of specimens. *A. glomerata* = *Adercotryma glomerata*, *C. wuellerstorfi* = *Cibicides wuellerstorfi*, *E. bradyi* = *Eggerella bradyi*, *E. exigua* = *Epistominella exigua*, *E. foliaceus* = *Eratidus foliaceus*, *G. subglobosa* = *Globocassidulina subglobosa*, *G. polia* = *Gyroidina polia*, *G. aff. soldanii* = *Gyroidina aff. soldanii*, *G. umbonata* = *Gyroidina umbonata*, *K. apicularis* = *Karrerulina apicularis*, *M. barleeanus* = *Melonis barleeanus*, *M. pompilioides* = *Melonis pompilioides*, *N. dentaliniformis* = *Nodulina dentaliniformis*, *N. umboniferus* = *Nuttaliides umboniferus*, *O. globosa* = *Oolina globosa*, *O. umbonatus* = *Oridorsalis umbonatus*, *P. aurantiaca* = *Placopsilinella aurantiaca*, *P. murrayi* = *Portatrochammina murrayi*, *P. murrhina* = *Pyro murrhina*, *Q. venusta* = *Quinqueloculina venusta*, *S. bulloides* = *Sphaeroidina bulloides*.

Rank	H1	N	Rank	H4	N	Rank	P3	N	Rank	P4	N	Rank	Total	N
	Species			Species			Species			Species			Species	
1	<i>E. exigua</i>	216	1	<i>S. bulloides</i>	564	1	<i>E. exigua</i>	146	1	<i>E. exigua</i>	129	1	<i>E. exigua</i>	669
2	<i>G. subglobosa</i>	112	2	<i>E. exigua</i>	178	2	<i>G. subglobosa</i>	34	2	<i>G. subglobosa</i>	57	2	<i>S. bulloides</i>	634
3	<i>E. bradyi</i>	87	3	<i>G. subglobosa</i>	86	2	<i>E. bradyi</i>	34	3	<i>A. glomerata</i>	27	3	<i>G. subglobosa</i>	289
4	<i>O. umbonatus</i>	79	4	<i>P. murrhina</i>	82	4	<i>N. umboniferus</i>	29	3	<i>M. barleeanus</i>	27	4	<i>P. murrhina</i>	199
5	<i>M. pompilioides</i>	69	5	<i>M. barleeanus</i>	80	5	<i>P. murrhina</i>	27	5	<i>P. murrhina</i>	26	5	<i>M. barleeanus</i>	191
6	<i>P. murrhina</i>	64	6	<i>C. wuellerstorfi</i>	76	6	<i>C. wuellerstorfi</i>	22	6	<i>E. bradyi</i>	24	6	<i>O. umbonatus</i>	186
7	<i>M. barleeanus</i>	63	7	<i>M. pompilioides</i>	74	6	<i>O. umbonatus</i>	22	6	<i>L. aff. arenulata</i>	24	7	<i>E. bradyi</i>	184
8	<i>C. wuellerstorfi</i>	46	8	<i>O. umbonatus</i>	70	8	<i>M. barleeanus</i>	21	8	<i>S. bulloides</i>	22	8	<i>M. pompilioides</i>	183
8	<i>L. aff. arenulata</i>	46	9	<i>N. umboniferus</i>	60	8	<i>M. pompilioides</i>	21	9	<i>M. pompilioides</i>	19	9	<i>C. wuellerstorfi</i>	159
10	<i>A. glomerata</i>	45	10	<i>G. polia</i>	45	10	<i>A. glomerata</i>	16	10	<i>C. wuellerstorfi</i>	15	10	<i>N. umboniferus</i>	130
11	<i>S. bulloides</i>	35	11	<i>Pullenia</i> sp. 1	44	11	<i>L. aff. arenulata</i>	14	10	<i>O. umbonatus</i>	15	11	<i>A. glomerata</i>	112
12	<i>N. dentaliniformis</i>	30	12	<i>E. bradyi</i>	39	12	<i>S. bulloides</i>	13	12	<i>N. umboniferus</i>	13	12	<i>L. aff. arenulata</i>	104
13	<i>N. umboniferus</i>	28	13	<i>P. aurantiaca</i>	30	13	<i>Gyroidina</i> sp. 1	12	13	<i>Hormosina</i> sp. 1	12	13	<i>G. polia</i>	80
14	<i>G. polia</i>	24	13	<i>Psammosphaera</i> sp. 1	30	14	<i>N. dentaliniformis</i>	9	14	<i>G. aff. soldanii</i>	10	14	<i>Gyroidina</i> sp. 1	60
14	<i>Gyroidinoina</i> sp. 1	24	15	<i>E. foliaceus</i>	25	14	<i>Oolina</i> sp. 4	9	14	<i>Oolina</i> sp. 4	10	15	<i>Pullenia</i> sp. 1	56
16	<i>Recurvoides</i> sp. 1	21	16	<i>A. glomerata</i>	24	14	<i>G. aff. soldanii</i>	9	14	<i>Parafissurina</i> sp. 3	10	16	<i>Recurvoides</i> sp. 1	53
17	<i>K. apicularis</i>	14	17	<i>P. murrayi</i>	23	17	<i>G. polia</i>	8	14	<i>Quinqueloculina</i> sp. 2	10	17	<i>N. dentaliniformis</i>	50
18	<i>O. globosa</i>	13	18	<i>Q. venusta</i>	21	18	<i>G. umbonata</i>	6	18	<i>Recurvoides</i> sp. 1	9	18	<i>Parafissurina</i> sp. 3	38
18	<i>Quinqueloculina</i> sp. 2	13	19	Multiple (3) spp.	20	19	Multiple (5) spp.	5	18	<i>Reophax</i> sp. 19	9	19	<i>G. aff. soldanii</i>	36
20	Multiple (5) spp.	12							20	<i>Lagenamma</i> sp. 19	8	19	<i>Quinqueloculina</i> sp. 2	36

four in two out of four samples). Other species had high rankings in one or two samples. For example, 'white domes' (distinctive form with a thick, white test made of finely agglutinated particles resembling the well-known agglutinated genus *Crithionina*) was ranked 1st and 8th in two samples but was entirely absent in others; *Reophax* sp. 28 was ranked in the top 8 twice; *Nodellum*-like sp. was ranked 2nd in one sample and 17th in another; *Sphaeroidina bulloides* was ranked 4th in one sample and 9th in another, and *Bolivina spathulata* was ranked 3rd in only one sample.

The top 20 species for the potential fossil fauna are summarised in Table 5.3. *Epistominella exigua* and *Globocassidulina subglobosa* were ranked 1st and 2nd in three out of four samples, and 2nd and 3rd in the fourth sample. Other species with consistently high rankings were *Pyrgo murrhina*, *Cibicides wuellerstorfi*, *Melonis barleeanus*, *M. pompilioides* and *Oridorsalis umbonatus*, all featuring in the top 10 of all four samples. *Sphaeroidina bulloides* was usually a medium-ranked species in three out of four samples (mean rank 10, mean density 23 specimens per sample), but it achieved the highest abundance (564 specimens per sample) of any single species at site H4, which is located on top of a relatively large (~500 m high) abyssal hill (see Fig. 5.1). Only two species with poor fossilisation potential were amongst the top 20 species in the dead assemblage: *Adercotryma glomerata* (top 10 in three out of four samples) and *Lagenammia* aff. *arenulata* (top 8 in two out of four samples).

5.3.3.3 L/D ratios

Considering the entire assemblage, a total of 17 species had a relative abundance >5% in the living and/or dead fauna (see Supplementary Material 5.A.4). Both count and relative abundance data were subsequently used for estimating the L/D ratios of these species (L_N/D_N and $L\%/D\%$, respectively; Table 5.4). Nine species had finely agglutinated walls and were inferred to have poor fossilisation potential. Four of these, *Nodellum*-like sp., 'white domes', *Reophax* sp. 9 and *Reophax* sp. 21, were consistently more common in the live than in the dead assemblage, both in counts and in relative proportions (Table 5.4). Other four species (*Lagenammia* aff. *arenulata*, *Nodulina dentaliniformis*, *Reophax* sp.

Table 5.4 Live/dead (L/D) ratios for all major species (i.e. relative abundance >5% in at least one sample), considering the 'entire' (fossilisable plus non-fossilisable) assemblage. L/D ratios are calculated based on counts (N; L_N/D_N) and relative abundance (%; $L\%/D\%$). L_{only} = only live (Rose-Bengal-stained) specimens found, D_{only} = only dead specimens found, A = absent from both live and dead fraction. Lag = *Lagenammia*, Nod = *Nodellum*-like group, Sph = Spheres (no aperture), Hor = Hormosinacea, Rot = Rotaliida, Tex = Textulariida, Tro = Trochamminacea.

Group	Species	H1		H4		P3		P4	
		L_N/D_N	$L\%/D\%$	L_N/D_N	$L\%/D\%$	L_N/D_N	$L\%/D\%$	L_N/D_N	$L\%/D\%$
	Poor fossilisation potential								
Lag	<i>Lagenammia</i> aff. <i>arenulata</i>	0.30	2.56	D_{only}	D_{only}	0.14	0.74	0.17	1.48
Nod	<i>Nodellum</i> -like sp.	L_{only}	L_{only}	9	156.18	L_{only}	L_{only}	D_{only}	D_{only}
Sph	White domes	3	25.22	A	A	L_{only}	L_{only}	A	A
Hor	<i>Nodulina dentaliniformis</i>	0.10	0.84	0.14	2.48	0.89	4.59	0.25	2.22
Hor	<i>Reophax bilocularis</i>	D_{only}	D_{only}	3	52.06	D_{only}	D_{only}	1.67	14.79
Hor	<i>Reophax</i> sp. 9	4	33.63	0.29	4.96	L_{only}	L_{only}	2	17.74
Hor	<i>Reophax</i> sp. 21	5	42.04	0.89	15.43	L_{only}	L_{only}	4	35.49
Hor	<i>Reophax</i> sp. 28	0.83	7.01	D_{only}	D_{only}	4.67	24.10	0.33	2.96
Tro	<i>Adercotryma glomerata</i>	0.24	2.06	1	17.35	0.13	0.65	0.33	2.96
	High fossilisation potential								
Rot	<i>Bolivina spathulata</i>	A	A	A	A	10	51.64	A	A
Rot	<i>Epistominella exigua</i>	0.03	0.27	0.04	0.68	0.11	0.57	0.10	0.89
Rot	<i>Globocassidulina subglobosa</i>	0.04	0.38	0.02	0.40	0.15	0.76	0.02	0.16
Rot	<i>Melonis pompilioides</i>	D_{only}	D_{only}	D_{only}	D_{only}	0.05	0.25	0.05	0.47
Rot	<i>Nuttallides umboniferus</i>	0.04	0.30	0.03	0.58	0.03	0.18	0.08	0.68
Rot	<i>Oridorsalis umbonatus</i>	0.06	0.53	0.01	0.25	0.05	0.23	0.07	0.59
Rot	<i>Sphaeroidina bulloides</i>	0.06	0.48	0.01	0.22	0.23	1.19	D_{only}	D_{only}
Tex	<i>Eggerella bradyi</i>	D_{only}	D_{only}	0.05	0.89	0.06	0.30	D_{only}	D_{only}

28, *Adercotryma glomerata*) were more common in the dead assemblage ($L_N/D_N < 1$), although their relative abundance was usually greater in the live assemblage ($L\%/D\% > 1$). *Reophax bilocularis* had mixed patterns. All of the 8 species with good fossilisation potential, except for *Bolivina spathulata*, were always more abundant in the dead than in the live assemblage (L_N/D_N and $L\%/D\% < 1$, Table 5.5). *B. spathulata* had by far the highest L_N/D_N ratio, even in comparison with the easily-degradable species (Table 5.4).

When considering only the potential fossil foraminifera, a total of 17 species had a relative abundance >5% in the living and/or dead fauna (see Supplementary Material 5.A.5). Except for *B. spathulata*, L_N/D_N ratios were all <1, reflecting a greater abundance in the dead than in the live assemblage (Table 5.5). However,

Table 5.5 Live/dead (L/D) ratios for all major species (i.e. relative abundance >5% in at least one sample), considering potential fossil species only. L/D ratios are calculated based on counts (N; L_N/D_N) and relative abundance (%; $L\%/D\%$). L_{only} = only live (Rose-Bengal-stained) specimens found, D_{only} = only dead specimens found, A = absent from both live and dead fractions. Mil = Milioliida, Rot = Rotaliida, Tex = Textulariida.

Group	Species	H1		H4		P3		P4	
		L_N/D_N	$L\%/D\%$	L_N/D_N	$L\%/D\%$	L_N/D_N	$L\%/D\%$	L_N/D_N	$L\%/D\%$
Mil	<i>Pyrgo murrhina</i>	0.08	2.06	0.05	2.17	0.07	0.69	0.08	1.30
Mil	<i>Quinqueloculina venusta</i>	0.33	8.79	0.05	2.12	D_{only}	D_{only}	D_{only}	D_{only}
Mil	<i>Quinqueloculina</i> sp. 2	0.15	4.06	D_{only}	D_{only}	D_{only}	D_{only}	D_{only}	D_{only}
Rot	<i>Spirosigmoilina tenuis</i>	0.08	2.20	0.67	29.62	D_{only}	D_{only}	D_{only}	D_{only}
Rot	<i>Alabaminella weddellensis</i>	0.29	7.54	D_{only}	D_{only}	D_{only}	D_{only}	A	A
Rot	<i>Bolivina spathulata</i>	A	A	A	A	10	93.6	A	A
Rot	<i>Cibicides wuellerstorfi</i>	0.04	1.15	0.03	1.17	0.14	1.28	0.07	1.13
Rot	<i>Epistominella exigua</i>	0.03	0.85	0.04	1.75	0.11	1.03	0.10	1.70
Rot	<i>Globocassidulina subglobosa</i>	0.04	1.18	0.02	1.03	0.15	1.38	0.02	0.30
Rot	<i>Gyroidina</i> sp. 1	0.08	2.20	0.05	2.34	D_{only}	D_{only}	D_{only}	D_{only}
Rot	<i>Melonis barleeanus</i>	D_{only}	D_{only}	D_{only}	D_{only}	D_{only}	D_{only}	0.07	1.25
Rot	<i>Melonis pompilioides</i>	D_{only}	D_{only}	D_{only}	D_{only}	0.05	0.45	0.05	0.89
Rot	<i>Nuttallides umboniferus</i>	0.04	0.94	0.03	1.48	0.03	0.32	0.08	1.30
Rot	<i>Oridorsalis tenerus</i>	D_{only}	D_{only}	0.5	22.22	A	A	0.2	3.38
Rot	<i>Oridorsalis umbonatus</i>	0.06	1.67	0.01	0.63	0.05	0.43	0.07	1.13
Rot	<i>Sphaeroidina bulloides</i>	0.06	1.51	0.01	0.55	0.23	2.16	D_{only}	D_{only}
Tex	<i>Eggerella bradyi</i>	D_{only}	D_{only}	0.05	2.28	0.06	0.55	D_{only}	D_{only}

$L\%/D\%$ indicated that in addition to *B. spathulata*, a further 5 species (*Pyrgo murrhina*, *Cibicides wuellerstorfi*, *Epistominella exigua*, *Globocassidulina subglobosa*, *Oridorsalis tenerus*), were relatively more abundant in the live than in the dead assemblages ($L\%/D\%>1$; Table 5.5). The remaining species had mixed patterns.

5.4 Discussion

5.4.1 Limitations

Our study was limited to foraminiferal tests retained on a 150- μm mesh sieve. Finer size fractions (e.g. 63–150 μm) often include some abundant, opportunistic species that are absent or under-represented in the >150- μm fraction (Gooday, 1988; 1993; Sun et al., 2006). Unfortunately, analysis of the 63–150- μm fraction is extremely time consuming, especially when taking into account dead foraminifera,

and could not be accomplished during the time frame of this study. Nevertheless, coarser-meshed sieves (125 or 150 μm) are commonly used in paleoceanographic research (Gooday, 2003), and size-fractionated data from the NE Atlantic (>150 and >63 μm) resulted in similar correlations between diversity measures and benthic foraminiferal densities (Gooday et al., 2012).

5.4.2 To what extent are dead benthic foraminiferal assemblages representative of the original live fauna?

Comparisons of live and dead foraminiferal faunas have been the focus of several studies, with varying degrees of agreement between the two assemblages for fossilisable (mainly calcareous) foraminifera (de Stigter et al., 1999; Douglas et al., 1980; Mackensen and Douglas, 1989; Mackensen et al., 1990), agglutinating foraminifera (Bernstein and Meador, 1979; Murray and Pudsey, 2004), and combined assemblages (Duros et al., 2012; Duros et al., 2014; Murray and Alve, 1999).

Our results revealed an important change between the 'entire' live and the dead assemblages in the surface 0–1 cm at each station (Fig. 5.3a). This trend persisted even when we restricted our comparisons to potential fossil species (Fig. 5.3b). A mixture of taphonomic processes and biological factors (population dynamics) (see sections 1.4.3–1.4.4) is likely responsible for these differences in composition. Species similarity between samples was greater for the dead compared to the live assemblage even when we did not consider delicate agglutinated taxa ($\text{MVDISP}_{\text{dead}} < \text{MVDISP}_{\text{live}}$ in both entire and fossilisable cases). This likely reflects the fact that dead assemblages provide a time averaged record integrating different seasonal conditions and changing microenvironments. In the present case the dead assemblage in the 0–1 cm layer could be from 300 to 3100 years old, given sedimentation rates of 3.5 cm ky^{-1} and the depth (11 cm) of the sediment mixed layer (Billett and Rice, 2001; Smith and Rabouille, 2002). Integration over time also potentially explains the greater number of species in the dead compared to the live assemblage (163 versus 83). Nevertheless, rarefied alpha diversity (species richness, exponential Shannon index, inverse Simpson index, Chao 1) was always similar. In fact, the rarefied number of species in the

live assemblage was linearly correlated with that of both the entire and the potential fossil dead assemblage (Fig. 5.2). Thus, for the PAP-SO area, the number of live species is a good indicator of the number of dead species and vice versa.

5.4.3 Taphonomic processes affecting the composition of dead assemblages

The main taphonomic processes that can modify dead foraminiferal faunas in the area of PAP-SO include i) post-mortem physicochemical destruction of tests, ii) transportation of tests and iii) predation.

5.4.3.1 Post-mortem physicochemical destruction of tests

Selective destruction of organic-walled tests and agglutinated tests with organic cement may result in the poor representation or absence of certain taxa in the dead assemblage (Denne and Sen Gupta, 1989; Douglas et al., 1980; Schröder, 1988). In the present study fragile species, including *Lagenammina* spp., *Nodellum*-like sp., *Saccamina* spp. and *Reophax* spp., as well as species with more robust tests (e.g. *A. glomerata*), all of which have organic cement, were found mainly in the living fauna (Tables 5.2, 5.4), suggesting that significant post-mortem destruction took place. However, agglutinated species with calcitic cement, notably *Eggerella bradyi*, were mainly found in the dead assemblages (Table 5.3). This is consistent with previous evidence that the use of calcitic cement by agglutinating foraminifera enhances the preservation potential of their tests (Bender, 1989; de Stigter et al., 1999; Harloff and Mackensen, 1997).

Since the PAP-SO area is located above the CCD but close to or within the lysocline (Biscaye et al., 1976; van der Loeff and Lavaleye, 1986) dissolution could have affected some calcareous tests (Berger, 1968, 1970), including those of miliolids, a group that is particularly sensitive to dissolution (Douglas, 1983; Jorissen and Wittling, 1999). Typical visual indicators of carbonate dissolution are etching of the wall surface, test breakage, and the translucent or opaque appearance of hyaline test walls that are normally transparent (Murray, 1967;

Murray and Wright, 1970). Corliss and Honjo (1981) found a good statistical correlation between the proportion of broken benthic foraminiferal tests and bottom-water carbonate undersaturation. Our samples yielded numerous miliolid fragments (constituting 32% of all picked fragments; Supplementary Material 5.A.1), mostly belonging to the genera *Pyrgo* and *Quinqueloculina*, which may have resulted from dissolution. Gooday and Alve (2001) considered carbonate dissolution a potentially important environmental factor in this area. However, the consistently low L/D ratios of most major calcareous species (Table 5.5) as well as the transparent walls of most hyaline species, indicates that this process is unlikely to have been particularly important in this case.

5.4.3.2 Transport of tests

The transport of dead foraminifera tests in the deep sea can be caused by bottom currents (bed- and suspended load), turbidity currents and submarine slides (Murray, 1976; Murray, 2006). Living foraminifera are less likely to be transported, at least by bottom currents, since they can utilise their reticulopodial network to anchor among sediment particles (Goldstein, 1999).

Visual inspection of the sediment cores from which our samples were taken provides information on the sedimentary processes operating at each site (Ruhl, 2012; Durden et al., 2015, Supplementary Material 5.B.1). The P3 core, which was collected adjacent to a large, (~900 m high) steep hill, had a uniform light greyish colour, and was poorly consolidated for its full length (c. 40 cm) – common characteristics for cores collected in that area, but very distinct from other locations on the Porcupine Abyssal Plain (Supplementary Material 5.B.1; Ruhl, 2013). It is possible that run out of slope failures from the large, steep-sided hill could have transported some benthic foraminiferal tests to this site. In a more detailed comparison of live benthic foraminiferal assemblages from hill and plain sites in the PAP-SO area (Chapter 4), including the data used in this study, we found that site P3 was more similar to hill samples (especially H1) than site P4, which is located >10 km away from the nearest hill (Fig. 5.1). The core from P4, in common with most cores from the Porcupine Abyssal Plain, had a dark band ~25 cm below the sediment surface (Supplementary Material 5.B.1). This is interpreted

as a turbidite deposit (Thomson et al., 1987) and/or chemical oxidation front (Wallace et al., 1988), potentially dating to the glacial/Holocene transition. Cores from the hills (H1, H4) were more variable (Supplementary Material 5.B.1); in general, they were light brown in colour with the lower quarter to a third being somewhat darker but with no evidence of a turbidite layer.

The abyssal hills in the PAP-SO area have coarser (greater proportion of particles $>63\ \mu\text{m}$) sediments than the plain (Chapter 3; Durden et al., 2015; Stefanoudis et al., 2016; Turnewitsch et al., 2004, 2013, 2015), a winnowing effect of the stronger bottom currents above the hills that preferentially remove fine particles and redeposit them on the adjacent plain. It is possible that some dead tests could be transported in this way. This might contribute to the enhanced homogeneity between dead foraminiferal faunas (Fig. 5.3), although current-induced transport is thought to mainly influence tests $<150\ \mu\text{m}$ (Jorissen and Wittling, 1999; Murray, 2006).

5.4.3.3 Predation

Shell etching and boring by fungi, protozoans and metazoan meiofauna and macrofauna can lead to the weakening or complete destruction of foraminiferal tests (Culver and Lipps, 2003; Hickman and Lipps, 1983; Lipps, 1983). In our samples, a total of 60 dead tests (42 *Pyrgo*, 10 *Quinqueloculina*, 7 *Melonis*, 1 *Eggerella*) displayed rather irregular punctures, reminiscent of holes observed in other benthic foraminiferal tests that were suggested to be a result of nematode predation (Sliter, 1971; Douglas, 1983; Fig. 5.1 therein). However, some of the etching we observed could be the result of selective or unselective deposit-feeding by invertebrates (Mageau and Walker, 1976) or carbonate dissolution (see section 4.2.1). For example, Bé et al. (1975) and Hecht et al. (1975) illustrated similar-shaped holes in planktonic foraminiferal tests caused by carbonate undersaturation in a series of dissolution experiments. Freiwald (1995) has also reported etching on *C. lobatulus* tests, presumed to result from bacterially-induced carbonate degradation. In any case, borings and or signs of etching were rare, occurring in only $\sim 0.01\%$ of all dead specimens of the present study. We conclude

that predation and dissolution were unlikely to have had a major influence on the composition of the observed dead assemblage.

5.4.4 The influence of population dynamics on the composition of dead assemblages

Living foraminiferal faunas vary throughout the year in response to inputs of organic matter (phytodetritus) from primary production that may trigger reproductive events (e.g. Gooday, 1988; Kitazato et al., 2000; Gooday & Hughes, 2002; Fontanier et al., 2003; Smart, 2008). After such events, certain species may show a sudden increase in population size through reproduction (Gooday, 1993) or a change in their microhabitat occupancy (Jorissen et al., 1995; Ohga and Kitazato, 1997), leading to considerable differences between the living and time-averaged dead assemblages. Our samples were collected on 5–22 August 2011, after the spring phytoplankton bloom and the subsequent peak in particulate organic carbon flux that occurred in June 2011 (Frigstadt et al., 2015).

Phytodetritus was visible on the surface some of our studied cores, mainly from P3 and less so from H4 (Supplementary Material 5.B.2–3).

Epistominella exigua, an opportunistic species that reproduces rapidly during pulsed fluxes of phytodetritus, was common in both the live and dead assemblages (Tables 5.2–3) with counts being substantially higher in the latter. However, considering only the potential fossil fauna, its relative abundance was consistently higher in the live assemblage ($L\%/D\% > 1$, Table 5.5). This may indicate that we captured part of the reproductive period of this highly opportunistic species. The high abundance of *E. exigua* in the dead assemblage (Table 5.3), suggests that the ‘phytodetrital signal’ will also be expressed in the fossil fauna (Smart, 2008). *Alabaminella weddellensis*, another rotaliid species often associated with phytodetritus deposits in the PAP-SO area (Gooday, 1988, 1993; Smart and Gooday, 1997), was relatively scarce in our samples (Supplementary Material 5.A.3). *Epistominella exigua* and *A. weddellensis* appear to have distinct ecologies, the former being associated with regions of high seasonality, the latter with areas of high productivity (Fariduddin and Loubere, 1997; Hayward et al., 2002; Loubere, 1996; Sun et al., 2006). However, the relative scarcity of this small

species probably also reflects the fact that we analysed the relatively coarse 150- μm fraction in which *A. weddellensis* is poorly represented.

Like those of *E. exigua*, the L%/D% ratios for *Cibicidoides wuellerstorfi* and *Globocassidulina subglobosa* were consistently >1 . Jorissen and Wittling (1999) suggested that *C. wuellerstorfi* might be positively related to phytodetritus, and Gooday (1988) reports that this species inhabits phytodetrital aggregates, but a link with seasonal food input was not confirmed by other studies (Corliss et al., 2006; Smart, 2008). In the PAP area, *G. subglobosa* has also been found embedded within phytodetritus aggregates (Gooday, 1988, 1993, 1996), while in the Southern Ocean it has been shown to feed selectively on phytodetritus (Suhr and Pond, 2006; Suhr et al., 2003). However, Sun et al. (2006) again reported a negative correlation between *G. subglobosa* and seasonality in primary production. Our results provide some evidence that these two species (*C. wuellerstorfi*, *G. subglobosa*) behave in a manner similar to that of *E. exigua* by rapidly reproducing once food becomes available. However, the magnitude of their response is much less evident, at least for the size fraction $>150\ \mu\text{m}$, as evidenced by their considerably lower contribution to the living and dead assemblages in comparison to *E. exigua* (Tables 5.2–3).

The case of *Sphaeroidina bulloides* also warrants attention. L%/D% ratios showed that it was relatively more abundant in the live assemblages of two of the three samples in which it occurred, the exception being H4 (Table 5.5). The density of this species in the dead assemblage at site H4 was at least an order of magnitude higher than at other PAP-SO sites (Table 5.3). Topographic features such as the abyssal hill on which H4 was located, are characterised by stronger currents, potentially enhanced organic matter supply, and coarser sediments, factors that could influence the composition of modern foraminiferal faunas (Chapter 4). Interestingly, small patches of phytodetritus were present on the surface of the sediment core from H4 (Supplementary Material 5.B.3). *Sphaeroidina bulloides* has been suggested to be positively associated with high organic carbon fluxes (Altenbach et al., 2003), which might explain its unusually high densities at H4. Linke and Lutze (1993) found that *S. bulloides* rapidly changed its habit from epifaunal to infaunal depending on food supply and environmental conditions. The

infaunal tests were often enclosed within agglutinated mud coatings ('cysts'), a behaviour commonly observed among live specimens in our study area (Appendix B; Stefanoudis and Gooday, 2016). Additional information on the ecology of this species would be valuable in interpreting its relative abundance in the living and dead fractions in the PAP-SO area.

Miliolid species (*Pyrgo murrhina*, *Quinqueloculina auberiana*, *Quinqueloculina* sp. 2, *Spirosigmoilina tenuis*) had positive L%/D% ratios at most of the hill locations (H1, H4), while being absent from the living fauna in samples from the plain (Table 5.5). Moreover, their densities in the living and dead fractions were generally higher on the hills (Supplementary Material 5.A.3). A previous study at the PAP-SO central site found that an unnamed *Quinqueloculina* species, probably identical to *Quinqueloculina* sp. 2 of the present study, moved towards the sediment surface when food availability was high and retreated back into deeper layers once food resources had been exhausted (Gooday et al., 2010). As previously indicated, food supply is probably higher on the hills (e.g. Morris et al., 2016), which may help to explain the larger populations of *Quinqueloculina* spp. there in comparison to the plain.

5.4.5 *Bolivina spathulata*

This species was absent from the living and dead fractions of all samples except for P3. Here, it was 10 times more abundant in absolute terms (i.e. L_N/D_N values) in the live than in the dead assemblage (Table 5.5), although the actual numbers of specimens (10 live and 1 dead) were fairly low (Supplementary Material 5.A.3). *Bolivina* species are generally considered to be indicative of low oxygen, high productivity environments (Altenbach et al., 1999; Jorissen et al., 1992; Schmiedl et al., 1997), typically at bathyal depths. In the southern Adriatic Sea, de Stigter et al. (1998) found *B. spathulata* penetrating deep into the sediment and efficiently exploiting the subsurface food resources available there, mainly degraded organic material. Nevertheless, in the PAP-SO area this species occurred in the upper sediment layer, suggesting that it is also able to exploit fresh organic material in well-oxygenated, abyssal settings. This is consistent with the fact that the surface of the core from the P3 site had a clearly developed phytodetritus layer

(Supplementary Material 5.B.2). It appears that *B. spathulata* was able to flourish in a local patch of fresh organic matter. The opportunist species *Epistominella exigua* was also common in this sample (Table 5.2).

5.4.6 Concluding remarks

Our results from the PAP-SO area indicate that the transition from live to dead benthic foraminiferal assemblages involves a significant loss of delicate agglutinated and organic-walled tests (e.g. *Lagenammina*, *Nodellum*, *Reophax*), and to a lesser extent of some fragile calcareous tests (mostly miliolids), the latter possibly the result of dissolution. Other processes, such as hydrodynamically induced transport of tests and predation by metazoans, are unlikely to have significantly modified the dead assemblages. Relatively high live to dead ratios in some samples suggest that a few species (e.g. *Bolivina spathulata*, *Cibicidoides wuellerstorfi*, *Epistominella exigua*, *Globocassidulina subglobosa*) might have responded to recent food deposition by rapid reproduction.

In the PAP-SO area it seems that, for foraminifera in the >150 µm fraction of surficial sediments, taphonomic rather than life processes are largely responsible for the composition of dead assemblages. The magnitude of these processes is comparable between samples from the plain and the hills, suggesting that the preservation potential of benthic foraminifera is not markedly affected by local topography (Fig. 5.4). Particularly notable is the fact that the composition of the dead assemblages is quite similar between samples from the hills and the plain, despite the fact that live faunas are more distinct between these two settings, particularly between H4 and all other samples (Figs. 5.3–5.4; see also Chapter 4, Fig. 4.4 therein). This suggests that it may not be possible to differentiate between foraminiferal faunas originating from (modestly) topographically contrasting sites in the fossil record, despite potentially substantial differences in organic matter supply between such sites (Durden et al., 2015; Morris et al., 2016).

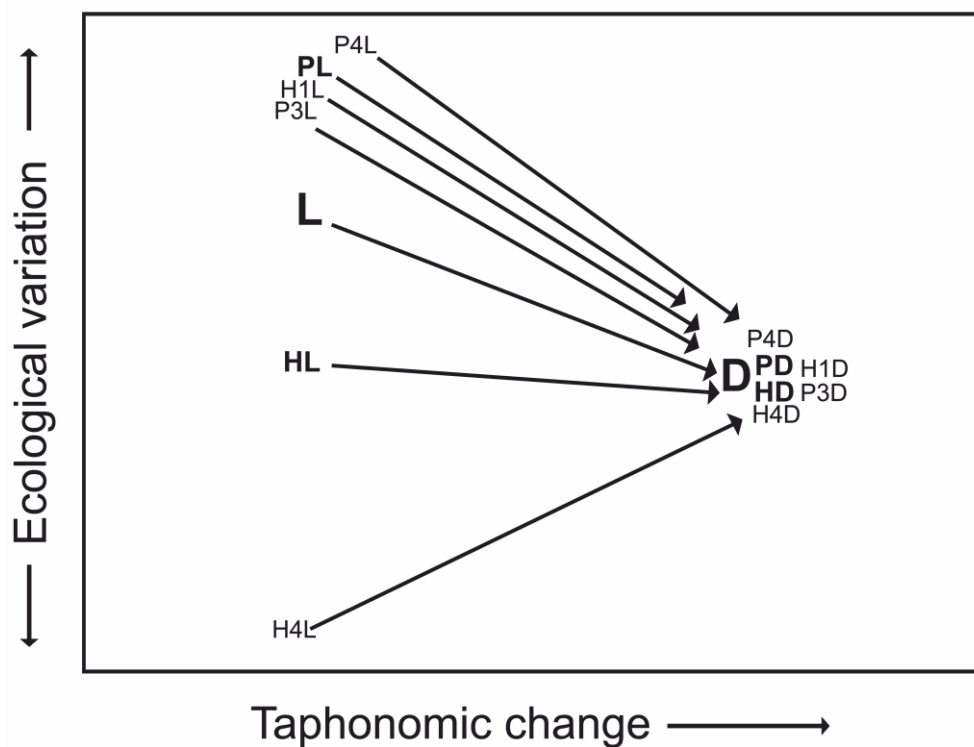


Fig. 5.4. 2-d non-metric multi-dimensional scaling ordination plot of live (L) and dead (D) foraminiferal assemblage composition in samples from the PAP-SO area, based on Bray-Curtis dissimilarity of $\log(x+1)$ transformed relative abundance data. Note compositional shift related to topographic setting (hills, H; plain, P), and striking difference between live and dead assemblages. (HL, hills live [H1L+H4L]; PL, plain live [P3L+P4L]), HD, hills dead [H1D+H4D]; PD, plain dead [P3D+P4D]; L, live [HL+PL]; D, dead [HD+PD]).

References of Chapter 5

- Altenbach, A.V., Pflaumann, U., Schiebel, R., Thies, A., Timm, S., Trauth, M., 1999. Scaling percentages and distributional patterns of benthic foraminifera with flux rates of organic carbon. *Journal of Foraminiferal Research*, 29, 173–185.
- Altenbach, A.V., Lutze, G.F., Schiebel, R., Schönfeld, J., 2003. Impact of interrelated and interdependent ecological controls on benthic foraminifera: an example from the Gulf of Guinea. *Palaeogeography, Palaeoclimatology, Palaeoecology*, 197, 213–238.
- Bé, A.W.H., Morse, J.W., Harrison, S.M., 1975. Progressive dissolution and ultrastructural breakdown of planktonic foraminifera. In: Sliter, W.V., Bé, A.W.H., Berger, W.H. (Eds.), *Dissolution of Deep-Sea Carbonates*, Vol. 13 (pp. 27–55). Washington, DC.
- Bender, H., 1989. Gehäuseaufbau, Gehäusegenese und Biologie agglutiniertes Foraminiferen (Sarcodina, Textulariina). *Jahrbuch der Geologischen Bundesanstalt*, 133, 259–347.
- Berger, W.H., 1968. Planktonic Foraminifera: selective solution and paleoclimatic interpretation. *Deep-Sea Research and Oceanographic Abstracts*, 15, 31–43.
- Berger, W.H., 1970. Planktonic Foraminifera: selective solution and lysocline. *Marine Geology*, 8, 111–138.
- Berger, W.H., Bonneau, M.C., Parker, F.L., 1982. Foraminifera on the deep-sea floor: lysocline and dissolution rate. *Oceanologica Acta*, 5, 249–258.
- Bernstein, B.B., Meador, J.P., 1979. Temporal persistence of biological patch structure in an abyssal benthic community. *Marine Biology*, 51, 179–183.
- Bett, B.J., Malzone, M.G., Narayanaswamy, B.E., Wigham, B.D., 2001. Temporal variability in phytodetritus and megabenthic activity at the seabed in the deep Northeast Atlantic. *Progress in Oceanography*, 50, 349–368.
- Billett, D.S.M., Rice, A.L., 2001. The BENGAL programme: introduction and overview. *Progress in Oceanography*, 50, 13–25.
- Biscaye, P.E., Kolla, V., Turekian, K.K., 1976. Distribution of calcium carbonate in surface sediments of the Atlantic Ocean. *Journal of geophysical research*, 81, 2595–2603.
- Bouchet, V.M.P., Sauriau, P.G., Debenay, J.P., Mermillod-Blondin, F., Schmidt, S., Amiard, J.C., Dupas, B., 2009. Influence of the mode of macrofauna-mediated bioturbation on the vertical distribution of living benthic foraminifera: First insight from axial tomodesitometry. *Journal of Experimental Marine Biology and Ecology*, 371, 20–33.
- Colwell, R.K., Chao, A., Gotelli, N.J., Lin, S.Y., Mao, C.X., Chazdon, R.L., Longino, J.T., 2012. Models and estimators linking individual-based and sample-based rarefaction, extrapolation and comparison of assemblages. *Journal of Plant Ecology*, 5, 3–21.
- Corliss, B.H., Honjo, S., 1981. Dissolution of deep-sea benthonic foraminifera. *Micropaleontology*, 27, 356–378.
- Corliss, B.H., Sun, X., Brown, C.W., Showers, W.J., 2006. Influence of seasonal primary productivity on $\delta^{13}\text{C}$ of North Atlantic deep-sea benthic foraminifera. *Deep-Sea Research Part I—Oceanographic Research Papers*, 53, 740–746.

- Culver, S.J., Lipps, J.H., 2003. Predation on and by Foraminifera. In: Kelley, P.H., Kowalewski, M., Hansen, T.A. (Eds.), *Predator-Prey Interactions in the Fossil Record* (pp. 7–32): Springer US.
- de Stigter, H.C., Jorissen, F.J., van der Zwaan, G.J., 1998. Bathymetric distribution and microhabitat partitioning of live (Rose Bengal stained) benthic foraminifera along a shelf to bathyal transect in the southern Adriatic Sea. *Journal of Foraminiferal Research*, 28, 40–65.
- de Stigter, H.C., van der Zwaan, G.J., Langone, L., 1999. Differential rates of benthic foraminiferal test production in surface and subsurface sediment habitats in the southern Adriatic Sea. *Palaeogeography Palaeoclimatology Palaeoecology*, 149, 67–88.
- Denne, R.A., Sen Gupta, B.K., 1989. Effects of taphonomy and habitat on the record of benthic foraminifera in modern sediments. *Palaaios*, 4, 414–423.
- Douglas, R.G., Liestman, J., Walch, C., Blake, G., Cotton, M.L., 1980. The transition from live to sediment assemblages in benthic foraminifera from the southern California borderland. In: Field, M.E., Bouma, A.H., Colburn, I.P., Douglas, R.G., Ingle, I.C. (Eds.), *Quaternary Depositional Environments of the Pacific Coast, Pacific Coast Paleogeography Symposium* (pp. 257–280): Society of Economic Paleontologists and Mineralogists.
- Douglas, R.G., 1983. Benthonic foraminiferal biostratigraphy in the central North Pacific. *Deep Sea Drilling Project: Initial Report Deep Sea Drilling Project v. 17* (pp. 607–671).
- Durden, J.M., Bett, B.J., Jones, D.O.B., Huvenne, V.A.I., Ruhl, H.A., 2015. Abyssal hills – hidden source of increased habitat heterogeneity, benthic megafaunal biomass and diversity in the deep sea. *Progress in Oceanography*, 137, 209–218.
- Duros, P., Fontanier, C., de Stigter, H.C., Cesbron, F., Metzger, E., Jorissen, F.J., 2012. Live and dead benthic foraminiferal faunas from Whittard Canyon (NE Atlantic): Focus on taphonomic processes and paleo-environmental applications. *Marine Micropaleontology*, 94–95, 25–44.
- Duros, P., Jorissen, F.J., Cesbron, F., Zaragosi, S., Schmidt, S., Metzger, E., Fontanier, C., 2014. Benthic foraminiferal thanatocoenoses from the Cap-Ferret Canyon area (NE Atlantic): A complex interplay between hydro-sedimentary and biological processes. *Deep-Sea Research Part II—Topical Studies in Oceanography*, 104, 145–163.
- Fariduddin, M., Loubere, P., 1997. The surface ocean productivity response of deeper water benthic foraminifera in the Atlantic Ocean. *Marine Micropaleontology*, 32, 289–310.
- Fischer, G., Wefer, G., 1999. *Use of proxies in paleoceanography: examples from the South Atlantic*. Berlin: Springer.
- Fontanier, C., Jorissen, F., Chaillou, G., David, C., Anschutz, P., Lafon, V., 2003. Seasonal and interannual variability of benthic foraminiferal faunas at 550m depth in the Bay of Biscay. *Deep-Sea Research Part I—Oceanographic Research Papers*, 50, 457–494.
- Fontanier, C., Koho, K.A., Goni-Urriza, M.S., Deflandre, B., Galaup, S., Ivanovsky, A., Gayet, N., Dennielou, B., Gremare, A., Bichon, S., Gassie, C., Anschutz, P., Duran, R., Reichart, G.J., 2014. Benthic foraminifera from the deep-water Niger delta (Gulf of Guinea): Assessing present-day and past activity of hydrate pockmarks. *Deep-Sea Research Part I—Oceanographic Research Papers*, 94, 87–106.

- Freiwald, A., 1995. Bacteria-induced carbonate degradation: a taphonomic case study of *Cibicides lobatulus* from a high-boreal carbonate setting. *Palaios*, 10, 337–346.
- Frigstad, H., Henson, S.A., Hartman, S.E., Omar, A.M., Jeansson, E., Cole, H., Pebody, C., Lampitt, R.S., 2015. Links between surface productivity and deep ocean particle flux at the Porcupine Abyssal Plain sustained observatory. *Biogeosciences*, 12, 5885–5897.
- Gage, J.D., Bett, B.J., 2005. Deep-sea benthic sampling. In: Eleftheriou, A., MacIntyre, A.D. (Eds.), *Methods for the study of marine benthos*, 3rd ed. (pp. 273–325). Oxford, UK: Blackwell Scientific.
- Goineau, A., Fontanier, C., Mojtahid, M., Fanget, A.S., Bassetti, M.A., Berne, S., Jorissen, F., 2015. Live-dead comparison of benthic foraminiferal faunas from the Rhône prodelta (Gulf of Lions, NW Mediterranean): Development of a proxy for palaeoenvironmental reconstructions. *Marine Micropaleontology*, 119, 17–33.
- Goldstein, S.T., 1999. Foraminifera: a biological overview. In: Sen Gupta, B.K. (Ed.), *Benthic foraminiferal microhabitats below the sediment-water interface* (pp. 37–56). Dordrecht: Kluwer Academic Publishers.
- Gooday, A.J., 1988. A response by benthic foraminifera to the deposition of phytodetritus in the deep sea. *Nature*, 332, 70–73.
- Gooday, A.J., 1993. Deep-sea benthic foraminiferal species which exploit phytodetritus: characteristic features and controls on distribution. *Marine Micropaleontology*, 22, 187–205.
- Gooday, A.J., 1996. Epifaunal and shallow infaunal foraminiferal communities at three abyssal NE Atlantic sites subject to differing phytodetritus input regimes. *Deep-Sea Research Part I—Oceanographic Research Papers*, 43, 1395–1421.
- Gooday, A.J., Alve, E., 2001. Morphological and ecological parallels between sublittoral and abyssal foraminiferal species in the NE Atlantic: a comparison of *Stainforthia fusiformis* and *Stainforthia* sp. *Progress in Oceanography*, 50, 261–283.
- Gooday, A.J., Hughes, J.A., 2002. Foraminifera associated with phytodetritus deposits at a bathyal site in the northern Rockall Trough (NE Atlantic): seasonal contrasts and a comparison of stained and dead assemblages. *Marine Micropaleontology*, 46, 83–110.
- Gooday, A.J., 2003. Benthic foraminifera (protista) as tools in deep-water palaeoceanography: Environmental influences on faunal characteristics. *Advances in Marine Biology*, 46, 1–90.
- Gooday, A.J., Cedhagen, T., Kamenskaya, O.E., Cornelius, N., 2007. The biodiversity and biogeography of komokiaceans and other enigmatic foraminiferan-like protists in the deep Southern Ocean. *Deep-Sea Research Part II—Topical Studies in Oceanography*, 54, 1691–1719.
- Gooday, A.J., Malzone, M.G., Bett, B.J., Lamont, P.A., 2010. Decadal-scale changes in shallow-infaunal foraminiferal assemblages at the Porcupine Abyssal Plain, NE Atlantic. *Deep-Sea Research Part II—Topical Studies in Oceanography*, 57, 1362–1382.
- Gooday, A.J., Bett, B.J., Jones, D.O.B., Kitazato, H., 2012. The influence of productivity on abyssal foraminiferal biodiversity. *Marine Biodiversity*, 42, 415–431.

- Gooday, A.J., 2014. Deep-sea benthic foraminifera. *Reference Module in Earth Systems and Environmental Sciences* (pp. 1–20).
- Harloff, J., Mackensen, A., 1997. Recent benthic foraminiferal associations and ecology of the Scotia Sea and Argentine Basin. *Marine Micropaleontology*, 31, 1–29.
- Hartman, S.E., Lampitt, R.S., Larkin, K.E., Pagnani, M., Campbell, J., Gkritzalis, T., Jiang, Z.P., Pebody, C.A., Ruhl, H.A., Gooday, A.J., Bett, B.J., Billett, D.S.M., Provost, P., McLachlan, R., Turton, J.D., Lankester, S., 2012. The Porcupine Abyssal Plain fixed-point sustained observatory (PAP-SO): variations and trends from the Northeast Atlantic fixed-point time-series. *ICES Journal of Marine Science: Journal du Conseil*, 69, 776–783.
- Hayward, B.W., Neil, H., Carter, R., Grenfell, H.R., Hayward, J.J., 2002. Factors influencing the distribution patterns of recent deep-sea benthic foraminifera, east of New Zealand, Southwest Pacific Ocean. *Marine Micropaleontology*, 46, 139–176.
- Hecht, A.D., Eslinger, E.V., Garmon, L.B., 1975. Experimental studies on the dissolution of planktonic foraminifera. In: Sliter, W.V., Bé, A.W.H., Berger, W.H. (Eds.), *Dissolution of Deep-Sea Carbonates*, Vol. 13 (pp. 56–69). Washington, DC.
- Hickman, C.S., Lipps, J.H., 1983. Foraminiferivory: selective ingestion of foraminifera and test alterations produced by the neogastropod *Olivella*. *Journal of Foraminiferal Research*, 13, 108–114.
- Jorissen, F.J., Barmawidjaja, D.M., Puskaric, S., Vanderzwaan, G.J., 1992. Vertical distribution of benthic foraminifera in the northern Adriatic Sea: The relation with the organic flux. *Marine Micropaleontology*, 19, 131–146.
- Jorissen, F.J., de Stigter, H.C., Widmark, J.G.V., 1995. A conceptual model explaining benthic foraminiferal microhabitats. *Marine Micropaleontology*, 26, 3–15.
- Jorissen, F.J., Wittling, I., 1999. Ecological evidence from live-dead comparisons of benthic foraminiferal faunas off Cape Blanc (Northwest Africa). *Palaeogeography, Palaeoclimatology, Palaeoecology*, 149, 151–170.
- Jorissen, F.J., Fontanier, C., Thomas, E., 2007. Paleooceanographical proxies based on deep-sea benthic foraminiferal assemblage characteristics. In: Hillaire-Marcel, C., de Vernal, A. (Eds.), *Proxies in Late Cenozoic Paleooceanography: Pt. 2: Biological tracers and biomarkers* (pp. 263–326).
- Kitazato, H., Shirayama, Y., Nakatsuka, T., Fujiwara, S., Shimanaga, M., Kato, Y., Okada, Y., Kanda, J., Yamaoka, A., Masuzawa, T., Suzuki, K., 2000. Seasonal phytodetritus deposition and responses of bathyal benthic foraminiferal populations in Sagami Bay, Japan: preliminary results from "Project Sagami 1996-1999". *Marine Micropaleontology*, 40, 135–149.
- Lampitt, R.S., Bett, B.J., Kiriakoulakis, K., Popova, E.E., Ragueneau, O., Vangriesheim, A., Wolff, G.A., 2001. Material supply to the abyssal seafloor in the Northeast Atlantic. *Progress in Oceanography*, 50, 27–63.

- Lampitt, R.S., Billett, D.S.M., Martin, A.P., 2010a. The sustained observatory over the Porcupine Abyssal Plain (PAP): Insights from time series observations and process studies *Deep-Sea Research Part II—Topical Studies in Oceanography*, 57, 1267–1271.
- Lampitt, R.S., Salter, I., de Cuevas, B.A., Hartman, S., Larkin, K.E., Pebody, C.A., 2010b. Long-term variability of downward particle flux in the deep northeast Atlantic: Causes and trends. *Deep-Sea Research Part II—Topical Studies in Oceanography*, 57, 1346–1361.
- Lipps, J.H., 1983. Biotic interactions in benthic foraminifera. In: Tevesz, M.J.S., McCall, P.L. (Eds.), *Biotic interactions in recent and fossil benthic communities* (pp. 331–376): Springer, US.
- Loeblich, A.R., Tappan, H., 1987. *Foraminiferal genera and their classification*. New York: Van Nostrand Reinhold.
- Loubere, P., Gary, A., 1990. Taphonomic process and species microhabitats in the living to fossil assemblage transition of deeper water benthic foraminifera. *Palaios*, 375–381.
- Loubere, P., Gary, A., Lagoe, M., 1993. Generation of the benthic foraminiferal assemblage: Theory and preliminary data. *Marine Micropaleontology*, 20, 165–181.
- Loubere, P., 1996. The surface ocean productivity and bottom water oxygen signals in deep water benthic foraminiferal assemblages. *Marine Micropaleontology*, 28, 247–261.
- Loubere, P., 1997. Benthic foraminiferal assemblage formation, organic carbon flux and oxygen concentrations on the outer continental shelf and slope. *Journal of Foraminiferal Research*, 27, 93–100.
- Loubere, P., Rayray, S., 2016. Benthic foraminiferal assemblage formation: Theory and observation for the European Arctic margin. *Deep Sea Research Part I: Oceanographic Research Papers*, 115, 36–47.
- Mackensen, A., Douglas, R.G., 1989. Down-core distribution of live and dead deep-water benthic foraminifera in box cores from the Weddell Sea and the California continental borderland. *Deep-Sea Research Part A—Oceanographic Research Papers*, 36, 879–900.
- Mackensen, A., Grobe, H., Kuhn, G., Futterer, D.K., 1990. Benthic foraminiferal assemblages from the eastern Weddell Sea between 68° and 73° S: Distribution, ecology and fossilization potential. *Marine Micropaleontology*, 16, 241–283.
- Mackensen, A., Grobe, H., Schmiedl, G., 1993. Benthic foraminiferal assemblages from the eastern South Atlantic Polar Front region between 35 and 57 S: distribution, ecology and fossilization potential. *Marine Micropaleontology*, 22, 33-69.
- Mackensen, A., Schmiedl, G., Harloff, J., Giese, M., 1995. Deep-sea foraminifera in the South Atlantic ocean: Ecology and assemblage generation. *Micropaleontology*, 41, 342–358.
- Mageau, N.C., Walker, D.A., 1976. Effects of ingestion of foraminifera by larger invertebrates. In: Schafer, C.T., Pelletier, B.R. (Eds.), *First International Symposium on Benthonic Foraminifera of Continental Margins* (pp. 89–105).
- McIlroy, D., Green, O.R., Brasier, M.D., 2001. Palaeobiology and evolution of the earliest agglutinated Foraminifera: Platysolenites, Spirosolenites and related forms. *Lethaia*, 34, 13–29.

- Mendes, I., Dias, J.A., Schönfeld, J., Ferreira, O., Rosa, F., Lobo, F.J., 2013. Living, dead and fossil benthic foraminifera on a river dominated shelf (northern Gulf of Cadiz) and their use for paleoenvironmental reconstruction. *Continental Shelf Research*, 68, 91–111.
- Moodley, L., 1990. Southern North Sea sea floor and subsurface distribution of living benthic foraminifera. *Netherlands Journal of Sea Research*, 27, 57–71.
- Morris, K., Bett, B., Durden, J., Benoist, N., Huvenne, V., Jones, D., Robert, K., Ichino, M., Wolff, G., Ruhl, H., 2016. Landscape-scale spatial heterogeneity in phytodetrital cover and megafauna biomass in the abyss links to modest topographic variation. *Scientific Reports*, 6, 34080.
- Murray, J.W., 1967. Transparent and opaque foraminiferid tests. *Journal of Paleontology*, 41, 791.
- Murray, J.W., Wright, C.A., 1970. Surface textures of calcareous foraminiferids. *Palaeontology*, 13, 184–187.
- Murray, J.W., 1976. Comparative studies of living and dead benthic foraminiferal distributions. In: Hedley, R.H., Adams, C.G. (Eds.), *Foraminifera*, Vol. 2 (pp. 45–109).
- Murray, J.W., Alve, E., 1999. Natural dissolution of modern shallow water benthic foraminifera: taphonomic effects on the palaeoecological record. *Palaeogeography Palaeoclimatology Palaeoecology*, 146, 195–209.
- Murray, J.W., 2003. Foraminiferal assemblage formation in depositional sinks on the continental shelf west of Scotland. *Journal of Foraminiferal Research*, 33, 101–121.
- Murray, J.W., Pudsey, C.J., 2004. Living (stained) and dead foraminifera from the newly ice-free Larsen Ice Shelf, Weddell Sea, Antarctica: ecology and taphonomy. *Marine Micropaleontology*, 53, 67–81.
- Murray, J.W., 2006. *Ecology and applications of benthic foraminifera*. New York: Cambridge University Press.
- Ohga, T., Kitazato, H., 1997. Seasonal changes in bathyal foraminiferal populations in response to the flux of organic matter (Sagami Bay, Japan). *Terra Nova*, 9, 33–37.
- Pawlowski, J., Holzmann, M., Tyszka, J., 2013. New supraordinal classification of Foraminifera: molecules meet morphology. *Marine Micropaleontology*, 100, 1–10.
- Rice, A.L., Billett, D.S.M., Thurston, M.H., Lampitt, R.S., 1991. The Institute of Oceanographic Sciences Biology Program in the Porcupine Seabight: background and general introduction. *Journal of the Marine Biological Association of the United Kingdom*, 71, 281–310.
- Rice, A.L., Thurston, M.H., Bett, B.J., 1994. The IOSDL DEEPSEAS Program: introduction and photographic evidence for the presence and absence of a seasonal input of phytodetritus at contrasting abyssal sites in the northeastern Atlantic. *Deep-Sea Research Part I—Oceanographic Research Papers*, 41, 1305–1320.
- Ruggiero, M.A., Gordon, D.P., Orrell, T.M., Bailly, N., Bourgoin, T., Brusca, R.C., Cavalier-Smith, T., Guiry, M.D., Kirk, P.M., 2015. A higher level classification of all living organisms. *Plos One*, 10, 1–60.

- Ruhl, H.A., 2012. RRS James Cook Cruise 62, 24 Jul-29 Aug 2011. Porcupine Abyssal Plain - sustained observatory research. *National Oceanography Centre Cruise Report* (p. 119). Southampton, UK: National Oceanography Centre.
- Ruhl, H.A., 2013. RRS Discovery Cruise 377 & 378, 05 - 27 Jul 2012, Southampton to Southampton. Autonomous ecological surveying of the abyss: understanding mesoscale spatial heterogeneity at the Porcupine Abyssal Plain. *National Oceanography Centre Cruise Report* (p. 73). Southampton, UK: National Oceanography Centre.
- Saidova, K.M., 1965. Distribution of benthic foraminifera in the Pacific. *Okeanologiya*, 5, 332–476.
- Saidova, K.M., 1966. Benthic foraminiferal faunas of the Pacific. *Oceanology*, 6, 222–227.
- Schmiedl, G., Mackensen, A., Muller, P.J., 1997. Recent benthic foraminifera from the eastern South Atlantic Ocean: Dependence on food supply and water masses. *Marine Micropaleontology*, 32, 249–287.
- Schröder, C.J., 1988. Subsurface preservation of agglutinated foraminifera in the Northwest Atlantic Ocean. *Abhandlungen der Geologischen Bundesanstalt*, 41, 325–336.
- Schumacher, S., Jorissen, F.J., Dissard, D., Larkin, K.E., Gooday, A.J., 2007. Live (Rose Bengal stained) and dead benthic foraminifera from the oxygen minimum zone of the Pakistan continental margin (Arabian Sea). *Marine Micropaleontology*, 62, 45–73.
- Sliter, W.V., 1971. Predation on benthic foraminifers. *The Journal of Foraminiferal Research*, 1.
- Smart, C.W., Gooday, A.J., 1997. Recent benthic foraminifera in the abyssal northeast Atlantic Ocean: relation to phytodetrital inputs. *Journal of Foraminiferal Research*, 27, 85–92.
- Smart, C.W., 2008. Abyssal NE Atlantic benthic foraminifera during the last 15 kyr: Relation to variations in seasonality of productivity. *Marine Micropaleontology*, 69, 193–211.
- Smith, C.R., Rabouille, C., 2002. What controls the mixed-layer depth in deep-sea sediments? The importance of POC flux. *Limnology and Oceanography*, 47, 418–426.
- Snider, L.J., Burnett, B.R., Hessler, R.R., 1984. The composition and distribution of meiofauna and nanobiota in a central North Pacific deep-sea area. *Deep-Sea Research Part I – Oceanographic Research Papers*, 31, 1225–1249.
- Snyder, S.W., Hale, W.R., Kontrovitz, M., 1990. Assessment of postmortem transportation of modern benthic foraminifera of the Washington continental shelf. *Micropaleontology*, 36, 259–282.
- Stefanoudis, P.V., Gooday, A.J., 2015. Basal monothalamous and pseudo-chambered benthic foraminifera associated with planktonic foraminiferal shells and mineral grains from the Porcupine Abyssal Plain, NE Atlantic. *Marine Biodiversity*, 45, 357–369.
- Stefanoudis, P.V., Gooday, A.J., 2016. Formation of agglutinated cysts by the foraminiferan *Sphaeroidina bulloides* on the Porcupine Abyssal Plain (NE Atlantic). *Marine Biodiversity*, 1–3.
- Stefanoudis, P.V., Schiebel, R., Mallet, R., Durden, J.M., Bett, B.J., Gooday, A.J., 2016. Agglutination of benthic foraminifera in relation to mesoscale bathymetric features in the abyssal NE Atlantic (Porcupine Abyssal Plain). *Marine Micropaleontology*, 123, 15–28.

- Suhr, S.B., Pond, D.W., Gooday, A.J., Smith, C.R., 2003. Selective feeding by benthic foraminifera on phytodetritus on the western Antarctic Peninsula shelf: evidence from fatty acid biomarker analysis. *Marine Ecology Progress Series*, 262, 153–162.
- Suhr, S.B., Pond, D.W., 2006. Antarctic benthic foraminifera facilitate rapid cycling of phytoplankton-derived organic carbon. *Deep-Sea Research Part II—Topical Studies in Oceanography*, 53, 895–902.
- Sun, X., Corliss, B.H., Brown, C.W., Showers, W.J., 2006. The effect of primary productivity and seasonality on the distribution of deep-sea benthic foraminifera in the North Atlantic. *Deep-Sea Research Part I—Oceanographic Research Papers*, 53, 28–47.
- Tendal, O.S., Hessler, R.R., 1977. An introduction to the biology and systematics of Komokiacea (Textulariina, Foraminiferida). *Galathea Report*, 14, 165–194.
- Thomson, J., Colley, S., Higgs, N., Hydes, D., Wilson, T., Sorensen, J., 1987. Geochemical oxidation fronts in NE Atlantic distal turbidites and their effects in the sedimentary record. In: Weaver, P.P., Thomson, J. (Eds.), *Geology and Geochemistry of the Abyssal Plains* (pp. 167–177).
- Thomson, J., Colley, S., Anderson, R., Cook, G.T., Mackenzie, A.B., Harkness, D.D., 1993. Holocene sediment fluxes in the northeast Atlantic from $\delta^{13}C_{org}$ and radiocarbon measurements. *Paleoceanography*, 8, 631–650.
- Turnewitsch, R., Reyss, J.L., Chapman, D.C., Thomson, J., Lampitt, R.S., 2004. Evidence for a sedimentary fingerprint of an asymmetric flow field surrounding a short seamount. *Earth and Planetary Science Letters*, 222, 1023–1036.
- Turnewitsch, R., Falahat, S., Nycander, J., Dale, A., Scott, R.B., Furnival, D., 2013. Deep-sea fluid and sediment dynamics—Influence of hill- to seamount-scale seafloor topography. *Earth-Science Reviews*, 127, 203–241.
- Turnewitsch, R., Lahajnar, N., Haeckel, M., Christiansen, B., 2015. An abyssal hill fractionates organic and inorganic matter in deep-sea surface sediments. *Geophysical Research Letters*, 42, 7663–7672.
- van der Loeff, M.R., Lavaleye, M., 1986. Sediments, fauna, and the dispersal of radionuclides at the NE Atlantic dumpsite for low-level radioactive waste: Report of the Dutch DORA program. (p. 134). NIOZ: Den Burg: Netherlands Institute for Sea Research.
- Wallace, H.E., Thomson, J., Wilson, T.R.S., Weaver, P.P.E., Higgs, N.C., Hydes, D.J., 1988. Active diagenetic formation of metal-rich layers in NE Atlantic sediments. *Geochimica Et Cosmochimica Acta*, 52, 1557–1569.

Chapter 6: Synthesis and future directions

6.1 Main conclusions

The overall purpose of this project was to investigate the effects of mesoscale topographic heterogeneity generated by abyssal hills on benthic foraminiferal assemblages in the PAP-SO area of the NE Atlantic. This objective has been approached from various angles, which reveal that the hills exert a subtle influence on 'live' (stained) foraminiferal assemblages that is not apparent in the corresponding dead assemblages. The main findings of the preceding chapters are as follows:

In chapter 2, I described 18 distinct morphotypes of poorly known primitive benthic foraminifera associated with (i.e. sessile on) planktonic foraminiferal shells and mineral grains. These represented up to 31–33% and 23–36% of the total live and dead foraminiferal assemblages, respectively. Some forms were more common on the hills (monothalamids with tests composed of mineral grains; spheres with short tube), while others were more common on the plain (thick-walled spheres with red interior; chain-like forms), although analysis of additional replicate samples is needed to confirm these patterns. Similar forms have been described from the NE Atlantic (Gooday et al., 1995b) as well as from the Pacific (Nozawa et al., 2006; Ohkawara et al., 2009; Snider et al., 1984). In the latter case they are found close to or below the CCD and are therefore associated with the siliceous shells of radiolarians rather than calcareous planktonic foraminiferan shells. They therefore represent an overlooked but potentially important facet of deep-sea biodiversity that warrants closer attention and taxonomic effort.

In chapter 3, I demonstrated that foraminifera selected different sized particles on hills and plains, mirroring the distinct hydrodynamic conditions and by extension the distinct sedimentary profiles of the two settings. I also found differences in the visual appearance of their tests related to seafloor topography, which was confirmed by morphometric analyses. Test elemental composition was similar (silica-dominated) for all studied specimens irrespective of topography, despite the

fact that the bulk elemental composition of hill sediments was distinct from that of the plain; the difference in the elemental composition of the sediment presumably reflected a difference in mineralogy, probably a result of current-induced winnowing on the hills. I concluded that the test characteristics (morphometry, particle size composition) of agglutinated benthic foraminifera could be used as a proxy for paleoflow dynamics in 'flysch-type' or 'high latitude slope deep-water agglutinated foraminifera' faunas.

In chapter 4, I compared 'live' (Rose-Bengal-stained) benthic foraminiferal assemblages between three abyssal hill and two adjacent plain locations (8 samples per setting; 1–4 replicates per site). Density and diversity were higher on the hills but not significantly so. Nevertheless, hills supported a higher species density, distinct fauna, and increased regional diversity. I proposed enhanced bottom-water flow on hills, which affects organic matter supply and local sedimentology, to be responsible for these differences. I concluded that hill-induced mesoscale habitat complexity is potentially important in regulating abyssal foraminiferal diversity, and as such hills should be incorporated into any assessment of abyssal ecology.

In chapter 5, I compared live and dead benthic foraminiferal faunas from 4 samples (2 on hills, 2 on the plain) in order to gain a better understanding of the main processes influencing the composition of the dead assemblage and hence ultimately of fossil assemblages. The results suggest that the most important process operating during the transition from live to dead faunas is a significant loss of delicate agglutinated and organic-walled forms, while other factors (dissolution of fragile calcareous tests, transport of tests by currents, predation) are of minor significance. Live to dead ratios also indicated that some species (e.g. *Epistominella exigua*, *Bolivina spathulata*) may have responded to a recent phytodetritus input. However, unlike live assemblages (Chapter 4), the composition of the dead assemblages was very similar in hill and plain settings. I conclude that it would not be possible for paleoceanographers to differentiate between fossil foraminiferal faunas originating from these topographically contrasting settings.

6.2 Limitations of data set

Due to the number of samples processed ($n=16$, 1–4 replicates per site) the analysis had to be limited to individuals retained on a 150- μm mesh sieve. In addition, I incorporated into my analysis soft-walled monothalamous forms ('monothalamids'), which substantially increased the amount of time needed to process a single sediment sample. However, monothalamids have been shown to dominate foraminifera in deep-sea sediments (e.g. Gooday 1986; Pawlowski et al., 2011; Lejzerowicz et al., 2014), and thus cannot be overlooked in a biologically orientated study such as the present one. Moreover, the patchy distribution of benthic foraminifera in coastal environments (e.g. Buzas et al., 2002; 2015) and in the deep sea (Barras et al., 2010; Bernstein et al., 1978; Fontanier et al., 2003; Griveaud et al., 2010) makes it essential to follow well-established ecological practice by analysing replicate samples at each site (Schönfeld et al., 2012), something not always done in geologically-orientated studies. The lack of finer fractions ($<150\ \mu\text{m}$) in the present study was unavoidable for practical reasons. Examination of fine residues (e.g. 63–125 μm , 125–150 μm) is particularly time consuming, especially in deep-sea settings where small-sized individuals dominate foraminifera assemblages (e.g. Gooday, 1986, 1996; Gooday et al., 1995b), making it impossible to process replicates on a realistic timescale. Although some information on species diversity and dominance might be lost (Sen Gupta et al., 1987), in particular that related to the small, opportunistic taxa that have a strong response to food inputs (Gooday, 1993; Smart et al., 1994), it is also true that numerous studies focusing on foraminifera retained on a 150- μm mesh sieve have yielded significant ecological results (e.g. Barras et al., 2010; Caille et al., 2015; Fontanier et al., 2002; Goineau et al., 2012; Mojtahid et al., 2010), also shown in Chapters 3–5. Finally, another advantage of working with the $>150\text{-}\mu\text{m}$ size fraction is that it allows direct comparison with other studies on deep-sea benthic foraminifera, which are often based on the >125 or $>150\text{-}\mu\text{m}$ fractions (Murray, 2007, 2015).

Time constraints also confined the present analysis to the upper (0–1 cm) sediment layer. Benthic foraminiferal microhabitats are mainly controlled by organic matter and oxygen availability (Corliss and Emerson, 1990; Jorissen et al.,

1995) and it is now well known that deep-sea foraminiferans penetrate into deeper sediment layers when conditions are favourable (e.g. Corliss, 1985; Fontanier et al., 2002; Gooday, 1986; Jorissen et al., 1999). Consequently, in the present study some of the deeper-dwelling species were certainly undersampled. Nevertheless, epifaunal and shallow infaunal foraminifera living on and in the top 1-cm layer are more in touch with sediment surface/bottom-water environment and thereby are more responsive to changes in food supply compared to intermediate infaunal (1–4 cm) and deep infaunal (>4 cm) species (Heinz et al., 2002; Nomaki et al., 2005). Moreover, Gooday et al. (1998) reports only a slight effect on diversity measures when deeper sediment layers are excluded. As a result, it is unlikely that analysis of deeper sediment layers would have led to substantially different results.

6.3 Suggestions for future work

Chapter 2: The answer to the question of whether many of the chain-like and tubular forms described here, in particular those containing dark material (decayed stercomata), were 'alive' or dead was ambiguous. In many cases it would be difficult to determine the status of such forms without a more detailed and probably destructive examination. As a result ~16% of all picked specimens were termed ?Live. In a study of foraminifera encrusting nodules and dropstones, Gooday et al. (2015) faced similar challenges and suggested a range of methods for tackling these problems that included the use of: a) non-specific fluorescent markers such as CellTracker™ Green (Bernhard et al., 2006b), fluorescein diacetate (FDA) (Bernhard et al., 1995) and DAPI (4',6-diamidino-2-phenylindole) (Lecroq et al., 2009b), b) the FISH (fluorescent in situ hybridization) technique, c) transmission electron microscopy, which might prove helpful in discovering additional features of test morphology as well as of cellular organization (e.g. Bernhard et al., 2006a). In practice, however, these methods are unlikely to yield any significant results for the forms described here. Considering the depths they were recovered from (~4350–4850 m), most of the specimens that were alive on the seafloor were probably dead when they reached the ship, and even if still alive their metabolic rates were likely to be very low (Gooday et al., 2008). Thus the success of the fluorescent techniques is doubtful. In addition, such forms are very fragile and

likely to be damaged during sample recovery (see examples of specimens that collapsed when transferred onto an SEM stub, Chapter 2, Figs. 2.3d–e, 2.5d–e therein). Considering these shortcomings, improved knowledge of these poorly-known foraminifera might be best achieved by 1) using scanning electron microscopy (SEM) to examine specimens that had been critical-point dried, 2) using thin sections of optimally fixed specimens for SEM and TEM observations, and 3) picking and fixing multiple fresh specimens in order to obtain small subunit ribosomal RNA gene sequences, which would shed light on their phylogenetic position. Similar methods have been applied to giant foraminifera (xenophyophores) from the Japan Trench (Lecroq et al., 2009b), a group of foraminifera whose study entails similar challenges to the ones outlined here.

Chapter 3: The investigation of agglutination patterns of benthic foraminifera in relation to topography was based on 65 specimens belonging to 10 species. In the future, additional specimens and species from the two topographic settings (hills and plain) could be analysed in order to improve the reliability and wider application of the results. Ideally, the number of analysed specimens per species should be at least 4 for each setting (total of 8 for hills and plain combined), which would then allow species-specific non-parametric comparisons (e.g. ANOSIM and MDS; Clarke et al., 1993) to be made between different topographic settings. Alternatively, more effort could be devoted to those species that showed the clearest differences between topographic settings (e.g. *Reophax* sp. 21), making them possible indicators of enhanced current flow. Specimens could originate from the hills from which I have already analysed samples (H1, H4), but a wider study could also include material from 'Ben Billett', a much larger hill (~900 m high) located next to site P3 (Chapter 4, Fig. 4.1 therein; Turnewitsch et al., 2015; Fig. 1 therein). I have already shown that specimens from H4 (~500 m high) had significantly coarser agglutination compared to H1 (~200 m high), so I would expect that effect to be more pronounced on top of 'Ben Billett'. Finally, a detailed analysis on the mineralogy of the studied tests and comparison with that of the corresponding sediments would provide information on mineral selectivity, which is common in some agglutinated taxa (Corliss and Milliman, 1981; Gooday and Claugher, 1989; Gooday et al., 1995c; Jørgensen, 1977; Lipps, 1973; Mancin et al., 2012).

Chapter 4: Here, I demonstrated that abyssal hills enhance the mesoscale diversity of benthic foraminifera. However, other key questions remain regarding the scale and nature of environmental heterogeneity associated with these features and the processes controlling them. Further work is required to quantify the detailed contributions of factors that cause such heterogeneity, such as slope, slope failures, hydrodynamic regime, sedimentation events (both sinking from the surface and re-suspended sediments), and bioturbation. To understand the roles of these factors in structuring benthic foraminiferal communities, the topography of abyssal hills should be examined at higher resolution. Based on previous observations on seamounts (Koslow et al., 2001; Raymore, 1982; Rogers, 1994) and mid-ocean ridges (Priede et al., 2013), such a survey would probably reveal a great variety of topographic and microrelief features on the hills in the form of slumps, gullies and exposed hard substratum (rocky outcrops, cliff faces), in stark contrast with the surrounding sedimented abyssal plain. Hard substrata are known to host diverse assemblages of sessile suspension feeders (e.g. Mortensen et al., 2008), including benthic foraminifera (e.g. Linke and Lutze, 1993; Lutze and Altenbach, 1988; Mullineaux, 1988; Schönfeld et al., 2002a,b). Consequently, the presence of extensive areas of hard substrates on the hills is certain to enhance foraminiferal diversity at smaller (within-hill; centimetres to metres) and larger (plain and hills; kilometres) scales. Finally, it would be interesting to progressively extend the scale of the study to test if other hills in the PAP-SO area (notably 'Ben Billett'), hills from other parts of the Atlantic, and abyssal hills in other oceans, also influence benthic foraminiferal communities. This would help to clarify if the effect of hill-related heterogeneity on benthic foraminifera revealed in this study is a widespread phenomenon in the deep sea, with important implications for global abyssal diversity.

Chapter 5: Due to time constraints, the present study was based on a limited number of samples ($n= 4$). Analysis of replicated samples from each site would remove any potential bias stemming from the patchy distribution of foraminifera, and allow for statistical comparisons of dead assemblage composition between the plain and the hills. Addition of finer size fractions ($<150 \mu\text{m}$) would provide a better insight into population dynamics of some small-sized species (e.g.

Alabaminella weddellensis), while examination of deeper sedimentary microhabitats (>1 cm) would provide information on the deeper infaunal populations and their contribution to the dead and fossil assemblage (see Loubere and Gary, 1990; Loubere et al., 1993). Finally, comparisons between dead assemblages and the 'real' fossil assemblages below the mixed layer (e.g. Mackensen and Douglas, 1989) merit further investigation, as they would offer a better understanding of the diagenetic processes (related to pore-water geochemistry and sediment compaction) affecting fossil fauna composition.

Foraminifera encrusting dropstones: Ice-rafted dropstones are pebble to boulder-sized stones of various shapes, which were dropped from melting icebergs during the last glacial maximum (Bennett et al., 1996; Gilbert, 1990). They are a common feature of the seafloor at high latitudes, and can be abundant on abyssal hills further south in the NE Atlantic (Kidd and Huggett, 1981), including the hills within the PAP-SO area (Ruhl, 2012). Dropstones are an important source of small-scale heterogeneity, providing patches of firm substratum in an otherwise soft, sedimentary habitat. Nevertheless, very little is known about the encrusting fauna of glacially transported dropstones. Some information originates from studies conducted in Arctic shallow waters (Kuklinski, 2009, 2013), while a handful of studies considered deeper settings (e.g. Oschmann, 1990; Weston, 1985). In all cases, a variety of attached organisms that were not found in the surrounding sediment have been reported, including significant numbers of benthic foraminifera.

I am not aware of any in-depth study of dropstone-associated fauna from abyssal habitats. A preliminary study of material collected from the BIOTRANS area in the NE Atlantic (3900–4500 metres water depth), recognised up to 36 putative species of benthic foraminifera living on 28 stones (Gooday, unpubl. data). Recently, Gooday et al. (2015) reported a further 39 foraminiferal species and two types of metazoans encrusting 8 dropstones from the PAP and also included some information from stones collected in the BIOTRANS area in the 1980s.

These previous efforts prompted me to examine the encrusting fauna of dropstones found on hills within the PAP-SO in more detail. During RV *Meteor*

Cruise 108 (ME108, 6 to 24 July 2014) and RRS *Discovery* Cruise 032 (DY032, 20 June to 8 July 2015) I collected a total of 125 dropstones from two hill locations in the PAP-SO area (Table 6.1) in order to study their attached fauna. Preliminary examination of the collected material revealed that a diverse sessile fauna colonised the dropstones (Table 6.2). A total of 99 morphotypes (presumed to be morphospecies) was recognised. Some (21 spp.; 21%) were metazoans, mostly sponges, polychaete tubes and occasionally branchiopods (*Pelagodiscus*) or scyphozoans (*Stephanoscyphus*) (Fig. 6.1). The majority (78 spp.; 79%), however, were foraminifera or foraminifera-like protists (Table 6.2, Fig. 6.2). Between 0 and 15 morphotypes were present on individual stones. Faunal cover varied greatly from stone to stone, ranging from total absence of attached organisms to 100% coverage. The foraminifera were dominated by a variety of mat- and chain-like formations, isolated domes, anastomosing trails, reticulated networks and simpler branched or unbranched tubular structures, interpreted as monothalamous foraminifera (monothalamids). Most had agglutinated tests but a few were

Table 6.1. Site and station information.

Site	Station	Water depth (m)	Lat (°N)	Long (°W)	Equipment	No of stones
Ben Billett	ME108–795	3903	49.115	16.630	Megacorer	39
H4	DY032–45	4295	49.074	16.264	Box core	69
H4	DY032–83	4292	49.074	16.264	Megacorer	17

Table 6.2. Numbers of foraminiferal and metazoan morphospecies attached to 125 dropstones collected from two hill locations during the ME108 and DY032 cruises in the PAP-SO area.

Major group	No of spp.	Figure
Foraminifera		
Multichambered		
<i>Globothalamea</i>	18 (13)	6.2g
<i>Tubothalamea</i>	2 (2)	6.2h–i
Monothalamids		
<i>Spheres and domes</i>	8 (4)	6.2c
<i>Chains of chambers</i>	16	6.2e
<i>Networks of tubes</i>	17	6.2d
<i>Komokiaceans</i>	13	6.2a–b
<i>Mats and patches</i>	4	6.2f
Metazoa	21	6.1a–d
Indeterminate	3	

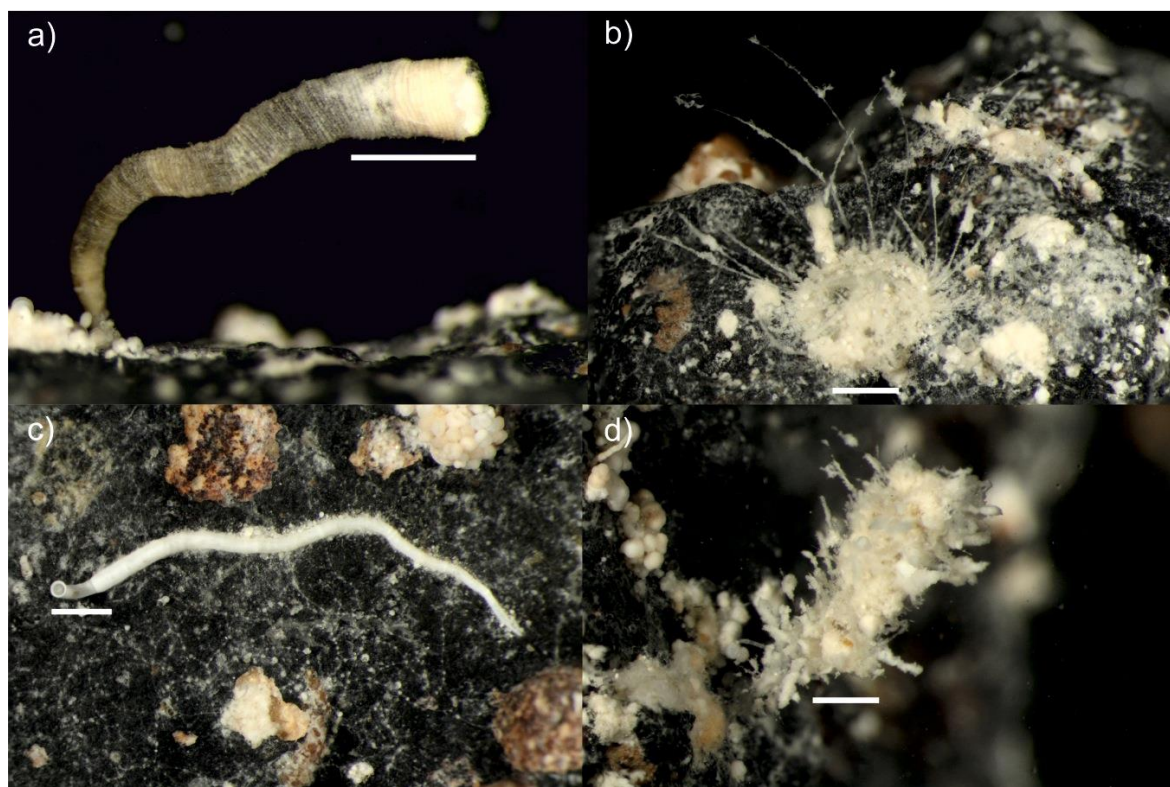


Fig. 6.1. Common encrusting metazoans on dropstones from hills within the PAP-SO area. In brackets the major taxon to which each organism belongs. a) *Stephanoscyphus* sp. (Cnidaria, Scyphozoa), b) *Pelagodiscus* sp. (Brachiopoda), c) Serpulid tube (Polychaeta), d) Sponge (Porifera). Scale bar = 1 mm.

predominately organic. Some could be assigned to the Komokiaceae (Fig. 6.2a–b) or the genera *Psammosphaera* (Fig. 6.2c) and *Telamina* (Fig. 6.2d), while others (e.g. many of the chains and mats; Fig. 6.3e–f) were difficult to place into existing taxa. Polythalamous foraminifera were also fairly common and included calcareous (mostly *Cibicides* spp.; Fig. 6.3g) and agglutinated (various trochamminaceans) species of the class Globothalamea (*sensu* Pawlowski et al., 2013), as well as agglutinated forms such as *Ammodiscus* (Fig. 6.4h) and *Glomospira* (Fig. 6.4i) of the class Tubothalamea (*sensu* Pawlowski et al., 2013).

Comparisons with the sediment-dwelling foraminiferan fauna from the PAP-SO area (Chapter 4) indicated that, with the exception of some domes and polythalamous species, the morphotypes were restricted to the dropstones. As dropstones are a very common small-scale feature on hills within the PAP-SO area they must enhance foraminifera diversity at small (within-hill; centimetres to metres) to intermediate (plain vs hills; kilometres) scales. Future efforts will aim at

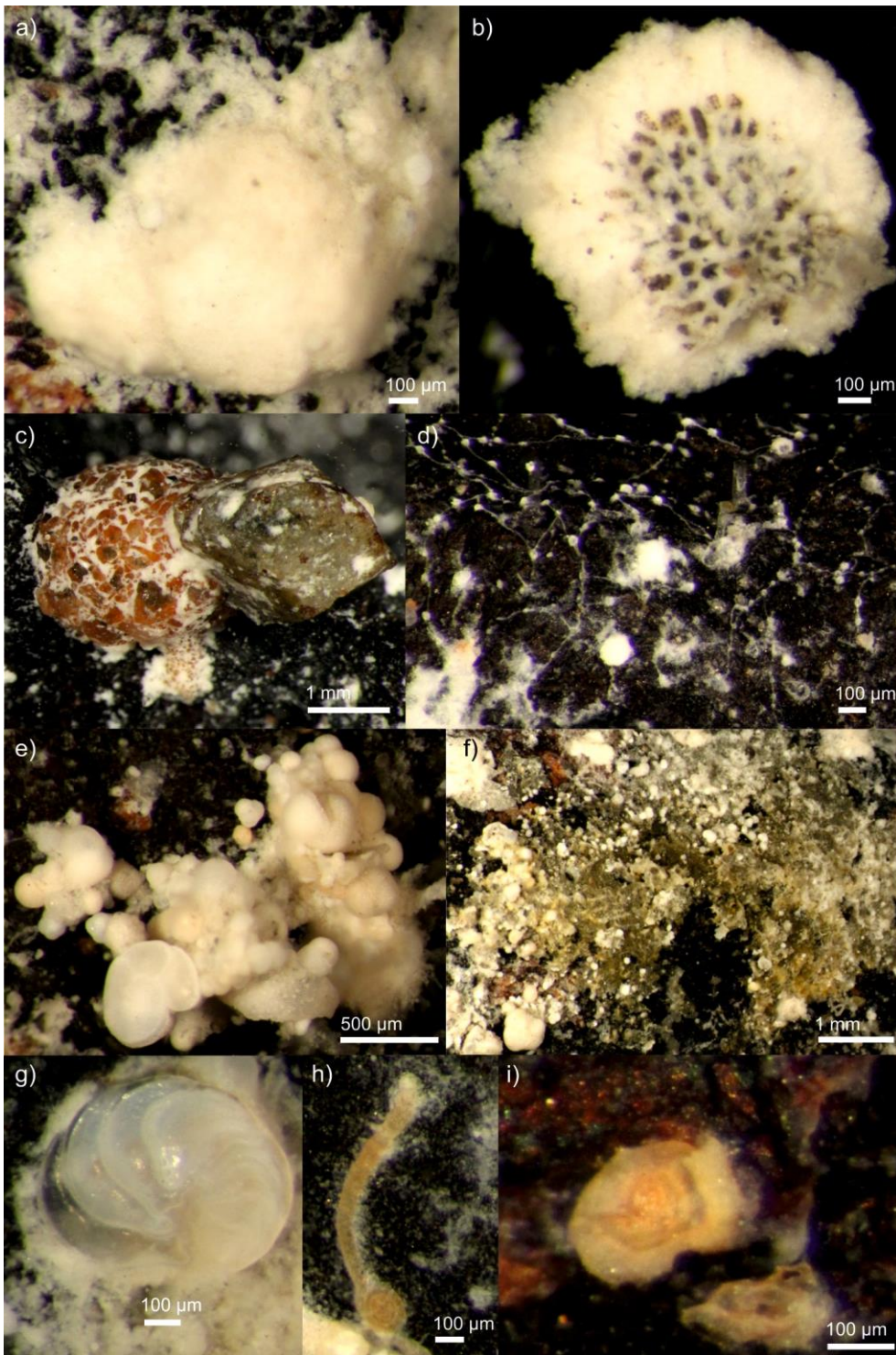


Fig. 6.2. Common encrusting foraminifera on dropstones from hills within the PAP-SO area. In brackets are the major groupings (formal or informal) to which each morphotype belongs. a–b) Solid, domed komokiacean with internal chambers (Komokiacea) similar to some specimens illustrated by Gooday et al. (2015, Figs. 14a–b, 15f–g), c) *Psammospaera* sp. ('spheres and domes'), d) *Telamina* sp. ('network of tubes'), e) Irregular chain ('chain of chambers'), f) Yellow agglutinated mat ('mats and patches'), g) *Cibicides wuellerstorfi* (Globothalamea: Rotaliida), h) *Ammodiscus* sp. (Tubothalamea: Ammodiscidae) similar to the specimen illustrated by Gooday et al. (2015, Fig. 15e), i) *Glomospira* sp. (Tubulothalamea: Ammodiscidae).

i) providing a brief description of the main foraminiferal morphotypes attached on the stones, ii) comparing the generated data against similar assemblages reported from abyssal polymetallic nodules and crusts (e.g. Mullineaux, 1987; Gooday et al. 2015), and iii) combining that information with existing knowledge of the sediment dwelling faunas (Chapter 4) in order to estimate the total foraminiferal diversity on the hills, and the wider area of the PAP-SO.

Biomass of benthic foraminifera: A variety of methods has been used to estimate the biomass of benthic foraminifera (Murray and Alve, 2000). Early approaches involved estimation of the test volumes from the volumes of geometric shapes that approximated those of the tests (Murray, 1968, 1969, 1970a,b); Saidova (1967) went a step further and multiplied these volumes by the protoplasmic density to estimate biomass. Since then, Saidova's method has been applied in a series of papers (e.g. Basov, 1974, Basov and Khusid, 1983, Khusid, 1974) although the conversion of external test volume to internal volume has only occasionally been considered (e.g. Wefer and Lutze, 1976). Authors have also often made the assumption that protoplasm fills the entire test interior. Although true for some taxa (e.g. *Uvigerina akitaensis* and *Ammonia beccarii*, Goldstein and Corliss, 1994; Nomaki et al., 2010), for many foraminifera, cytoplasm only partly fills the internal space, and numerous vacuoles further reduce the volume (Altenbach, 1987; Bernhard et al., 2012; Gerlach et al., 1985; Snider et al., 1984). Hannah et al. (1994) estimated foraminiferal test volume using scaled clay models to derive a best fitting formula, and then took into account shell thickness and assumed 75% cytoplasmic content in order to calculate biomass. Finally, Korsun et al. (1998) determined biomass following the method of Saidova (1967), although they also took into account shell thickness and used a slightly different factor to convert foraminiferal protoplasm to biomass.

DeLaca (1986) tried to overcome the uncertainties involved in volume-estimation methods by using the ATP content of the cell as a measure of biomass. This was thought to better reflect the amount of protoplasm present in the test and has since then been successfully applied in other studies (e.g. Bernhard, 1992; Gooday et al., 1995a). Nevertheless, there are some disadvantages notably that the technique is expensive, it destroys the specimens, and the samples need to be

processed within a few hours of collection. In another approach, Altenbach (1985, 1987) determined the organic carbon of foraminiferal tests by using wet oxidation and infrared analysis, and then developed conversion factors based on test size to calculate biomass (see also works of Altenbach, 1992 and Thomsen and Altenbach, 1993 for further applications of the technique). Similarly, Moodley et al. (2000) measured organic carbon content of decalcified foraminifera specimens using an elemental analyser and reported results comparable to Altenbach's method. However, both of these methods, like DeLaca's, destroy the test impeding any further analysis. Other authors have measured foraminiferal wet weights (Kamenskaya, 1988; Kamenskaya et al., 2013; Smith et al., 1978), dry weights (Olsson, 1975), dry weights of the protoplasm (Boltovskoy and Lena, 1969), ash-free dry weights (Shirayama, 1983, 1984; Widbom, 1984) for foraminiferal assemblages and species. Nevertheless, it has been argued that wet and dry weights greatly overestimate the organic matter content of foraminifera with heavy tests and/or sparse cytoplasm (Goody et al., 1992; Widbom, 1984).

Recently, Movellan et al. (2012) quantified the protein content (a proxy for biomass) of benthic and planktic foraminifera using nano-spectrophotometry. Although reliable and inexpensive, this method has been applied so far only to calcareous (i.e. hard-shelled) shallow-water species. Consequently, it might not be applicable to the smaller-sized deep-sea foraminifera many of which are loosely agglutinated (i.e. soft-walled) (Movellan, pers. comm). In addition, this method requires the use of freshly collected specimens and cannot be applied to specimens fixed in formalin, which is the standard fixative for deep-sea biological material.

Micro-X-ray computed tomography (CT), a powerful tool for observing and reconstructing the internal structures of target objects including benthic foraminifera (Briguglio et al., 2011; Nomaki et al., 2015; Speijer et al., 2008), might be a promising future approach. This technique has a number of key advantages. It is rapid (typically <1h) and non-destructive, so that specimens can be saved for further analysis. It can generate 3D images of foraminiferal tests. It can reveal both the total cytoplasmic volume and the volume occupied by vacuoles, which allows the calculation of actual cytoplasmic volume. In theory it is possible to then convert

the obtained data to organic carbon content and other parameters (Nomaki et al., 2015). Nevertheless, for the moment this method is relatively expensive if applied to a large number of specimens, which would be the case for estimating foraminiferal biomass at the community level. Moreover, it has not been tested on small-sized benthic foraminifera that are common in the deep sea. Despite these challenges, I believe it is worth exploring this method further and applying it to benthic foraminifera from abyssal depths.

At present, deep-sea foraminiferal biomass data are scarce and, with the exception of Kurbjeweit et al. (2000), none are available from abyssal depths, despite the fact that they are a major component of the benthos worldwide. The resulting data would allow the conversion of taxon-specific counts and body size data into biomass estimates and ultimately into models of carbon stocks and flow, as has been done for metazoan meio- and macrofauna (Kelly-Gerreyn B.A. et al., 2014). Similarly, estimates of megafaunal biomass from photogrammetric methods has led to substantially revised stocks and flows of benthic carbon in the Porcupine Abyssal Plain (Durden, 2016). Accurate estimates of foraminiferal biomass would also be a useful tool for palaeontologists aiming to reconstruct trophic conditions in past oceanic ecosystems.

Molecular genetics: During the last 20 years DNA barcoding has become an affordable and practical means for inferring molecular phylogenies and supporting species descriptions of foraminifera from a plethora of marine environments (Apotheloz-Perret-Gentil and Pawlowski, 2015; Pillet et al., 2013; Voltski et al., 2014; Voltski and Pawlowski, 2015), including the deep-sea floor (Cedhagen et al., 2009; Gooday et al., 2004; Gooday and Pawlowski, 2004; Lecroq et al., 2009b; Lejzerowicz et al., 2015b; Pawlowski, 2000). However, still only a few deep-sea foraminiferal species have been studied genetically (Pawlowski and Holzmann, 2014). More analyses using the small subunit (SSU) of the ribosomal RNA gene would help to clarify the degree of genetic differentiation in the case of morphologically indistinct species that occur across wide geographic and bathymetric ranges (e.g. Lecroq et al., 2009a; Pawlowski et al., 2007; Tsuchiya et al., 2009). The detection of cryptic speciation (Brandt et al., 2007; Saad and Wade, 2016) is another important application of genetic data. Cryptic species have

been suggested to be particularly prevalent in monothalamids (Pawlowski and Holzmann, 2008) due to their relatively simple morphology and numerous small-sized species.

There has also been a considerable development recently in biodiversity assessments using DNA barcoding and more recently DNA metabarcoding (Taberlet et al., 2012b). These methods refer to the identification of multiple species from environmental DNA (eDNA) (Taberlet et al., 2012a) samples using traditional Sanger sequencing for the former, and high-throughput sequencing (HTS) technologies, sometimes known as next generation sequencing (NGS), for the latter. eDNA surveys for the assessment of foraminiferal diversity have been successfully conducted in freshwater (Holzmann et al., 2003), coastal (Edgcomb et al., 2014; Habura et al., 2008; Habura et al., 2004), deep-water (Edgcomb et al., 2014; Lecroq et al., 2011; Lejzerowicz et al., 2014) and even terrestrial settings (Lejzerowicz et al., 2010). To some extent, the development of these methods, as applied to foraminifera and other taxa, has been driven by their potential application in marine and freshwater biomonitoring activities (Lejzerowicz et al., 2015a; Pawlowski et al., 2014a; Pawlowski et al., 2016; Pochon et al., 2015; Vivien et al., 2016). These new approaches represent a rapid and cost-effective way to identify species in sediment samples, which will be particularly useful in the case of tiny deep-sea species that cannot easily be detected visually.

At the present there are a number of challenges related to next-generation eDNA surveys, most notably the lack of a comprehensive 'molecular database' (DNA barcode reference library) to which assigned foraminifera species (known or unknown) can be compared with, or the bias in the interpretation of the obtained data, facilitated by the lack of standardised bioinformatics and visualisation tools (reviewed in Pawlowski et al., 2014). Addressing these issues in the upcoming years will help HTS eDNA surveys to cement their position as a standard tool for biodiversity assessments.

6.4 Implications for understanding of the PAP-SO area and the wider abyss

The present research is part of the wider NERC-funded efforts of the Autonomous Ecological Survey of the Abyss project (AESAs NE/H021787/1) and the Porcupine Abyssal Plain Sustained Observatory Programme. One of the key aims of these projects was to examine how spatial heterogeneity in seafloor attributes relates to the distribution of meio- (foraminifera), macro- (polychaetes) and megafaunal abundance and biomass.

Hills appeared to have a significant effect on benthic foraminifera (community composition; Chapter 4) and megafauna (biomass, community composition; Durden et al., 2015) but not on polychaetes (Laguionie-Marchais, 2015). Laguionie-Marchais (2015) speculated that the lack of effect in the case of polychaetes might be a) down to the small sample size used for the analysis, which resulted to some rare species being missed, leading to a likely underestimation of differences among sites, b) due to enhanced within-hill spatial heterogeneity making the distinction between hills and plain less clear, and c) the fact that the classification of sites as abyssal hill or plain may be too simplistic. For example, visual observations of the sediment cores from some plain sites, suggested that different physical disturbances occurred at each location (Durden et al., 2015; see also section 5.4.3.2 in Chapter 5).

Abyssal hills might not be more diverse than surrounding areas but they nevertheless contributed to an enhanced regional biodiversity for all three studied groups, an observation that also applies to seamounts (e.g., Chivers et al., 2013). It is believed that historical and contemporary differences in local flow conditions, namely difference in near-bed current flows as observed in other systems (Bongiorni et al., 2013; Levin et al., 2001; Snelgrove and Butman, 1994), may be the primary factor influencing sediment particle size distribution (% of particles >63 μm), food availability and therefore faunal composition.

The findings of the present thesis, together with studies on macrofauna and megafauna from the same (PAP-SO) area, indicated that biodiversity estimations in abyssal systems have been greatly under-appreciated. This is important as estimation of deep-sea diversity has been a recurring theme in deep-sea biology since the 1960s (Grassle and Maciolek, 1992; Gray, 1994; Hessler and Sanders, 1967; Mora et al., 2011; Sanders, 1968) and remains a debated topic (McClain and Schlacher, 2015). An increasing number of studies have suggested that biodiversity regulates functioning in all ecosystems (Cardinale et al., 2002; Worm et al., 2006), and in the deep sea, exponential relationships between biodiversity and ecosystem functioning and efficiency have been found across a wide range of habitats (Danovaro, 2012; Danovaro et al., 2008). As abyssal hills are one of the most common topographic features on Earth, they may promote higher abyssal benthic meio-, macro- and megafauna diversity at regional scales than previously thought, with important implications of deep-sea ecosystem functioning.

References of Chapter 6

- Altenbach, A.V., 1985. Die Biomasse der Benthischen Foraminiferen. Auswertungen von "Meteor"-Expeditionen im Östlichen Nordatlantik. PhD thesis. *Christian-Albrechts University Kiel* (p. 167).
- Altenbach, A.V., 1987. The measurement of organic carbon in foraminifera. *Journal of Foraminiferal Research*, 17, 106–109.
- Altenbach, A.V., 1992. Short term processes and patterns in the foraminiferal response to organic flux rates. *Marine Micropaleontology*, 19, 119–129.
- Apotheloz-Perret-Gentil, L., Pawlowski, J., 2015. Molecular phylogeny and morphology of *Leannia veloxifera* n. gen. et sp. unveils a new lineage of monothalamous Foraminifera. *Journal of Eukaryotic Microbiology*, 62, 353–361.
- Barras, C., Fontanier, C., Jorissen, F., Hohenegger, J., 2010. A comparison of spatial and temporal variability of living benthic foraminiferal faunas at 550m depth in the Bay of Biscay. *Micropaleontology*, 56, 275–295.
- Basov, I.A., 1974. Biomass of benthic foraminifers in the region of the South Sandwich Trench and Falkland Islands. *Oceanology*, 14, 277–279.
- Basov, I.A., Khusid, T.A., 1983. Biomass of benthic foraminifera sediments of the Sea of Okhotsk. *Oceanology*, 23, 489–495.
- Bennett, M.R., Doyle, P., Mather, A.E., 1996. Dropstones: their origin and significance. *Palaeogeography Palaeoclimatology Palaeoecology*, 121, 331–339.
- Bernhard, J.M., 1992. Benthic foraminiferal distribution and biomass related to pore-water oxygen content: central California continental slope and rise. *Deep-Sea Research Part A–Oceanographic Research Papers*, 39, 585–605.
- Bernhard, J.M., Newkirk, S.G., Bowser, S.S., 1995. Towards a non-terminal viability assay for foraminiferan protists. *Journal of Eukaryotic Microbiology*, 42, 357–367.
- Bernhard, J.M., Habura, A., Bowser, S.S., 2006a. An endobiont-bearing allogromiid from the Santa Barbara Basin: Implications for the early diversification of foraminifera. *Journal of Geophysical Research-Biogeosciences*, 111.
- Bernhard, J.M., Ostermann, D.R., Williams, D.S., Blanks, J.K., 2006b. Comparison of two methods to identify live benthic foraminifera: A test between Rose Bengal and CellTracker Green with implications for stable isotope paleoreconstructions. *Paleoceanography*, 21.
- Bernhard, J.M., Casciotti, K.L., McIlvin, M.R., Beaudoin, D.J., Visscher, P.T., Edgcomb, V.P., 2012. Potential importance of physiologically diverse benthic foraminifera in sedimentary nitrate storage and respiration. *Journal of Geophysical Research-Biogeosciences*, 117.
- Bernstein, B.B., Hessler, R.R., Smith, R., Jumars, P.A., 1978. Spatial dispersion of benthic foraminifera in abyssal central North Pacific. *Limnology and Oceanography*, 23, 401–416.
- Boltovskoy, E., Lena, H., 1969. Seasonal occurrences. standing crop and production in benthic foraminifera of Puerto Deseado. *Contributions from the Cushman Foundation for Foraminiferal Research*, 20, 87–95.

- Bongiorni, L., Ravara, A., Parretti, P., Santos, R.S., Rodrigues, C.F., Amaro, T., Cunha, M.R., 2013. Organic matter composition and macrofaunal diversity in sediments of the Condor seamount (Azores, NE Atlantic). *Deep Sea Research Part II–Topical Studies in Oceanography*, 98, 75–86.
- Brandt, A., Gooday, A.J., Brandao, S.N., Brix, S., Brokeland, W., Cedhagen, T., Choudhury, M., Cornelius, N., Danis, B., De Mesel, I., Diaz, R.J., Gillan, D.C., Ebbe, B., Howe, J.A., Janussen, D., Kaiser, S., Linse, K., Malyutina, M., Pawlowski, J., Raupach, M., Vanreusel, A., 2007. First insights into the biodiversity and biogeography of the Southern Ocean deep sea. *Nature*, 447, 307–311.
- Briguglio, A., Metscher, B., Hohenegger, J., 2011. Growth rate biometric quantification by X-ray microtomography on larger benthic foraminifera: three-dimensional measurements push nummulitids into the fourth dimension. *Turkish Journal of Earth Sciences*, 20, 683–699.
- Buzas, M.A., Hayek, L.-A.C., Reed, S.A., Jett, J.A., 2002. Foraminiferal densities over five years in the Indian River Lagoon, Florida: a model of pulsating patches. *Journal of Foraminiferal Research*, 32, 68–92.
- Buzas, M.A., Hayek, L.A.C., Jett, J.A., Reed, S.A., 2015. *Pulsating patches: history and analyses of spatial, seasonal, and yearly distribution of living benthic foraminifera*. Washington D.C.: Smithsonian Institution Scholarly Press.
- Cardinale, B.J., Palmer, M.A., Collins, S.L., 2002. Species diversity enhances ecosystem functioning through interspecific facilitation. *Nature*, 415, 426–429.
- Caulle, C., Mojtahid, M., Gooday, A.J., Jorissen, F.J., Kitazato, H., 2015. Living (Rose-Bengal-stained) benthic foraminiferal faunas along a strong bottom-water oxygen gradient on the Indian margin (Arabian Sea). *Biogeosciences*, 12, 5005–5019.
- Cedhagen, T., Gooday, A.J., Pawlowski, J., 2009. A new genus and two new species of saccamminid foraminiferans (Protista, Rhizaria) from the deep Southern Ocean. *Zootaxa*, 9–22.
- Chivers, A.J., Narayanaswamy, B.E., Lamont, P.A., Dale, A., Turnewitsch, R., 2013. Changes in polychaete standing stock and diversity on the northern side of Senghor Seamount. *Biogeosciences*, 10, 3535–3546.
- Clarke, K.R., 1993. Non-parametric multivariate analyses of changes in community structure. *Australian Journal of Ecology*, 18, 117–143.
- Corliss, B.H., Milliman, J.D., 1981. The use of phillipsite in test construction of agglutinated deep-sea benthonic foraminifera. *Sedimentology*, 28, 401–406.
- Corliss, B.H., 1985. Microhabitats of benthic foraminifera within deep-sea sediments. *Nature*, 314, 435–438.
- Corliss, B.H., Emerson, S., 1990. Distribution of Rose Bengal stained deep-sea benthic foraminifera from the Nova Scotian continental margin and Gulf of Maine. *Deep-Sea Research Part I–Oceanographic Research Papers*, 37, 381–400.

- Danovaro, R., Gambi, C., Dell'Anno, A., Corinaidesi, C., Fraschetti, S., Vanreusel, A., Vincx, M., Gooday, A.J., 2008. Exponential decline of deep-sea ecosystem functioning linked to benthic biodiversity loss. *Current Biology*, 18, 1–8.
- Danovaro, R., 2012. Extending the approaches of biodiversity and ecosystem functioning to the deep ocean. In: Solan, M., Aspden, R.J., Paterson, D.M. (Eds.), *Marine Biodiversity and Ecosystem Functioning: Frameworks, methodologies, and integration* (pp. 115–126). Oxford: Oxford University Press.
- DeLaca, T.E., 1986. Determination of benthic rhizopod biomass using ATP analysis. *Journal of Foraminiferal Research*, 16, 285–292.
- Durden, J.M., Bett, B.J., Jones, D.O.B., Huvenne, V.A.I., Ruhl, H.A., 2015. Abyssal hills – hidden source of increased habitat heterogeneity, benthic megafaunal biomass and diversity in the deep sea. *Progress in Oceanography*, 137, 209–218.
- Durden, J.M., 2016. Spatial and temporal variation in abyssal megabenthic communities, as assessed with seabed photography. Doctoral Thesis. *University of Southampton, Ocean & Earth Science* (p. 203).
- Edgcomb, V.P., Bernhard, J.M., Summons, R.E., Orsi, W., Beaudoin, D., Visscher, P.T., 2014. Active eukaryotes in microbialites from Highborne Cay, Bahamas, and Hamelin Pool (Shark Bay), Australia. *Isme Journal*, 8, 418–429.
- Fontanier, C., Jorissen, F.J., Licari, L., Alexandre, A., Anschutz, P., Carbonel, P., 2002. Live benthic foraminiferal faunas from the Bay of Biscay: faunal density, composition, and microhabitats. *Deep-Sea Research Part I–Oceanographic Research Papers*, 49, 751–785.
- Fontanier, C., Jorissen, F., Chaillou, G., David, C., Anschutz, P., Lafon, V., 2003. Seasonal and interannual variability of benthic foraminiferal faunas at 550m depth in the Bay of Biscay. *Deep-Sea Research Part I–Oceanographic Research Papers*, 50, 457–494.
- Gerlach, S.A., Hahn, A.E., Schrage, M., 1985. Size spectra of benthic biomass and metabolism. *Marine Ecology Progress Series*, 26, 161–173.
- Gilbert, R., 1990. Rafting in glaci-marine environments. In: Dowdeswell, J.A., Scourse, J.D. (Eds.), *Glaci-marine Environments: Processes and Sediments* (pp. 105–120).
- Goineau, A., Fontanier, C., Jorissen, F., Buscail, R., Kerhervé, P., Cathalot, C., Pruski, A., Bourgeois, S., Metzger, E., Legrand, E., 2012. Temporal variability of live (stained) benthic foraminiferal faunas in a river-dominated shelf–faunal response to rapid changes of the river influence (Rhône prodelta, NW Mediterranean). *Biogeosciences*, 9, 1367–1388.
- Goldstein, S.T., Corliss, B.H., 1994. Deposit-feeding in selected deep-sea and shallow-water benthic foraminifera. *Deep-Sea Research Part I–Oceanographic Research Papers*, 41, 229–241.
- Gooday, A.J., 1986. Meiofaunal foraminiferans from the bathyal Porcupine Seabight (northeast Atlantic): size structure, standing stock, taxonomic composition, species-diversity and vertical-distribution in the sediment. *Deep Sea Research Part A–Oceanographic Research Papers*, 33, 1345–1373.

- Gooday, A.J., Claugher, D., 1989. The genus *Bathysiphon* (Protista, Foraminiferida) in the northeast Atlantic: SEM observations on the wall structure of seven species. *Journal of Natural History*, 23, 591–611.
- Gooday, A.J., Levin, L.A., Linke, P., Heeger, T., 1992. The role of benthic foraminifera in deep-sea food webs and carbon cycling. *Deep-Sea Food Chains and the Global Carbon Cycle*, 360, 63–91.
- Gooday, A.J., 1993. Deep-sea benthic foraminiferal species which exploit phytodetritus: characteristic features and controls on distribution. *Marine Micropaleontology*, 22, 187–205.
- Gooday, A.J., Bernhard, J.M., Bowser, S.S., 1995a. The taxonomy and ecology of *Crithionina delacai* sp. nov., an abundant large agglutinated foraminifer from Explorers Cove, Antarctica. *Journal of Foraminiferal Research*, 25, 290–298.
- Gooday, A.J., Carstens, M., Thiel, H., 1995b. Microforaminifera and nanoforaminifera from abyssal northeast Atlantic sediments: a preliminary report. *Internationale Revue Der Gesamten Hydrobiologie*, 80, 361–383.
- Gooday, A.J., Nott, J.A., Davis, S., Mann, S., 1995c. Apatite particles in the test wall of the large agglutinated foraminifer *Bathysiphon major* (Protista). *Journal of the Marine Biological Association of the United Kingdom*, 75, 469–481.
- Gooday, A.J., 1996. Epifaunal and shallow infaunal foraminiferal communities at three abyssal NE Atlantic sites subject to differing phytodetritus input regimes. *Deep-Sea Research Part I—Oceanographic Research Papers*, 43, 1395–1421.
- Gooday, A.J., Bett, B.J., Shires, R., Lamshead, P.J.D., 1998. Deep-sea benthic foraminiferal species diversity in the NE Atlantic and NW Arabian sea: a synthesis. *Deep-Sea Research Part II—Topical Studies in Oceanography*, 45, 165–201.
- Gooday, A.J., Holzmann, M., Guiard, J., Cornelius, N., Pawlowski, J., 2004. A new monothalamous foraminiferan from 1000 to 6300 m water depth in the Weddell Sea: morphological and molecular characterisation. *Deep-Sea Research Part II—Topical Studies in Oceanography*, 51, 1603–1616.
- Gooday, A.J., Pawlowski, J., 2004. *Conqueria laevis* gen. and sp. nov., a new soft-walled, monothalamous foraminiferan from the deep Weddell Sea. *Journal of the Marine Biological Association of the United Kingdom*, 84, 919–924.
- Gooday, A.J., Nomaki, H., Kitazato, H., 2008. Modern deep-sea benthic foraminifera: a brief review of their morphology-based biodiversity and trophic diversity. *Geological Society, London, Special Publications*, 303, 97–119.
- Gooday, A.J., Goineau, A., Voltski, I., 2015. Abyssal foraminifera attached to polymetallic nodules from the eastern Clarion Clipperton Fracture Zone: a preliminary description and comparison with North Atlantic dropstone assemblages. *Marine Biodiversity*, 391–412.
- Grassle, J.F., Maciolek, N.J., 1992. Deep-Sea species richness: regional and local diversity estimates from quantitative bottom samples. *American Naturalist*, 139, 313–341.
- Gray, J.S., 1994. Is the deep sea really so diverse? Species diversity from the Norwegian continental shelf. *Marine Ecology Progress Series*, 112, 205–209.

- Griveaud, C., Jorissen, F., Anschutz, P., 2010. Spatial variability of live benthic foraminiferal faunas on the Portuguese margin. *Micropaleontology*, 56, 297–322.
- Habura, A., Pawlowski, J., Hanes, S.D., Bowser, S.S., 2004. Unexpected foraminiferal diversity revealed by small-subunit rDNA analysis of Antarctic sediment. *Journal of Eukaryotic Microbiology*, 51, 173–179.
- Habura, A., Goldstein, S.T., Broderick, S., Bowser, S.S., 2008. A bush, not a tree: The extraordinary diversity of cold-water basal foraminiferans extends to warm-water environments. *Limnology and Oceanography*, 53, 1339–1351.
- Hannah, F., Rogerson, A., Laybourn-Parry, J., 1994. Respiration rates and biovolumes of common benthic foraminifera (protozoa). *Journal of the Marine Biological Association of the UK*, 74, 301–312.
- Heinz, P., Hemleben, C., Kitazato, H., 2002. Time-response of cultured deep-sea benthic foraminifera to different algal diets. *Deep-Sea Research Part I—Oceanographic Research Papers*, 49, 517–537.
- Hessler, R.R., Sanders, H.L., 1967. Faunal diversity in the deep-sea. *Deep Sea Research and Oceanographic Abstracts*, 14, 65–78.
- Holzmann, M., Habura, A., Giles, H., Bowser, S.S., Pawlowski, J., 2003. Freshwater foraminiferans revealed by analysis of environmental DNA samples. *Journal of Eukaryotic Microbiology*, 50, 135–139.
- Jørgensen, N.O., 1977. Wall structure of some arenaceous foraminifera from the Maastrichtian White Chalk (Denmark). *Journal of Foraminiferal Research*, 7, 313–321.
- Jorissen, F.J., de Stigter, H.C., Widmark, J.G.V., 1995. A conceptual model explaining benthic foraminiferal microhabitats. *Marine Micropaleontology*, 26, 3–15.
- Jorissen, F.J., 1999. Benthic foraminiferal microhabitats below the sediment-water interface. *Modern foraminifera* (pp. 161–180): Kluwer Academic Publishers.
- Kamenskaya, O.E., 1988. Quantitative distribution of komoki and xenophyophores in the southern Atlantic. *Structural and Functional Researches of the Marine Benthos* (pp. 15–20). P.P. Shirshov Institute of Oceanology: Academy of Sciences of the USSR.
- Kamenskaya, O.E., Melnik, V.F., Gooday, A.J., 2013. Giant protists (xenophyophores and komokiaceans) from the Clarion-Clipperton ferromanganese nodule field (Eastern Pacific). *Biology Bulletin Reviews*, 3, 388–398.
- Kelly-Gerrey B.A., Martin A.P., Bett B.J., Anderson T.R., Kaariainen J.I., Main C.E., Marcinko C.J., A., Y., 2014. Benthic biomass size spectra in shelf and deep-sea sediments. *Biogeosciences*, 11, 6401–6416.
- Khusid, T.A., 1974. Distribution of benthic foraminifers off the west coast of South America. *Oceanology*, 14, 900–904.
- Kidd, R.B., Huggett, Q.J., 1981. Rock debris on abyssal plains in the northeast Atlantic: a comparison of epibenthic sledge hauls and photographic surveys. *Oceanologica Acta*, 4, 99–104.

- Korsun, S., Hald, M., Panteleeva, N., Tarasov, G., 1998. Biomass of foraminifera in the St. Anna Trough, Russian Arctic continental margin. *Sarsia*, 83, 419–431.
- Kuklinski, P., 2009. Ecology of stone-encrusting organisms in the Greenland Sea—A review. *Polar Research*, 28, 222–237.
- Kuklinski, P., 2013. Biodiversity and abundance patterns of rock encrusting fauna in a temperate fjord. *Marine Environmental Research*, 87–88, 61–72.
- Kurbjeweit, F., Schmiedl, G., Schiebel, R., Hemleben, C., Pfannkuche, O., Wallmann, K., Schafer, P., 2000. Distribution, biomass and diversity of benthic foraminifera in relation to sediment geochemistry in the Arabian Sea. *Deep-Sea Research Part II—Topical Studies in Oceanography*, 47, 2913–2955.
- Laguionie-Marchais, C., 2015. Polychaete community structure and biodiversity change in space and time at the abyssal seafloor. Doctoral thesis. *University of Southampton, Ocean & Earth Science* (p. 301).
- Lecroq, B., Gooday, A.J., Pawlowski, J., 2009a. Global genetic homogeneity in the deep-sea foraminiferan *Epistominella exigua* (Rotaliida: Pseudoparrellidae). *Zootaxa*, 23–32.
- Lecroq, B., Gooday, A.J., Tsuchiya, M., Pawlowski, J., 2009b. A new genus of xenophyophores (Foraminifera) from Japan Trench: morphological description, molecular phylogeny and elemental analysis. *Zoological Journal of the Linnean Society*, 156, 455–464.
- Lecroq, B., Lejzerowicz, F., Bachar, D., Christen, R., Esling, P., Baerlocher, L., Osteras, M., Farinelli, L., Pawlowski, J., 2011. Ultra-deep sequencing of foraminiferal microbarcodes unveils hidden richness of early monothalamous lineages in deep-sea sediments. *Proc Natl Acad Sci U S A*, 108, 13177–13182.
- Lejzerowicz, F., Pawlowski, J., Fraissinet-Tachet, L., Marmeisse, R., 2010. Molecular evidence for widespread occurrence of Foraminifera in soils. *Environmental Microbiology*, 12, 2518–2525.
- Lejzerowicz, F., Esling, P., Pawlowski, J., 2014. Patchiness of deep-sea benthic Foraminifera across the Southern Ocean: Insights from high-throughput DNA sequencing. *Deep-Sea Research Part II—Topical Studies in Oceanography*, 108, 17–26.
- Lejzerowicz, F., Esling, P., Pillet, L., Wilding, T.A., Black, K.D., Pawlowski, J., 2015a. High-throughput sequencing and morphology perform equally well for benthic monitoring of marine ecosystems. *Scientific Reports*, 5.
- Lejzerowicz, F., Voltski, I., Pawlowski, J., 2015b. Foraminifera of the Kuril-Kamchatka Trench area: The prospects of molecular study. *Deep-Sea Research Part II—Topical Studies in Oceanography*, 111, 19–25.
- Levin, L.A., Etter, R.J., Rex, M.A., Gooday, A.J., Smith, C.R., Pineda, J., Stuart, C.T., R., H.R., Pawson, D., 2001. Environmental influences on regional deep-sea species diversity. *Annual Review of Ecology and Systematics*, 32, 51–93.
- Linke, P., Lutze, G.F., 1993. Microhabitat preferences of benthic foraminifera - a static concept or a dynamic adaptation to optimize food acquisition. *Marine Micropaleontology*, 20, 215–234.
- Lipps, J.H., 1973. Test Structure in Foraminifera. *Annual Review of Microbiology*, 27, 471–488.

- Loubere, P., Gary, A., 1990. Taphonomic process and species microhabitats in the living to fossil assemblage transition of deeper water benthic foraminifera. *Palaios*, 375–381.
- Loubere, P., Gary, A., Lagoe, M., 1993. Generation of the benthic foraminiferal assemblage: Theory and preliminary data. *Marine Micropaleontology*, 20, 165–181.
- Lutze, G.F., Altenbach, A.V., 1988. *Rupertina stabilis* (Wallich), a highly adapted, Suspension feeding foraminifer. *Meyniana*, 40, 55–69.
- Mackensen, A., Douglas, R.G., 1989. Down-core distribution of live and dead deep-water benthic foraminifera in box cores from the Weddell Sea and the California continental borderland. *Deep-Sea Research Part A—Oceanographic Research Papers*, 36, 879–900.
- Mancin, N., Basso, E., Pirini, C., Kaminski, M.A., 2012. Selective mineral composition, functional test morphology and paleoecology of the agglutinated foraminiferal genus *Colominella* Popescu, 1998 in the Mediterranean Pliocene (Liguria, Italy). *Geologica Carpathica*, 63, 491–502.
- McClain, C.R., Schlacher, T.A., 2015. On some hypotheses of diversity of animal life at great depths on the sea floor. *Marine Ecology*, 36, 849–872.
- Mojtahid, M., Griveaud, C., Fontanier, C., Anschutz, P., Jorissen, F.J., 2010. Live benthic foraminiferal faunas along a bathymetrical transect (140–4800m) in the Bay of Biscay (NE Atlantic). *Revue de micropaléontologie*, 53, 139–162.
- Moodley, L., Boschker, H.T.S., Middelburg, J.J., Pel, R., Herman, P.M.J., de Deckere, E., Heip, C.H.R., 2000. Ecological significance of benthic foraminifera: 13C labelling experiments. *Marine Ecology Progress Series*, 202, 289–295.
- Mora, C., Tittensor, D.P., Adl, S., Simpson, A.G.B., Worm, B., 2011. How many species are there on Earth and in the ocean? *PLoS biology*, 9.
- Mortensen, P.B., Buhl-Mortensen, L., Gebruk, A.V., Krylova, E.M., 2008. Occurrence of deep-water corals on the Mid-Atlantic Ridge based on MAR-ECO data. *Deep-Sea Research Part II—Topical Studies in Oceanography*, 55, 142–152.
- Movellan, A., Schiebel, R., Zubkov, M.V., Smyth, A., Howa, H., 2012. Protein biomass quantification of unbroken individual foraminifers using nano-spectrophotometry. *Biogeosciences*, 9, 3613–3623.
- Mullineaux, L.S., 1987. Organisms encrusting manganese nodules and crusts: distribution and abundance at three North Pacific sites. *Deep-Sea Research Part I—Oceanographic Research Papers*, 34.
- Mullineaux, L.S., 1988. The role of settlement in structuring a hard-substratum community in the deep sea. *Journal of Experimental Marine Biology and Ecology*, 120, 247–261.
- Murray, J.W., 1968. Living foraminifers of lagoons and estuaries. *Micropaleontology*, 14, 435–455.
- Murray, J.W., 1969. Recent foraminifers from the Atlantic continental shelf of the United States. *Micropaleontology*, 15, 401–419.
- Murray, J.W., 1970a. The Foraminiferida of the Persian Gulf: 6. Living forms in the Abu Dhabi Region. *Journal of Natural History*, 4, 55–67.

- Murray, J.W., 1970b. The foraminifera of the hypersaline Abu Dhabi lagoon, Persian Gulf. *Lethaia*, 3, 51–68.
- Murray, J.W., Alve, E., 2000. Major aspects of foraminiferal variability (standing crop and biomass) on a monthly scale in an intertidal zone. *Journal of Foraminiferal Research*, 30, 177–191.
- Murray, J.W., 2007. Biodiversity of living benthic foraminifera: How many species are there? *Marine Micropaleontology*, 64, 163–176.
- Murray, J.W., 2015. Some trends in sampling modern living (stained) benthic foraminifera in fjord, shelf and deep sea: Atlantic Ocean and adjacent seas. *Journal of Micropalaeontology*, 34, 101–104.
- Nomaki, H., Heinz, P., Hemleben, C., Kitazato, H., 2005. Behavior and response of deep-sea benthic foraminifera to freshly supplied organic matter: a laboratory feeding experiment in microcosm environments. *Journal of Foraminiferal Research*, 35, 103–113.
- Nomaki, H., Ogawa, N.O., Ohkouchi, N., Toyofuku, T., Kitazato, H., 2010. The role of meiofauna in deep-sea benthic food webs revealed by carbon and nitrogen stable isotope analyses. In: Ohkouchi, N., Tayasu, I., Koba, K. (Eds.), *Earth, Life, and Isotopes* (pp. 119–138): Kyoto University Press.
- Nomaki, H., Toyofuku, T., Tsuchiya, M., Matsuzaki, T., Uematsu, K., Tame, A., 2015. Three-dimensional observation of foraminiferal cytoplasmic morphology and internal structures using uranium-osmium staining and micro-X-ray computed tomography. *Marine Micropaleontology*, 121, 32–40.
- Nozawa, F., Kitazato, H., Tsuchiya, M., Gooday, A.J., 2006. 'Live' benthic foraminifera at an abyssal site in the equatorial Pacific nodule province: Abundance, diversity and taxonomic composition. *Deep-Sea Research Part I—Oceanographic Research Papers*, 53, 1406–1422.
- Ohkawara, N., Kitazato, H., Uematsu, K., Gooday, A.J., 2009. A minute new species of *Saccamina* (monothalamous Foraminifera; Protista) from the abyssal Pacific. *Journal of Micropalaeontology*, 28, 143–151.
- Olsson, I., 1975. On methods concerning marine benthic meiofauna. *Zoon*, 3, 49–60.
- Oschmann, W., 1990. Dropstones – rocky mini-islands in high-latitude pelagic soft substrate environments. *Seckenbergiana Maritima*, 21, 55–75.
- Pawlowski, J., 2000. Introduction to the molecular systematics of foraminifera. *Micropaleontology*, 46, 1–12.
- Pawlowski, J., Fahrni, J., Lecroq, B., Longet, D., Cornelius, N., Excoffier, L., Cedhagen, T., Gooday, A.J., 2007. Bipolar gene flow in deep-sea benthic foraminifera. *Molecular Ecology*, 16, 4089–4096.
- Pawlowski, J., Holzmann, M., 2008. Diversity and geographic distribution of benthic foraminifera: a molecular perspective. *Biodiversity and Conservation*, 17, 317–328.
- Pawlowski, J., Christen, R., Lecroq, B., Bachar, D., Shahbazkia, H.R., Amaral-Zettler, L., Guillou, L., 2011. Eukaryotic richness in the abyss: insights from pyrotag sequencing. *Plos One*, 6.
- Pawlowski, J., Holzmann, M., Tyszka, J., 2013. New supraordinal classification of Foraminifera: molecules meet morphology. *Marine Micropaleontology*, 100, 1–10.

- Pawlowski, J., Esling, P., Lejzerowicz, F., Cedhagen, T., Wilding, T.A., 2014a. Environmental monitoring through protist next-generation sequencing metabarcoding: assessing the impact of fish farming on benthic foraminifera communities. *Molecular Ecology Resources*, 14, 1129–1140.
- Pawlowski, J., Holzmann, M., 2014. A plea for DNA barcoding of foraminifera. *Journal of Foraminiferal Research*, 44, 62–67.
- Pawlowski, J., Lejzerowicz, F., Esling, P., 2014b. Next-Generation environmental diversity surveys of Foraminifera: preparing the future. *Biological Bulletin*, 227, 93–106.
- Pawlowski, J., Esling, P., Lejzerowicz, F., Cordier, T., Visco, J.A., Martins, C.I.M., Kvalvik, A., Staven, K., Cedhagen, T., 2016. Benthic monitoring of salmon farms in Norway using foraminiferal metabarcoding. *Aquaculture Environment Interactions*, 8, 371–386.
- Pillet, L., Voltzki, I., Korsun, S., Pawlowski, J., 2013. Molecular phylogeny of Elphidiidae (foraminifera). *Marine Micropaleontology*, 103, 1–14.
- Pochon, X., Wood, S.A., Keeley, N.B., Lejzerowicz, F., Esling, P., Drew, J., Pawlowski, J., 2015. Accurate assessment of the impact of salmon farming on benthic sediment enrichment using foraminiferal metabarcoding. *Marine pollution bulletin*, 100, 370–382.
- Ruhl, H.A., 2012. RRS James Cook Cruise 62, 24 Jul-29 Aug 2011. Porcupine Abyssal Plain - sustained observatory research. *National Oceanography Centre Cruise Report* (p. 119). Southampton, UK: National Oceanography Centre.
- Saad, S.A., Wade, C.M., 2016. Biogeographic distribution and habitat association of *Ammonia* genetic variants around the coastline of Great Britain. *Marine Micropaleontology*, 124, 54–62.
- Saidova, K.M., 1967. The biomass and quantitative distribution of live Foraminifera in the Kurile-Kamchatka trench area. *Doklady Akademii Nauk SSSR*, 174, 216–217.
- Sanders, H.L., 1968. Marine benthic diversity: a comparative study. *American Naturalist*, 102, 243–282.
- Schönfeld, J., 2002a. Recent benthic foraminiferal assemblages in deep high-energy environments from the Gulf of Cadiz (Spain). *Marine Micropaleontology*, 44, 141–162.
- Schönfeld, J., 2002b. A new benthic foraminiferal proxy for near-bottom current velocities in the Gulf of Cadiz, northeastern Atlantic Ocean. *Deep-Sea Research Part I—Oceanographic Research Papers*, 49, 1853–1875.
- Schönfeld, J., Alve, E., Geslin, E., Jorissen, F., Korsun, S., Spezzaferri, S., 2012. The FOBIMO (FOraminiferal Blo-MONitoring) initiative-towards a standardised protocol for soft-bottom benthic foraminiferal monitoring studies. *Marine Micropaleontology*, 94–95, 1–13.
- Sen Gupta, B.K., Shin, I.C., Wendler, S.T., 1987. Relevance of specimen size in distribution studies of deep-sea benthic foraminifera. *Palaios*, 2, 332–338.
- Shirayama, Y., 1983. Size structure of deep-sea meiobenthos and macrobenthos in the Western Pacific. *Internationale Revue Der Gesamten Hydrobiologie*, 68, 799–810.
- Shirayama, Y., 1984. The abundance of deep-sea meiobenthos in the Western Pacific in relation to environmental factors. *Oceanologica Acta*, 7, 113–121.

- Smart, C.W., King, S.C., Gooday, A.J., Murray, J.W., Thomas, E., 1994. A benthic foraminiferal proxy of pulsed organic matter paleofluxes. *Marine Micropaleontology*, 23, 89–99.
- Smith, K.L., White, G.A., Laver, M.B., Haugness, J.A., 1978. Nutrient exchange and oxygen consumption by deep-sea benthic communities: Preliminary in situ measurements. *Limnology and Oceanography*, 23, 997–1005.
- Snelgrove, P.V.R., Butman, C.A., 1994. Animal sediment relationships revisited: cause versus effect. *Oceanography and Marine Biology: An Annual Review*, 32, 111–177.
- Snider, L.J., Burnett, B.R., Hessler, R.R., 1984. The composition and distribution of meiofauna and nanobiota in a central North Pacific deep-sea area. *Deep-Sea Research Part I—Oceanographic Research Papers*, 31, 1225–1249.
- Speijer, R.P., Van Loo, D., Masschaele, B., Vlassenbroeck, J., Cnudde, V., Jacobs, P., 2008. Quantifying foraminiferal growth with high-resolution X-ray computed tomography: New opportunities in foraminiferal ontogeny, phylogeny, and paleoceanographic applications. *Geosphere*, 4, 760–763.
- Taberlet, P., Coissac, E., Hajibabaei, M., Rieseberg, L.H., 2012a. Environmental DNA. *Molecular Ecology*, 21, 1789–1793.
- Taberlet, P., Coissac, E., Pompanon, F., Brochmann, C., Willerslev, E., 2012b. Towards next-generation biodiversity assessment using DNA metabarcoding. *Molecular Ecology*, 21, 2045–2050.
- Thomsen, L., Altenbach, A.V., 1993. Vertical and areal distribution of foraminiferal abundance and biomass in microhabitats around inhabited tubes of marine echinurids. *Marine Micropaleontology*, 20, 303–309.
- Tsuchiya, M., Grimm, G.W., Heinz, P., Stogerer, K., Ertan, K.T., Collen, J., Bruchert, V., Hemleben, C., Hemleben, V., Kitazato, H., 2009. Ribosomal DNA shows extremely low genetic divergence in a world-wide distributed, but disjunct and highly adapted marine protozoan (*Virgulinema fragilis*, Foraminiferida). *Marine Micropaleontology*, 70, 8–19.
- Turnewitsch, R., Lahajnar, N., Haeckel, M., Christiansen, B., 2015. An abyssal hill fractionates organic and inorganic matter in deep-sea surface sediments. *Geophysical Research Letters*, 42, 7663–7672.
- Vivien, R., Ferrari, B.J., Pawlowski, J., 2016. DNA barcoding of formalin-fixed aquatic oligochaetes for biomonitoring. *BMC Research Notes*, 9, 1.
- Voltski, I., Korsun, S., Pawlowski, J., 2014. *Toxisarcon taimyr* sp. nov., a new large monothalamous foraminifer from the Kara Sea inner shelf. *Marine Biodiversity*, 44, 213–221.
- Voltski, I., Pawlowski, J., 2015. *Flexammina islandica* gen. nov. sp. nov. and some new phylotypes of monothalamous foraminifera from the coast of Iceland. *Zootaxa*, 3964, 245–259.
- Wefer, G., Lutze, G.F., 1976. Benthic foraminifera biomass production in the western Baltic. *Kieler Meeresforschungen Sonderheft*, 3, 76–81.
- Weston, J.F., 1985. Comparison between recent benthic foraminiferal faunas of the Porcupine Seabight and Western Approaches continental slope. *Journal of Micropalaeontology*, 4, 165–183.

- Widbom, B., 1984. Determination of average individual dry weights and ash-free dry weights in different sieve fractions of marine meiofauna. *Marine Biology*, 84, 101–108.
- Worm, B., Barbier, E.B., Beaumont, N., Duffy, J.E., Folke, C., Halpern, B.S., Jackson, J.B.C., Lotze, H.K., Micheli, F., Palumbi, S.R., Sala, E., Selkoe, K.A., Stachowicz, J.J., Watson, R., 2006. Impacts of biodiversity loss on ocean ecosystem services. *Science*, 314, 787–790.

Appendix A Taxonomic Appendix

The following notes include all named species and all open nomenclature species. For named species, we give the author, the original generic designation, and references to representative illustrations. Open nomenclature species are briefly characterized and compared, where possible, to a published illustration. NHM registration numbers (prefix ZF) refer to specimens housed in the Natural History Museum, London that we have personally examined.

MONOTHALAMIDS

Lagenammia

Lagenammia aff. *arenulata* (Skinner 1961) (Fig. A.1a–d) illustrated as *Lagenammia* sp. 1 by Stefanoudis et al. (2016, Pl. 3, Fig. 5–12). We included here two similar morphotypes with tests composed of mineral grains. One morphotype (Chapter 3, Pl. 3.3, Figs. 5–8; Stefanoudis et al., 2016, Pl. 3, Figs. 5–8) has an oval-shaped chamber with a relatively narrow apertural neck and closely resembles *Reophax* cf. *diffflugiformis* Brady 1879 of Timm (1992, Pl. 1, Fig. 13a–b), *Lagenammia diffflugiformis* of Schiebel (1992, Pl. 8, Fig. 9), *L. diffflugiformis* subsp. *arenulata* (Skinner 1961) of Wollenburg (1992, Pl. 2, Fig. 3), as well as the ‘morphotype resembling *L. diffflugiformis*’ of Gooday et al. (2010, Fig. 13c) from the PAP-SO central site. The second morphotype has a generally more elongate test with a relatively wider apertural neck (Chapter 3, Pl. 3.3, Figs. 9–12; Stefanoudis et al., 2016, Pl. 3, Figs. 9–12) and resembles another of the *Lagenammia* species illustrated by Gooday et al. (2010, Fig. 13f). The two forms could not be separated consistently, particularly in the case of specimens from the abyssal hills where the shape of the test was partly or completely obscured by coarse mineral grains. Consequently, we consider them to represent the same species. Length up to 650 µm.

Remarks: We compared our specimens with *R. diffflugiformis* of Brady (1884, Pl. 30, Figs. 1–3, 5; NHM reg. nos ZF2267 and ZF2269). Our specimens are more coarsely-grained, less elongate and lack the characteristic yellow-orange test of those on slide ZF2267. They are more similar to those on slide ZF2269,

considered to belong to *L. arenulata* by Jones (1994), although Brady's specimens have less pronounced necks and were collected from much shallower depths (approx. 1000 m).

Lagenammina difflugiformis (Brady 1879) (Fig. A.1g–h), illustrated by Brady (1884, Pl. 30, Figs. 1–3) as *Reophax difflugiformis* Brady 1879. The test is elongate, flask-shaped with a long neck and a neatly constructed wall with a characteristic yellow-orange colour. Our specimens are identical to those of Brady on slide ZF2267.

Lagenammina tubulata Rhumbler 1931 (Fig. A.1i–j) = *Saccammina tubulata* Rhumbler 1931 in Wiesner (1931, Pl. 23, Fig. A). Occasional specimens in which mineral grains or planktonic foraminiferal shells obscure the spherical chamber can be identified as this species by the presence of a long, straight apertural neck.

Lagenammina sp. 2 (Fig. A.1e–f). Narrow elongate test with short but distinct apertural neck. Wall is composed predominantly of fine mineral grains, but specimens from the hills also incorporate coarser particles. Length up to 680 μm . *Remarks:* This species differs from *Lagenammina* aff. *arenulata* in being much more elongate with a shorter neck.

Lagenammina sp. 3 (Fig. A.1k). Flask-shaped test composed of planktonic foraminiferal shell fragments. Agglutinated particles weakly cemented, making the test rather fragile.

Remarks: Our specimens look identical to *Proteonina* (= *Lagenammina*) *difflugiformis* (Brady 1879), as illustrated by Rhumbler (1904, Fig. 80c) and Cushman (1918, Pl. 21, Fig. 1). They differ from *L. difflugiformis* of Brady in being composed of planktonic foraminiferal shell fragments rather than mineral grains. This species is most likely conspecific with *Lagenammina* sp. 1 of Gooday (1996) and *Lagenammina* sp. 89 of Gooday et al. (2010). Other similar specimens have been illustrated by Gooday (1986, Fig.10B) , Gooday et al. (1995, Pl. 1, Figs. E–F) and Gooday and Hughes (2002, Pl. 3, Fig. a). It also resembles *Ammolagena* sp. 1 of Duchemin et al. (2007, Pl. 2, Fig. 17), although our species certainly does not belong to this genus. Length up to 350 μm .

Lagenammina sp. 12 (Fig. A.2a–b). Test composed of mineral grains and consisting of an oval chamber with a long apertural neck that is almost as long as the chamber. It is similar to our morphotype of *Lagenammina difflugiformis* with the narrow neck, but the neck is much longer. Length up to 370 μm .

Remarks: This species is most similar to *Reophax* cf. *longicolis* (Wiesner 1931) in Timm (1992, Pl. 1, Figs. 10a–c); however, our specimens are uniserial, which would exclude them from the genus *Reophax*. It also bears a close resemblance to *Lagenammina arenulata* Skinner 1961 of Zheng and Fu (2001, Pl. VI, Figs. 6–7), although it differs from *L. arenulata* in having a much longer neck.

Lagenammina sp. 17 (Fig. A.2c). Oval chamber composed of large planktonic foraminiferal shells set in a matrix of fine mineral grains and extending into a relatively long apertural neck. Length ~730 μm .

Lagenammina sp. 18 (Fig. A.2d). Spherical to broadly oval chamber composed of small planktonic foraminiferal shells set in a matrix of fine mineral particles and with a short apertural neck. The incorporation of complete planktonic shells rather than fragments, as well as its globular to subglobular shape, helps to distinguish this species from *Lagenammina* sp. 3. Length up to 410 μm .

Lagenammina sp. 19 (Fig. A.2e–g). Oval chamber composed of larger and smaller planktonic foraminiferal shells and fine mineral grains and with a relatively long trumpet-shaped neck, 2–3 times the length of the chamber. The globigerinacean shells obscure the chamber to a lesser or greater extent, although the apertural neck is devoid of large shells and clearly defined. Length up to 930 μm .

Remarks: This species is probably conspecific with *Lagenammina* sp. 88 of Gooday et al. (2010, Fig. 13A–B). It differs from *Lagenammina* sp. 18 in being much larger with a longer and wider neck.

***Nodellum*-like**

Nodellum-like sp. (Fig. A.2h–i) = *Nodellum*-like form 2 of Gooday et al. (2004, Fig. 3F–H). This species was always found attached to planktonic foraminiferal shells.

Placopsilinella aurantiaca Earland 1934 (Fig. A.2j–k). Our specimens of this distinctive species resemble those illustrated by Earland (1934, Pl. III, Fig. 18), Thomas et al. (1990, Pl. 1, Fig. 1), Wollenburg (1992, Pl. 1, Fig. 3), Wollenburg and Mackensen (1998, Pl. 1, Figs. 1–2) and Hayward et al. (2010, Pl. 1, Fig. 1). A spiral initial part is clearly present in some specimens.

Resigella-like form 1 (Fig. A.2l) *sensu* Gooday et al. (2004, Fig. 4A–E); this species has been recorded from the North and West Equatorial Pacific and the NE Atlantic (PAP-SO area). Length ~100 µm.

Organic-walled

Allogromiid sp. 1 (Fig. A.3a). A morphologically simple organic-walled form, broadly oval in shape with a single, relatively simple aperture. Test interior is filled with brightly stained, rather featureless cytoplasm. Length ~300 µm.

Allogromiid sp. 3 (Fig. A.3b). Elongate, organic-walled test with a terminal aperture. The test interior is filled with brightly-stained protoplasm. This single specimen was found inside a much larger spherical structure made of planktonic foraminiferal shells. Length ~300 µm.

Nemogullmia sp. (Fig. A.3c). Elongate, fairly long, organic-walled tube with an agglutinated sheath. The sheath is made of fine sediment particles and has a smooth surface; occasionally some globigerinacean shells are also incorporated; in some specimens the sheath is not well developed. Protoplasm is well-stained and lacks stercomata. Length up to 2400 µm.

Organic-walled domes (Fig. A.3d). Small, organic-walled domes, each giving rise to a short tubular extension, attached to planktonic foraminiferal shells or mineral grains. They are overlain by a thin cocoon of fine sediment. Test interior stained red and containing numerous stercomata (waste pellets). One specimen is usually present on each shell or grain but multiple individuals also occur on a single particle. Length of individual ~100 µm.

Tinogullmia riemanni Gooday 1990 (Fig. A.3e). See also illustrations by Gooday (1990). This deep-water species was described from the central PAP-SO site in the NE Atlantic where it is often associated with phytodetrital deposits (Gooday, 1990).

‘Saccamminids’

Saccamina sp. 1 (Fig. A.3f). Test consisting of one to two chambers; with thin and short apertural neck. Wall is mostly finely agglutinated, of brown to orange colour. Length up to 790 µm.

Remarks: Our specimens look similar to the single- and two-chambered specimens of *Hormosina globulifera* Brady 1879 specimens as illustrated by Brady

(1884, Pl. 39, Figs. 1–2), but are smaller (660–800 μm). The single-chambered specimens also resemble *Saccamina sphaerica* Brady 1871, but again are too small to be assigned to this species.

Saccaminid sp. 1 (Fig. A.3g). Elongate species, with test tapering towards both ends where nipple-like apertural structures are located. Test wall has a whitish surface and is composed of finely agglutinated material. Test interior filled with cytoplasm and also contains stercomata. Length $\sim 560 \mu\text{m}$.

Saccaminid sp. 2 (Fig. A.3h). Test rather elongate and shaped like a rugby ball, widest in the middle and tapering towards the two bluntly pointed ends; with one aperture at each end. The wall is translucent with a slightly reflective surface, and consists of fine sediment particles. Cytoplasm fills the entire test interior and contains numerous stercomata. Similar rugby-ball-shaped saccaminids are often encountered in deep-sea samples (e.g. Gooday et al., 2004). Length $\sim 440 \mu\text{m}$.

Saccaminid sp. 3 (Fig. A.3i–j). More or less droplet-shaped test tapering towards the slightly produced, bluntly pointed apertural end, which terminates in a simple circular aperture of variable diameter. The wall is composed of tiny plate-like mineral grains that are responsible for its silvery, reflective surface. It is usually thicker at the proximal end of the test and the thickening occasionally creates a blunt point that can be mistaken for a second apertural structure (Fig. A.3j). The finely granular cytoplasm usually fills the entire test interior, devoid of stercomata. Length $\sim 500 \mu\text{m}$.

Saccaminid sp. 4 (Fig. A.4a). Test oval, with a single aperture located at one end. The test has a slightly shiny surface and appears silver under the stereomicroscope. Test wall consists of finely agglutinated material; test interior contains well-stained protoplasm and scattered stercomata. Length $\sim 640 \mu\text{m}$.

Saccaminid sp. 5 (Fig. A.4b). Broadly oval, almost circular test with nipple-like apertural structure. Wall made of finely agglutinated particles, with smooth, slightly reflective silvery surface. Test interior completely filled with heterogeneous cytoplasm that contains stercomata. Length $\sim 180 \mu\text{m}$.

Saccaminid sp. 6 (Fig. A.4c). This distinctive form has a test with a central broadly spindle-shaped capsule from either end of which arise two slightly curved, flimsy tubular extensions. Length $\sim 280 \mu\text{m}$.

Remarks: This is probably conspecific to Sacamminid sp. 6 of Gooday (2004, Fig. 6 I–J), especially the more globular form from the North Pacific.

Thurammina albicans Brady 1879 (Fig. A.4d) illustrated by Brady (1884, Pl. 37, Figs. 2–7).

Thurammina papillata Brady 1879 (Fig. A.4e) illustrated by (1884, Pl. 36, Figs. 7–18).

Spheres

Monothalamous sp. 3 (Fig. A.4f). Finely agglutinated sphere with smooth surface and no distinct aperture. Test of single specimen test filled with brightly-stained protoplasm. Length ~340 µm.

Psammosphaera fusca Schultz 1875 (Fig. A.4g). The PAP-SO specimens agglutinate large quartz grains with fine material filling the intervening spaces. They resemble specimens illustrated by Brady (1884, Pl. 18, Fig. 1) as well as some by Heron-Allen and Earland (1913, Pl. II, Fig. 3.10–12).

Psammosphaera sp. 1 (Fig. A.4h). Small, irregularly spherical or dome-shaped monothalamid, maximum dimension up to 200 µm, that uses mineral grains to construct its test, suggesting a placement in the genus *Psammosphaera*. The grains comprise a variety of whitish, yellow and orange particles, some of them plate-like. It is found free-living or attached to planktonic foraminiferal shells. This species is the same as the “monothalamids associated with mineral grains” of Stefanoudis and Gooday (2015, Fig. 6a–c). See also Chapter 2 (Fig. 2.6a–c).

Psammosphaera sp. 2 (Fig. A.4i). Agglutinated, subspherical test composed of large quartz grains, and a few dark grains, set in a fairly copious fine-grained matrix. Test interior filled with brightly stained protoplasm. Length ~900 µm.

White domes (Fig. A.4j) = *Crithionina*-like spheres *sensu* Stefanoudis and Gooday (2015). A distinctive form with a thick, white test made of finely agglutinated particles (mainly coccoliths). See also illustration in Stefanoudis and Gooday (2015, Fig. 3i–j) and in Chapter 2 (Fig. 2.3i–j). These specimens resemble the well-known agglutinated genus *Crithionina* Goës, 1894, although they are much smaller (~150 µm) than any described species of the genus.

Tubular

Bathysiphon sp. 1 (Fig. A.5a). Gently curved tube open at both ends, gradually increasing in width towards one end; test slender, yellow to brown. Wall fairly thick, made of fine mineral particles. Length up to 520 μm ; width $\sim 30 \mu\text{m}$.

Bathysiphon sp. 2. Test a narrow sinuous tube open at both ends, increasing in width towards one end; with silvery, reflective surface. Wall thin, made of fine mineral particles. Length up to 800 μm , width $\sim 25 \mu\text{m}$.

Hippocrepinella sp. (Fig. A.5b). Test elongate, irregularly cylindrical, almost straight, with two apertures, one at each end. Wall is thin, made of fine mineral particles and has a granular appearance; light brown to whitish in colour. Length of fragments $\sim 940 \mu\text{m}$, width $\sim 100 \mu\text{m}$.

Rhizammina algaeformis Brady 1879 *sensu* Cartwright et al. (1989) (Fig. A.5c). The name *Rhizammina algaeformis* is commonly applied to a variety of tubular foraminifera. The PAP-SO species is probably not the same as any of the specimens illustrated by Brady (1884). Fragments up to 2250 μm in length and $\sim 100 \mu\text{m}$ in width.

Rhizammina-like formation (Fig. A.5d). Complex structure comprising a central mass with several tubular extensions; a few finer tubules are also present. The wall is heavily dominated by large planktonic foraminiferal shells and has small tubular structures resembling Tubular sp. 19 (see below) attached to its surface. Length $\sim 2200 \mu\text{m}$.

Xenophyophore-like tube type 1 (Fig. A.5e). Elongate tube, occasionally with short side-branches. The wall is made of fine sediment particles and has a rather fuzzy surface; globigerinacean shells are occasionally incorporated into the test. The protoplasm contains a few, sparse stercomata. Length of fragments up to 2000 μm , width 200–250 μm .

Xenophyophore-like tube type 2 (Fig. A.5f). Tubular test fairly wide, rather fragile and white in colour; fragments form a circuit, suggesting that complete specimens have a net-like appearance. The wall is composed of globigerinacean shells and fragments, some large but mostly small, embedded within a matrix of fine sediment. Test interior filled with stercomata. Length of fragments $\sim 1600 \mu\text{m}$, width up to 350 μm .

Tubular sp. 1 (Fig. A.5g). Pale white, fragile, branching tube. Wall thin, made of finely agglutinated mineral particles, sometimes incorporating a few

globigerinacean shells. Test interior partly filled with protoplasm and some stercomata. Length of fragments up to 1000 μm , width 80–90 μm .

Remarks: This species somewhat resembles fragments of the xenophyophore *Septuma*, which is known to occur at the PAP-SO central site. However, as it lacks septae it is unlikely to belong to this genus.

Tubular sp. 2 (Fig. A.5h). Delicate, pale whitish, flexible tubes. The wall is thin, transparent, composed of fine mineral grains and occasionally incorporates globigerinacean shells. Early parts of the tube are narrow (~100 μm), finely agglutinated with no protoplasm; later parts are wider (~150 μm), less finely agglutinated and filled with stercomata.. Length of fragments up to 2000 μm , although most fragments are <1000 μm .

Tubular sp. 3 (Fig. A.5i). Elongate, narrow, delicately agglutinated tube fragments. Fine-grained wall consisting of mineral particles and occasionally including some globigerinacean shells. Protoplasm contains a few stercomata. Length of fragments up to 1700 μm , width ~70 μm .

Tubular sp. 4 (Fig. A.5j). Long, narrow, delicate tube. Wall consists of fine mineral particles and a few globigerinacean shells. Fairly similar to Tubular sp. 3, but the test is much more flexible. Length of fragments up to 1200 μm , width ~80 μm .

Tubular sp. 5 (Fig. A.6a). Soft, flimsy tube filled with stercomata. Wall translucent, composed of fine mineral particles, occasionally incorporating globigerinacean shells. Length of fragments up to 900 μm , width ~80 μm .

Tubular sp. 6 (Fig. A.6b2; c). Relatively wide, robust tube fragments, whitish in colour. The wall is composed predominantly of globigerinacean and some benthic foraminiferal shells set in a thin fine-grained matrix. Test interior with numerous stercomata. Length of fragments up to 4000 μm , width ~700 μm .

Tubular sp. 7 (Fig. A.6b1; d). Relatively wide, whitish to brown tube fragments made of small and larger planktonic foraminiferal shells set in a matrix of fine sediment particles. The fragments are up to 4000 μm long, 900–1000 μm wide and unbranched. Test interior with a solid mass of stercomata.

Remarks: This species resembles Tubular sp. 6 but is wider and less robust with a lower ratio of globigerinacean shells to fine sediment particles in the wall. The wall is similar to that of Xenophyophore-like tube type 2 but the tubes are much wider and never form a circuit.

Tubular sp. 8 (Fig. A.6e–f). Elongate, rigid, distinctly yellow tube made of fine-grained mineral particles and incorporating a variable number of globigerinacean shells that overlie the layer of mineral grains. Protoplasm well-stained without stercomata. Length of fragments up to 1400 μm , width 100–150 μm .

Tubular sp. 9 (Fig. A.6g). Elongate, rigid test, often branching dichotomously; the wall consists of coarse protruding quartz grains set in a matrix of fine, yellow mineral particles. Protoplasm well-stained, without stercomata. Length of fragments up to 2200 μm , width \sim 100 μm .

Remarks: Tubular sp. 8 and sp. 9 resemble each other as both have tests of similar size that are primarily made of fine yellow mineral particles. However, the former includes globigerinacean shells (sp. 8) while the latter agglutinates some large quartz grains. As both species have been recorded from the same locality it is unlikely that they represent the same species.

Tubular sp. 10 (Fig. A.6h). Large, wide tube made of coarse mineral particles that give it a rather irregular appearance. Length of fragments up to 2100 μm , width \sim 300 μm .

Tubular sp. 11 (Fig. A.6i). Narrow, elongate, branching tube. Wall loosely agglutinated, consisting of fine sediment material. Stercomata are numerous, forming a fairly compact mass that occupies most of the test interior. Length of fragments up to 550 μm , width \sim 100 μm .

Remarks: This species differs from Tubular sp. 1 in having a thinner, more transparent and less firmly agglutinated wall. It also has a compact mass of stercomata that fills the entire test interior rather than only part of it.

Tubular sp. 12 (Fig. A.6j). Pale white to light brown, slightly fuzzy, thick-walled tubes. Wall consists of fine sediment particles and sporadic juvenile globigerinacean shells. Protoplasm well-stained, containing a few stercomata. Length of fragments up to 800 μm , width \sim 150 μm .

Tubular sp. 13 (Fig. 6k). Narrow, elongate, unbranched tube. Wall consists of a mixture of fine and coarse mineral particles and has a granular and sparkling appearance; occasionally incorporates some large globigerinacean shells. Length of fragments up to 1000 μm , width \sim 50 μm .

Tubular sp. 14 (Fig. A.7a). Large, flimsy tubes. Wall primarily consists of fine, loosely agglutinated sediment particles, but also contains some planktonic

shells. Protoplasm very well-stained and contains stercomata. All fragments found were quite wide (approx. 400 μm in width) and up to 1800 μm long.

Tubular sp. 15 (Fig. A.7b). Wide tubes made of planktonic foraminiferal shells and fragments set in a matrix of fine sediment particles. Test interior entirely filled with well-stained protoplasm and some stercomata. Length of fragments up to 1000 μm , width \sim 300 μm .

Remarks: This species differs from Tubular sp. 12 in being wider and incorporating a number of larger planktonic foraminiferal shells in its wall, making the test rather more rigid.

Tubular sp. 16 (Fig. A.7c). Pale tubes. Wall consists of fine sediment material and occasionally incorporates some planktonic foraminiferal shells. Protoplasm contains a few stercomata. Length of fragments up to 900 μm , width \sim 150 μm .

Tubular sp. 19 (Fig. A.7d). Radiating tubular network attached to a substrate (e.g., globigerinacean shells and fragments). The protoplasm is well stained and apparently lacks stercomata. Length of fragments up to 400 μm , width \sim 20 μm .

Tubular sp. 20 (Fig. A.7e). Large, segmented tube gradually increasing in width. The wall is robust and fairly coarsely agglutinated, made of mineral particles with a few planktonic foraminiferan shells. Single available specimen was covered by a cyst-like structure made of fine sediment, globigerinacean shells and filaments. Length of fragment \sim 1600 μm , width 100–170 μm .

Tubular sp. 25 (Fig. A.7f). Coarsely-grained tube that agglutinates a few globigerinacean shells and/or large quartz grains. Test interior contains stercomata. Length of fragment \sim 700 μm , width \sim 100 μm .

Tubular sp. 27 (Fig. A.7g). Flimsy, transparent, organic-walled tube containing numerous stercomata. The wall is thin, very flexible and its surface slightly reflective. Numerous fragments of this species have been found in a single sample. Length of fragments \sim 600 μm , width \sim 100 μm .

Tubular sp. 28 (Fig. A.7h). The tubular test forms a circuit. The wall is fairly thick and composed mainly of fine sediment particles with scattered globigerinacean shells. Test interior with stercomata. Length of fragments \sim 1700 μm , width 200–300 μm .

Remarks: This species appears similar to Xenophyophore-like tube type 2, which also forms a circuit of tubes, but the wall is made mainly of fine sediment rather than planktonic foraminiferal shells. It is possibly a fragment of a xenophyophore (e.g. *Syringamina*).

Others

Monothalamous sp. 1 (Fig. A.8a). Flask-shaped chamber with apertural neck at distal end. Finely agglutinated wall made of mineral grains over an organic layer and occasionally incorporating a few planktonic foraminiferal shells. The test is sometimes covered by a thin sediment coating. Test interior contains stercomata as well as cytoplasm. The test morphology suggests a placement in *Lagenamina*. However, the strongly developed organic layer of the wall and the presence of stercomata are features that are not typical of this genus. Length ~330 μm .

Monothalamous sp. 2 (Fig. A.8b–c). Elongate, fusiform test, tapered at both ends with a single aperture located at the less strongly tapered end. Coarsely agglutinated wall made of mineral particles creating a granular appearance, although the surface is relatively smooth. The wall is thickened towards the two ends. Test interior almost completely filled with cytoplasm. Length ~660 μm .

Monothalamous sp. 4 (Fig. A.8d). Elongate, fusiform test that extends out into two narrow, flimsy tubular extensions. Wall finely agglutinated with slightly granular appearance. Protoplasm occupies only the central part of the test. Length up to 1000 μm .

Remarks: This distinctive form is distinguished from Saccamminid sp. 6 by the shape of the central chamber (elongate rather than subglobular) and the degree to which the protoplasm fills the chamber (partial rather than almost complete).

Monothalamous sp. 5 (Fig. A.8e). Globular to subglobular test, with two tubular extensions, not necessarily opposite each other. Wall made of fine sediment particles, loosely agglutinated to give a somewhat fuzzy appearance. Test interior filled with stercomata. Length up to 460 μm .

Monothalamous sp. 6 (Fig. A.8f). Agglutinated sphere that gives rise to up to three short tubular extensions. Relatively thick, finely agglutinated wall made of mineral grains with a thin coating of very fine particles ('sediment') but also

incorporating small globigerinacean shells and shell fragments. Test interior filled with cytoplasm. Length up to 200 μm .

Vanhoeffenella sp. (Fig. A.8g). Single test is ~220 μm long, very flat with an agglutinated rim and transparent upper and lower membranes through which the central cell body is visible. Test interior partly filled with cytoplasm. The morphological variability of *Vanhoeffenella* (e.g. Gooday et al., 2004) suggests that several distinct species of this well-known and widely distributed genus exist in the deep sea.

MULTICHAMBERED

Ammodiscacea

Ammodiscus anguillae Höglund 1947 (Fig. A.9a–c). See illustration in Enge et al. (2012, Pl. 1, Fig. 13). Jones (1994) considers *A. anguillae* to be the same as Brady's (1884, Pl. 38, Figs. 1–3) *Ammodiscus incertus* (d'Orbigny 1839).

Remarks: Our specimens are very similar in size and test characteristics (e.g. the width of the coiled tube) to some of Brady's specimens (slide ZF 1059). Those on slide ZF 1078 are also similar but much smaller than ours.

Ammodiscus sp. 1 (Fig. A.9d–f). Test circular, planispirally enrolled with a somewhat irregular coiling pattern in which some later whorls overlap onto earlier ones; width of coiling chambers increases steadily. Wall agglutinated, roughly finished. Length up to 470 μm .

Remarks: This species is most similar to *Ammodiscus tenuis* (Brady 1881) illustrated by Brady (1884, Pl. 38, Figs. 4–6). However, Brady's specimen (slide ZF 1064) is narrower, regularly coiled and with a shinier surface.

Glomospira gordialis (Jones and Parker 1860) (Fig. A.9g–i) = *Ammodiscus gordialis* Jones and Parker 1860. Our specimens look identical to those identified as *A. gordialis* on Brady's slide ZF 1057 as all have the same irregular coiling pattern, shiny surface and are similar in size; see illustrations in Brady (1884, Pl. 38, Figs. 7–9).

Repmamina charoides (Jones and Parker 1860) (Fig. A.9j–l) = *Ammodiscus charoides* Jones and Parker 1860 illustrated by Brady (1884, Pl. 3, Figs. 10–16). See also *Usbekistania charoides* (Jones and Parker 1860) of Murray and Alve (1994, Pl. 1, Fig. 20), Murray and Alve (2011, Fig. 18.17).

Hormosinacea

Hormosina aff. *monile* (Cushman 1912) (Fig. A.10a–b). See Cushman (1920, Pl. 6, Fig. 4). Length ~400 µm.

Hormosina pilulifera (Brady 1884) (Fig. A.10e–f) = *Reophax pilulifera* Brady 1884. See Brady (1884, Pl. 30, Figs. 18–20), Kaminski and Gradstein (2005, Pl. 53, fig. 53), and Holbourn et al. (2013, pg. 482).

Hormosina sp. 1 (Fig. A.10c–d). Test orange in colour, consisting of two to three spherical chambers arranged along a straight or slightly curved axis. Final chamber has a short apertural neck. Test wall comprises scattered coarse grains in a matrix of fine sediment particles. The species is commonly found attached or lodged between globigerinacean shells. Length up to 270 µm.

Hormosinella guttifera (Brady 1881) (Fig. A.10g–h) = *Reophax guttifera* Brady 1881. Our specimens have more globular chambers compared to those illustrated by Brady (1884, Pl. 31, Figs. 10–15); however, some specimens on the syntype slide (ZF2276) are identical to ours.

Hormosinella ovicula (Brady 1879) (Fig. A.10i–j) = *Reophax ovicula* Brady 1884. Single available test consists of three chambers, connected by short necks, placed along a more or less linear axis. Last chamber produced into a long, thin apertural neck. Wall finely agglutinated, consisting of mineral grains. Our single specimen is identical to the one illustrated by Brady (1884, Pl. 39, Fig. 8). Length ~870 µm.

Hormosinella sp. 1 (Fig. A.10k–l). Test with two elongate, symmetrical chambers, final chamber ending in a short apertural neck. Wall is pale yellow with a smooth surface and consists of finely agglutinated mineral grains. Length up to 870 µm.

Remarks: This species resembles *Hormosinella ovicula* in Brady (1884, Pl. 39, Figs. 8–10) although Brady's species has short necks connecting successive chambers, which are generally more globular in shape. In our species the two chambers merge together without an intervening neck.

Hormosina/Saccamina sp. (Fig. A.11a). Test comprises one to two chambers with a relatively long apertural neck (half the length of the chamber). Wall is an agglutinated matrix of fine sediment particles with a few scattered coarse grains; the apertural neck is always composed of fine material. Length up to 390 µm.

Nodulina dentaliniformis (Brady 1881) (Fig. A.11b–d) = *Reophax dentaliniformis* Brady 1881. Typical specimens from the PAP-SO area are illustrated in Stefanoudis et al. (2016, Pl. 2, Figs. 1–2) and Chapter 3 (Pl. 3.2, Figs. 1–2). Test long and slender, consisting of up to seven clearly defined chambers arranged along a straight or slightly curved axis. Chambers are clearly defined and become larger and more elongate distally, although never parallel-sided. Final chamber is elongate with a short apertural neck. Test wall consists of mineral grains. Specimens from abyssal hills slightly deviate from the typical morphology of this species, due to the coarser material that they agglutinate. Length up to 1400 µm.

Remarks. A search of the literature suggests that a range of different morphotypes has been placed in this species. Our specimens closely resemble those illustrated by Brady (1884, Pl. 30, Figs. 21–22).

Reophax agglutinatus Cushman 1913 (Fig. A.11e–f). Test large, compact, comprising at least three chambers of increasing size. Test wall dominated by globigerinacean shells that often obscure the morphology of the chambers. Length up to 1500 µm. Our specimens are fairly similar to those from the type area in the Philippines, illustrated by Cushman (1920, Pl. 2, Figs. 4–5).

Reophax bilocularis Flint 1899 (Fig. A.11 g–i). Test large, compact, comprising two chambers the second much bigger than the first. Test wall is composed mainly of globigerinacean shells that partly obscure test interior. Fine sediment material fills the intervening spaces. Length up to 1300 µm. This name has been applied in the literature to a variety of different bilocular morphotypes. Our specimens resemble some of the type specimens illustrated by Flint (1899, Pl. 17, Fig. 2) as well as those of Cushman (1921, Pl. 12, Fig. 7).

Reophax helenae Rhumbler 1931 (Fig. A.11j). Test comprising four to five chambers that increase rapidly in size. Terminal chamber is produced into a relatively long apertural neck. Test wall composed of planktonic foraminiferal shell fragments with a fine-grained matrix of mineral particles.

Remarks: According to the original description (Rhumbler 1911), based on material collected at >4,000 m depth off St Vincent in the Caribbean, *R. helenae* has a test composed of large planktonic foraminiferal shell fragments, very similar to the wall structure of the PAP-SO species. Several authors assigned specimens with tests composed entirely of mineral grains to this species (e.g. Kuhnt et al.,

2000; Pl. 3, Figs. 2–3; Schröder, 1986, Pl. 15, Fig. 8; Timm, 1992, Pl. 2, Fig. 5). These may represent a different species.

Reophax aff. *scorpiurus* de Montfort 1808 (Fig. A.11k–n). Test comprising four to five chambers that increase in size distally. Most chambers have ventricose asymmetry (shorter on one side than the other) and the final chamber has a short apertural neck. The earliest chambers are typically curved or angled upwards. Test wall consists predominantly of mineral grains. Length up to 370 μm .

Remarks: Since *Reophax scorpiurus* was first described from Adriatic beach sands (Brönnimann and Whittaker 1980), the name has been applied to a wide range of forms from shallow and deep water, which almost certainly represent different species. Our specimens most closely resemble some of those identified as *R. scorpiurus* by Schröder (1986, Pl. 14, Figs. 4–5). However, given the range of test morphologies illustrated by Schröder (1986) it is likely that she also included several genetically distinct entities within this species.

Reophax sp. 1 (Fig. A.12a). Large (up to 1700 μm), gently curved test comprising 4–5 chambers that increase in size distally; final chamber has a short apertural neck. Wall is made of coarse mineral grains that partly obscure test interior.

Remarks: Our specimens resemble some coarsely agglutinated *Reophax scorpiurus* specimens illustrated by Schröder (1986, Pl. 14, Fig. 1) and Timm (1992, Pl. 1, Fig. 15b), although the lack of the curved tail that is typical of this species and the small apertural neck, lead us to regard it as a distinct species.

Reophax sp. 4 (Fig. A.12b). Species with three to four chambers arranged on a slightly curved axis. Short apertural neck developed on the final chamber. Test wall mainly composed of large mineral grains but often incorporating some large globigerinacean shells. Length up to 1100 μm .

Reophax sp. 6 (Fig. A.12c). Single specimen comprising three chambers arranged along a straight axis. Chamber size increases gradually; final chamber ends in a short apertural neck. Wall composed of globigerinacean fragments in a fine-grained matrix. Length ~1400 μm .

Reophax sp. 7 (Fig. A.12d–f). Slender test composed of five or more symmetrical chambers that increase rapidly in size. The final chamber ends into a fairly wide apertural neck. Test wall generally smooth and composed of fine

sediment particles in the abyssal plain samples, but can be quite coarse in specimens from hill sites. Length up to 620 μm .

Remarks: This species is probably conspecific with *Reophax* sp. 7 from the PAP-SO central site (Gooday, pers. comm.) that was included, although not illustrated, in the study by Gooday et al. (2010).

Reophax sp. 8 (Fig. A.12g–h). Generally fusiform test composed of 2–3 chambers that increase rapidly in size. Final chamber produced into a short, wide apertural neck. Test wall is made of planktonic foraminiferal shells fragments in a matrix of coccoliths. Length up to 840 μm .

Remarks: Our specimens resemble *Reophax agglutinans sensu* Zheng and Fu (2001, Pl. XIV, Figs. 1–3) .

Reophax sp. 9 (Fig. A.12i–j) *sensu* Stefanoudis et al. (2016, Pl. 1, Figs. 11–12). See also illustrations in Chapter 3 (Pl. 3.1, Figs. 11–12). Test comprising 2–4 chambers, the second being substantially larger than the first and produced into a clearly developed apertural neck. Wall is composed predominantly of mineral grains, which can be quite coarse in the case of specimens from abyssal hills. Length up to 370 μm .

Remarks: This species is probably conspecific with *Reophax* sp. 112/113 of Gooday et al. (2010) from the PAP-SO central site, as well as *Reophax* sp. 14 of Cornelius and Gooday (2004, Fig. 5c) and *Reophax* sp. of Wollenburg and Mackensen (1998, Pl. 1, Fig. 9). It is somewhat similar to *Reophax subfusiformis* of Earland (1933, Pl. II, Figs. 16–19) and *Reophax fusiformis sensu* Jones (1994, Pl. 30, Figs. 7–10), but is much smaller and more delicately constructed.

Reophax sp. 11 (Fig. A.12k). Test fragile, comprising 3–4 chambers that increase in size distally, with the final chamber extending into a short apertural neck. Wall consists of loosely agglutinated globigerinacean fragments. Length up to 1300 μm .

Remarks: This species looks similar to some specimens of *Reophax subfusiformis* with a short apertural neck in Höglund (1947, Figs. 43–50) . However, since these have tests made of mineral particles and originate from much shallower depths, they are unlikely to represent the same species.

Reophax sp. 19 (Fig. A.13a–b). Compact test comprising 2–3 chambers of increasing size. Terminal chamber tapers into a short apertural tube with a pronounced rim ('flange'). Wall comprising globigerinacean shell fragments with a

fine-grained matrix of coccoliths. The apertural neck is made solely from mineral particles. Length ~ 400 µm.

Remarks: Conspecific with *Reophax* sp. 107 from the PAP-SO central site (Gooday, pers. comm.), a species that was included but not illustrated in the Gooday et al. (2010) study. It also resembles *Reophax rostrata* Höglund 1947 illustrated by Höglund (1947, Figs. 57–60) and Zheng and Fu (2001, Pl. XXII, Figs. 1–7) .

Reophax sp. 20 (Fig. A.13c–d). Large, slender test that consists of 4–5 chambers arranged along a linear axis. Wall is made predominantly of globigerinacean shells with intervening small mineral grains. Final chamber ends in a short apertural neck free of planktonic shells. A single specimen found in a sample from the large hill (JC062–126; H4) has much coarser agglutination and a wider apertural neck. Length up to 2100 µm.

Remarks: This species resembles *Reophax* sp. 104 from the PAP-SO central site (Gooday, pers. comm.), a species that was included but not illustrated in the study of Gooday et al. (2010). It is somewhat similar to *Reophax scorpiurus* of Brady (1884, Pl. 30, Fig. 17) and to the *Reophax scorpiurus* specimen 'of questionable character' in Cushman (1910, Fig. 116) .

Reophax sp. 21 (Fig. A.13e–i) *sensu* Stefanoudis et al. (2016, Pl. 2, Figs. 3–6). See also Chapter 3 (Pl. 3.2, Figs. 3–6). Test rather elongate, occasionally slightly curved, comprising 4–6 more or less globular chambers, sometimes connected by short necks. Chambers increase in size distally; final chamber with a relatively long apertural neck. Wall consists predominantly of mineral grains. Length up to 880 µm.

Remarks: This species closely resembles *Reophax* sp. 116 of Gooday et al. (2010, Fig. 14E) from the PAP-SO central site. It also looks similar to *Reophax scorpiurus* de Montfort 1808 in Schröder et al. (1988, Pl. 5, Figs. 1–2). In plain samples where tests are fairly fine grained it is clear that this species is distinct from *Reophax scorpiurus*. However, the two species are more difficult to distinguish in hill samples where large grains obscure the chambers.

Reophax sp. 23 (Fig. A.13j–l). Distinctive test comprising up to six globular, closely adjoined chambers arranged along a linear axis. Final chamber produced into a short apertural neck. The test wall is thick, made mainly of fine sediment particles giving it a smooth outer surface, although occasionally some coarser

particles are also included. When 'live' (Rose-Bengal-stained) protoplasm fills the entire test interior. Length up to 530 μm .

Remarks: This species is very similar to *Hormosina monile sensu* Zheng and Fu (2001, Pl. XXVI, Figs. 1–10), although clearly distinct from Brady's original *H. monile*, and to *Reophax paucus* Hada 1957 illustrated in Zheng and Fu (2001, Pl. XVIII, Figs. 11–16). It may be the same as *Reophax horridus* Cushman 1912 of Schröder et al. (1988, Pl. 5, Fig. 5) from the abyssal central North Pacific, although it is clearly different from Cushman's (1912) original species in lacking projecting sponge spicules. In the scanning electron microscope the test resembles that of specimens that we placed in *Hormosina pilulifera*, although the wall is more transparent when viewed with transmitted light and the chambers are less globular.

Reophax sp. 27 (Fig. A.13m–n). Test comprising 2 chambers connected by a short neck. Final chamber terminates in a slightly produced aperture or a short apertural neck. Wall composed of fine-grained mineral particles with scattered coarser grains, the latter often concentrated close to or on the apertural neck and the short neck connecting the chambers. Protoplasm almost completely fills the final chamber of 'live' specimens. Length up to 910 μm .

Remarks: This species is similar to *Reophax bilocularis* Flint 1899 illustrated in Schröder (1986, Pl. 14, Figs. 8–10) and Timm (1992, Pl. 2, Fig. 3b). However, the type specimens in Flint (1899, Pl. 17, Fig. 2) are primarily made of globigerinacean shells, while those in Timm and some in Schröder are made of mineral grains, hence, it is unlikely that these two forms are conspecific. The name *Reophax bilocularis* has been applied to a variety of bilocular morphotypes that probably encompass a number of species.

Reophax sp. 28 (Fig. A.14a–b) *sensu* Stefanoudis et al. (2016, Pl. 1, Figs. 7–10). See also Chapter (Pl. 3.2, Figs. 7–10). Test elongate, more or less straight, comprising 4–5 slim chambers, which gradually increase in size. The wall is largely made of mineral grains and often incorporates a small number of long sponge spicules. The final chamber is often particularly elongated, terminating in a slender apertural neck. Length up to 830 μm .

Remarks: This species was referred to as *Reophax* sp. 117 by Gooday et al. (2010, Fig. 14C) in their study of the PAP-SO central site.

Reophax sp. 34 (Fig. A.14c–d). Test comprising 5 chambers, arranged along a nearly linear axis. Initial chambers are small and spherical, later ones increase rapidly in size, resulting in a relatively short but strongly tapered test shape. Terminal chamber produces into a very short apertural neck. Wall is made of fine sediment with scattered coarser particles, including mica plates. Length ~490 μm .

Remarks: This distinctive species bears a slight resemblance to *Reophax gibberus* Zheng and Fu 2001 in Zheng and Fu (2001, Pl. XXIV, Figs. 1–10) .

Reophax sp. 38 (Fig. A.14e). Coarsely-agglutinated test consisting of 2–3 chambers; final chamber with short apertural neck. Wall is made of large mineral grains that obscure the chambers. Length ~360 μm .

Reophax sp. 40 (Fig. A.14f–g). Test bilocular with the 2 chambers at a slight angle to each other. The single specimen has a narrow and relatively long apertural neck at the end of the terminal chamber. Test wall composed of globigerinacean shells fragments. Length ~480 μm .

Reophax sp. 42 (Fig. A.14h–i). Single specimen with test consisting of 3 chambers that become larger and more elongate distally. Terminal chamber produced into a short apertural neck. Wall with smooth outer surface, composed of mainly small mineral grains with some larger particles. Length ~500 μm .

Remarks: This species resembles *Reophax* sp. 199 from the PAP-SO central site (Gooday, pers. comm.), included but not illustrated in the study of Gooday et al. (2010). It also resembles *Reophax praegracilis* Rhumbler 1936 illustrated by Zheng and Fu (2001, Pl. XXI, Figs. 1–2) but differs in having a narrower apertural opening and more globular chambers.

Reophax sp. 43 (Fig. A.14j). Test comprising two to three chambers; the final chamber has a fairly long, narrow apertural neck. Wall composed of globigerinacean shells. Length ~520 μm .

Reophax sp. 110/111 (Fig. A.14 k–l) *sensu* Gooday et al. (2010, Fig. 14B). Delicate, fragile species consisting of two, sometimes three chambers that increase rapidly in size. Test wall is made of globigerinacean shell fragments and mineral grains. Length ~300 μm .

Remarks: Resembles *Reophax* sp. 112/113 of Gooday et al. (2010, Fig. 14A) in overall test morphology, but the test incorporates planktonic foraminiferal fragments which *Reophax* sp. 112/113 never does.

Lageniida

Buchnerina iberica Jones 1984 (Fig. A.15a). See Jones (1984, Pl. 1, Figs. 4–6), and Loeblich and Tappan (1987, Pl. 462, Figs. 4–6) .

Fissurina aff. *alveolata* (Brady 1884) *sensu* Jones (1984) (Fig. A.15b). Test compressed, sub-circular with a strongly tapered apertural neck. Wall smooth and mostly opaque, apart from the apertural neck where a centrally placed entosolenian tube is visible. See illustrations in Jones (1984, Pl. 1, Figs. 14–15). Length ~450 µm.

Fissurina annectens (Burrows and Holland 1895) (Fig. A.15c). Jones (1994) regards the specimens illustrated by Brady (1884, Pl. 59, Figs. 7, 15) as *Lagena quadricostulata* Reuss 1870 to belong to *F. annectens*.

Fissurina fimbriata (Brady 1881) (Fig. A.15d) = *Lagena fimbriata* Brady 1881. Overall outline resembles a compressed rocket. Test relatively longer than broad, slightly compressed. Periphery with a thin keel that is narrow in the distal part of the test but widens around the base; spherical to elliptical aperture developed at the slightly produced distal end. Test wall smooth, pale white and slightly opaque. Length up to 340 µm.

Remarks: Our specimens are less elongate and a bit shorter compared to those on Brady's slides (ZF1654, ZF 1655, as *L. fimbriata*), although in other respects they are identical; see illustrations in Brady (1884, Pl. 60, Fig. 60). They also closely resemble *Fissurina fimbriata fimbriata* in Jones (1984, Pl. 3, Figs. 3–4), although again these illustrations show specimens that are more elongate and bullet-shaped than ours.

Fissurina cf. *quinqueannulata* Parr 1950 (Fig. A.15e) illustrated by Parr (1950, Pl. VIII, Figs. 13a–b). Length ~1100 µm.

Fissurina seminiformis (Schwager 1866) (Fig. A.15f) illustrated as *Lagena seminiformis* Schwager 1866 by Brady (1884, Pl. 59, Figs. 28–30) and Cushman (1913, Pl. 11, Fig. 2) , and as *Lagenosolenia seminiformis* (Schwager 1866) by Jones (1984, Pl. 4, Figs. 11–12).

Remarks: Since our specimens have an entosolenian tube it is unlikely that they belong to *Lagena*. Moreover, the slit-like to fissurine aperture and the absence of an apertural neck suggest that this species is a member of *Fissurina* rather than *Lagenosolenia* (see Patterson and Richardson, 1987).

Fissurina sp. 1 (Fig. A.15g–h). Test nearly circular test in lateral view and slightly inflated when viewed from above. The apertural end forms a small hood with a rounded opening. The margin of the test has a pronounced keel, especially on the lower half of the test. Wall is semi-transparent with a smooth surface. Length ~300 µm.

Lagena hispida Reuss 1858 (Fig. A.15i) in Brady (1884, Pl. 57, Figs. 1–2).

Lagena flatulenta Loeblich and Tappan 1953 (Fig. A.15j) in Jones (1984, Pl. 7, Fig. 1).

Lagena spinigera Earland 1934 (Fig. A.15k) = *Lagena semilineata* var. *spinigera* Earland 1934 in Brady (1884, Pl. 58, Figs. 4, 17). Very similar to *Lagena* sp. 5 in Jones (1984, Pl. 8, Fig. 5).

Lagena staphyllearia (Schwager 1866) (Fig. A.15l) illustrated by Brady (1884, Pl. 59, Figs. 8–11) and as *Fissurina staphyllearia* by Enge et al. (2012, Pl. 3, Fig. 7). Jones (1994) regards *F. staphyllearia* the same as *Fissurina kerguelenensis* Parr 1950 of Parr (1950, Pl. VIII, Figs. 7a–b).

Lagena aff. *striata* (d'Orbigny 1839) (Fig. A.16a). Our specimen has fewer striations than the one depicted in Brady (1884, Pl. 57, Figs. 22, 24), but in other respects they are identical. Length ~400 µm.

Lagenid sp. 1 (Fig. A.16b). Test pyriform, elongate to rugby-ball shaped with 3 or more chambers. It tapers towards both ends and is widest just behind the middle; the proximal end is somewhat pointed, the apertural end has a distinctly pointed apertural hood and the aperture itself is triangular with a pointed apex. Wall smooth and transparent. Length ~350 µm.

Lagenid sp. 2 (Fig. A.16c). Test pyriform, flask-shaped with 3 or more chambers, widest and most inflated in the distal 1/3. Nipple-like apertural structure associated with small hood developed at distal end. The wall is smooth and transparent. Length ~400 µm.

Oolina aff. *exsculpta* (Brady 1881) (Fig. A.16d–e). The single available specimen differs from the one illustrated in Brady (1884, Pl. 58, Fig. 1) as *Lagena exsculpta* in having striations covering most of the test, and being less tapered towards the apertural end. Length ~220 µm.

Oolina globosa (Montagu 1803) (Fig. A.16f–i). Test spherical to subspherical, shaped somewhat like a short light bulb. The apertural opening is circular and placed slightly to one side of the axis of the test. Wall is smooth, semi-

transparent, often with some visible scattered pores; entosolenian tube extends for about half the height of the test.

Remarks: Our spherical specimens are identical to *Oolina globosa globosa* Montagu 1803 illustrated by Jones (1984, Pl. 1, Figs. 10–11), except for the slightly asymmetrically-placed aperture. They are also very similar, although much smaller, than those on Brady's slide (ZF 1666), identified as *Lagena globosum* (Montagu 1803); see Brady (1884, Pl. 56, Fig. 3). Subspherical specimens are identical, although again smaller, than those on Brady's slides (ZF 1664, ZF 1665), despite the fact that some of them (ZF 1665) came from a very shallow setting (<100 m deep).

Oolina setosa (Earland 1934) (Fig. A.16j–l) = *Lagena globosa* var. *setosa* Earland 1934. Our specimens are similar to the illustrations in Jones (1984, Pl. 1, Figs. 14–15) who calls this species *Oolina globosa setosa* Earland 1934. Jones (1994) also identifies as *O. globosa setosa* specimens referred to *Lagena longispina* Brady 1881 by Brady (1884, Pl. 56, 33–36).

Oolina sp. 4 (Fig. A.17a–b). Test elongate, droplet-shaped, slightly compressed and tapered towards the apertural end where a slight hood is developed around the apertural opening. Transparent wall with smooth surface. Length up to 300 µm.

Remarks: Our species is rather similar to *Oolina* sp. 4 *sensu* Jones (1984, Pl. 2, Fig. 2) but is droplet-shaped rather than spindle-shaped. It also resembles *Oolina* sp. 5 *sensu* Jones (1984, Pl. 2, Fig. 3) although the latter is more elongate and flask-shaped.

Parafissurina crassa (Boltovksy and Watanabe 1977) (Fig. A.17c). See Jones (1984, Pl. 6, Fig. 6). This species is probably conspecific with *Parafissurina* sp. 334 from the PAP-SO central site (Gooday, pers. comm.), which was included, although not illustrated, in the study by Gooday et al. (2010).

Parafissurina lateralis (Cushman 1913) (Fig. A.17d). See illustrations of *Lagena apiculata* (Reuss, 1851) in Brady (1884, Pl. 56, Figs. 17–18), which Jones (1994) considers to be *P. lateralis*.

Parafissurina pseudolateralis Jones 1984 (Fig. A.17e) illustrated by Jones (1984, Pl. 6, Figs. 17–18).

Parafissurina sp. 3 (Fig. A.17f–g). Test nearly circular in lateral view with the bluntly pointed apertural end forming a small hood above a rounded aperture. Wall

is semi-transparent with a smooth surface. We include here three similar morphotypes. i) Test with almost no peripheral keel and a small protuberance opposite the aperture; this type looks similar to *Parafissurina curta* Parr 1950 illustrated in Parr (1950, Pl. X, Fig. 6a–b; 7). ii) Test with no peripheral keel and no protuberance; this type resembles *Parafissurina ovata* (Wiesner 1931) in Parr (1950, Pl. X, Fig. 4). iii) Test with a pronounced peripheral keel in the lower half of the test and no protuberance; this type is rather similar to *Parafissurina schlichti* (Silvestri 1902) in Parr (1950, Pl. X, Fig. 5). However, as many specimens have intermediate characteristics, we regard all of them to be part of the same species. Length up to 330 μm .

Parafissurina sp. 7 (Fig. A.17h). Test spherical, slightly inflated, with a well-developed hood developed behind the aperture, giving it a short bulb-like appearance. The wall is translucent with a smooth surface and some scattered pores. Length ~300 μm .

Remarks: This species is probably conspecific with *Parafissurina* aff. *ventricosa*, illustrated in Jones (1984, Pl. 6, Fig. 1), although that specimen appears to be somewhat more inflated with a shorter hood and a slit-like aperture. However, these differences might be due to the angle at which Jones' specimen was photographed.

Pyrulina gutta (d'Orbigny 1839) (Fig. A.17i). Jones (1994) considers specimens identified as *Polymorphina lactea* (Walker and Jacob 1798) by Brady (1884, Pl. 71, Fig. 14) to belong to *P. gutta*.

Pyrulina sp. (Fig. A.17j). Our single specimen is similar to *Pyrulina* (= *Polymorphina*) *angusta* (Egger 1857) specimens on Brady's slide (ZF 2127), although it is somewhat less elongate than those illustrated by Brady (1884, Pl. 72, Figs. 1–2). Length ~620 μm .

Solenina subformosa subs. *fluens* Jones 1984 (Fig. A.17k) illustrated by Jones (1984, Pl. 5, Fig. 14).

Solenina sp. (Fig. A.17l). This species is fairly similar to *Solenina subformosa* subs. *fluens* but differs in having a more inflated chamber with fewer striations, a narrower peripheral keel, and shorter apertural neck. It looks identical to *Solenina?* illustrated by Jones (1984, Pl. 5, Figs. 3–5). Length ~320 μm .

Vaginulinopsis tasmanica Parr 1950 (Fig. A.17m) in Parr (1950, Pl. XI, Figs. 13-14). Jones (1994) considers *V. tasmanica* to be the same as Brady's illustration (1884, Pl. 67, Fig. 7) of *Cristellaria schloenbachi* Reuss 1863.

Milioliida

Edentostomina pseudodepressa (Mangin 1960) (Fig. A.18a–b) *sensu* Zheng (1988, pg. 220, Pl. 2, Figs. 2–8).

Pyrgo fischeri (Schlumberger 1891) (Fig. A.18c–d) = *Biloculina fischeri* Schlumberger 1891 in Schlumberger (1891, Pl. 6, Figs. 77–78).

Pyrgo murrhina (Schwager 1866) (Fig. A.18e–f) in Holbourn et al. (2013, pg. 458) = *Biloculina murrhina* Schwager = *Biloculina depressa* var. *murrhina* Schwager in Brady (1884, Pl. 2, Figs. 10–11). Our specimens are typical of this common and widespread abyssal species.

Pyrgoella sp. (Fig. A.18g–h). Single specimen with a subglobular test, slightly inflated in the middle; last chamber somewhat produced with an arch-shaped aperture. Wall semi-transparent. Length ~150 µm.

Remarks: This specimen is somewhat similar to *Biloculina irregularis* d'Orbigny 1839 in Brady (1884, Pl. 1, Figs. 17–18); however, *B. irregularis* is much more spherical and inflated. Jones (1994) considers *B. irregularis* of Brady as *Pyrgoella irregularis* (d'Orbigny 1839).

Quinqueloculina venusta Karrer 1868 (Fig. A.18i–j). See also Lohmann (1978, Pl. 4, Figs. 17–18), Corliss (1979, Pl. 1, Figs. 9–11), Hayward et al. (2010, Pl. 8, Figs. 12–14), and Brady (1884, Pl. 5, Fig. 7) as *Miliolina venusta* (Karrer 1868).

Remarks: Brady's specimens on slide ZF 1918 look indistinguishable to ours.

Quinqueloculina sp. 2 (Fig. A.18k–l) = *Quinqueloculina* sp. *sensu* Gooday et al. (2010, Fig. 10A–D). The lateral outline is rounded; when viewed from the apertural end, the test is subtriangular with rounded corners. Length up to 600 µm.

Remarks: Our species is closest to *Quinqueloculina auberiana* d'Orbigny 1839 illustrated by Hayward et al. (2010, Pl. 8, Figs. 12–14) as well as by Brady (1884, Pl. 5, Figs. 8–9) as *Miliolina auberiana* (d'Orbigny 1839). However, Brady's specimens (slide ZF1847) are more angular and originate from a much shallower setting (approx. 700 m deep), as do Hayward et al.'s (13–110 m). It is therefore unlikely that they represent the same species.

Quinqueloculina sp. 3 (Fig. A.19a–b). Test broadly spindle-shaped in lateral view, slightly inflated; last chamber protruding into short apertural neck; when viewed from the apertural end, the test is triangular with rounded corners. Length ~460 μm .

Remarks: *Quinqueloculina* sp. 3 differs from *Quinqueloculina* sp. 2, in having a less rounded outline, more angular in side view and less inflated.

Spirophthalmidium acutimargo (Brady 1884) (Fig. A.19c–d) = *Spiroloculina acutimargo* Brady 1884 in Brady (1884, Pl. 10, Fig. 13).

Spirosigmoilina pussila (Earland 1934) (Fig. A.19e) illustrated by Hayward et al. (2010, Pl. 9, Figs. 19–20). Jones (1994) considered *S. pussila* to be the same as *Spiroloculina tenuis* (Czjzek 1848) in Brady (1884, Pl. 10, Figs. 9–10).

Spirosigmoilina tenuis (Czjzek 1848) (Fig. A.19f–g) illustrated by Hayward et al. (2010, Pl. 9., Figs. 21–22), as well as by Brady (1884, Pl. 10, Figs. 7–8) as *Quinqueloculina tenuis* Czjzek 1848.

Rotaliida

Alabaminella weddellensis (Earland 1936) (Fig. A.19h–i) = *Eponides weddellensis* Earland 1936 illustrated by Earland (1936, Pl. 1, Figs. 65–67), and Gooday (1988, Fig. 1d). This abyssal species is common at the PAP-SO central site (Gooday et al., 2010) but too small to be routinely retained on a 150- μm screen.

Anomalinoides colligera (Chapman and Parr 1937) (Fig. A.19j–l). See illustration of *Anomalina ammonoides* (Reuss 1844) in Brady (1884, Pl. 94, Figs. 2–3), which Jones (1994) considers to represent *A. colligera*.

Bolivina decussata (Brady 1881) (Fig. A.20a) illustrated by Brady (1884, Pl. 53, Figs. 12–13).

Bolivina aff. *earlandi* Parr 1950 (Fig. A.20b) in Parr (1950, Pl. XII, Fig. 16), and in Brady (1884, Pl. 52, Figs. 18–19) as *Bolivina punctuata* (d'Orbigny 1848).

Remarks: Our specimens are somewhat smaller (~200 μm) but in other respects very similar to Brady's specimens (slide ZF 1191). However, as his specimens were collected at a shallow site (<150 m depth), it is unlikely that they represent the same species.

Bolivina spathulata (Williamson 1858) (Fig. A.20c) illustrated by Haake (1977, Pl. 2, Figs. 12–13). Jones (1994) considers *Bolivina dilatata* Reuss 1850 in Brady (1884, Pl. 52, Figs. 20–21) to be conspecific with *B. spathulata*.

Bolivina sp. 1 (Fig. A.20d). Test narrow, elongate ovate, slightly compressed with 14–16 chambers arranged biserially; aperture forms a narrow loop at the base of final chamber. Wall thin and translucent. Length ~250 µm. *Remarks:* Superficially this species resembles *Bolivina* aff. *earlandi*; both have narrow, elongate tests with translucent, hyaline walls. However, *Bolivina* sp. 1 has fewer chambers that are more rounded and inflated as well as larger. In addition, the initial chambers in *B. earlandi* are minute and successive ones increase rapidly in size, whereas in *Bolivina* sp. 1 the change in chamber size is much more gradual.

Bulimina elongata d'Orbigny 1826 (Fig. A.20e). See illustrations in Brady (1884, Pl. 50, Figs. 3–4) as *Bulimina elegans* d'Orbigny 1826 regarded by Jones (1994) as representing the same species.

Cibicides lobatulus (Walker and Jacob 1798) (Fig. A.20 f–j) illustrated by Holbourn et al. (2013, pg. 152). See also Brady (1884, Pl. 92, Fig. 10; Pl. 93, Figs. 1, 4–5; Pl. 115, Figs. 4–5) as *Truncatulina lobatula* (Walker and Jacob 1798).

Cibicides wuellerstorfi (Schwager, 1866) (Fig. A.21a–c) in Jones (1994, Pl. 93, Figs. 8–9) = *Fontbotia wuellerstorfi* (Schwager 1866) in Loeblich and Tappan (1987, Pl. 319, Figs. 7–13) = *Planulina wuellerstorfi* (Schwager 1866) in Lohmann (1978, Pl. 2, Figs. 1–4), Corliss (1979, Pl. 2, Figs. 13–18) and Holbourn et al. (2013, pg. 416).

Cibicidoides kullenbergi (Parker 1953) (Fig. A.21d–f) illustrated by Lohmann (1978, Pl. 2, Figs. 5–7).

Cibicidoides subhaidingerii (Parr 1950) (Fig. A.21g–h). See Brady's illustration (1884, Pl. 95, Fig. 7) as *Truncatulina haidingerii* (d'Orbigny 1846) regarded by Jones (1994) as representing the same species.

Ehrenbergina trigona Goës 1896 (Fig. A.22a). See illustration in Brady (1884, Pl. 55, Figs. 2–3, 5) as *Ehrenbergina serrata* Reuss 1850 regarded by Jones (1994) as *E. trigona*.

Epistominella exigua (Brady 1884) (Fig. A.22b–c) in Corliss (1979, Pl. 2, Figs. 7–9) = *Pulvinulina exigua* Brady 1884 in Brady (1884, Pl. 103, Figs. 13–14).

The global distribution of this widely reported abyssal species has recently been established using molecular methods (Lecroq et al., 2009).

Francesita sp. (Fig. A.22d–e). Test elongate approximately cylindrical with rounded ends. The aperture is characteristic, an elongate slit starting from one side at the base of the final chamber and extending across the distal end of the test to about halfway down on the opposite side. Wall calcareous, finely perforate; surface smooth. Length up to 600 μm .

Fursenkoina bradyi (Cushman 1922) (Fig. A.22f). See illustration by Brady (1884, Pl. 52, Fig. 9) as *Virgulina subsquamosa* Egger 1857 regarded by Jones (1994) as *F. bradyi*.

Fursenkoina complanata (Egger 1893) (Fig. A.22g) as illustrated by Hayward et al. (2010, Pl. 20, Figs. 15–16). Jones (1994) regarded *Virgulina* (= *Fursenkoina*) *schreibersiana* Czjzek 1848 in Brady (1884, Pl. 52, Figs. 1–3) as *F. complanata*.

Globocassidulina subglobosa (Brady, 1881) (Fig. A.22h–i) in Corliss (1979, Pl. 3, Figs. 3–12) = *Cassidulina subglobosa* Brady 1881 in Brady (1884, Pl. 54, Fig. 17).

Gyroidina bradyi (Trauth 1918) (Fig. A.23a–f) in Jones (1994, Pl. 95, Fig. 5) = *Truncatulina dutemplei* (d'Orbigny) in Brady (1884, Pl. 95, Fig. 5).

Gyroidina aff. *broeckhiana* (Karrer 1878) (Fig. A.23g–k) = *Rotalia broeckhiana* Karrer 1878 in Brady (1884, Pl. 107, Fig. 4). Length up to 300 μm . *Remarks:* Our specimens are very similar to Brady's specimens (slide ZF 2318), despite the fact that they originate from a shallower location (approx. 1000 m deep) in the Pacific. However, ours have fewer and easily distinguishable chambers, a more rounded periphery in end-on view and form a higher (i.e. more conical) spire.

Gyroidina polia (Phleger and Parker 1951) (Fig. A.24a–f) in van Leeuwen (1989, Pl. 12, Figs. 4–6) = *Eponides polius* in Phleger and Parker (1951, Pl. 11, Figs. 1–2).

Gyroidina aff. *soldanii* d'Orbigny 1826 (Fig. A.24g–l) = *Rotalia soldanii* (d'Orbigny 1826) illustrated by Brady (1884, Pl. 107, Figs. 6–7). Length up to 400 μm .

Remarks: Brady's specimens (slides ZF 2330 and ZF 2331) look similar to ours especially those on ZF 2330. In particular, the sutures between chambers lie at an

angle. Nevertheless, Brady's specimens are comparatively larger, fatter in side view and more strongly built. Our are also rather similar to the illustration of *Gyroidina soldanii* var. *altiformis* (Stewart and Stewart 1930) in Cushman (1931, Part 8, Fig. 1) .

Gyroidina umbonata (Silvestri 1898) (Fig. A.25a–c) in Duchemin et al. (2007, Pl. 2, Figs. 2–4) = *Rotalia soldanii* var. *umbonata* Silvestri (1896, Pl. 6, Figs. 14a–c).

Gyroidina sp. 1 (Fig. A.25d–f). Trochospiral test moderately inflated with smoothly rounded periphery in end-on view with 7–9 chambers in the final whorl, steadily increasing in size and with radial sutures; early chambers are orange in colour, gradually becoming transparent. Aperture an interiomarginal slit. Length up to 300 μm .

Remarks: Our specimens most resemble *Gyroidina soldanii* in Hayward et al. (2010, Pl. 27, Figs. 7–12). However, compared with Brady's specimens of *Rotalia* (= *Gyroidina*) *soldanii* (slides ZF 2330 and ZF 2331), ours are much smaller and less strongly built; they were most similar to specimens on slide ZF 2331 in having straight sutures. This species also slightly resembles *G. umbonata*, although the latter has a smaller, more porous test that lacks the characteristic orange colour of *Gyroidina* sp. 1.

Gyroidina sp. 2 (Fig. A.25g–i). Test trochospiral with a smoothly rounded periphery in end-on view. Chambers increasing steadily in size with 7 chambers in the final whorl and sutures curved towards the periphery. Aperture a central interiomarginal arch at the base of the final chamber. Length ~250 μm .

Gyroidina sp. 3 (Fig. A.25j–l). Test trochospiral; slightly inflated; with ten chambers on the final whorl, gradually increasing in size and with straight sutures. Aperture an elongate slit extending across the base of the final chamber. Length ~320 μm .

Remarks: This species differs from *Gyroidina* sp. 1 in that its test periphery in end-on view is slightly lobate, and the test is less inflated.

Gyroidina sp. 4 (Fig. A.26a–c). Test trochospiral, periphery in end-on view smoothly rounded and inflated on spiral side. Final whorl with 7 chambers that increase steadily in size; sutures slightly curved on spiral side and radial on umbilical side. Aperture a small crescentic slit at the base of final chamber. Length ~300 μm .

Remarks: This species looks somewhat similar to *Gyroidina kawagatai* (Ujiié 1995) illustrated by Hayward et al. 2010 (Pl. 26, Figs. 16-18), although *G. kawagatai* has a more rounded periphery, a longer slit-like aperture, and is flat on the spiral side.

Ioanella tumidula (Brady 1884) (Fig. A.26d) = *Truncatulina tumidula* in Brady (1884, Pl. 95, Fig. 8).

Melonis barleeanus (Williamson 1858) (Fig. A.26e-h). We included here specimens that closely resemble illustrations of *M. barleeanus* in Corliss (1979, Pl., Figs. 7-8), Loeblich and Tappan (1987, Pl. 347, Figs. 1-5) and van Leeuwen (1989, Pl. 13, Figs. 1-2).

Remarks: Several specimens differ from typical *M. barleeanus* in being less compressed with fewer chambers per whorl. In these respects they are rather similar to *Melonis formosus* (Sequenza 1880) and *Melonis sphaeroides* Voloshinova 1958, as described and illustrated by van Leeuwen (1989, Pl. 13, Figs. 3-8). However, as we encountered specimens that exhibited variation in the thickness of the test and number of chambers per whorl, we choose to regard all these forms as *M. barleeanus*.

Melonis pompilioides (Fichtel and Moll 1798) (Fig. A.26i-j) illustrated by Corliss (1979, Pl. 5, Figs. 9-10) as well as by Brady (1884, Pl. 109, Figs. 10-11) as *Nonionina pompilioides* (Fichtel and Moll 1798).

Nuttallides umboniferus (Cushman 1933) (Fig. A.26k-l) = *Epistominella umbonifera* in Lohmann (1978, Pl. 3, Figs. 1-6) and Corliss (1979, Pl. 2, Figs. 10-12).

Oridorsalis tenerus (Brady 1884) (Fig. A.26m-o) = *Oridorsalis tener* (Brady 1884) in Lohmann (1978, Pl. 4 Figs. 5-7) and Corliss (1979, Pl. 4, Figs. 10-15).

Oridorsalis umbonatus (Reuss 1851) (Fig. A.27a-c) in Lohmann (1978, Pl. 4, Figs. 1-3) = *Pulvinulina umbonata* (Reuss 1851) in Brady (1884, Pl. 95, Fig. 11).

Oridorsalis sp. 3 (Fig. A.27d-f). Trochospiral test with 7 chambers gradually increasing in size in the final whorl; sutures radial and depressed. Aperture slit-like at the base of final chamber. Length ~360 µm.

Pullenia bulloides (d'Orbigny 1846) (Fig. A.27g-i) illustrated by Lohmann (1978, Pl. 1, Figs. 10-11) and Corliss (1979, Pl. 4, Figs. 1-2). See also Brady (1884, Pl. 83, Figs. 12-13) as *Pullenia sphaeroides* (d'Orbigny 1826).

Pullenia osloensis Feyling and Hanssen 1954 (Fig. A.27k–m) illustrated by Feyling and Hanssen (1954, Pl. 1, Figs. 33–35), and Corliss (1979, Pl. 4, Figs. 3–4).

Remarks: *P. osloensis* differs from *P. bulloides* in being comparatively smaller, with a rounded rather than acute periphery in end-on view.

Pullenia simplex Rhumbler 1931 (Fig. A.28a–b). Test planispiral, slightly compressed with subrounded periphery in end-on view and 6–7 chambers that rapidly increase in size in final whorl; sutures almost radial. Aperture a narrow slit extending across the base of final chamber. See Corliss (1979, Pl. 4, Figs 5–6).

Pullenia sp. 1 (Fig. A.28c–d). Test planspiral with 5 chambers in the final whorl, steadily increasing in size with slightly curved sutures; slightly lobate periphery, rounded in end-on view. Aperture a crescentic slit extending across the base of the final chamber. Length up to 300 µm.

Remarks: Our specimens are most similar to *Pullenia salisburyi* (Stewart and Stewart 1930) illustrated by Mohan et al. (2011, Pl. 10, Figs. 3–4); both have 5 chambers in the final whorl, a sub-rounded periphery, a rounded cross-section and a similar aperture. However, the type specimen, illustrated by Stewart and Stewart (1930, Pl. 8, Fig. 2a–b), has six chambers in the final whorl, a less rounded cross-section and, like Mohan et al.'s specimens, originated from Neogene sediments (>2.58 Ma years old). As a result, we are cautious about assigning our specimens to this species. They also somewhat resemble *Noniona* (= *Pullenia*) *quinqueloba* Reuss 1851 illustrated by Brady (1884, Pl. 83, Figs. 14–15). However, Brady's specimens on slide ZF 2199 are larger, wider in end view, and have a pointed cross-section.

Rotaliid sp. (Fig. A.28e). Spiral test, with five chambers. The first chamber is big and bulbous and is followed by four smaller chambers of similar size. A small, oval-shaped aperture is located at the base of the final chamber. Whitish wall, slightly transparent, smooth surface. Length ~260 µm.

Sphaeroidina bulloides d'Orbigny 1826 (Fig. A.28f). See Brady (1884, Pl. 83, Figs. 1–2, 6–7), Lohmann (1978, Pl. 4, Fig. 4) and Corliss (1979, Pl. 2, Figs. 1–2). This species often forms cysts made of sediment particles (see Appendix B, Fig. B.1; Stefanoudis and Gooday, 2016, Fig. 1).

Uvigerina brunnensis Karrer 1857 (Fig. A.28g). See Brady (1884, Pl. 75, Figs. 4–5).

Uvigerina mediterranea Hofker 1932 (Fig. A.28h–j). See illustration in Brady (1884, Pl. 74, Figs. 11–12) as *Uvigerina pygmaea* d'Orbigny 1826.

Textulariida

Ammobaculites agglutinans (d'Orbigny 1846) (Fig. A.29a–b). See Stefanoudis et al. (2016, Pl. 1, Figs. 7–8) and Chapter 3 (Pl. 3.1, Figs. 7–8). Our specimens resemble those illustrated by Brady (1884, Pl. 32, Figs. 19–20, 24–26) as *Haplophragmium agglutinans* (d'Orbigny 1846). Kaminski and Kuhnt (1991) noted that specimens of this species from abyssal calcareous oozes have larger tests and usually possess more uniserial chambers compared to specimens from shallower depths on the continental margin.

Cribrostomoides subglobosus (Cushman 1910) (Fig. A.29c–d). Our specimens resemble those illustrated by Brady (1884, Pl. 34, Figs. 8–10) as *Haplophragmium latidorsatum* Bornemann 1858, which are identified as *C. subglobosus* by Jones (1994). This well-known species is widely reported from different oceans (Kaminski and Gradstein, 2005; Gooday and Jorissen, 2012). *Remarks:* Our specimens look identical to those on Brady's slides containing specimens of *H. latidorsatum* from Challenger Station 24 and 98. However, some of those from abyssal hill sites have a rather irregular appearance due to the incorporation of coarse quartz grains (e.g. Chapter 3, Pl. 3.1, Figs. 3–6; Stefanoudis et al., 2016, Pl. 1, Figs. 3–6; Fig. A.29c–d herein).

Cribrostomoides sp. 1 (Fig. A.29e–f). Test planispiral, relatively narrow and with rounded periphery in end-on view, last whorl with seven chambers that increase in size. Aperture an equatorial slit or elliptical opening located at the base of last chamber. Wall finely agglutinated, its surface smoothly finished and orange colour. Length ~250 µm.

Remarks: Our specimens are in many respects similar to those of *Trochammina trullissata* Brady 1879 on Brady's syntype slide (ZF 2519), regarded as *Veleroninoides wiesneri* (Parr 1950) by Jones (1994). In both cases the wall is fine-grained walls with a shiny surface, the number of chambers is similar and they are arranged more or less planispirally. However, the aperture of Brady's specimens is on the face of the last chamber and has well-developed lips, while in ours it is located at the base of the final chamber and has very narrow lips. As a

result, we assign our specimens to the genus *Cribrostomoides* (Loeblich and Tappan, 1987, pg. 65).

Cribrostomoides sp. 2 (Fig. A.29g–h). Test sub-rounded, streptospirally to planispirally coiled with 4–5 chambers in the last whorl. Thin, finely agglutinated wall, pale yellow in colour and semi-transparent in glycerol. Oval-shaped aperture located near the base of the final chamber. Length up to 500 µm.

Remarks: This species resembles *Cribrostomoides subglobosus*, but our specimens are noticeably smaller and have a much thinner wall.

Cyclammmina trullissata (Brady 1879) (Fig. A.29i–k) = *Trochammmina trullissata* Brady 1879 illustrated by Brady (1884, Pl. 40, Fig. 13).

Remarks: Brady's specimens (slide ZF2518) are larger than ours but in all other respects identical, despite the fact that they originate from a much shallower setting (approx. 700 m depth).

Dorothia inflata Colom 1945 (Fig. A.30a–b) illustrated by Colom (1945, Pl. 31, Figs. 1–18). Our specimens are identical to those found off NW Africa (Gooday, unpubl. data).

Eggerella bradyi (Cushman 1911) (Fig. A.30c–d). See Weston (1984, Fig. 2). Jones (1994) considered *E. bradyi* to be the same as *Verneuilina pygmaea* Egger 1857 in Brady (1884, Pl. 47, Figs. 4–7).

Eratidus foliaceus (Brady 1881) (Fig. A.30e–g) = *Haplophragmium foliaceum* Brady 1881 in Brady (1884, Pl. 33, Figs. 20–25).

Remarks: Specimens from abyssal hill samples differ from those from the plain. The former always incorporate large mineral grains and have a rather coarse and irregular appearance (Fig. 30g), whereas the latter are generally finer grained (Fig. 30e–f).

Karrerulina apicularis (Cushman 1911) (Fig. A.30h–i) = *Gaudryina apicularis* Cushman 1911 illustrated by Cushman (1922, Fig. 4).

Recurvoides contortus Earland 1934 (Fig. A.31a–f). See Loeblich and Tappan (1987, Pl. 68, Figs. 7–14), Zheng and Fu (2001, Pl. XLVI, Figs. 7–11), and Holbourn et al. (2013, pg. 478). Specimens assigned to this species have strong streptospiral coiling. The aperture is a small elliptical opening just above or at the base of the final chamber. The wall is pale orange to brown, with a rough unpolished surface. Although most specimens are finely agglutinated, a few from the hill sites incorporate coarser mineral grains.

Recurvoides sp. 1 (Fig. A.31g–h) = *Recurvoides* sp. 9 in Stefanoudis et al. (2016, Pl. 1, Figs. 1–2). See illustrations in Chapter 3 (Pl. 3.1, Figs. 1–2). Test sub-rounded, streptospirally coiled, occasionally incorporating large quartz grains. Last whorl consists of four to five chambers, which gradually increase in size. The aperture is small, simple, oval-shaped, and placed on the base of the final chamber. The wall is semi-opaque and its colour ranges from pale orange to yellowish brown. Length up to 420 μm .

Remarks: This species differs from *Recurvoides contortus* in having a coarsely rather than finely agglutinated wall, and a more regular coiling pattern.

Recurvoides sp. 4 (Fig. A.31i–k). Orange test with streptospiral coiling and almost square periphery when viewed end-on. The final whorl has 4 chambers that increase in size. The aperture is oval to slit-like, located at the base of the final chamber. Wall is coarsely agglutinated. Length up to 680 μm .

Remarks: This species differs from *Recurvoides contortus* in that its periphery is square rather than rounded, and there are fewer chambers in the final whorl (4 vs. 5–8). It also differs from *Recurvoides* sp. 1 in that its specimens are comparatively larger and more square.

Recurvoides sp. 8 (Fig. A.32a–c). Large, thick-walled, orange test; streptospirally coiled with sub-rounded periphery and relatively fine agglutination. The aperture is found on the base of the final chamber. Length ~800 μm .

Remarks: Our specimen is somewhat similar to *Recurvoides gigas* Zheng 1988 illustrated by Zheng and Fu (2001, Pl. XLVII, Fig. 2). It differs from all other *Recurvoides* spp. of the present study in having a much larger and robust test that is comparatively finer agglutinated.

Textularia sp. 1 (Fig. A.32d). Elongate, biserial test; with at least 10, usually 18–22, subglobular chambers that increase steadily in size. Aperture small circular opening near at the base of the final chamber. Length up 720 μm .

Textularia sp. 3 (Fig. A.32e). Test biserial, relatively short and fat, with test length being 1.5 times that of its width. Up to 12 chambers that increase steadily in size; aperture is a round opening with narrow lips, located in the middle of last chamber. Wall is semi-opaque and white. Length up to 360 μm .

Remarks: This species superficially resembles *Textularia* sp. 1, however, *Textularia* sp. 3 is less elongate and has always fewer, slightly angular chambers.

Textulariid sp. 1 (Fig. A.32f). Pale white, test with triserial chamber arrangement; test robust; wall calcareous, coarsely agglutinated. Length ~300 µm.

Veleroninoides sp. 1 (Fig. A.32g–k). Test planispirally coiled with a rounded periphery and compressed side-view. The last whorl has six chambers that increase only slightly in size. Aperture slit-like to oval with a slight lip, located at the base of the last chamber. Finely agglutinated wall with relatively smooth surface and orange in colour. Length up to 380 µm.

Remarks: Our species most resembles *Veleroninoides jeffresyii* (Williamson 1856) *sensu* Jones (1994), illustrated as *Haplophragmium canariensis* by Brady (1884, Pl. 35, Figs. 1–3, 5), although Brady's specimens (slides ZF1527 and ZF1528) have more chambers, are more coarsely grained, and have a dull surface.

Trochamminacea

Adercotryma glomerata (Brady 1878) (Fig. A.33a) = *Haplophragmium glomeratum* (Brady 1878). Test more or less rounded with four chambers in the final whorl, confirming its identification as *A. glomerata* rather than *A. wrighti*, which has 3 chambers in the final whorl. The almost circular shape is more pronounced in specimens from the abyssal plain than those from hill sites. In general, they closely resemble *A. glomerata* as illustrated by Brönnimann and Whittaker (1987, Fig. 4a–e), Timm (1992, Pl. 4, Fig. 1a), Hayward et al. (2010, Pl. 2, Fig. 20), as well as the oval-shaped morphotype of *A. glomerata* illustrated in Gooday et al. (2010, Fig. 15e). See also illustrations in Brady (1884, Pl. 34, Figs. 15–18), in Stefanoudis et al. (2016, Pl. 3, Figs. 1–4) and Chapter 3 (Pl. 3.3, Figs. 1–4).

Ammoglobigerina shannoni (Brönnimann and Whittaker 1988) (Fig. A.33b–c) illustrated by Dorst and Schönfeld (2015, Figs. 8.2, 8.5). See also illustrations in Brönnimann and Whittaker (1988, Fig. 15A–H) as *Globotrochamminopsis shannoni* Brönnimann and Whittaker 1988.

Buzasina galeata (Brady 1881) (Fig. A.33d–e) = *Trochammina galeata* Brady 1881 in Brady (1884, Pl. 40, Figs. 19–22).

Buzasina ringens (Brady 1879) (Fig. A.33f–g) = *Trochammina ringens* 1879 in Brady (1884, Pl. 40, Figs. 17–18).

Cystammina paucilocilata (Brady 1879) (Fig. A.33h) = *Trochammina pauciloculata* Brady 1879 in Brady (1884, Pl. 41, Fig. 1).

Deuterammia montagui Brönniman and Whittaker 1988 (Fig. A.33i) illustrated by Brönnimann and Whittaker (1988, Figs. 41–42).

Haplophragmoides sphaeriloculum Cushman 1910 (Fig. A.33j–m). Test planispiral with lobate periphery and 4–5 chambers in the final whorl. The chambers are inflated and increase gradually in size. The aperture is an oval opening at the bottom of the face of the final chamber. Wall is thin, finely agglutinated, pale orange in colour and semi-transparent. See illustrations in Cushman (1910, Fig. 165), Cushman (1921, Pl. 15, Fig. 3), Earland (1936, Pl. 1, Figs. 17–18), Kuhnt et al. (2000, Pl. 5, Figs. 16–18), and Zheng and Fu (2001, Pl. XXXV, Fig. 17; Pl. XXXVI, Figs. 4–5). This species has been commonly reported from NW European Seas mainly at depths >2900 m (Murray and Alve, 2011).

Remarks: It also resembles *Haplophragmium latidorsatum* (Bornemann 1855) in Jones (1994, Pl. 34, Fig. 14), which as Jones pointed out might be related to *H. sphaeriloculum*, although this requires further investigation.

Haplophragmoides sp. 2 (Fig. A.33n–o). Test planispiral with 4–6 chambers in the final whorl; chambers increase gradually in size and slightly overlap each other. Small oval-shaped aperture at the base of final chamber. Wall finely agglutinated, smoothly finished, like that of *Buzasina galeata* and *Buzasina ringens*. Length up to 200 µm.

Paratrochammina challengerii Brönnimann and Whittaker 1988 (Fig. A.34a–b) illustrated by Brönnimann and Whittaker (1988, Fig. 16H–K). Jones (1994) identifies the specimens assigned by Brady (1884, Pl. 35, Fig. 10) to *Haplophragmium globigeriniforme* (Parker and Jones 1865) as *P. challengerii*.

Paratrochammina aff. *scotiaensis* Brönnimann and Whittaker 1988 (Fig. A.34c–d). Test small, trochospiral, conical and bluntly pointed at the apex, with the height of the spire less than the diameter of the spiral side. Chambers gradually increase in size with four chambers in the final whorl and an aperture at the base of final chamber. Wall finely agglutinated, pale yellow in colour and translucent. Length ~160 µm.

Remarks: Our specimen has more bulbous chambers and a shorter spire compared to those illustrated by Brönniman and Whittaker (1988, Fig. 16A–G). However, in other respects (type of coiling, number of whorls, number of chambers in the final whorl, shape of the aperture) they are very similar. It is also somewhat similar to *Trochammina* sp. C in Zheng and Fu (2001, Pl. LXV, Fig. 8a–c).

Portatrochammina murrayi Brönnimann and Zaninetti 1984 (Fig. A.34e–f).

Our specimens resemble those illustrated in Brönnimann and Zaninetti (1984, Pl. 5, Figs. 7, 12–15), Gooday (1986, Fig. 10O–P) and Dorst and Schönfeld (2015, Figs. 3a, b and 4a–b), although in the latter study they were recorded from much shallower settings in the Celtic Sea (100–500 m water deep). See also Stefanoudis et al. (2016, Pl. 1, Figs. 9–10) and Chapter 3 (Pl. 3.1, Figs. 9–10). This species is reported across a very wide bathymetric range (17–4250 m) in NW European Seas, although it becomes proportionately less abundant at depths >1800 m (Murray and Alve, 2011).

Pseudotrochammina arenacea (Heron-Allen and Earland 1922) (Fig. A.34g–h). See Brönnimann and Whittaker (1988, Figs. 48 G–M; 49 A–Q).

Trochammina heronalleni (Mikhalevich 1972) (Fig. A.34i–j). Test trochospiral with 6 subglobular chambers in final whorl, increasing gradually in size. Umbilical side fairly flat, spiral side somewhat inflated. Small, arch-like aperture located at the base of the face of the final chamber. Wall is semi-transparent, finely agglutinated, pale orange in colour. See also description and illustrations in Brönnimann and Whittaker (1988, Fig. 11A–G).

Trochammina sp. 1 (Fig. A.34k–l). Test trochospiral with chambers arranged in 3 to 3.5 whorls, gradually increasing in size. Wall orange in colour, finely agglutinated. Length ~270 µm.

Remarks: This single specimen was not in a good condition and hence the aperture was not visible. However, its chamber arrangement, chamber shape and wall texture strongly resemble *Trochammina rotaliformis* Heron-Allen and Earland 1911 as illustrated by Cushman (1920, Fig. 2).

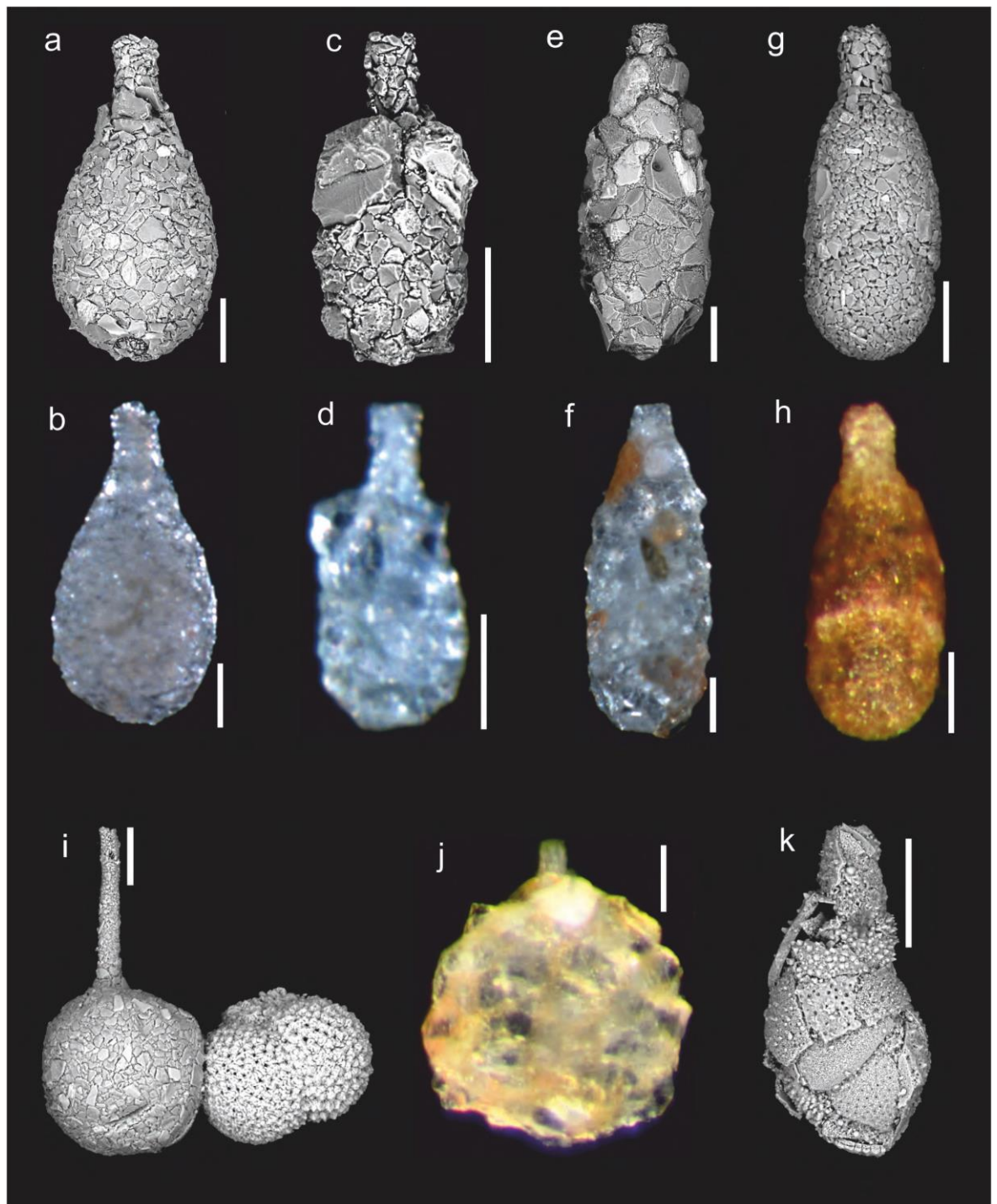


Fig. A.1. SEM and light (reflected) images. a–d) *Lagenammia* aff. *arenulata*, e–f) *Lagenammia* sp. 2, g–h) *Lagenammia difflugiformis*, i–j) *Lagenammia tubulata*, k) *Lagenammia* sp. 3. Scale bars = 100 μ m.

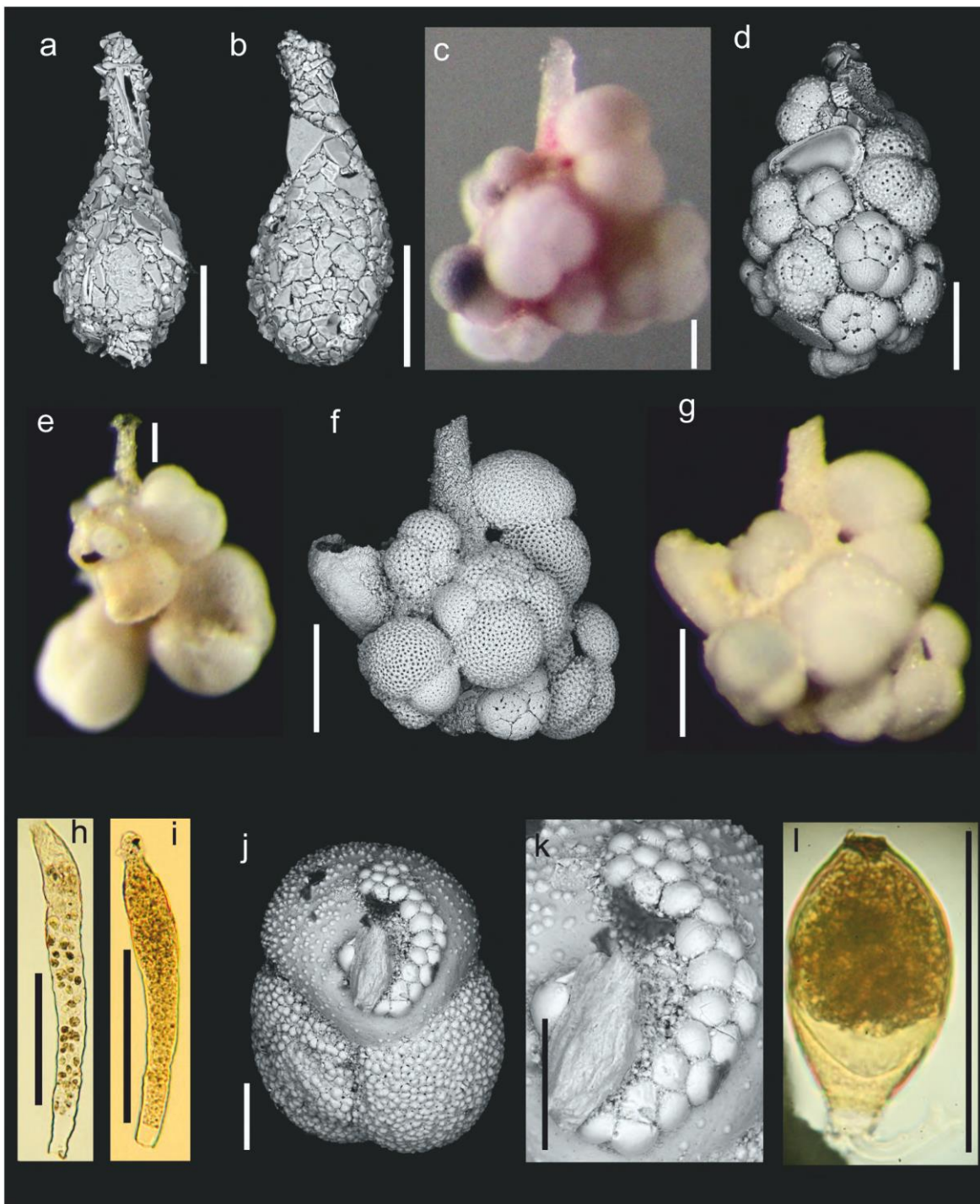


Fig. A.2. SEM and light (reflected, transmitted) images. a–b) *Lagenammia* sp. 12, c) *Lagenammia* sp. 17, d) *Lagenammia* sp. 18, e–g) *Lagenammia* sp. 19, h–i) *Nodellum*-like sp., j–k) *Placopsilinella aurantiaca*, l) *Resigella*-like form 1. Scale bars = 100 μ m.

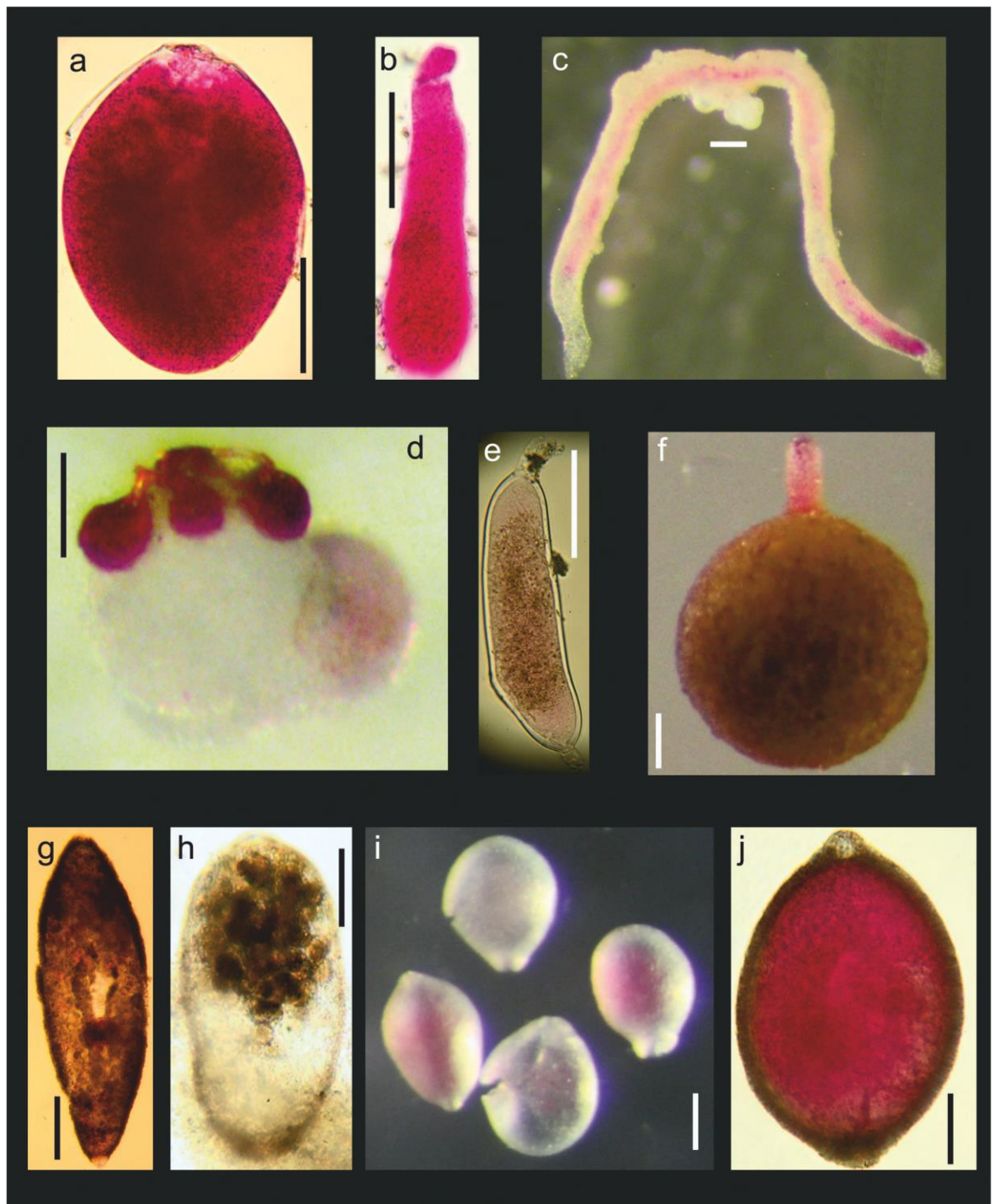


Fig. A.3. Light (reflected, transmitted) images. a) Allogromiid sp. 1, b) Allogromiid sp. 3, c) *Nemogullmia* sp., d) Organic-walled domes, e) *Tinogullmia riemanni*, f) *Saccamina* sp. 1, g) Saccamminid sp. 1, h) Saccamminid sp. 2, i–j) Saccamminid sp. 3. Scale bars = 100 µm.

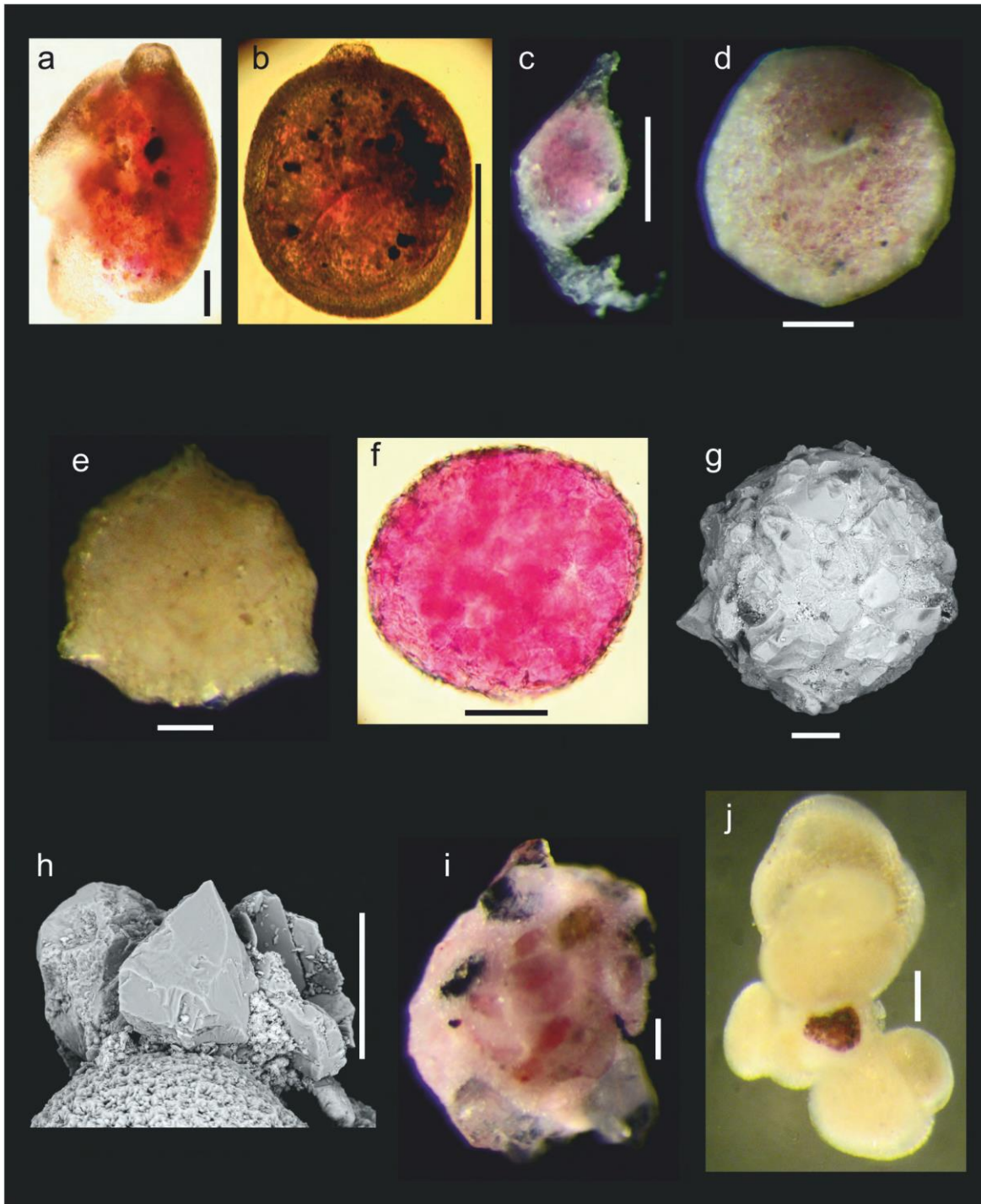


Fig. A.4. SEM and light (reflected, transmitted) images. a) Saccamminid sp. 4, b) Saccamminid sp. 5, c) Saccamminid sp. 6, d) *Thurammia albicans*, e) *Thurammia papillata*, f) Monothalamous sp. 3, g) *Psammosphaera fusca*, h) *Psammosphaera* sp. 1, i) *Psammosphaera* sp. 2, j) White domes. Scale bars = 100 μm .

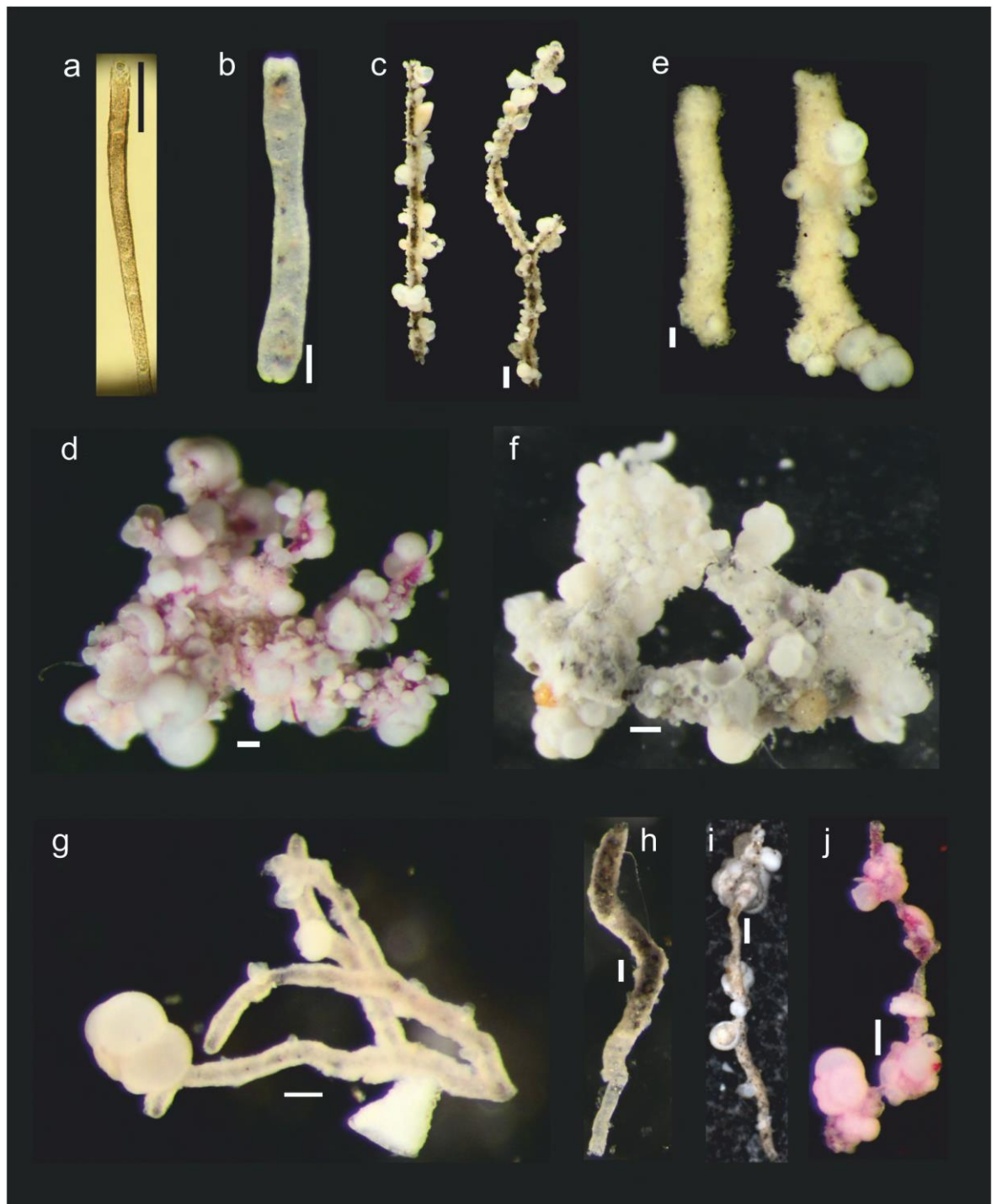


Fig. A.5. Light (reflected, transmitted) images. a) *Bathysiphon* sp. 1, b) *Hippocrepinella* sp., c) *Rhizammima algaeformis*, d) *Rhizammima*-like formation, e) Xenophyophore-like tube type 1, f) Xenophyophore-like tube type 2, g) Tubular sp. 1, h) Tubular sp. 2, i) Tubular sp. 3, j) Tubular sp. 4. Scale bars = 100 μ m.

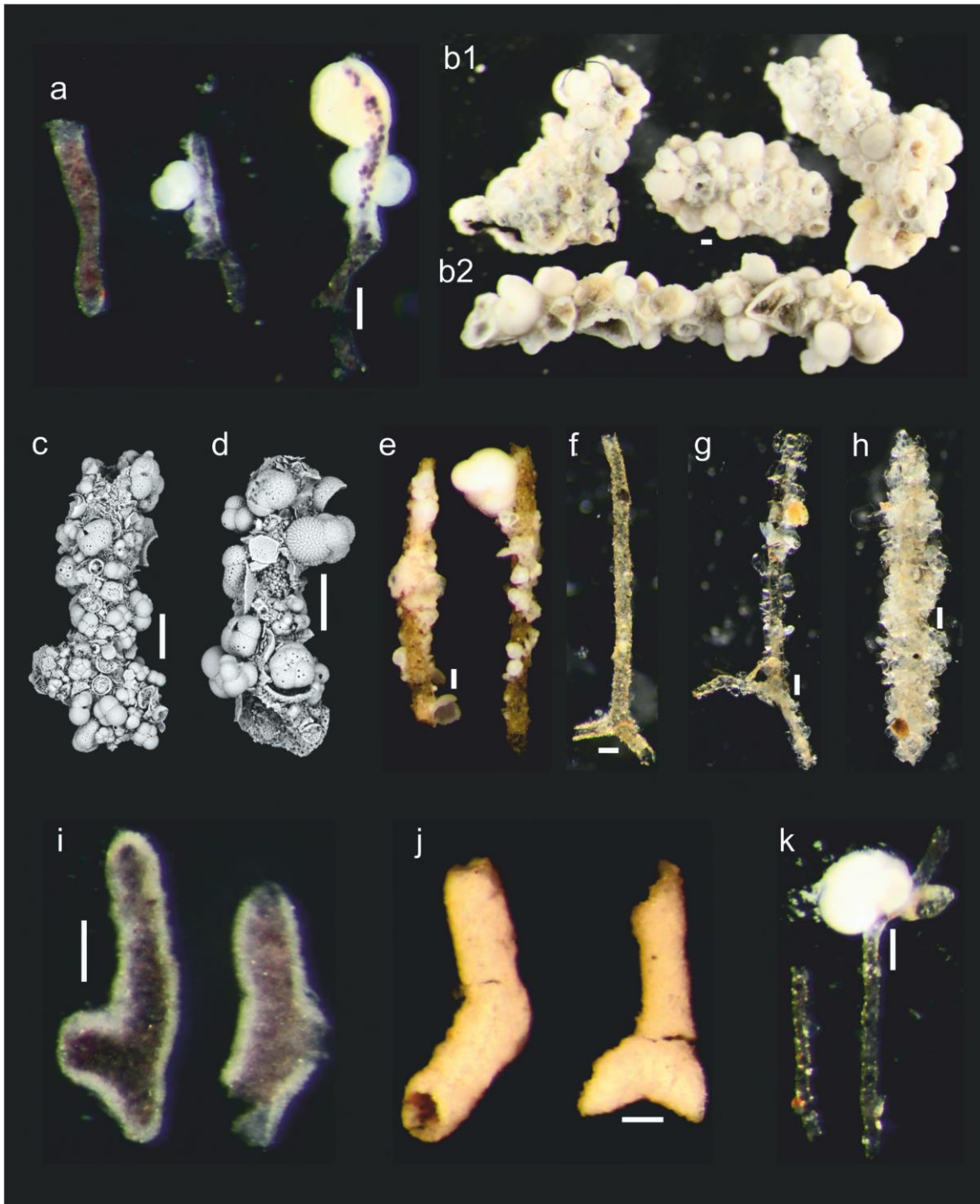


Fig. A.6. SEM and light (reflected) images. a) Tubular sp. 5, b1, d) Tubular sp. 7, b2, c) Tubular sp. 6, e–f) Tubular sp. 8, g) Tubular sp. 9, h) Tubular sp. 10, i) Tubular sp. 11, j) Tubular sp. 12, k) Tubular sp. 13. Scale bars = 100 μm .

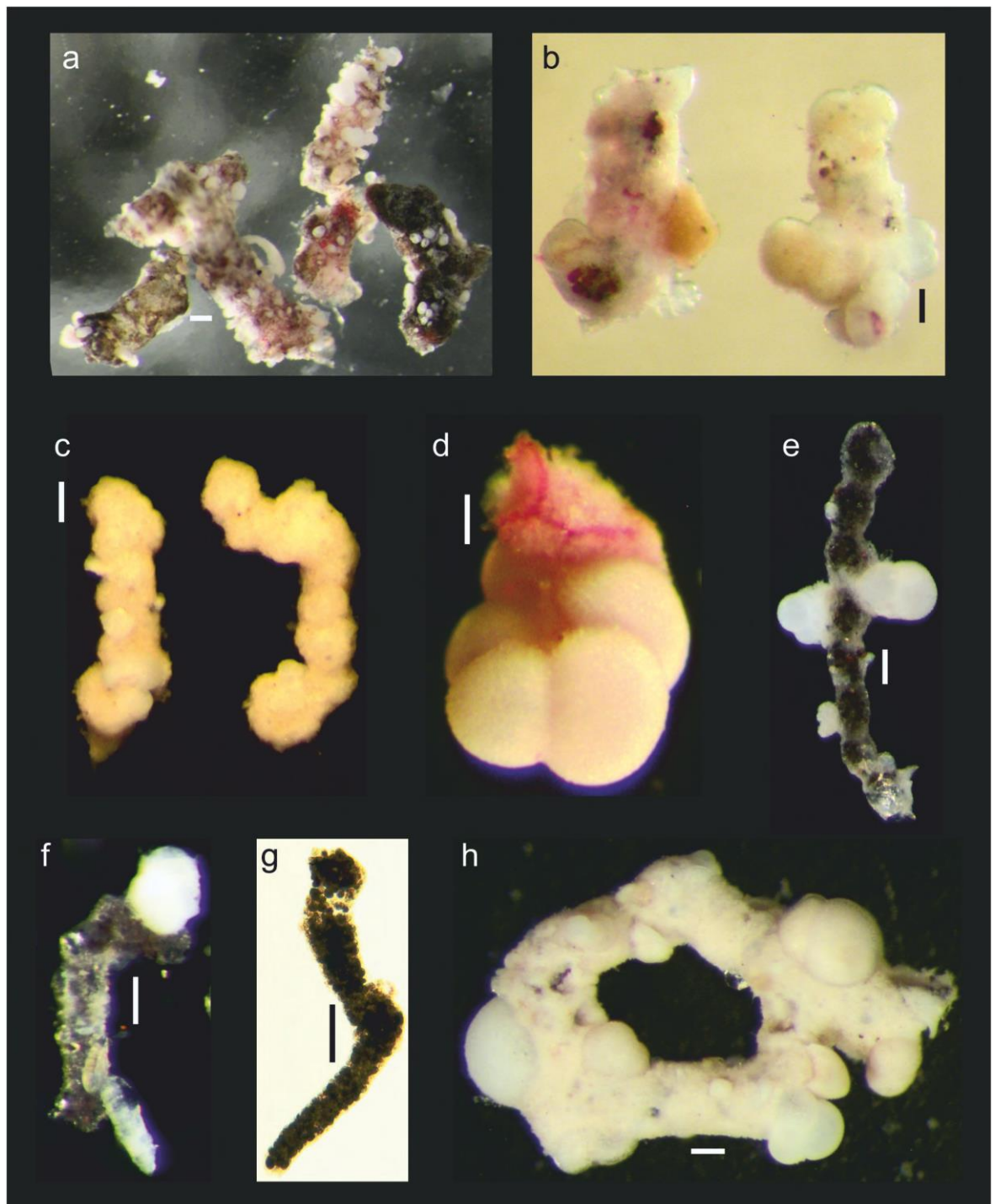


Fig. A.7. Light (reflected, transmitted) images. a) Tubular sp. 14, b) Tubular sp. 15, c) Tubular sp. 16, d) Tubular sp. 19, e) Tubular sp. 20, f) Tubular sp. 25, g) Tubular sp. 27, h) Tubular sp. 28. Scale bars = 100 μ m.

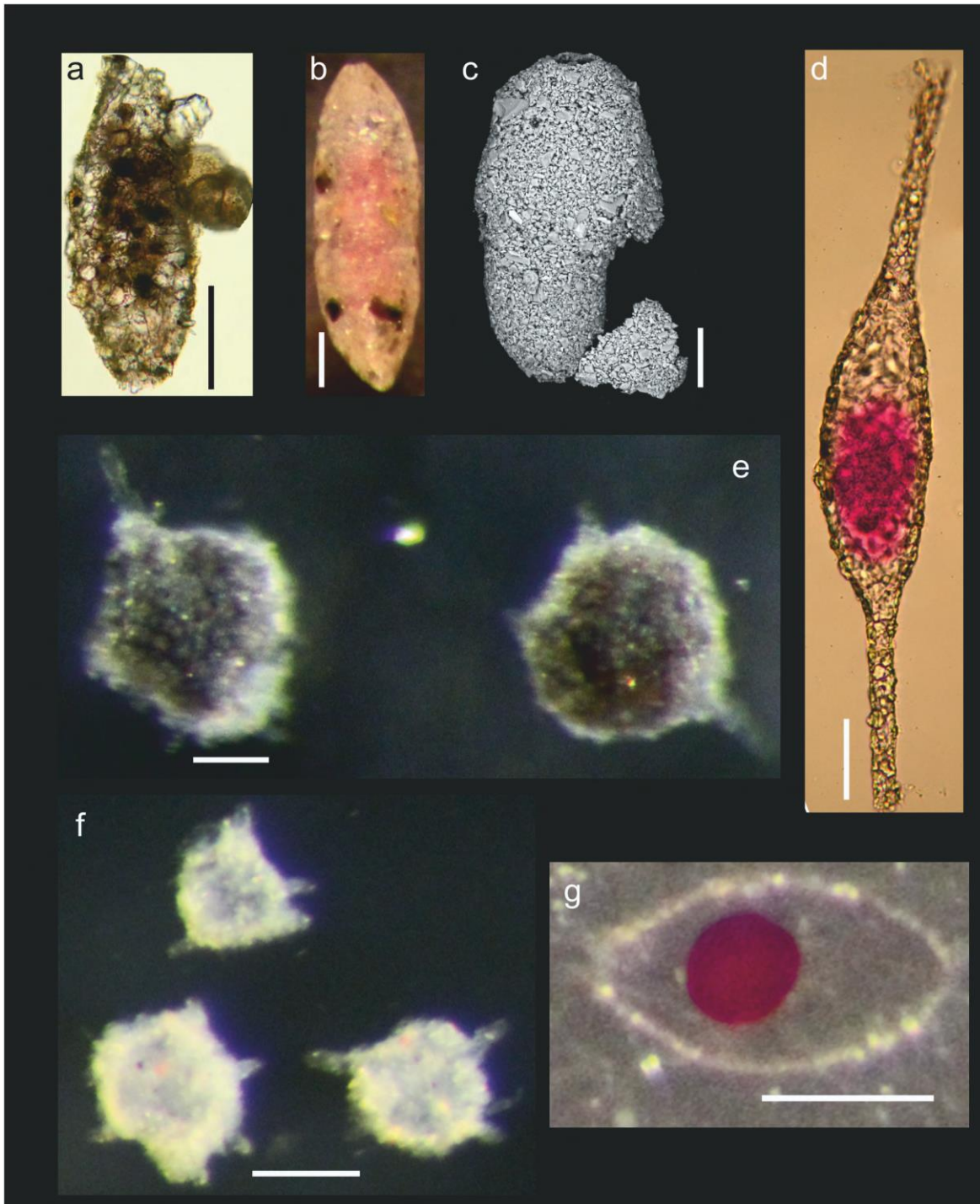


Fig. A.8. SEM and light (reflected, transmitted) images. a) *Monothalamous* sp. 1, b–c) *Monothalamous* sp. 2, d) *Monothalamous* sp. 4, e) *Monothalamous* sp. 5, f) *Monothalamous* sp. 6, g) *Vanhoeffenella* sp. Scale bars = 100 μm.

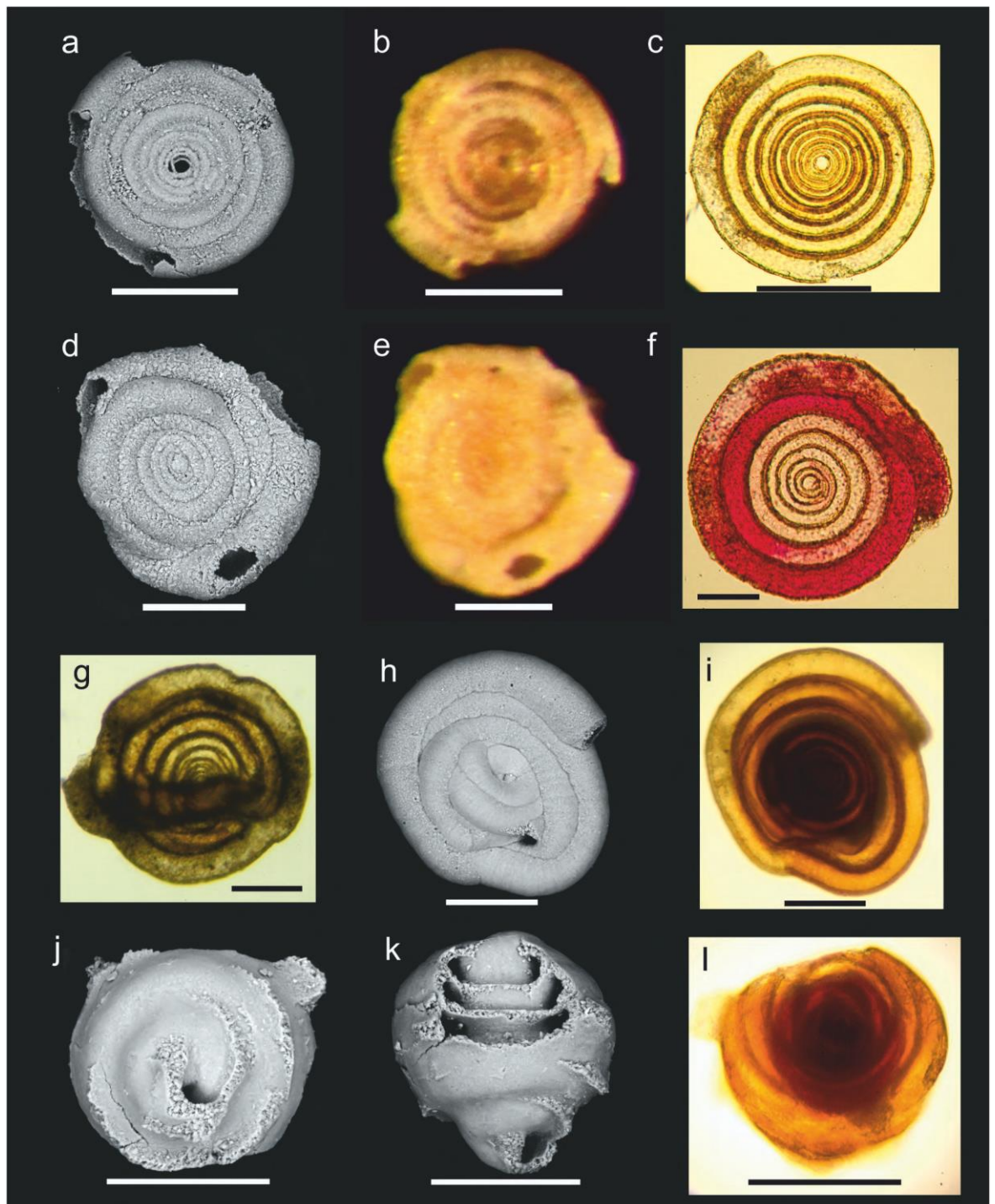


Fig. A.9. SEM and light (reflected, transmitted) images. a–c) *Ammodiscus anguillae*, d–f) *Ammodiscus* sp. 1, g–i) *Glomospira gordialis*, j–l) *Repmamina charoides*. Scale bars = 100 μ m.

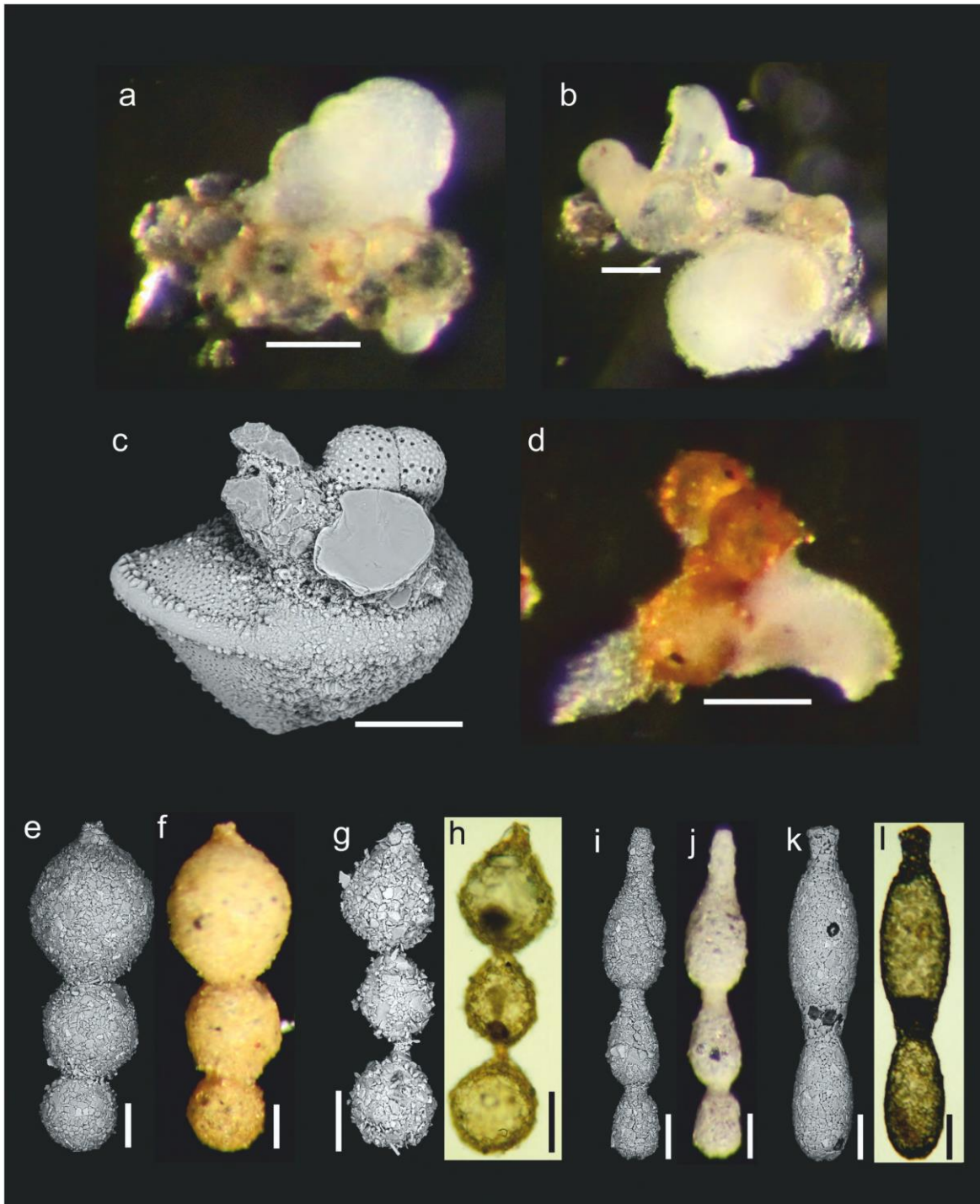


Fig. A.10. SEM and light (reflected, transmitted) images. a–b) *Hormosina* aff. *monile*, c–d) *Hormosina* sp. 1, e–f) *Hormosina pilulifera*, g–h) *Hormosinella guttifera*, i–j) *Hormosinella ovicula*, k–l) *Hormosinella* sp. 1. Scale bars = 100 µm.

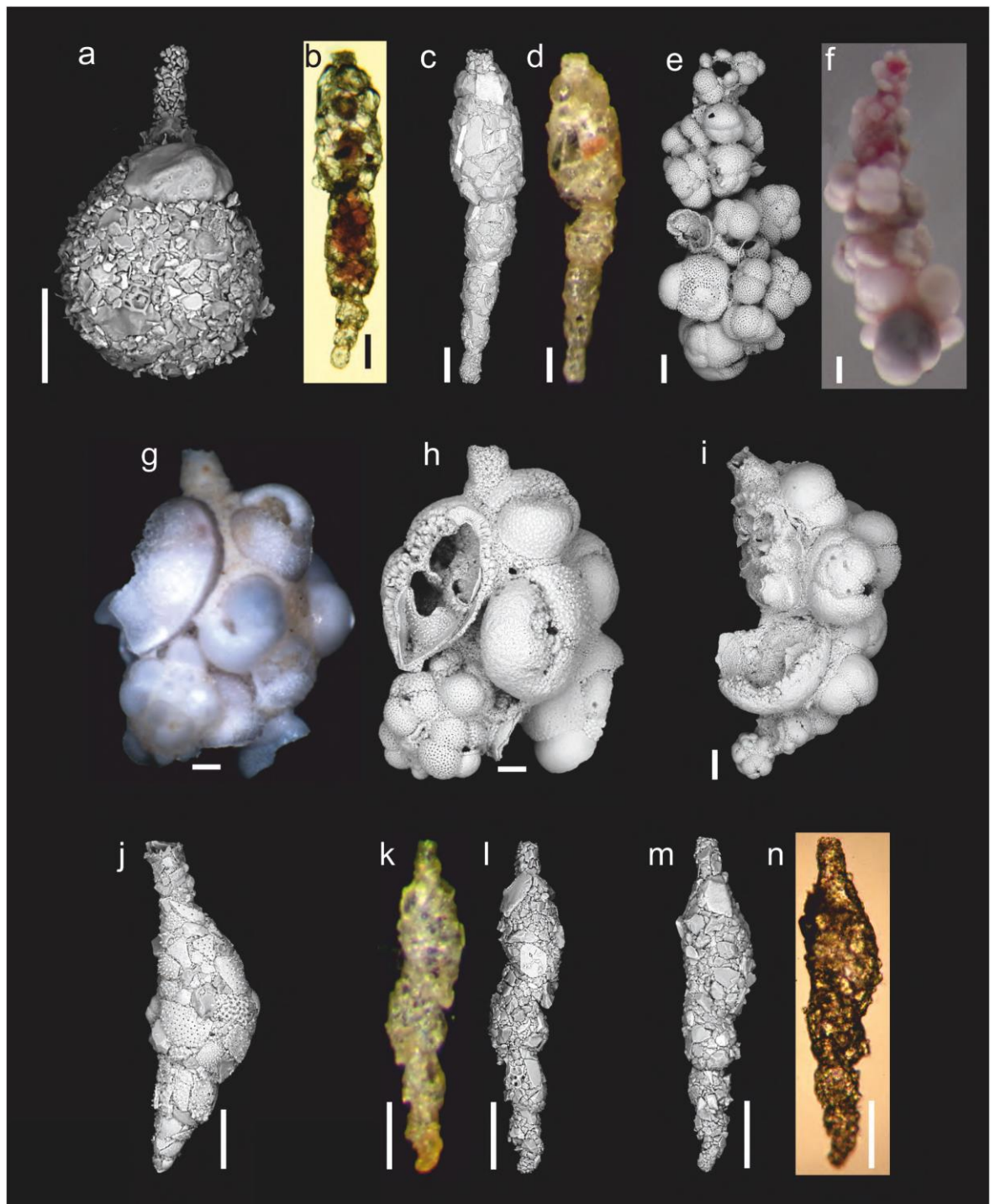


Fig. A.11. SEM and light (reflected, transmitted) images. a) *Hormosina/Saccammina* sp., b–d) *Nodulina dentaliniformis*, e–f) *Reophax agglutinatus*, g–i) *Reophax bilocularis*, j) *Reophax helenae*, k–n) *Reophax* aff. *scorpiurus*. Scale bars = 100 μ m.

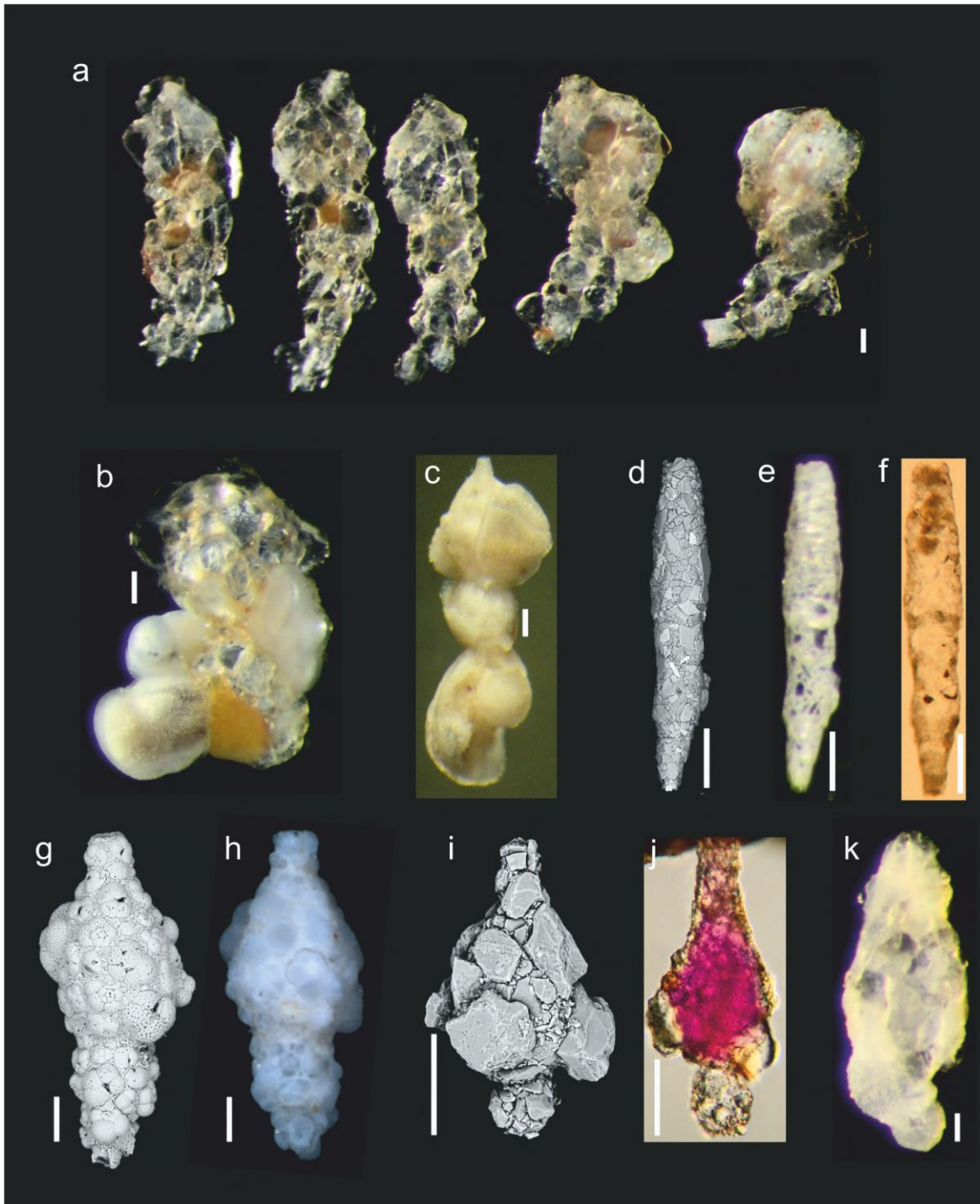


Fig. A.12. SEM and light (reflected, transmitted) images. a) *Reophax* sp. 1, b) *Reophax* sp. 4, c) *Reophax* sp. 6, d–f) *Reophax* sp. 7, g–h) *Reophax* sp. 8, i–j) *Reophax* sp. 9, k) *Reophax* sp. 11. Scale bars = 100 μm .

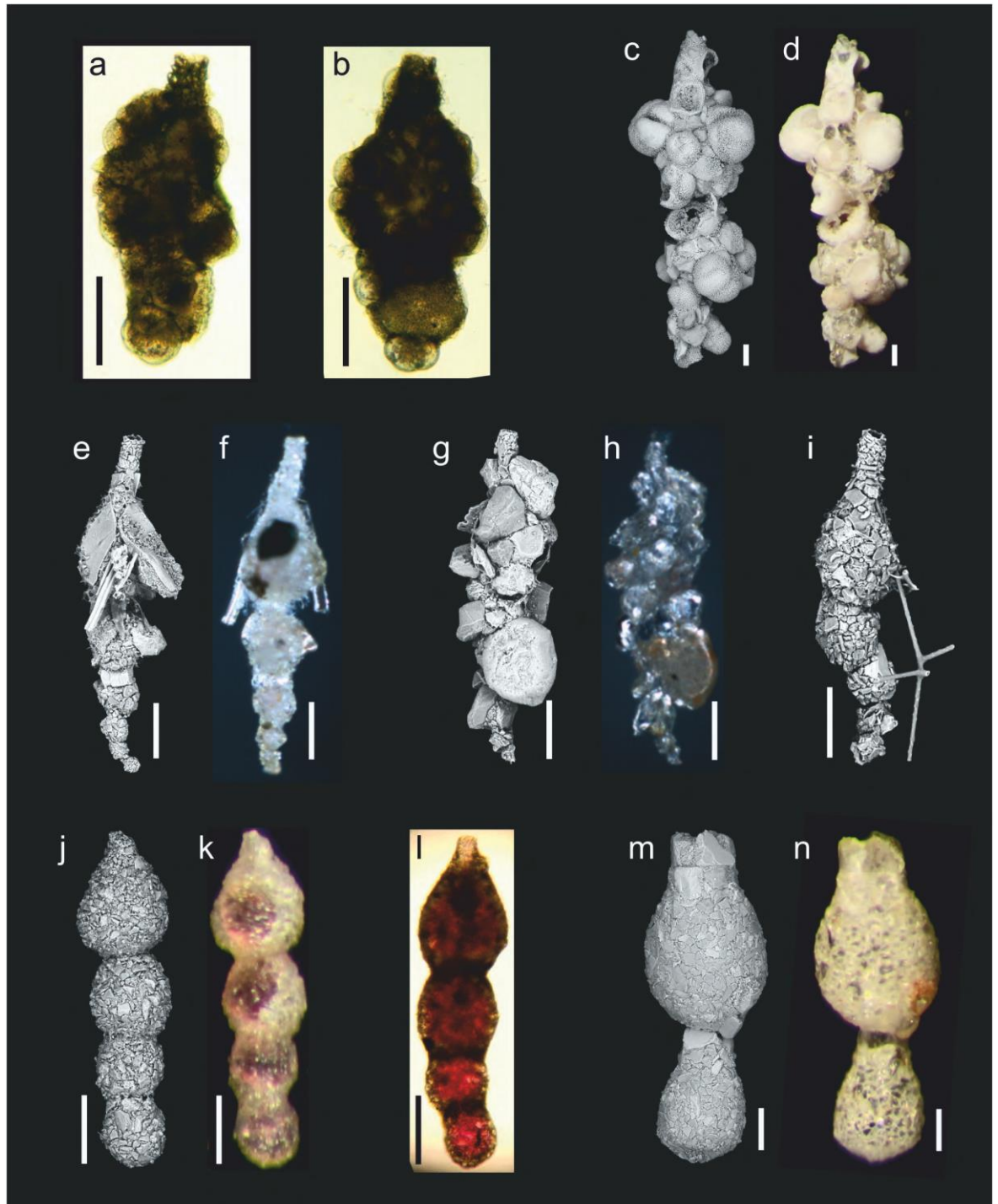


Fig. A.13. SEM and light (reflected, transmitted) images. a–b) *Reophax* sp. 19, c–d) *Reophax* sp. 20, e–i) *Reophax* sp. 21, j–l) *Reophax* sp. 23, m–n) *Reophax* sp. 27. Scale bars = 100 μ m.

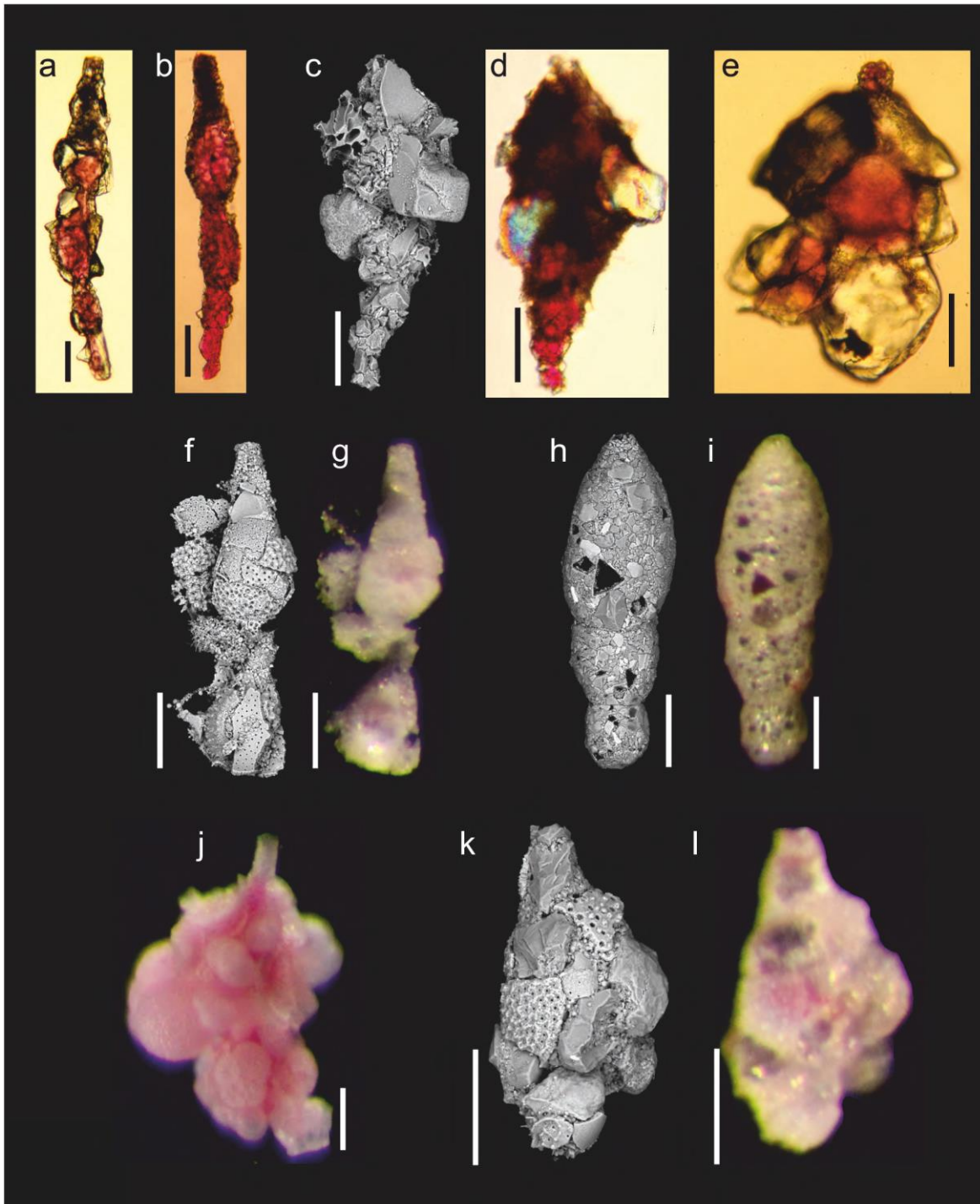


Fig. A.14. SEM and light (reflected, transmitted) images. a–b) *Reophax* sp. 28, c–d) *Reophax* sp. 34, e) *Reophax* sp. 38, f–g) *Reophax* sp. 40, h–i) *Reophax* sp. 42, j) *Reophax* sp. 43, k–l) *Reophax* sp. 110/111. Scale bars = 100 μ m.

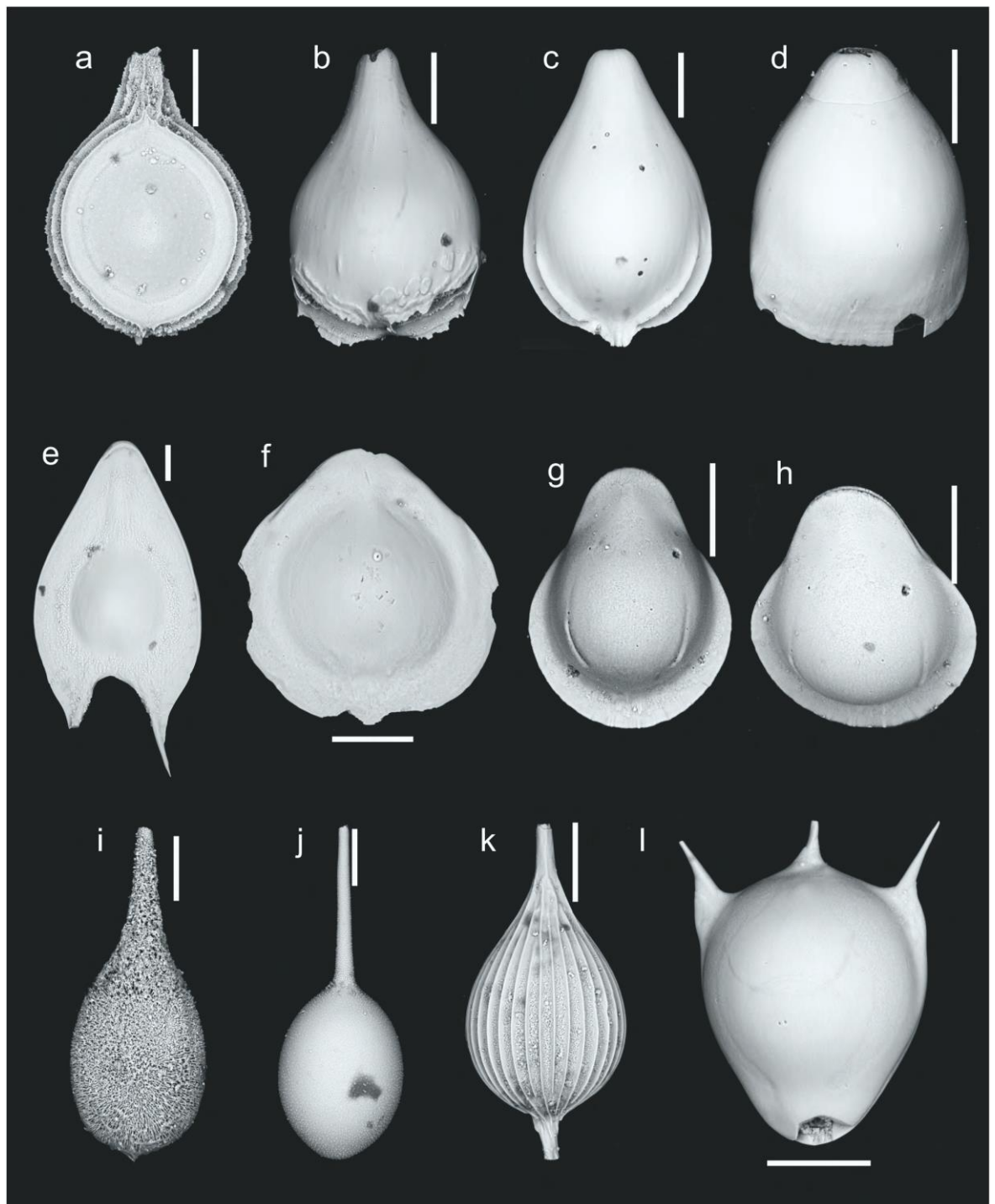


Fig. A.15. SEM images. a) *Buchnerina iberica*, b) *Fissurina* aff. *alveolata*, c) *Fissurina annectens*, d) *Fissurina fimbriata*, e) *Fissurina* cf. *quinqueannulata*, f) *Fissurina seminiformis*, g–h) *Fissurina* sp. 1, i) *Lagena hispida*, j) *Lagena flatulenta*, k) *Lagena spinigera*, l) *Lagena staphyllearia*. Scale bars = 100 μ m.

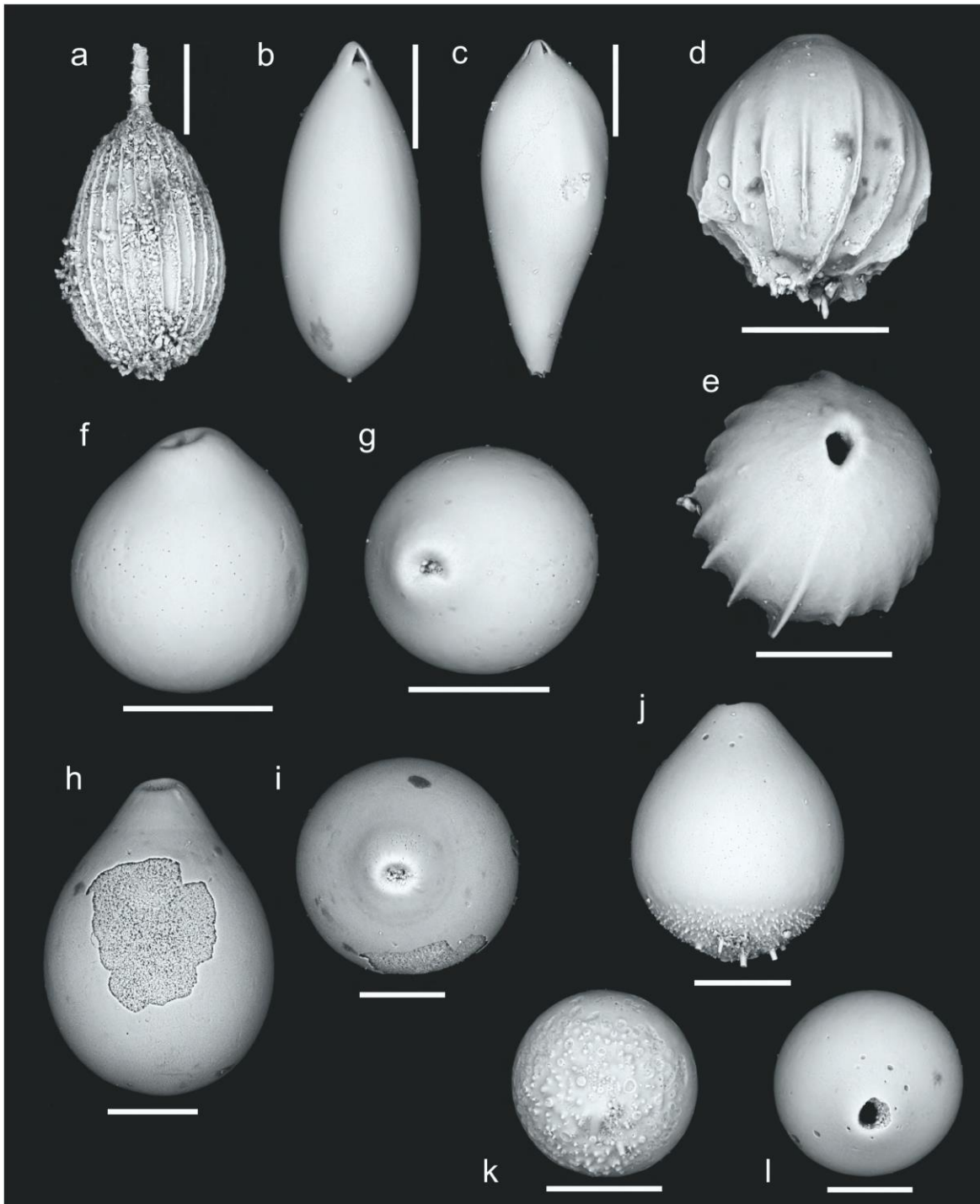


Fig. A.16. SEM images. a) *Lagena* aff. *striata*, b) Lagenid sp. 1, c) Lagenid sp. 2, d–e) *Oolina* aff. *exsculpta*, f–i) *Oolina* *globosa*, j–l) *Oolina* *setosa*. Scale bars = 100 μ m.

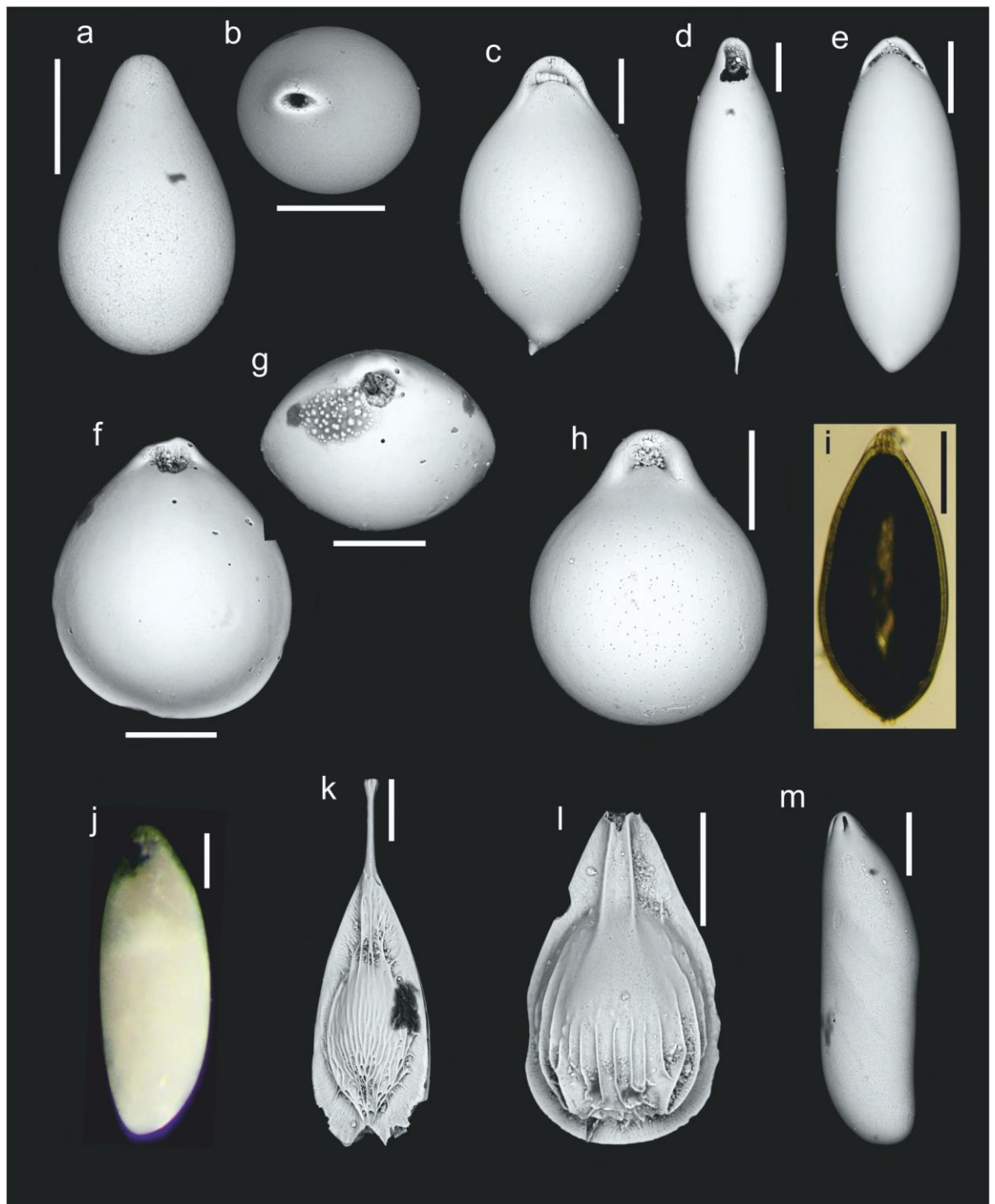


Fig. A.17. SEM and light (reflected, transmitted) images. a–b) *Oolina* sp. 4, c) *Parafissurina crassa*, d) *Parafissurina lateralis*, e) *Parafissurina pseudolateralis*, f–g) *Parafissurina* sp. 3, h) *Parafissurina* sp. 7, i) *Pyrulina gutta*, j) *Pyrulina* sp., k) *Solenina subformosa* subs. *fluens*, l) *Solenina* sp., m) *Vaginulinopsis tasmanica*. Scale bars = 100 μ m.

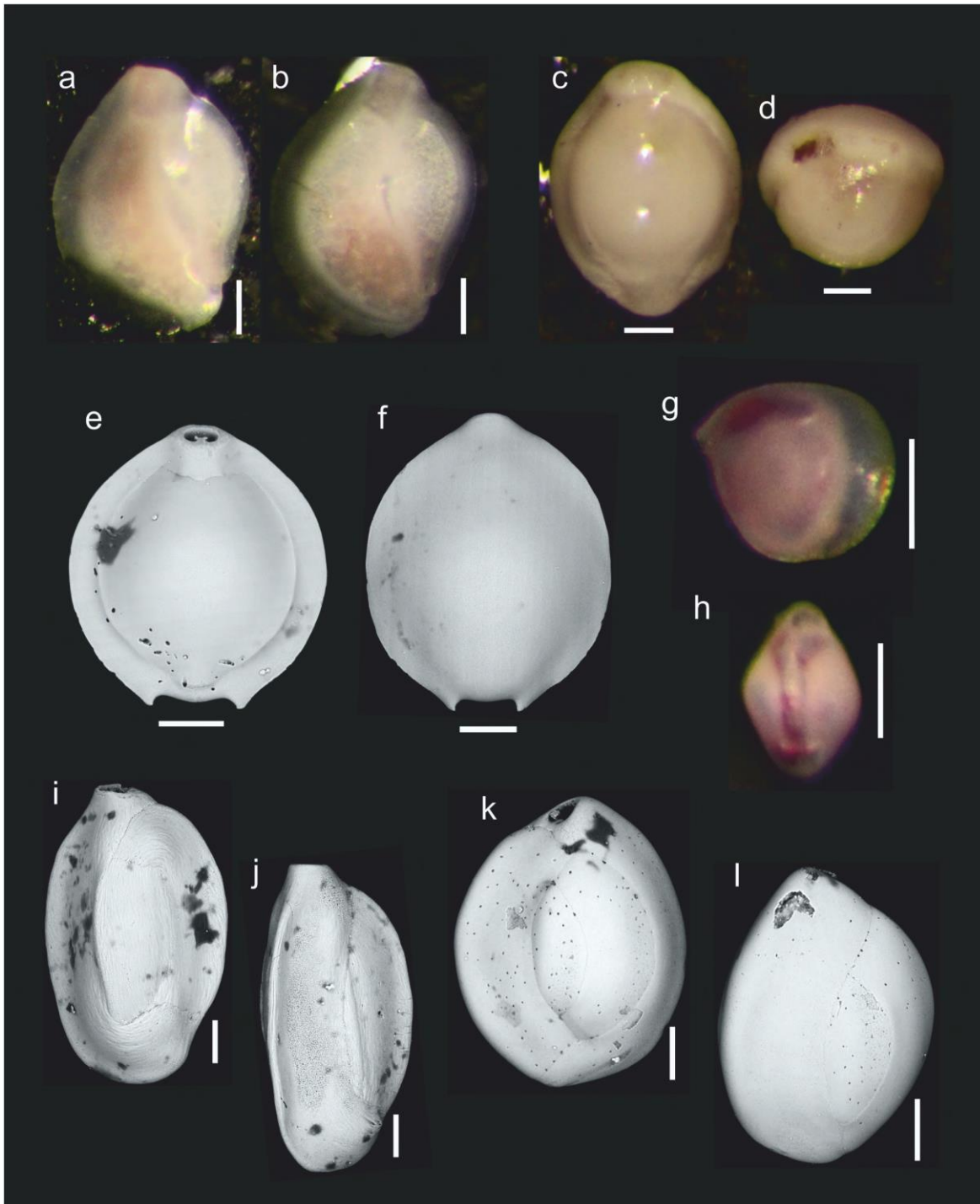


Fig. A.18. SEM and light (reflected) images. a–b) *Edentostomina pseudodepressa*, c–d) *Pyrgo fischeri*, e–f) *Pyrgo murrhina*, g–h) *Pyrgoella* sp, i–j) *Quinqueloculina venusta*, k–l) *Quinqueloculina* sp. 2. Scale bars = 100 μ m.

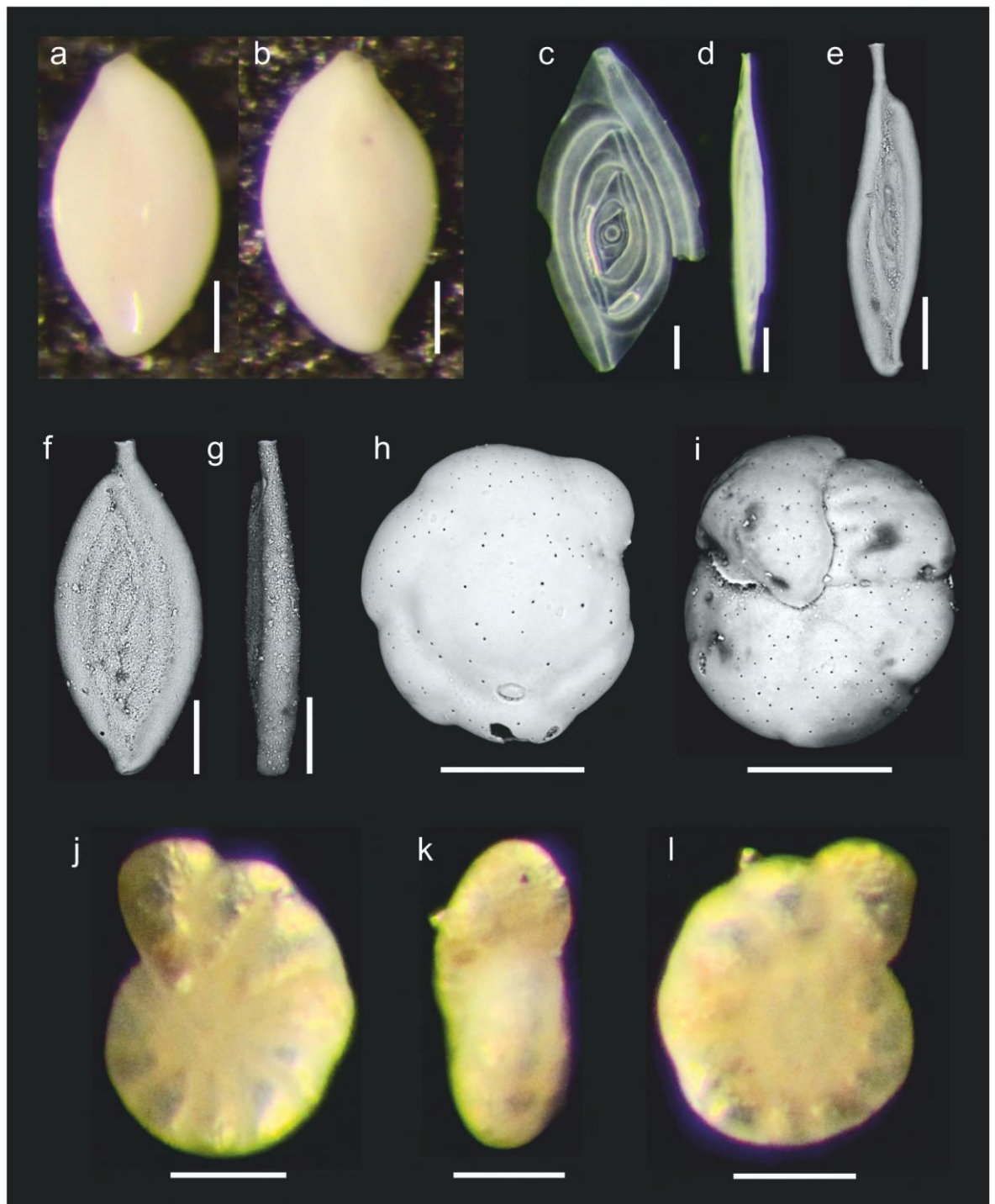


Fig. A.19. SEM and light (reflected) images. a–b) *Quinqueloculina* sp. 3, c–d) *Spirophthalmidium acutimargo*, e) *Spirosigmoilina pussila*, f–g) *Spirosigmoilina tenuis*, h–i) *Alabaminella weddellensis*, j–l) *Anomalinooides colligera*. Scale bars = 100 μ m.

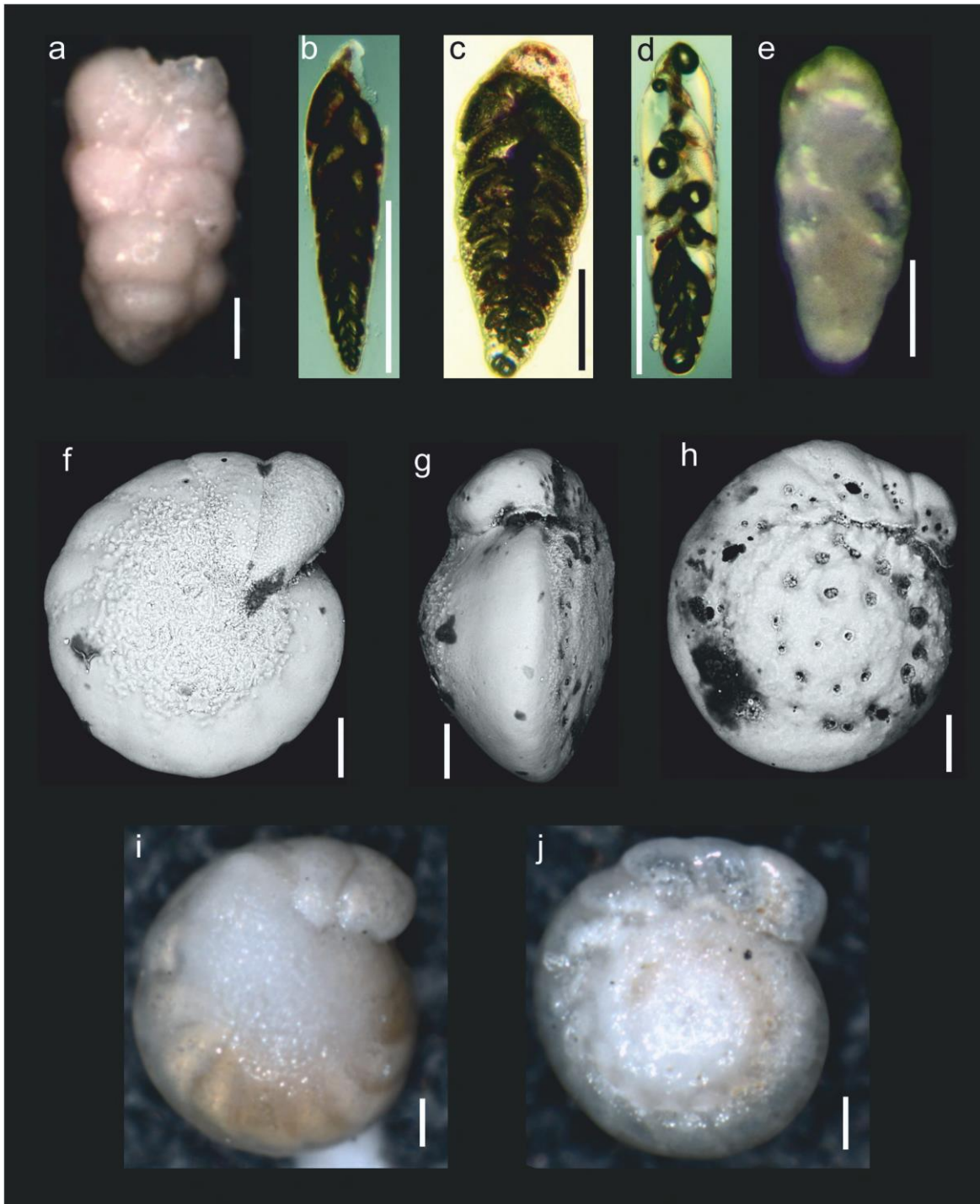


Fig. A.20. SEM and light (reflected, transmitted) images. a) *Bolivina decussata*, b) *Bolivina* aff. *earlandi*, c) *Bolivina spathulata*, d) *Bolivina* sp. 1, e) *Bulimina elongata*, f–j) *Cibicides lobatulus*. Scale bars = 100 μm .

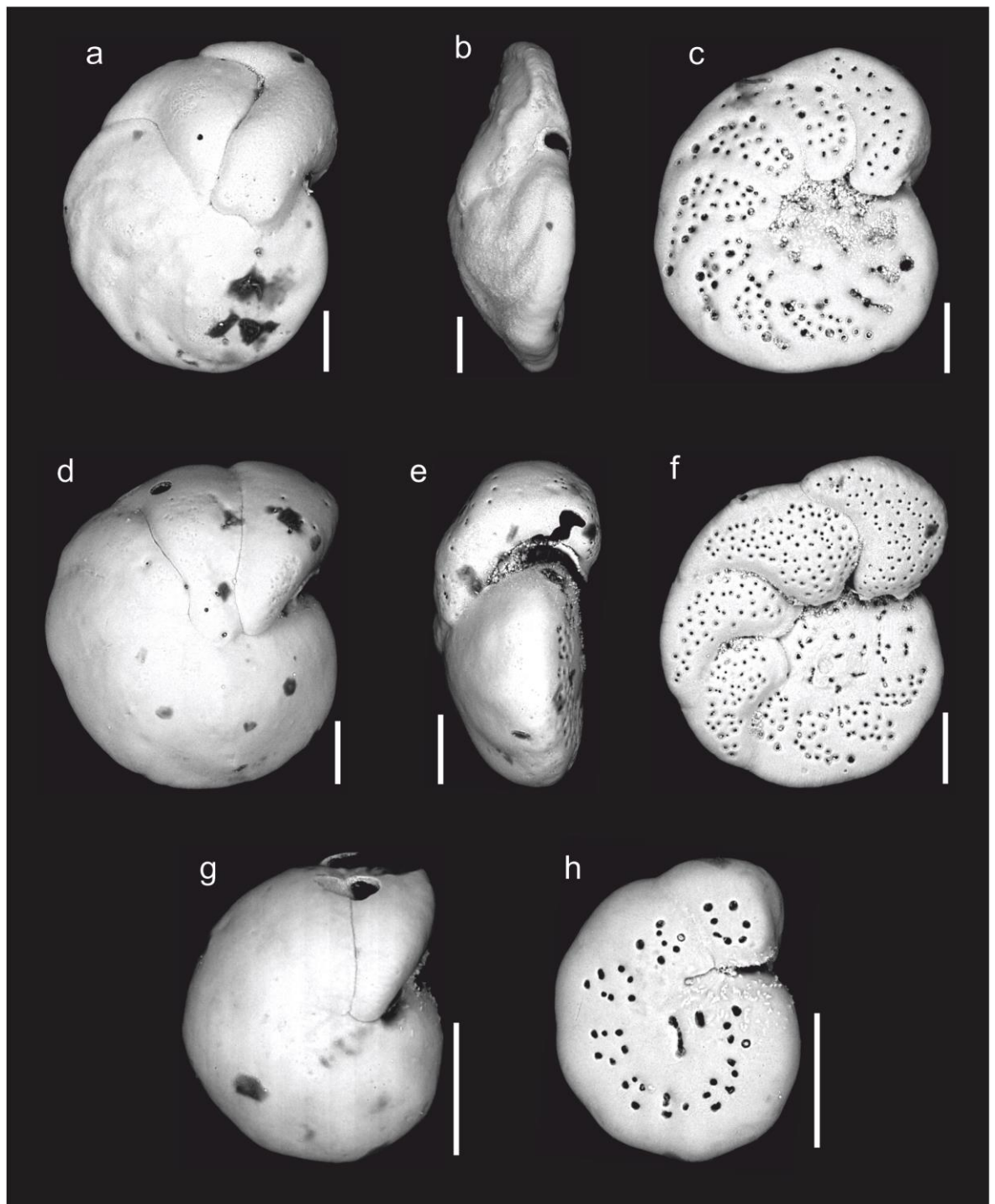


Fig. A.21. SEM images. a–c) *Cibicides wuellerstorfi*, d–f) *Cibicoides kullenbergi*, g–h) *Cibicoides subhaidingerii*. Scale bars = 100 μm .

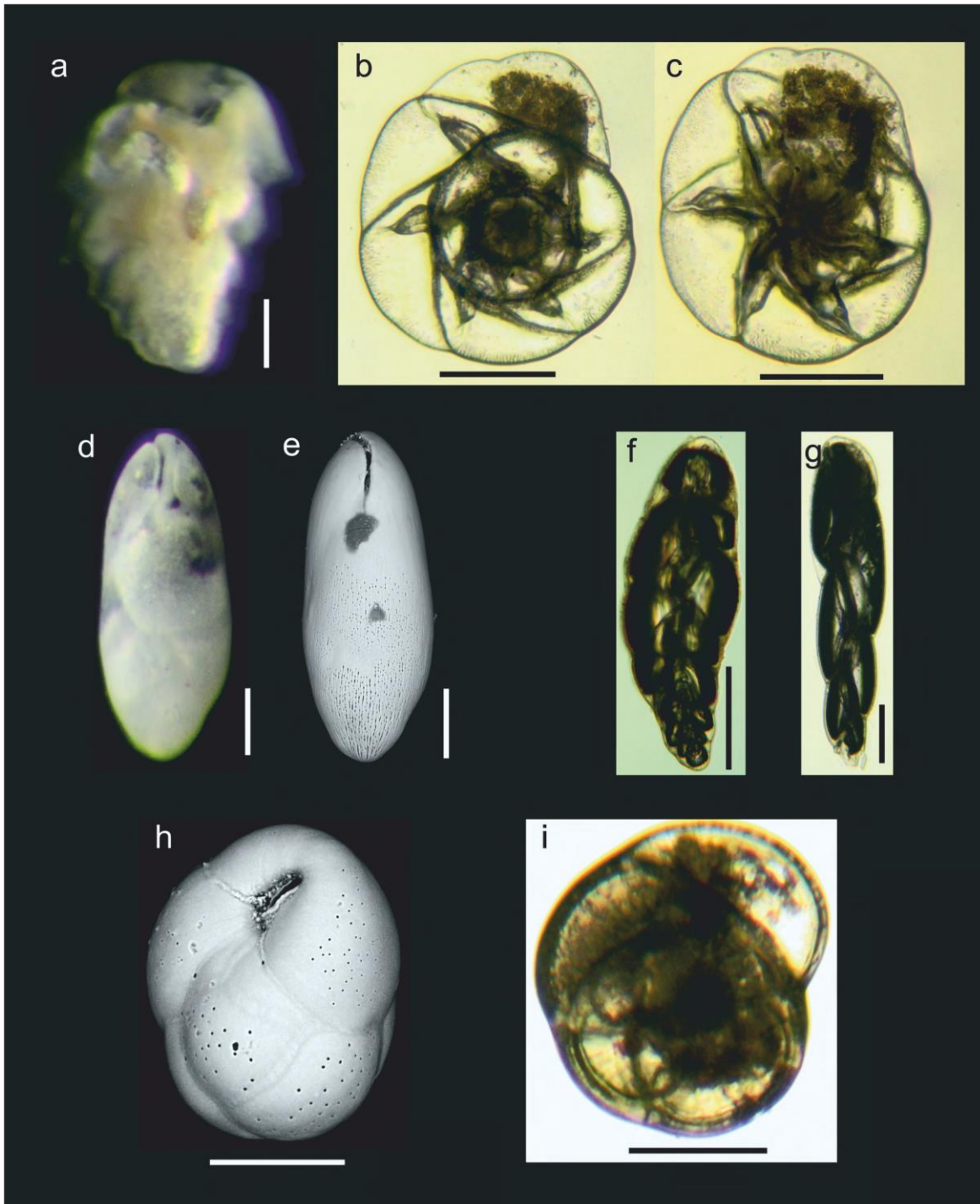


Fig. A.22. SEM and light (reflected, transmitted) images. a) *Ehrenbergina trigona*, b–c) *Epistominella exigua*, d–e) *Francesita* sp., f) *Fursenkoina bradyi*, g) *Fursenkoina complanata*, h–i) *Globocassidulina subglobosa*. Scale bars = 100 μm.

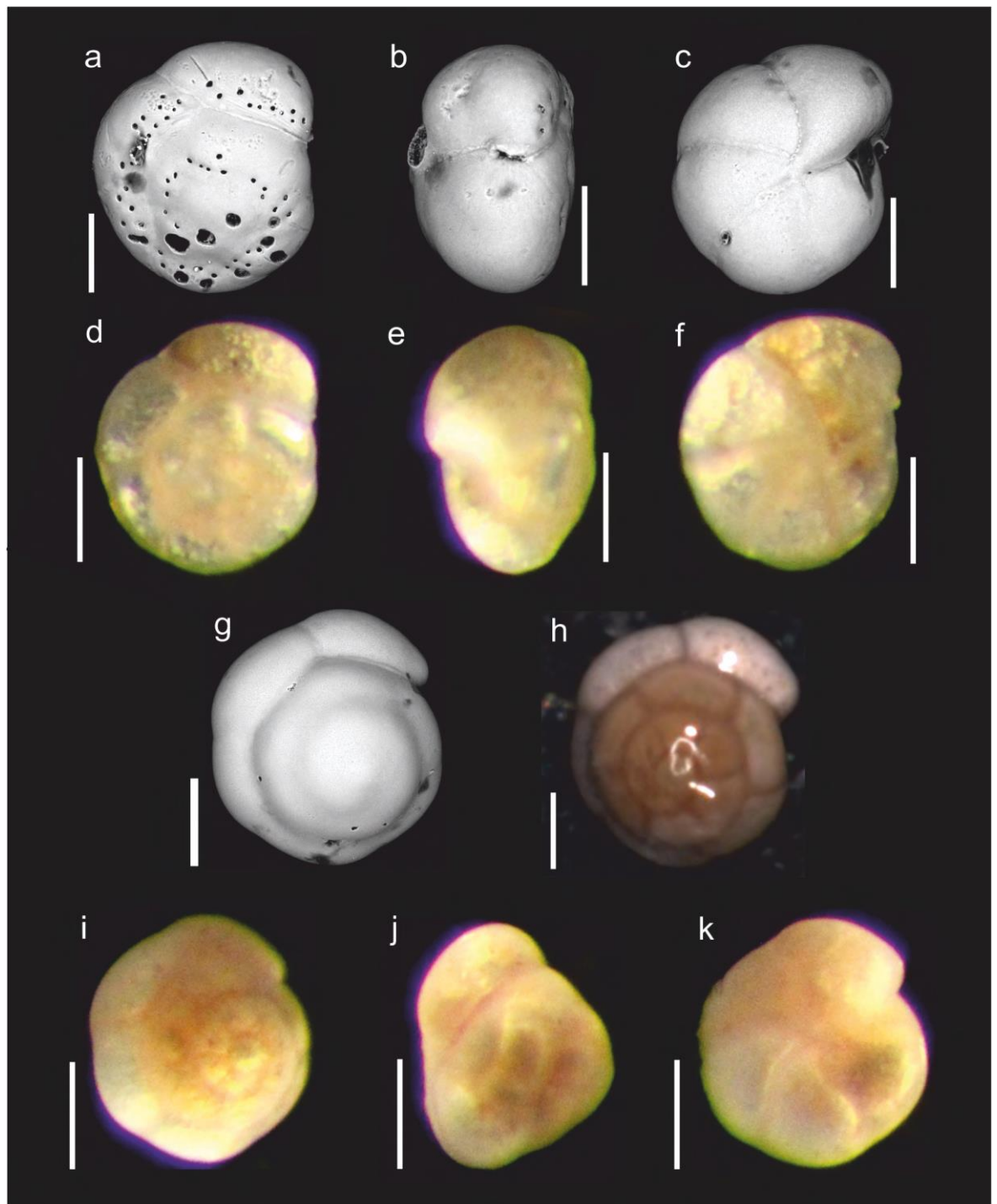


Fig. A.23. SEM and light (reflected) images. a–f) *Gyroidina bradyi*, g–k) *Gyroidina* aff. *broeckhiana*. Scale bars = 100 μ m.

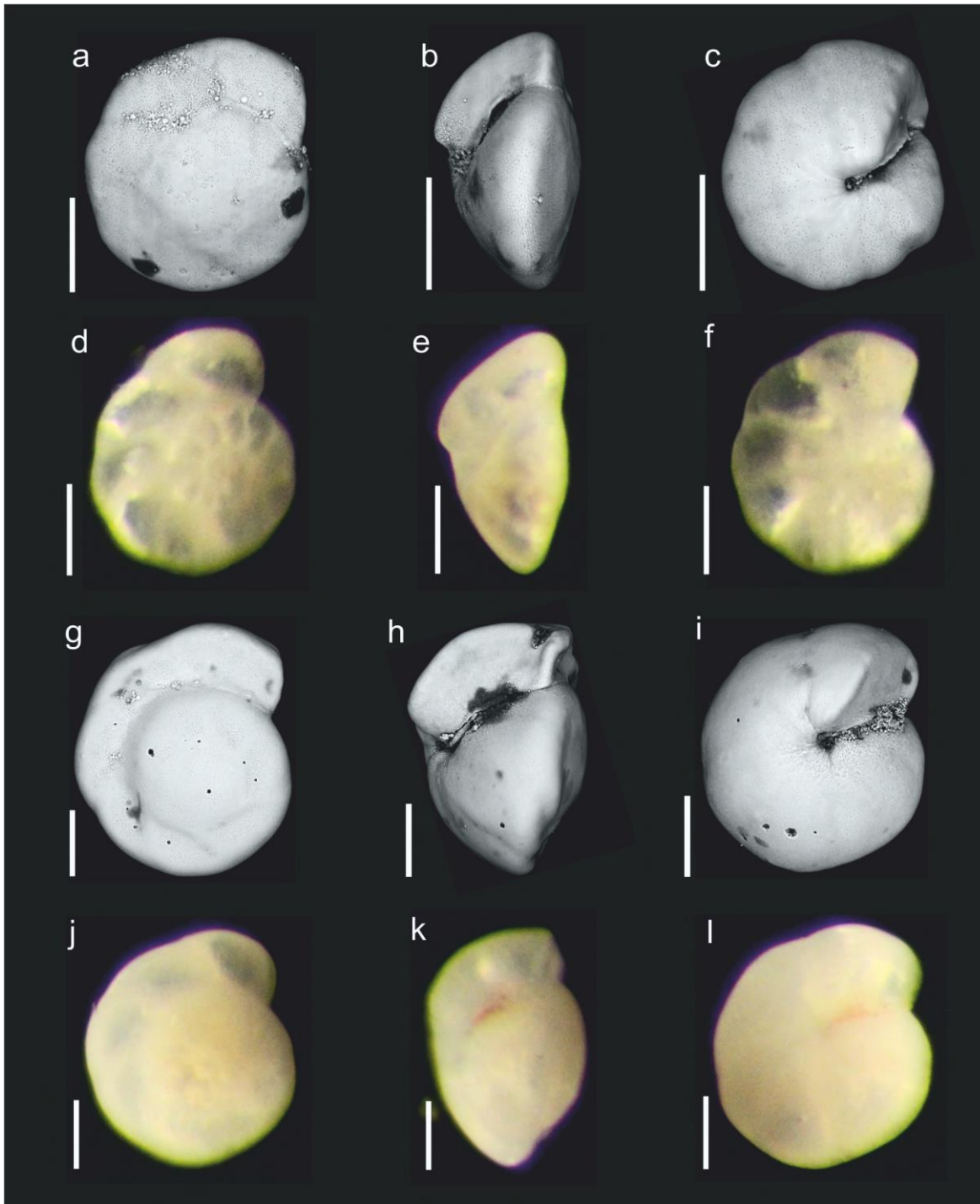


Fig. A.24. SEM and light (reflected) images. a–f) *Gyroidina polia*, g–l) *Gyroidina* aff. *soldanii*. Scale bars = 100 μm.

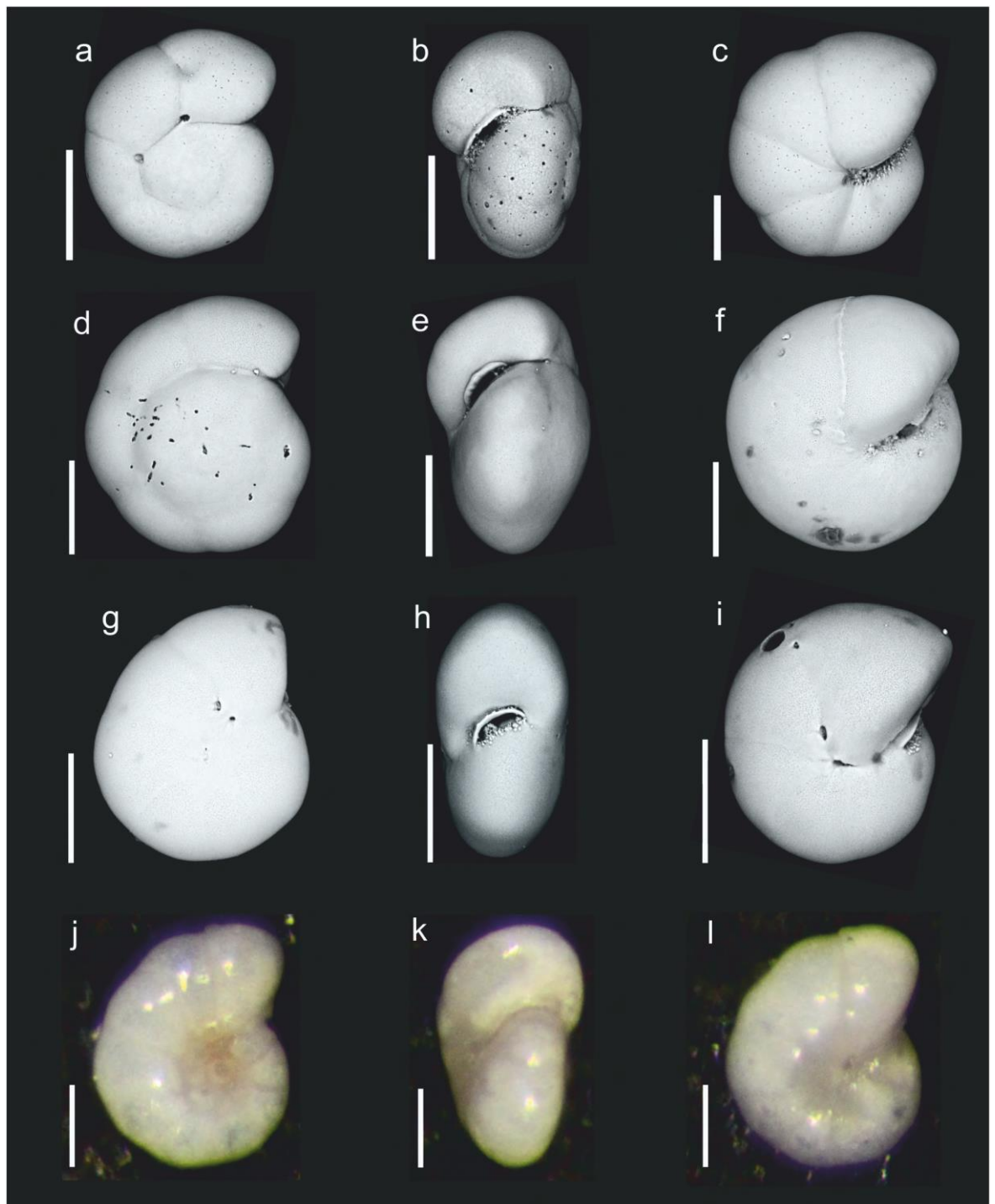


Fig. A.25. SEM and light (reflected) images. a–c) *Gyroidina umbonata*, d–f) *Gyroidina* sp. 1, g–i) *Gyroidina* sp. 2, j–l) *Gyroidina* sp. 3. Scale bars = 100 μ m.

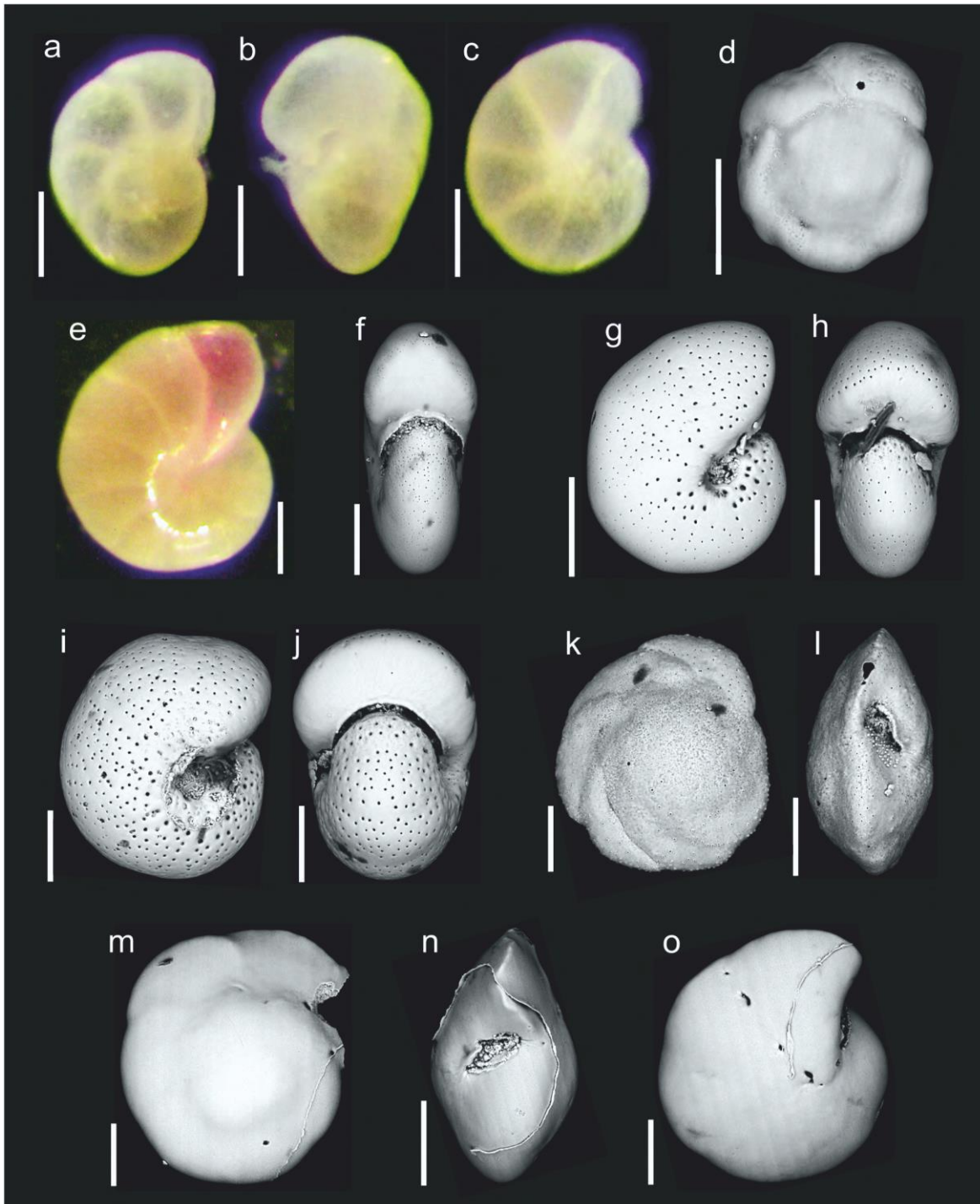


Fig. A.26. SEM and light (reflected) images. a–c) *Gyroidina* sp. 4, d) *Ioanella tumidula*, e–h) *Melonis barleeanus*, i–j) *Melonis pompilioides*, k–l) *Nuttallides umboniferus*, m–o) *Oridorsalis tenerus*. Scale bars = 100 μ m.

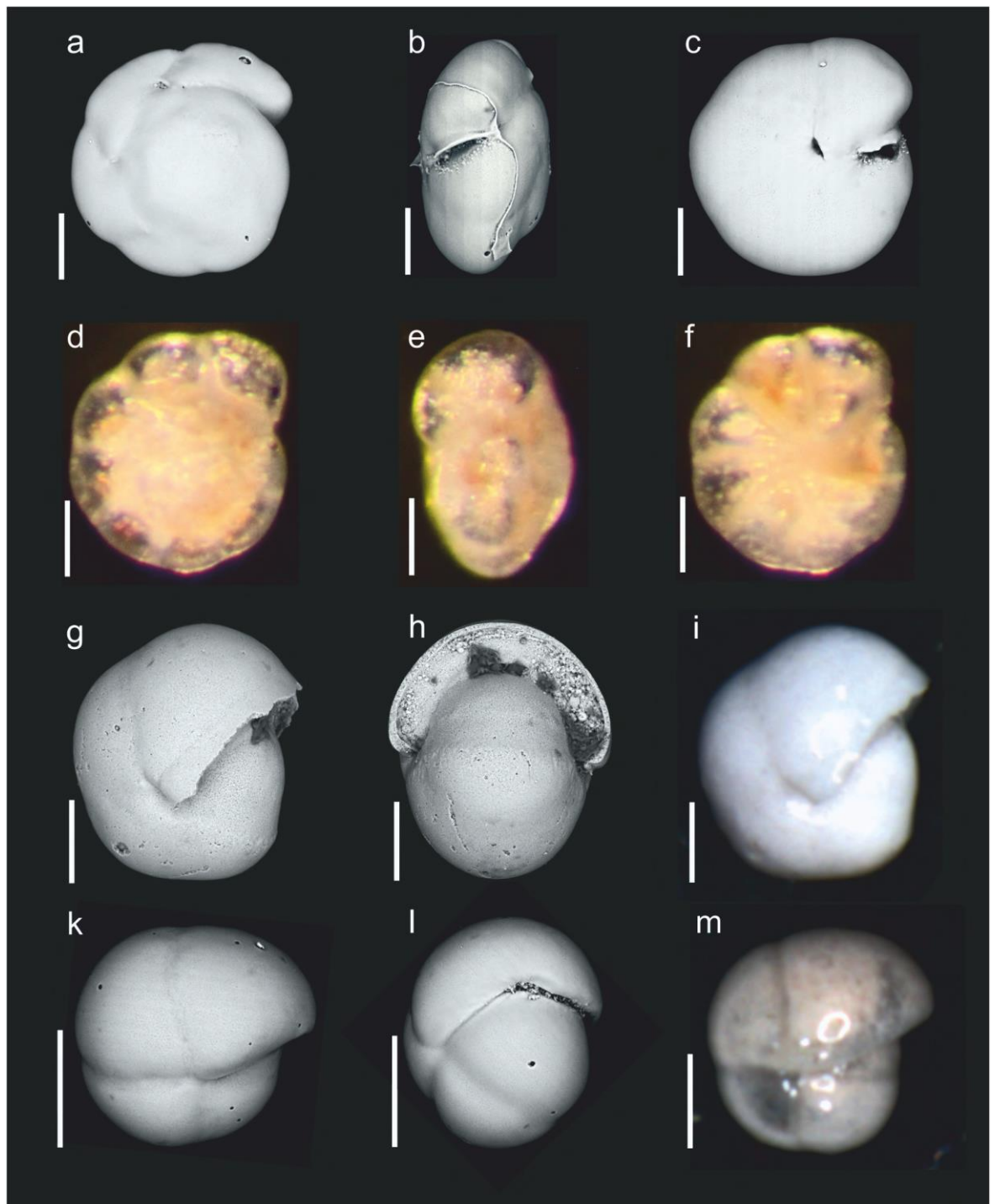


Fig. A.27. SEM and light (reflected) images. a–c) *Oridorsalis umbonatus*, d–f) *Oridorsalis* sp. 3, g–i) *Pullenia bulloides*, k–m) *Pullenia osloensis*. Scale bars = 100 μ m.

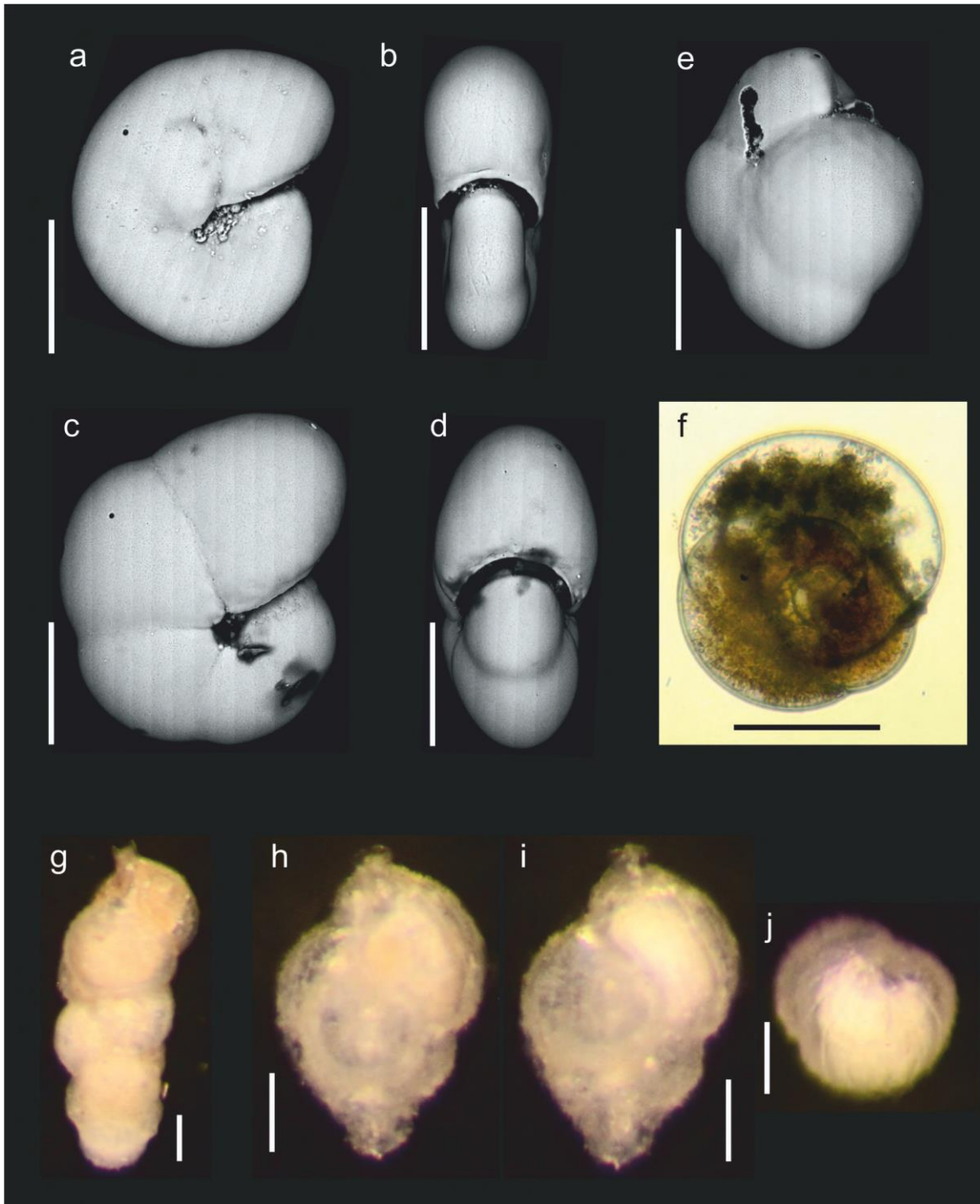


Fig. A.28. SEM and light (reflected, transmitted) images. a–b) *Pullenia simplex*, c–d) *Pullenia* sp. 1, e) Rotaliid sp., f) *Sphaeroidina bulloides*, g) *Uvigerina brunnensis*, h–j) *Uvigerina mediterranea*. Scale bars = 100 μ m.

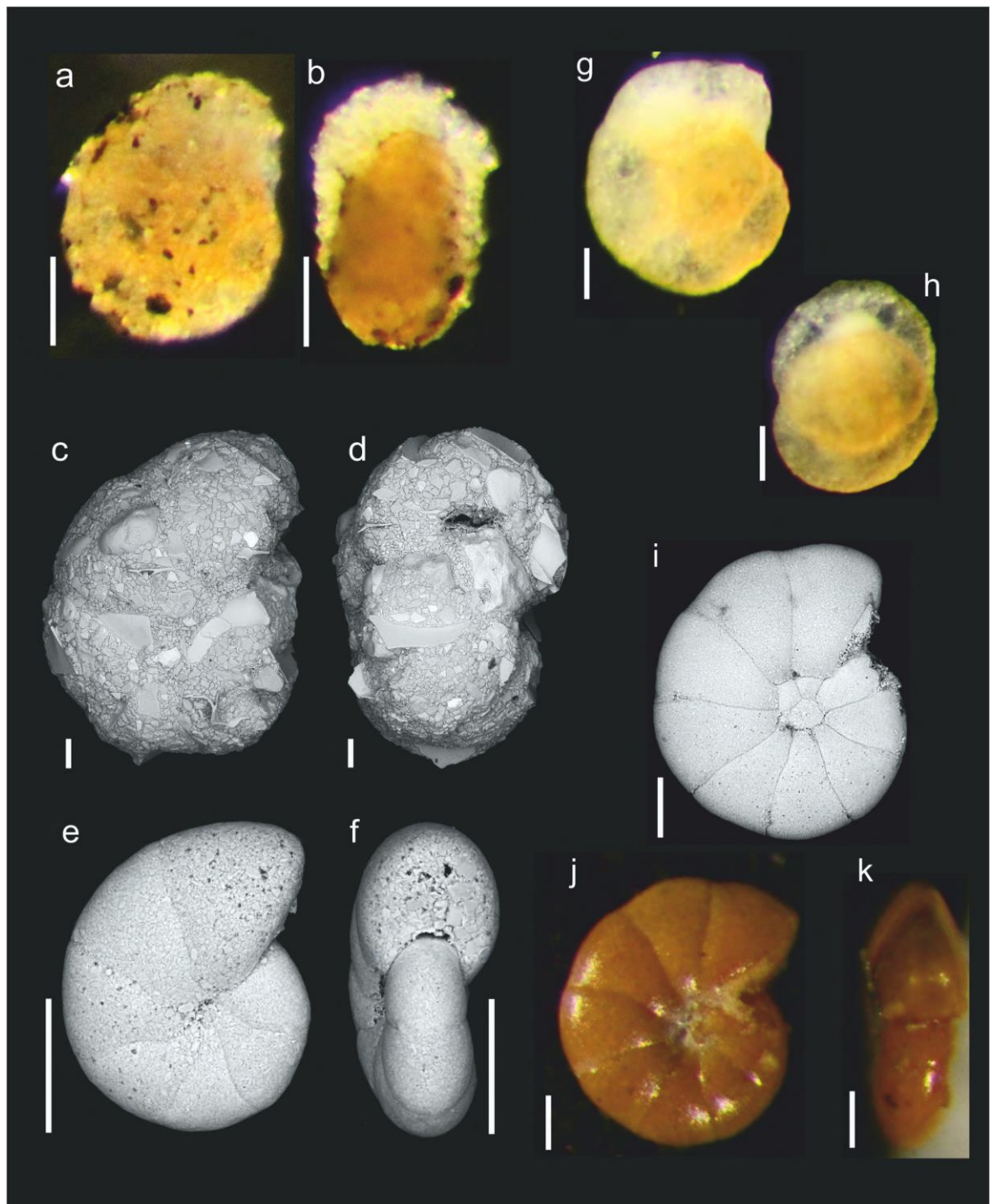


Fig. A.29. SEM and light (reflected) images. a–b) *Ammobaculites agglutinans*, c–d) *Cribrostomoides subglobosus*, e–f) *Cribrostomoides* sp. 1, g–h) *Cribrostomoides* sp. 2, i–k) *Cyclammmina trullissata*. Scale bars = 100 µm.

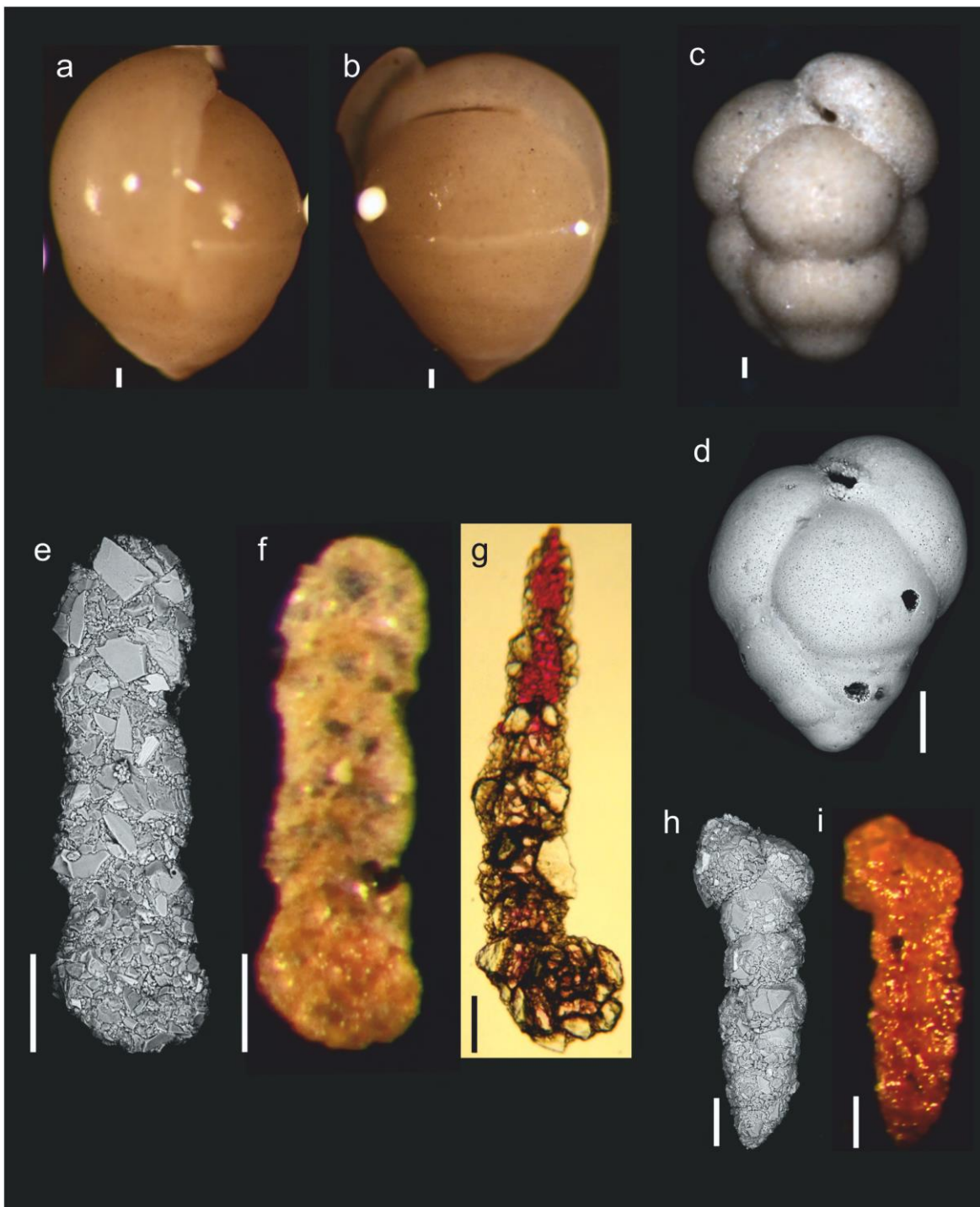


Fig. A.30. SEM and light (reflected, transmitted) images. a–b) *Dorothia inflata*, c–d) *Eggerella bradyi*, e–g) *Eratidus foliaceus*, h–i) *Karrerulina apicularis*. Scale bars = 100 μm .

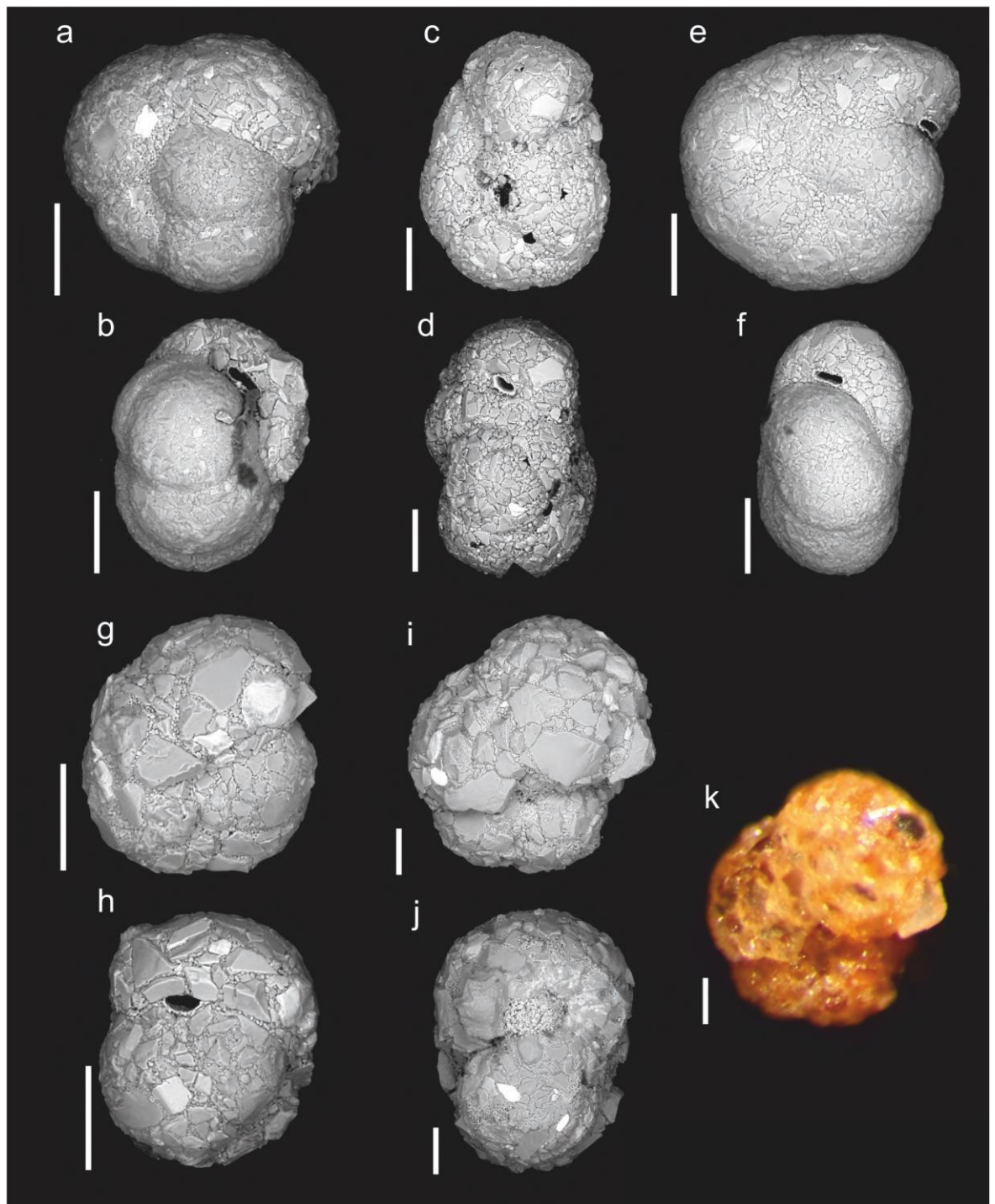


Fig. A.31. SEM and light (reflected) images. a–f) *Recurvoides contortus*, g–h) *Recurvoides* sp. 1, i–k) *Recurvoides* sp. 4. Scale bars = 100 μm .

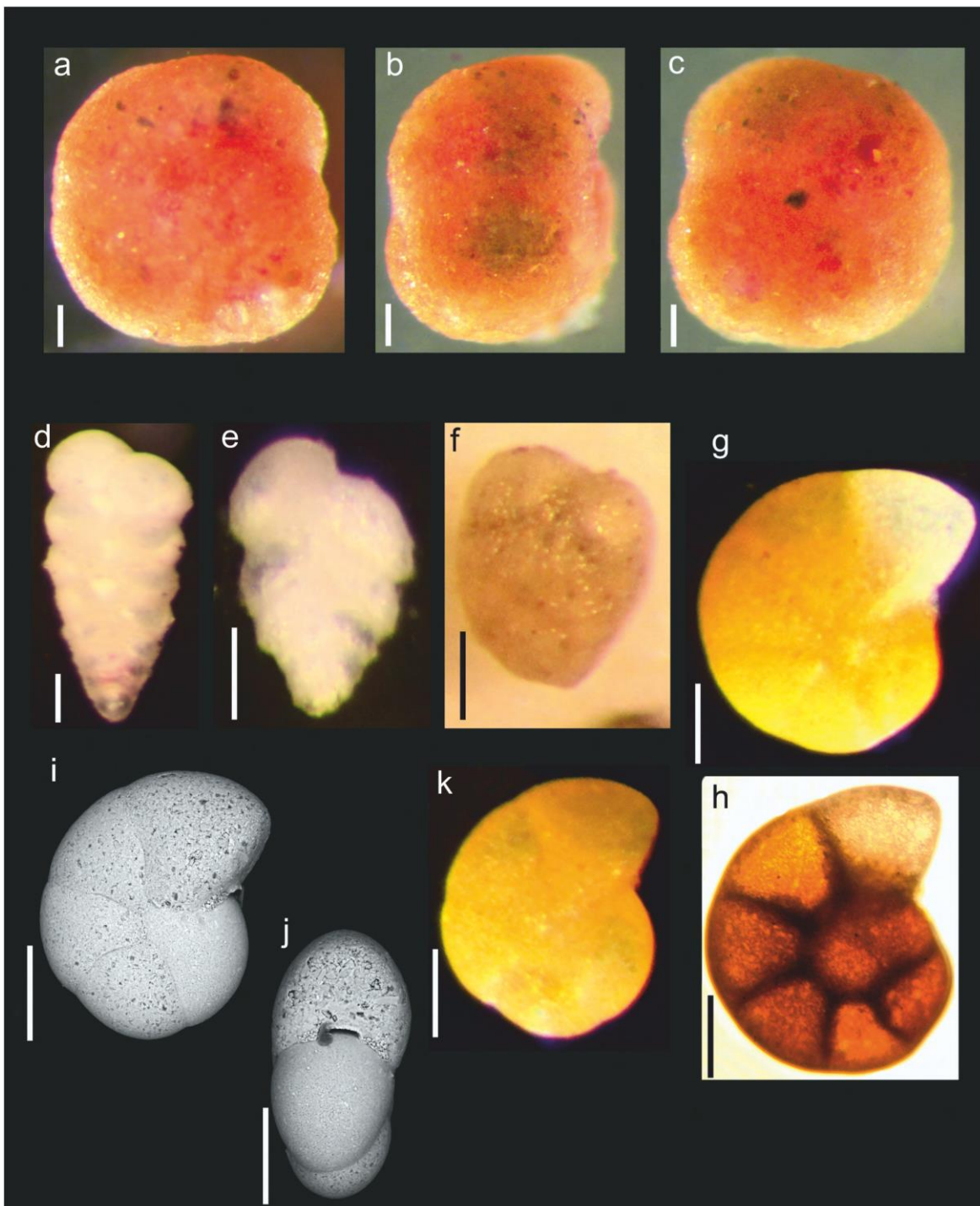


Fig. A.32. SEM and light (reflected, transmitted) images. a–c) *Recurvoides* sp. 8, d) *Textularia* sp. 1, e) *Textularia* sp. 3, f) Textulariid sp. 1, g–k) *Veleroninoides* sp. 1. Scale bars = 100 μ m.

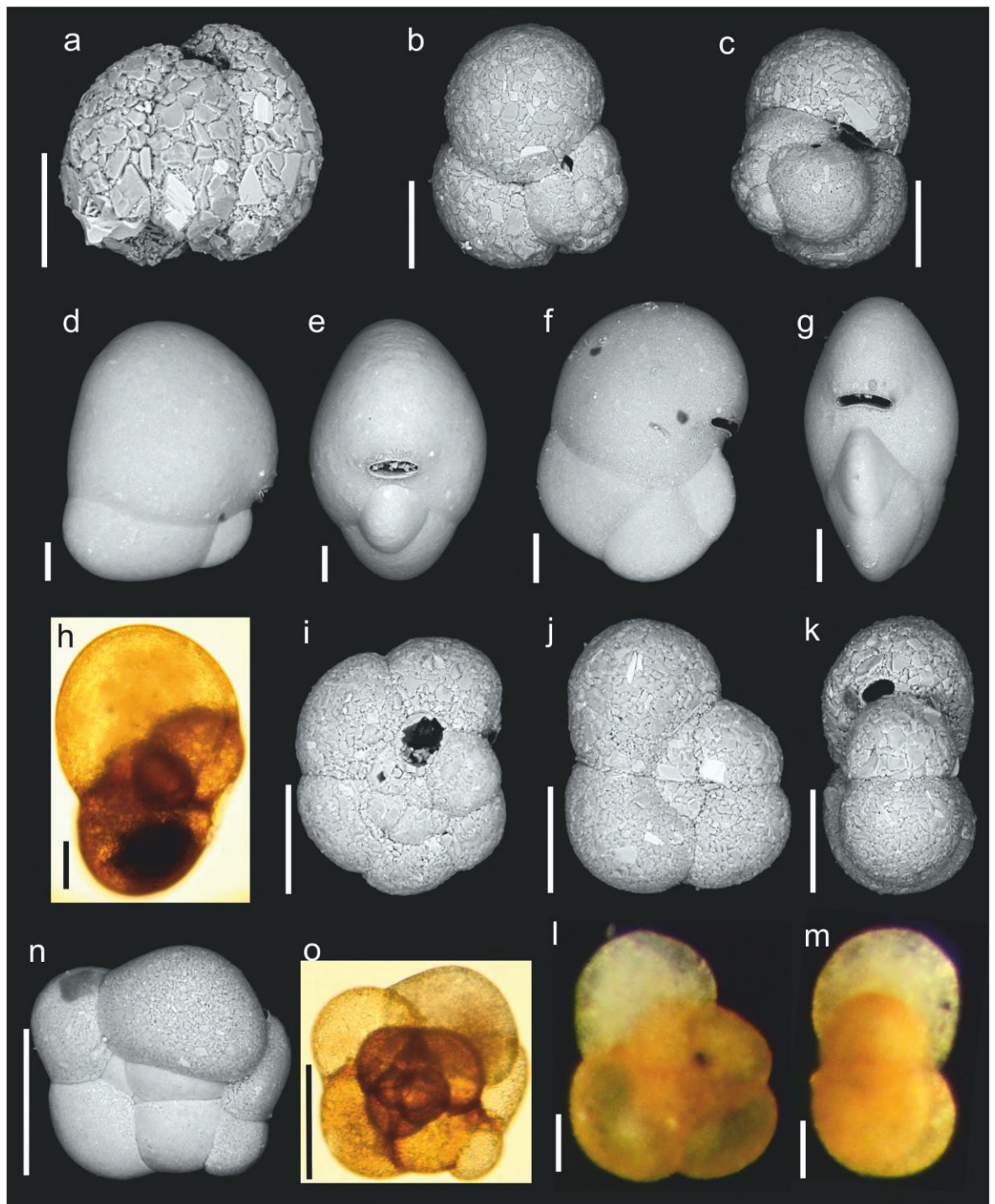


Fig. A.33. SEM and light (reflected, transmitted) images. a) *Adercotryma glomerata*, b–c) *Ammoglobigerina shannoni*, d–e) *Buzasina galeata*, f–g) *Buzasina ringens*, h) *Cystammina paucilocilata*, i) *Deuterammina montagui*, j–m) *Haplophragmoides sphaeriloculum*, n–o) *Haplophragmoides* sp. 2. Scale bars = 100 μ m.

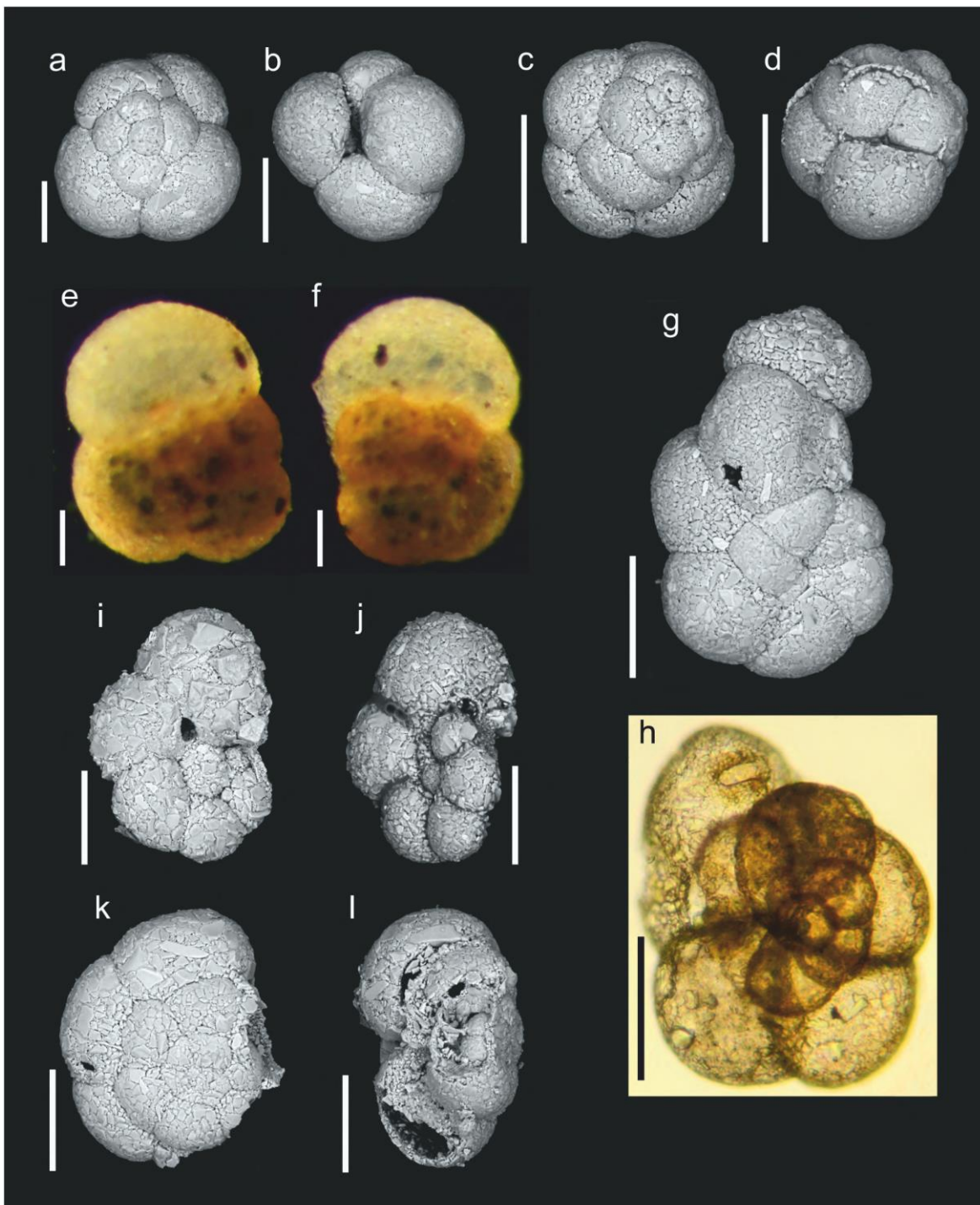


Fig. A.34. SEM and light (reflected, transmitted) images. a–b) *Paratrochammina challengeri*, c–d) *Paratrochammina* aff. *scotiaensis*, e–f) *Portatrochammina murrayi*, g–h) *Pseudotrochammina arenacea*, i–j) *Trochammina heronalleni*, k–l) *Trochammina* sp. 1. Scale bars = 100 μm .

References of Appendix A

- Brady, H.B., 1884. Report on the Foraminifera dredged by H.M.S. Challenger during the years 1873–1876: Report of the Scientific Results of the Voyage of H.M.S. Challenger, 1873–1876. *Zoology*, 9, 1–814.
- Brönnimann, P., Whittaker, J.E., 1980. A revision of *Reophax* and its type species with remarks on several other recent hormosinids (Protozoa: Foraminifera) in the collections of the British Museum (Natural History). *Bulletin of the British Museum (Natural History) Zoology*, 39, 259–272.
- Brönnimann, P., Zaninetti, L., 1984. Agglutinated foraminifera mainly Trochamminacea from the Baia de Sepetiba, near Rio de Janeiro, Brazil. *Revue de Paléobiologie*, 3, 63–115.
- Brönnimann, P., Whittaker, J.E., 1987. A revision of the foraminiferal genus *Adercotryma* Loeblich & Tappan, with a description of *A. wrighti* sp. nov. from British waters. *Bulletin British Museum Natural History (Zoology)*, 52, 19–28.
- Brönnimann, P., Whittaker, J.E., 1988. *The Trochamminacea of the Discovery Reports*. British Museum (Natural History), London.
- Cartwright, N.G., Gooday, A.J., Jones, A.R., 1989. The morphology, internal organization, and taxonomic position of *Rhizammina algaeformis* Brady, a large, agglutinated, deep-sea foraminifer. *Journal of Foraminiferal Research*, 19, 115–125.
- Colom, G., 1945. Estudio preliminar de las microfaunas de foraminíferos de las margas eocenas y oligocenas de Navarra. *Spain. Inst. Invest. Geol. "Lucas Mallada", Estud. Geol.*, Vol. 2 (pp. 35-84). Madrid.
- Corliss, B.H., 1979. Taxonomy of recent deep-sea benthonic foraminifera from the southeast Indian Ocean. *Micropaleontology*, 25, 1–19.
- Cushman, J.A., 1910. A monograph of the foraminifera of the North Pacific Ocean. Part I. Astrorhizidae and Lituolidae. *Bulletin of the United States National Museum*, 71, 1–134.
- Cushman, J.A., 1912. New arenaceous foraminifera from the Philippine Islands and contiguous waters. *Proceedings of the United States National Museum*, 42, 227–230.
- Cushman, J.A., 1913. A monograph of the Foraminifera of the North Pacific Ocean. Part III. Lagenidae. *Bulletin of the United States National Museum*, 71, 1–125.
- Cushman, J.A., 1918. The foraminifera of the Atlantic Ocean. Part 1. Astrorhizidae. *Bulletin of the United States National Museum*, 104, 1–111.
- Cushman, J.A., 1920. The foraminifera of the Atlantic Ocean. Part 2. Lituolidae. *Bulletin of the United States National Museum*, 104, 1–111.
- Cushman, J.A., 1921. Foraminifera of the Philippines and adjacent seas. *United States National Museum Bulletin*, 4, 1–488.
- Cushman, J.A., 1922. The foraminifera of the Atlantic Ocean. Part 3. Textulariidae. *Bulletin of the United States National Museum*, 104, 1–149.

- Cushman, J.A., 1931. The foraminifera of the Atlantic Ocean. Part 8. Rotaliidae, Amphisteginidae, Calcarinidae, Cymbaloporetidae, Globorotaliidae, Anomalinidae, Planorbulinidae, Rupertiidae, and Homotremidae. *Bulletin of the United States National Museum*, 104, 1–179.
- Dorst, S., Schönfeld, J., 2015. Taxonomic notes on recent benthic foraminiferal species of the family Trochamminidae from the Celtic Sea. *Journal of Foraminiferal Research*, 45, 167–189.
- Duchemin, G., Fontanier, C., Jorissen, F.J., Barras, C., Griveaud, C., 2007. Living small-sized (63–150 µm) foraminifera from mid-shelf to mid-slope environments in the Bay of Biscay. *Journal of Foraminiferal Research*, 37, 12–32.
- Earland, A., 1933. Foraminifera. Part II. South Georgia. *Discovery Reports*, Vol. 7 (pp. 27–138).
- Earland, A., 1934. Foraminifera. Part III. The Falklands sector of the Antarctic (excluding South Georgia). *Discovery Reports*, Vol. 10 (pp. 1–208).
- Earland, A., 1936. Foraminifera. Part IV. Additional records from the Weddel Sea sector from material obtained by the S.Y. 'Scotia'. *Discovery Reports*, Vol. 10 (pp. 1–76).
- Enge, A.J., Kucera, M., Heinz, P., 2012. Diversity and microhabitats of living benthic foraminifera in the abyssal Northeast Pacific. *Marine Micropaleontology*, 96–97, 84–104.
- Feyling-Hanssen, R.W., 1954. The stratigraphic position of the Quick Clay at Bekkelaget, Oslo. *Norsk Geologisk Tidsskrift*, 33, 185–197.
- Flint, J.M., 1899. Recent foraminifera. A descriptive catalogue of specimens dredged by the U.S. Fish Commission steamer Albatross. *Report of the United States National Museum for 1897* (pp. 249–349).
- Gooday, A.J., 1986. Meiofaunal foraminiferans from the bathyal Porcupine Seabight (northeast Atlantic): size structure, standing stock, taxonomic composition, species-diversity and vertical-distribution in the sediment. *Deep Sea Research Part A—Oceanographic Research Papers*, 33, 1345–1373.
- Gooday, A.J., 1988. A response by benthic foraminifera to the deposition of phytodetritus in the deep sea. *Nature*, 332, 70–73.
- Gooday, A.J., 1990. *Tinogullmia riemanni* sp. nov. (Allogromiina; Foraminiferida), a new species associated with organic detritus in the deep sea. *Bulletin British Museum Natural History (Zoology)*, 56, 93–103.
- Gooday, A.J., Carstens, M., Thiel, H., 1995. Microforaminifera and nanoforaminifera from abyssal northeast Atlantic sediments: a preliminary report. *Internationale Revue Der Gesamten Hydrobiologie*, 80, 361–383.
- Gooday, A.J., 1996. Epifaunal and shallow infaunal foraminiferal communities at three abyssal NE Atlantic sites subject to differing phytodetritus input regimes. *Deep-Sea Research Part I—Oceanographic Research Papers*, 43, 1395–1421.
- Gooday, A.J., Hughes, J.A., 2002. Foraminifera associated with phytodetritus deposits at a bathyal site in the northern Rockall Trough (NE Atlantic): seasonal contrasts and a comparison of stained and dead assemblages. *Marine Micropaleontology*, 46, 83–110.

- Gooday, A.J., Hori, S., Todo, Y., Okamoto, T., Kitazato, H., Sabbatini, A., 2004. Soft-walled, monothalamous benthic foraminiferans in the Pacific, Indian and Atlantic Oceans: aspects of biodiversity and biogeography. *Deep-Sea Research Part I—Oceanographic Research Papers*, 51, 33–53.
- Gooday, A.J., Malzone, M.G., Bett, B.J., Lamont, P.A., 2010. Decadal-scale changes in shallow-infaunal foraminiferal assemblages at the Porcupine Abyssal Plain, NE Atlantic. *Deep-Sea Research Part II—Topical Studies in Oceanography*, 57, 1362–1382.
- Gooday, A.J., Jorissen, F.J., 2012. Benthic foraminiferal biogeography: controls on global distribution patterns in deep-water settings. *Annual Review of Marine Science*, 4, 237–262.
- Haake, F.-W., 1977. Living benthic foraminifera in the Adriatic Sea: influence of water depth and sediment. *The Journal of Foraminiferal Research*, 7, 62–75.
- Hayward, B.W., Grenfell, H.R., Sabaa, A.T., Neil, H.L., Buzas, M.A., 2010. *Recent New Zealand deep-water benthic foraminifera: taxonomy, ecologic distribution, biogeography, and use in paleoenvironmental assessment*. Lower Hutt, New Zealand.
- Heron-Allen, E., Earland, A., 1913. On some foraminifera from the North Sea, etc, dredged by the Fisheries cruiser 'Goldseeker' (International North Sea Investigations—Scotland). II. On the distribution of *Saccamina sphaerica* (M. Sars) and *Psammosphaera fusca* (Schulze) in the North Sea: particularly with reference to the suggested identity of the two species. *Journal of the Royal Microscopical Society*, 1–26.
- Höglund, H., 1947. Foraminifera of the Gullmar Fjord and the Skagerak. *Zoologiska bidrag från Uppsala*, 26, 1–328.
- Holbourn, A.E.L., Henderson, A.S., MacLeod N., 2013. *Atlas of benthic foraminifera*. Natural History Museum.: Blackwell Publishing Ltd.
- Jones, R.W., 1984. A revised classification of the unilocular Nodosariida and Buliminida (Foraminifera). *Revista Espanola de Micropaleontologia*, 16, 91–160.
- Jones, R.W., 1994. *The Challenger Foraminifera*. The Natural History Museum, London: Oxford University Press.
- Kaminski, M.A., Kuhnt, W., 1991. Depth-related shape variation in *Ammobaculites agglutinans*. *Annales Societatis Geologorum Poloniae*, 61.
- Kaminski, M.A., Gradstein, F.M., 2005. *Atlas of paleogene cosmopolitan deep-water agglutinated foraminifera*.
- Kuhnt, W., Collins, C., Scott, D.B., 2000 Deep-water agglutinated foraminiferal assemblages across the Gulf Stream: distribution patterns and taphonomy. In: Hart, M.B., Kaminski, M.A., Smart, C.W. (Eds.), *Proceedings of the 5th International Workshop on Agglutinated Foraminifera* (pp. 261–298).
- Loeblich, A.R., Tappan, H., 1987. *Foraminiferal genera and their classification*. New York: Van Nostrand Reinhold.
- Lohmann, G.P., 1978. Abyssal benthonic foraminifera as hydrographic indicators in the western South Atlantic Ocean. *The Journal of Foraminiferal Research*, 8, 6–34.

- Mohan, K., Gupta, A.K., Bhaumik, A.K., 2011. Distribution of deep-sea benthic foraminifera in the Neogene of Blake Ridge, NW Atlantic Ocean. *Journal of Micropalaeontology*, 30, 33–74.
- Murray, J.W., Alve, E., 1994. High diversity agglutinated foraminiferal assemblages from the NE Atlantic: dissolution experiments. In: Sejrup, H.P., Knudsen, K.L. (Eds.), *Late Cenozoic benthic foraminifera: taxonomy, ecology and stratigraphy* (pp. 33–51).
- Murray, J.W., Alve, E., 2011. The distribution of agglutinated foraminifera in NW European seas: Baseline data for the interpretation of fossil assemblages. *Palaeontologia Electronica*, 14, 1–41.
- Parr, W.J., 1950. Foraminifera. *Reports B.A.N.Z. Antarctic Research Expedition 1929–1931, Series B (Zoology, Botany)*, 5, 232–392.
- Phleger, F.B., Parker, F.L., 1951. Ecology of foraminifera, northwest Gulf of Mexico. Part II. Foraminifera species. *Geological Society of America Memoir*, 46, 1–64.
- Rhumbler, L., 1904. Systematische Zusammenstellung der recenten Reticulosa (Nuda + Foraminifera). Teil 1. *Archiv für Protistenkunde*, 3, 181–294.
- Rhumbler, L., 1911. *Die Foraminiferen (Thalamophoren) der Plankton Expedition. Part 1. Die allgemeinen Organisationsverhältnisse der Foraminiferen*. Kiel und Leipzig.
- Schiebel, R., 1992. Rezente benthische Foraminiferen in Sedimenten des Schelfes und oberem Kontinentalhang im Golf von Guinea (Westafrika). *Berichte–Reports, Geologisch-Paläontologisches Institut Universität Kiel*, 51, 1–179.
- Schlumberger, C., 1891. Revision des Biloculines des grands fonds. *Mémoires de la Société Zoologique de France*, 4, 542–579.
- Schröder, C.J., 1986. Deep-water arenaceous foraminifera in the northwest Atlantic Ocean. *Canadian Technical Report of Hydrography and Ocean Sciences*, 71, 1–191.
- Schröder, C.J., Scott, D.B., Medioli, F.S., Bernstein, B.B., Hessler, R.R., 1988. Larger agglutinated Foraminifera: comparison of assemblages from central North Pacific and Western North Atlantic (Nares Abyssal Plain). *Journal of Foraminiferal Research*, 18, 25–41.
- Silvestri, A., 1896. Foraminiferi Pliocenici della Provincia di Siena. Parte I. *Atti della Pontificia Accademia Romana dei Nuovi Lincei*, 12, 1–381.
- Stefanoudis, P.V., Gooday, A.J., 2015. Basal monothalamous and pseudochambered benthic foraminifera associated with planktonic foraminiferal shells and mineral grains from the Porcupine Abyssal Plain, NE Atlantic. *Marine Biodiversity*, 45, 357–369.
- Stefanoudis, P.V., Gooday, A.J., 2016. Formation of agglutinated cysts by the foraminiferan *Sphaeroidina bulloides* on the Porcupine Abyssal Plain (NE Atlantic). *Marine Biodiversity*, 1–3.
- Stefanoudis, P.V., Schiebel, R., Mallet, R., Durden, J.M., Bett, B.J., Gooday, A.J., 2016. Agglutination of benthic foraminifera in relation to mesoscale bathymetric features in the abyssal NE Atlantic (Porcupine Abyssal Plain). *Marine Micropaleontology*, 123, 15–28.
- Stewart, R.E., Stewart, K.C., 1930. Post-Miocene foraminifera from the Ventura quadrangle, Ventura County, California. *Journal of Paleontology*, 4, 60–72.

- Thomas, F.C., Medioli, F.S., Scott, D.B., 1990. Holocene and latest Wisconsinan benthic foraminiferal assemblages and paleocirculation history, lower Scotian slope and rise. *Journal of Foraminiferal Research*, 20, 212–245.
- Timm, S., 1992. Rezente Tiefsee-Benthosforaminiferen aus Oberflächen-sedimenten des Golfes von Guinea (Westafrika) - Taxonomie, Verbreitung, Ökologie und Korngrößenfraktionen. *Berichte–Reports, Geologisch-Päontologisches Institut und Christian-Albrechts-Universität Kiel*, 59, 1–155.
- Van Leeuwen, R.J.W., 1989. *Seafloor distribution and the Quaternary faunal patterns of planktonic and benthic Foraminifers in the Angola basin*. Utrecht, Netherlands.
- Weston, J.F., 1984. Wall structure of the agglutinated foraminifera *Eggerella bradyi* (Cushman) and *Karreriella bradyi* (Cushman). *Journal of Micropalaeontology*, 3, 29–31.
- Wiesner, H., 1931. Die Foraminiferen der deutschen Südpolar-Expedition. In: von Drygalski, E. (Ed.), *Deutsche Südpolar-Expedition* Berlin, Leipzig.
- Wollenburg, J.E., 1992. Zur Taxonomie von resented benthischen Foraminiferen aus dem Nansen Becken, Arktischer Ozean. *Berichte zur Polarforschung*, 112, 1–137.
- Wollenburg, J.E., Mackensen, A., 1998. Living benthic foraminifers from the central Arctic Ocean: faunal composition, standing stock and diversity. *Marine Micropaleontology*, 34, 153–185.
- Zheng, S., 1988. *The agglutinated and porcelaneous foraminifera of the East China Sea*. Beijing, China: Science Press.
- Zheng, S., Fu, Z., 2001. *Fauna Sinica; Phylum Granuloreticulosa, Class Foraminifera, Agglutinated Foraminifera*. Beijing, China: Science Press.

Appendix B Formation of agglutinated cysts by the foraminiferan *Sphaeroidina bulloides* on the Porcupine Abyssal Plain (NE Atlantic)

Benthic foraminiferal species sometimes produce a covering made of sediment and detrital material around their tests (shells). These sedimentary envelopes, termed 'cysts', have been observed in a number of species, from organic-walled and agglutinated to calcareous (e.g., Linke and Lutze 1993; Cedhagen 1996; Gross 2000, 2002; Gooday and Hughes 2002; Heinz et al. 2005). However, almost all published records of this phenomenon originate from coastal or bathyal settings, and there are very few examples from abyssal depths, i.e. deeper than 3500 m.

During the analysis of Megacorer samples (25.5 cm² surface area, formalin-buffered, 0–1 cm sediment horizon, >150 µm fraction) collected in the area of the Porcupine Abyssal Plain Sustained Observatory (PAP-SO) in the northeast Atlantic (49°N 16.5°W, 4850 m water depth), we observed benthic foraminifera that had created partial or complete muddy coatings. Most belonged to *Sphaeroidina bulloides* d'Orbigny 1826 (Fig. B.1), and a few to *Melonis barleeanus* (Williamson 1858). The *S. bulloides* cysts occasionally incorporated juvenile planktonic foraminiferal tests (<50 µm), and always included one or more flexible agglutinated tubes (20–35 µm wide, 140–400 µm long) that extended out of the main structure (Fig. B.1a–e). There was no evidence of the presence within the cysts of microscopic organisms, comparable to the ciliates and nematodes observed by Linke and Lutze (1993) inside the cysts of *Elphidium incertum*. Although most of the *S. bulloides* cysts were unattached, some were sessile on large (>300 µm) planktonic foraminiferal tests (e.g., Fig. B.1b) that dominated the sand fraction of the PAP-SO sediments. All of the specimens found forming cysts were 'live' (i.e. stained with Rose Bengal) and filled with green-coloured cytoplasm (Fig. B.1g), which indicates that they were feeding on freshly deposited phytodetritus that formed patchy deposits on the seafloor at the time of sampling (Durden et al., 2015).

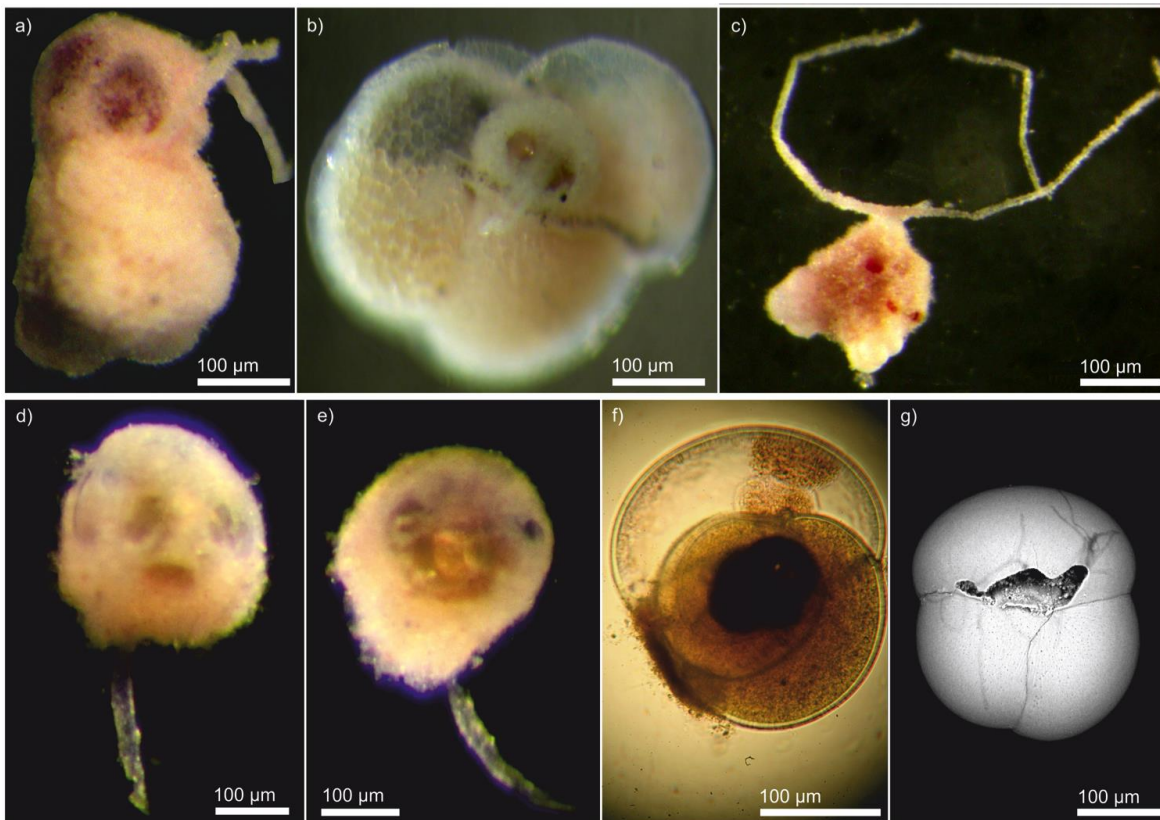


Fig. B.1. *Sphaeroidina bulloides* forming mud cysts. Reflected light images (a–e); scanning electron microscopy image (f); transmission light image (g). Unattached, complete cyst incorporating juvenile planktonic foraminiferal tests (<50 µm) and including long (approx. 400 µm) tubes (a). Partial mud cyst (indicated by an *arrow*) sitting on top of large (>300 µm) planktonic foraminiferal test (b). Partial mud cyst attached to planktonic foraminiferal tests (c). Specimen with partial muddy coating and short tube (approx. 200 µm) (d–e). Specimens of *S. bulloides* after the removal of the cyst (f–g). Note that the interior is filled with green protoplasm (g).

Encystment by *S. bulloides* was observed by Linke and Lutze (1993) from the Guinea Basin, off Ivory Coast (~700 m water depth). However, ours is the first record of this behavioural trait in *S. bulloides* at a much deeper abyssal site, despite the fact that this species has been recorded in other abyssal locations (Murray 2013; Table 16 in Supplementary Material). The only other example of which we are aware of an abyssal foraminiferal species creating a cyst is that of *Quinqueloculina* sp., also from the Porcupine Abyssal Plain (Gooday et al., 2010). Our analysis of ‘live’ benthic foraminifera in 16 Megacorer samples from the PAP-SO area revealed that *S. bulloides* had a density of 0–7 individuals per sample (i.e. up to 3.1 individuals per 10 cm²), or 0–6 % of the ‘live’ assemblage. These values are consistent with those recorded in other studies (Murray 2013, Table 2 therein). Overall, one of every four ‘live’ specimens of *S. bulloides* encountered in our samples had created a cyst.

The benefit of agglutinated cysts to the foraminifera is unclear, although it has been speculated that they serve various functions related to feeding, reproduction, growth and protection (Gross, 2002; Heinz et al., 2005). As sediments on the Porcupine Abyssal Plain are well oxygenated and situated above the carbonate compensation depth, encystment of *S. bulloides* in this area is unlikely to serve the purpose of protection against corrosion, as has been proposed by Murray (1991). The tubes arising from the cysts of this species may function as a guide or anchor for its pseudopodia, as suggested for *Cibicides refulgens* from an Antarctic coastal habitat (Alexander and Delaca, 1987) and *C. wuellerstorfi* from the bathyal Mediterranean (Heinz et al., 2005). Individuals of *Miliolinella subrotunda* collected at depths to 1419 m in the Atlantic Ocean constructed a sediment cyst extending into a tubular structure (up to 6 mm long) that elevated the test above the sediment surface, thus providing access to high quality suspended food particles advected by lateral currents (Altenbach et al., 1993). However, this structure clearly serves a different function from that of the flimsy, sometimes branched tubes described here.

References for Appendix B

- Alexander, S.P., Delaca, T.E., 1987. Feeding Adaptations of the Foraminiferan *Cibicides-Refulgens* Living Epizoically and Parasitically on the Antarctic Scallop *Adamussium-Colbecki*. *Biological Bulletin*, 173, 136-159.
- Altenbach, A.V., Heeger, T., Linke, P., Spindler, M., Thies, A., 1993. *Miliolinella subrotunda* (Montagu), a miliolid foraminifer building large detritic tubes for a temporary epibenthic life-style. *Marine Micropaleontology*, 20, 293–301.
- Cedhagen, T., 1996. Foraminiferans as food for cephalaspideans (Gastropoda: Opisthobranchia), with notes on secondary tests around calcareous foraminiferans. *Phuket Marine Biological Center Special Publication*, 16, 279–290.
- Durden, J.M., Bett, B.J., Jones, D.O.B., Huvenne, V.A.I., Ruhl, H.A., 2015. Abyssal hills – hidden source of increased habitat heterogeneity, benthic megafaunal biomass and diversity in the deep sea. *Progress in Oceanography*, 137, 209–218.
- Gooday, A.J., Hughes, J.A., 2002. Foraminifera associated with phytodetritus deposits at a bathyal site in the northern Rockall Trough (NE Atlantic): seasonal contrasts and a comparison of stained and dead assemblages. *Marine Micropaleontology*, 46, 83–110.
- Gooday, A.J., Malzone, M.G., Bett, B.J., Lamont, P.A., 2010. Decadal-scale changes in shallow-infaunal foraminiferal assemblages at the Porcupine Abyssal Plain, NE Atlantic. *Deep-Sea Research Part II–Topical Studies in Oceanography*, 57, 1362–1382.
- Gross, O., 2000. Influence of temperature, oxygen and food availability on the migrational activity of bathyal benthic foraminifera: evidence by microcosm experiments. *Hydrobiologia*, 426, 123–137.
- Gross, O., 2002. Sediment interactions of foraminifera: Implications for food degradation and bioturbation processes. *Journal of Foraminiferal Research*, 32, 414–424.
- Heinz, P., Geslin, E., Hemleben, C., 2005. Laboratory observations of benthic foraminiferal cysts. *Marine Biology Research*, 1, 149–159.
- Linke, P., Lutze, G.F., 1993. Microhabitat preferences of benthic foraminifera - a static concept or a dynamic adaptation to optimize food acquisition. *Marine Micropaleontology*, 20, 215–234.
- Murray, J.W., 1991. *Ecology and palaeoecology of benthic foraminifera*. New York: Longman Scientific & Technical.
- Murray, J.W., 2013. Living benthic foraminifera: biogeographical distributions and the significance of rare morphospecies. *Journal of Micropalaeontology*, 32, 1–58.